



University
of Glasgow

Foth, Mona (2014) *The role of FGFR3 mutation in tumour initiation, progression and invasion of urothelial cell carcinoma in mice.*
PhD thesis.

<http://theses.gla.ac.uk/5642/>

Copyright and moral rights for this thesis are retained by the author

A copy can be downloaded for personal non-commercial research or study, without prior permission or charge

This thesis cannot be reproduced or quoted extensively from without first obtaining permission in writing from the Author

The content must not be changed in any way or sold commercially in any format or medium without the formal permission of the Author

When referring to this work, full bibliographic details including the author, title, awarding institution and date of the thesis must be given

**The role of *FGFR3* mutation in tumour initiation,
progression and invasion of urothelial cell
carcinoma in mice**

Mona Foth

Submitted in fulfilment of the requirements for the Degree of PhD



Beatson Institute for Cancer Research

University of Glasgow

College of Medical, Veterinary and Life Sciences (MVLS)

2014

Abstract

Bladder cancer is the 5th most common and the 9th most lethal cancer in the UK. Based on histopathological and genomic analysis, a model of two independent pathogenesis pathways has been suggested, resulting in either non-invasive superficial or invasive urothelial tumours with potential to metastasise. Prominently, the fibroblast growth factor receptor 3 (FGFR3) is found mutated in up to 84% of non-invasive superficial tumours. Alterations in *FGFR3* such as mutation or wild type receptor overexpression are also found in 54% of muscle-invasive tumours. FGFR3 is a tyrosine kinase receptor for fibroblast growth factors (FGFs), which stimulates both the RAS/MAPK and the PI3K/AKT pathways and regulates a range of cellular processes such as cell growth and division during development. In this study we examined the role of *FGFR3* in bladder cancer by using mice as a model organism.

Firstly, we addressed whether combination of *Fgfr3* and *Pten* mutation, *Uro11Cre Fgfr3^{+ / K644E} Pten^{flox / flox}*, is able to drive non-invasive superficial bladder cancer. We observed that the thickness of the double mutant urothelium was significantly increased compared to singly mutated *Fgfr3* or *Pten*, *Uro11Cre Fgfr3^{+ / K644E}* and *Uro11Cre Pten^{flox / flox}*. Moreover, several cellular abnormalities were detected that were accompanied by differential expression of layer-specific markers, which strongly suggested that they were caused cooperatively by *Fgfr3* mutation and *Pten* deletion. The results supported the hypothesis that FGFR3 activation can play a causative role in urothelial pathogenesis of non-invasive superficial bladder cancer together with upregulated PI3K-AKT signalling.

Secondly, we aimed to identify mutations that cooperate with *Fgfr3* and with other common bladder cancer mutations such as *Pten* and *Ras*, in promoting urothelial tumourigenesis by Sleeping Beauty (SB) insertional mutagenesis in mice. The SB system may constitute an inefficient tool in the bladder to induce urothelial tumourigenesis, since it failed to produce bladder tumours in *Fgfr3* as well as in *Hras* mutant mice. In mice with *Pten* deletion, one tumour was generated and general hypertrophy with cellular abnormalities was observed in all samples. No direct association between *Fgfr3* and *Pten* mutations was found;

however, SB mutagenesis supported that *Fgfr3* and *Pten* cooperation may merge at the signalling downstream.

Thirdly, we examined the role of the most common mutation in *FGFR3*, *S249C*, in the urothelium and in tumour progression and invasion by subjecting *Fgfr3* mutant mice to a bladder-specific carcinogen, N-butyl-N-(hydroxybutyl)-nitrosamine (OH-BBN). We showed that *FGFR3 S249C* mutation by itself does not lead to urothelial abnormalities. However, in OH-BBN-induced tumours the presence of *S249C* increased the number of animals that formed bladder tumours by 4.4-fold. Our results present for the first time an effect of *FGFR3 S249C* mutation in invasive bladder cancer.

Lastly, we sought to establish methods to generate and assess invasive bladder tumours using *in vivo* and *in vitro* techniques. First we examined the effectiveness of a Cre-expressing adenovirus (AdenoCre) to generate mouse models of bladder cancer with different combinations of genetic mutations. *p53* deletion or mutation together with *Pten* loss led to formation of aggressive bladder tumours; however the origin of these tumours was likely to be the bladder muscle. *Hras* activation in combination with *Pten* deletion did not produce tumours or any cellular abnormalities by 8 months. AdenoCre-mediated tumour induction was successful in the presence of *β-catenin* and *Hras* mutation. However, an issue of AdenoCre transduction was the frequent observation of tumours in various other tissues such as the pelvic soft tissue, liver, pancreas and lung. Using an optimised AdenoCre procedure, the technique would allow lineage tracing of cancer stem cells in a developing bladder tumour and potentially during metastatic spread. Secondly, we tested imaging techniques in the living animals and validated ultrasound as a functional method to detect bladder wall thickening, as well as to monitor tumour growth *in vivo*. Thirdly, with the aim to assess cell transformation, migration and response to drug treatment, we tested essential *ex vivo* techniques and assays such as 3D sphere culture, organotypic slice culture as well as a Collagen-I invasion assay. The 3D tumour sphere culture was successful with murine Wnt-activated tumours as well as with invasive human cell lines. The organotypic slice culture was assessed as a system to test the effect of therapeutic drugs on the tumour cells; however, an issue of tissue disintegration has yet to be overcome. The Collagen-I assay

successfully recapitulated invasion of a human bladder cancer cell line; however, the system needs to be adapted to murine bladder tumours.

Taken together, this study presents for the first time evidence that support the functional role of FGFR3 signalling in the early stages of non-invasive urothelial carcinoma as well as in tumour progression of established neoplasms in mice. Given the wide availability of inhibitors specific to FGF signalling, our FGFR3 mouse models in conjunction with optimised *ex vivo* assays and imaging systems may open the avenue for FGFR3-targeted translation in urothelial disease.

Table of Contents

Abstract	1
Table of Contents	4
List of Tables.....	9
List of Figures.....	10
Acknowledgements.....	13
Author's declaration	15
Abbreviations	16
Chapter 1 (Introduction).....	19
1.1 The Bladder	20
1.1.1 The Urothelium	22
1.1.2 Urothelial lineage and stem cells	24
1.2 Bladder cancer	26
1.2.1 Epidemiology	26
1.2.2 Causes	26
1.2.3 Types of bladder cancer	27
1.2.4 Symptoms	27
1.2.5 Diagnosis	28
1.2.6 Treatment	28
1.2.7 Prognosis	29
1.2.8 Pathology of urothelial cell carcinoma	29
1.2.9 Genetics behind bladder cancer.....	34
1.2.10 Model of two independent pathways of bladder cancer progression 40	
1.3 Fibroblast Growth Factor Receptors (FGFRs).....	42
1.3.1 Downstream signalling	44
1.3.2 Negative regulation of FGFRs	46
1.3.3 FGFRs in cancer	46
1.3.4 Fibroblast growth factor receptor 3 (FGFR3).....	48
1.3.5 FGFR as a target of therapy.....	52
1.4 Modelling bladder cancer <i>in vivo</i> and <i>in vitro</i>	55
1.4.1 Cell culture	55
1.4.2 Orthotopic models.....	57
1.4.3 Carcinogen-induced models.....	58
1.4.4 Genetically engineered models.....	60
1.5 Aims of the study	69

Chapter 2 (Materials and Method.....	71
2.1 Mice.....	72
2.1.1 Mouse lines and genotyping alleles	72
2.1.2 Genetic background of mice	73
2.2 Sleeping Beauty mutagenesis	74
2.2.1 T2/Onc3 excision PCR assay	74
2.2.2 Splinkerette PCR and Sequencing	75
2.3 Generation of Tg(UroII-hFGFR3IIIbS249C).....	75
2.4 OH-BBN treatment.....	78
2.5 Virus injections	79
2.5.1 Virus preparation	79
2.5.2 Anaesthesia.....	79
2.5.3 Surgical procedure	80
2.6 Live imaging.....	81
2.6.1 Fluorescent imaging.....	81
2.6.2 Ultrasound scanning.....	81
2.7 Tissue harvest and fixation.....	81
2.8 Histology	82
2.9 Immunohistochemistry.....	82
2.9.1 Chromogenic signals.....	85
2.9.2 Fluorescent signals	85
2.9.3 Scanning of slides.....	86
2.10 Microscopy	86
2.11 Measurements of urothelial thickness	86
2.12 Measurements of urothelial cell size	86
2.13 Human tissue microarray (TMA).....	87
2.14 Statistics.....	87
2.15 Cell and tissue culture	88
2.15.1 Preparation of cell stocks.....	88
2.15.2 Cell counting.....	88
2.15.3 Culture of human cell line EJ138	88
2.15.4 Primary cell culture from mouse bladder	88
2.15.5 Matrigel culture and colony formation assay	89
2.15.6 Collagen-I invasion assay.....	90
2.15.7 Organotypic slice culture	90
2.15.8 Tamoxifen induction of organotypic slice culture.....	91
2.15.9 R3Mab treatment of organotypic slice culture.....	91

Chapter 3 (Results).....	94
3.1 Introduction	95
3.2 Establishment of the <i>UroIIcre Fgfr3^{+ /K644E} Pten^{flox/flox}</i> mouse model	97
3.2.1 Generation of the cohorts	97
3.2.2 FGFR3 and PTEN protein expression	98
3.2.3 Recombination under the <i>UroIIcre</i> promoter	100
3.3 Increased thickness of the <i>UroIIcre Fgfr3^{+ /K644E} Pten^{flox/flox}</i> urothelium	101
3.4 Abnormal morphology of <i>UroIIcre Fgfr3^{+ /K644E} Pten^{flox/flox}</i> urothelium ..	104
3.5 Differential expression of layer-specific markers.....	105
3.6 Increase in the size of intermediate cells in <i>UroIIcre Fgfr3^{+ /K644E} Pten^{flox/flox}</i> urothelium.....	107
3.7 Increased proliferation in <i>UroIIcre Fgfr3^{+ /K644E} Pten^{flox/flox}</i> urothelium ..	109
3.8 Increased apoptosis in the <i>UroIIcre Fgfr3^{+ /K644E}</i> urothelium.....	111
3.9 Changes in MAPK/AKT signalling and cell cycle regulation.....	113
3.10 Analysis of pathway association between FGFR3 and AKT signalling by tissue microarray (TMA)	115
3.11 Discussion	118
3.11.1 The <i>UroIIcre Fgfr3^{+ /K644E} Pten^{flox/flox}</i> model.....	118
3.11.2 <i>UroIIcre</i> recombination	118
3.11.3 Urothelial thickening	119
3.11.4 Abnormal urothelial differentiation	120
3.11.5 Cell size and cell number	121
3.11.6 Changes in downstream signalling	121
3.11.7 Limitations of the model.....	122
3.11.8 Future plans.....	123
3.11.9 Conclusion.....	123
Chapter 4 (Results).....	124
4.1 Introduction	125
4.2 Sleeping Beauty mutagenesis in the urothelium of <i>UroIIcre Fgfr3^{+ /K644E}</i>	128
4.3 Sleeping Beauty mutagenesis in the urothelium of <i>UroIIcre Pten^{flox/flox}</i>	131
4.4 Sleeping Beauty mutagenesis in the urothelium of <i>UroIIcre Hras^{+ /G12V}</i> ..	138
4.5 Discussion	140
4.5.1 SB in <i>UroIIcre Fgfr3^{+ /K644E}</i>	140
4.5.2 SB in <i>UroIIcre Pten^{flox/flox}</i>	140
4.5.3 Identification of cooperating mutations in SB-induced <i>UroIIcre Pten^{flox/flox}</i> tumours.....	141
4.5.4 SB in <i>UroIIcre Hras^{+ /G12V}</i>	142
4.5.5 SB as an insertional mutagenesis tool in the bladder	142

4.5.6	Future work	143
4.5.7	Conclusion	144
Chapter 5 (Results).....		145
5.1	Introduction	146
5.2	Generation of the Tg(UroII-hFGFR3IIIbS249C) mouse.....	150
5.3	Mouse cohorts that were subjected to OH-BBN	154
5.4	<i>FGFR3 S249C</i> mutation increases sensitivity to tumourigenesis after long-term OH-BBN exposure.....	155
5.5	<i>Fgfr3 K644E</i> mutation increases sensitivity to tumourigenesis after long-term OH-BBN exposure.....	160
5.6	<i>FGFR3 S249C</i> mutation promotes pre-neoplastic changes in a time course of OH-BBN exposure	166
5.7	Analysis of DNA damage in <i>Wild type</i> and <i>FGFR3</i> mutants	169
5.8	Discussion	172
5.8.1	Tg(UroII-hFGFR3IIIbS249C) line	172
5.8.2	<i>FGFR3</i> mutation increases sensitivity to tumourigenesis after OH-BBN exposure.....	173
5.8.3	DNA damage response upon OH-BBN.....	175
5.8.4	OH-BBN as a tool to induce invasive bladder cancer in mice	176
5.8.5	Future work	177
5.8.6	Conclusion	178
Chapter 6 (Results).....		179
6.1	Introduction	180
6.1.1	AdenoCre	180
6.1.2	<i>In vivo</i> imaging.....	182
6.1.3	<i>In vitro</i> models.....	183
6.2	Establishment of techniques to generate and detect invasive bladder cancer in mice	185
6.2.1	Generation of mouse cohorts to test AdenoCre recombination efficiency.....	185
6.2.2	Assessment of recombination.....	186
6.2.3	Monitoring tumour formation and progression <i>in vivo</i>	190
6.3	Highly aggressive tumours in AdenoCre <i>p53 Pten</i> bladders.....	192
6.3.1	Tumours in AdenoCre <i>p53^{flox/flox} Pten^{flox/flox}</i> bladders.....	192
6.3.2	Tumours in AdenoCre <i>p53^{R172H/R172H} Pten^{flox/flox}</i> bladders.....	198
6.4	Exophytic tumours in AdenoCre <i>β-catenin^{exon3/exon3} Hras^{G12V/G12V}</i> bladders 203	
6.5	Hypertrophy in AdenoCre <i>Hras^{+G12V} Pten^{flox/flox}</i> bladders	208

6.6	AdenoCre off-target effects: soft tissue tumours and other non-urothelial tumours.....	211
6.7	The use of LentiCre as an alternative to AdenoCre	214
6.8	Establishment of techniques to assess growth and invasion <i>in vitro</i>	215
6.8.1	Development of an organotypic collagen-I invasion assay.....	215
6.8.2	Development of an <i>ex vivo</i> assay to test the effects of therapeutic drugs	217
6.9	Discussion	229
6.9.1	Recombination	229
6.9.2	<i>In vivo</i> imaging.....	231
6.9.3	AdenoCre	232
6.9.4	<i>In vitro</i> models.....	236
6.9.5	Future work	237
6.9.6	Conclusion	238
	Chapter 7 (Discussion).....	239
7.1	Summary of the findings.....	240
7.2	Contribution of FGFR3 to tumour initiation, progression and invasion .	241
7.3	Tumour progression across pathogenesis pathways	243
7.4	Cooperating mutations.....	244
7.5	Current models of bladder cancer	245
7.6	FGFR3 as a biomarker in bladder cancer.....	246
7.7	FGFR3-targeted therapy.....	248
7.8	Future direction	249
7.9	Significance.....	250
	References.....	252
	Appendices	278
	Appendix 1 - Publications.....	278

List of Tables

Table 1-1: WHO classification of urinary tumours in 1973 and 2004.....	32
Table 1-2: Common genetic alterations in urothelial tumours	39
Table 1-3: Human bladder cancer cell lines.....	56
Table 2-1: Mouse lines and genotyping alleles	73
Table 2-2: T2/Onc3 excision PCR primers	74
Table 2-3: T2/Onc3 excision PCR conditions	75
Table 2-4: Tg(UroII-hFGFR3IIIbS249C) PCR primers.....	77
Table 2-5: <i>FGFR3</i> S249C PCR conditions	78
Table 2-6: Cre viruses.....	79
Table 2-7: Processing methods for histological staining	82
Table 2-8: Primary antibodies	84
Table 2-9: Biotinylated secondary antibodies	85
Table 2-10: Fluorescent secondary antibodies	85
Table 2-11: Media components.....	92
Table 2-12: Growth factors	93
Table 3-1: Summary of mouse cohorts with <i>Fgfr3</i> and <i>Pten</i> mutation	97
Table 4-1: Sleeping Beauty mouse cohorts with <i>Fgfr3</i> mutation	128
Table 4-2: Sleeping Beauty mouse cohorts with <i>Pten</i> mutation	131
Table 4-3: Common insertional sites in <i>UroII</i> Cre <i>Pten</i> ^{flox/flox} <i>SB</i> ⁺	137
Table 4-4: Sleeping Beauty mouse cohorts with <i>Hras</i> mutation	138
Table 5-1: Summary of mouse cohorts for <i>FGFR3-S249C</i> transgene analysis	151
Table 5-2: OH-BBN-treated mouse cohorts	154
Table 5-3: Histological changes of OH-BBN-treated mouse cohorts (“10+10 weeks”)	159
Table 5-4: Histological changes of OH-BBN-treated mouse cohorts (“20 weeks”)	161
Table 6-1: Summary of mice injected for recombination analysis	185
Table 6-2: Summary of p53 and <i>Pten</i> deleted mice injected with AdenoCre ...	192
Table 6-3: Summary of p53 and <i>Pten</i> deleted mice injected with AdenoCre ...	198
Table 6-4: Summary of <i>β-catenin</i> and <i>Hras</i> mutant mice injected with AdenoCre	204
Table 6-5: Summary of <i>Hras</i> and <i>Pten</i> mutant mice injected with AdenoCre ...	208
Table 6-6: Summary of non-urothelial tumours upon AdenoCre injection	211
Table 6-7: Summary of <i>in vivo</i> imaging techniques tested in the study.....	231
Table 6-8: Summary of <i>in vitro</i> techniques tested in the study	236

List of Figures

Figure 1-1: Anatomy of the normal bladder	21
Figure 1-2: Normal mouse urothelium.....	23
Figure 1-3: Staging of bladder cancer	31
Figure 1-4: Current model of bladder cancer progression in two independent pathways.....	41
Figure 1-5: Fibroblast Growth Factor Receptor (FGFR)	43
Figure 1-6: Fibroblast growth factor receptor signalling	45
Figure 1-7: Mutations in Fibroblast growth factor receptor 3 (FGFR3)	50
Figure 2-1: Tg(Uro11-hFGFR3IIIbS249C) vector map.....	76
Figure 2-2: Virus injection into mouse bladder	80
Figure 3-1: FGFR3 and PTEN expression in the <i>Uro11Cre Fgfr3^{+/K644E} Pten^{flox/flox}</i> urothelium.....	99
Figure 3-2: Recombination in the urothelium under Uro11Cre	100
Figure 3-3: Increased thickness of the <i>Uro11Cre Fgfr3^{+/K644E} Pten^{flox/flox}</i> urothelium by H&E	101
Figure 3-4: Quantification of thickness in <i>Uro11Cre Fgfr3^{+/K644E} Pten^{flox/flox}</i> urothelium.....	102
Figure 3-5: Thickening of the urothelium in <i>Uro11Cre Fgfr3^{K644E/K644E}</i> and <i>Uro11Cre Fgfr3^{K644E/K644E} Pten^{flox/flox}</i>	103
Figure 3-6: Abnormal morphology of the <i>Uro11Cre Fgfr3^{+/K644E} Pten^{flox/flox}</i> urothelium.....	104
Figure 3-7: Abnormal cellular identity in the <i>Uro11Cre Fgfr3^{+/K644E} Pten^{flox/flox}</i> urothelium.....	106
Figure 3-8: Differential effects of <i>Fgfr3</i> and <i>Pten</i> mutations in regulation of cell size in the urothelium	108
Figure 3-9: Differential effects of <i>Fgfr3</i> and <i>Pten</i> mutations in regulation of proliferation in the urothelium.....	110
Figure 3-10: Increased apoptosis in the <i>Uro11Cre Fgfr3^{+/K644E} Pten^{flox/flox}</i> urothelium.....	112
Figure 3-11: Deregulation of downstream signalling and cell cycle arrest in the <i>Uro11Cre Fgfr3^{+/K644E} Pten^{flox/flox}</i> urothelium.....	114
Figure 3-12: Tissue microarray analysis of FGFR3 and p-mTOR expression levels in T1 urothelial tumours.....	115
Figure 3-13: Tissue microarray analysis of FGFR3 and p-mTOR expression levels according to tumour grade.....	117
Figure 4-1: T2/Onc3 excision PCR	129
Figure 4-2: Sleeping Beauty insertional mutagenesis in the presence of <i>Fgfr3</i> mutation	130
Figure 4-3: Sleeping Beauty insertional mutagenesis in the presence of <i>Pten</i> mutation	132
Figure 4-4: FGFR3 expression in <i>Uro11Cre Pten^{flox/flox} SB⁺</i> urothelium	133
Figure 4-5: Sleeping Beauty insertional mutagenesis in the presence of <i>Fgfr3</i> and <i>Pten</i> mutation.....	135
Figure 4-6: Upregulation of pAKT in the <i>Pten^{flox/flox} SB⁺</i> tumour.....	136
Figure 4-7: Sleeping Beauty insertional mutagenesis in the presence of <i>Hras</i> mutation and/or in combination with <i>Fgfr3</i> mutation.....	139
Figure 5-1: Establishment of the Tg(Uro11-hFGFR3IIIbS249C) model	150
Figure 5-2: Urothelial appearance of <i>Wild type</i> , <i>Fgfr3-K644E</i> , <i>FGFR3-S249C</i> and <i>FGFR3-S249C Pten</i> at 12 months	153
Figure 5-3: OH-BBN treated urothelia after 10+10 weeks	156

Figure 5-4: Abnormal features in <i>FGFR3-S249C</i> at high magnification upon OH-BBN treatment	157
Figure 5-5: Frequency of histological features and tumour formation in OH-BBN-treated cohorts after 10+10 weeks	159
Figure 5-6: Frequency of histological features and tumour formation in OH-BBN-treated cohorts with <i>Fgfr3 K644E</i> mutation after 20 weeks continuously	161
Figure 5-7: Abnormal protein expression in <i>Fgfr3-K644E</i> at high magnification after 20 weeks continuous OH-BBN treatment.....	163
Figure 5-8: The effects of <i>Fgfr3 K644E</i> mutation in tumour progression upon OH-BBN treatment	165
Figure 5-9: Histological changes of <i>Wild type</i> and <i>FGFR3-S249C</i> bladders after two and six weeks of OH-BBN exposure	166
Figure 5-10: Histological changes of <i>Wild type</i> , <i>FGFR3-S249C</i> and <i>UroIIICre Pten^{flox/flox}</i> bladders after 10+2 weeks of OH-BBN exposure	167
Figure 5-11: Frequency of histological features and tumour formation after 10+2 weeks.....	168
Figure 5-12: Double-strand breaks upon OH-BBN treatment.....	171
Figure 6-1: Cre recombination upon adenoviral transduction visualised by IVIS Spectrum.....	187
Figure 6-2: Cre recombination at cellular level upon high-dose AdenoCre transduction.....	189
Figure 6-3: Monitoring of tumour progression using Vevo 770 Visualsonics ultrasound	191
Figure 6-4: Ultrasound of AdenoCre <i>p53^{flox/flox} Pten^{flox/flox}</i> bladders at 3.5 months post injection	193
Figure 6-5: Histology of AdenoCre <i>p53^{flox/flox} Pten^{flox/flox}</i> bladders at 3.5 months post injection	194
Figure 6-6: Immunohistochemistry of AdenoCre-induced <i>p53^{flox/flox} Pten^{flox/flox}</i> bladders at 3.5 months post injection	196
Figure 6-7: Smooth muscle actin staining on AdenoCre-induced <i>p53^{flox/flox} Pten^{flox/flox}</i> bladders at 3.5 months post injection	197
Figure 6-8: Histology of AdenoCre-induced <i>p53^{R172H/R172H} Pten^{flox/flox}</i> bladders at 1.7 months post injection	200
Figure 6-9: Histology of an AdenoCre-induced <i>p53^{R172H/R172H} Pten^{flox/flox}</i> lung at 1.7 months post injection.....	201
Figure 6-10: Histology of an AdenoCre-induced <i>p53^{R172H/R172H} Pten^{flox/flox}</i> liver at 1.7 months post injection	202
Figure 6-11: AdenoCre <i>β-catenin^{exon3/exon3} Hras^{G12V/G12V}</i> bladders at 2 months (A-B) and 3.5 months (C-D) post injection.....	205
Figure 6-12: AdenoCre <i>β-catenin^{exon3/exon3} Hras^{G12V/G12V}</i> tumours in liver and pancreas	206
Figure 6-13: Ultrasound of AdenoCre <i>β-catenin^{exon3/exon3} Hras^{G12V/G12V}</i> bladders at 8 months post injection.....	207
Figure 6-14: Ultrasound of AdenoCre <i>Hras^{+G12V} Pten^{flox/flox}</i> bladders at 6.5 months post injection	209
Figure 6-15: Histology of AdenoCre <i>Pten^{flox/flox}</i> and <i>Hras^{+G12V} Pten^{flox/flox}</i> bladders at 8 months post injection	210
Figure 6-16: Pelvic tumour formation at 2.8 -3.5 post AdenoCre injection	212
Figure 6-17: Histology of pelvic tumours at 2.8 -3.5 post AdenoCre injection ..	213
Figure 6-18: EJ138 human cell line migrating into organotypic collagen-I matrix	216
Figure 6-19: Matrigel culture of wild type urothelium, non-invasive tumour, and invasive tumour.....	218

Figure 6-20: Effect of EGF on <i>UrollCre B-catenin^{exon3/exon3} Hras^{G12V/G12V}</i> tumour sphere culture	219
Figure 6-21: Effect of different growth factors on <i>UrollCre Hras^{+G12V}</i> sphere culture	221
Figure 6-22: Sphere culture of OH-BBN-treated <i>Wild type</i> and <i>Tg(Uroll-hFGFR3IIIbS249C)</i> after 3 and 14 days	223
Figure 6-23: Organotypic slice culture of fluorescent reporter bladders	226
Figure 6-24: Organotypic slice culture of <i>Wild type</i> and <i>Tg(Uroll-hFGFR3IIIbS249C)</i> tumours treated with FGFR3 inhibitor (R3Mab)	228

Acknowledgements

I would like to thank my supervisors Dr Tomoko Iwata and Prof Owen Samson, as well as my advisor Prof Hing Leung for collectively making this project possible, and for great supervision and helpful input; especially, Dr Tomoko Iwata and Prof Owen Samson for supporting me during grant applications, oversea collaborations, conference travel, scientific writing and publishing, and for giving career advice.

I'm indebted to Colin Nixon and the Histology Service at the Beatson Institute for Cancer Research for their significant contribution to my experiments, as well as to all the involved staff at the Beatson Animal Unit for indispensable practical support, especially Derek Miller for the surgical training in orthotopic virus injections.

Many thanks also to my colleagues from the Beatson Institute and Glasgow University for fruitful discussions and experimental support, especially the members of groups R18, R8 and P1. I would also like to thank Imran Ahmad, who significantly contributed to the *UroII*Cre *Fgfr3*^{+/*K644E*} *Pten*^{*flox/flox*} project, Max Nobis for experimental support with the organotypic Collagen-I invasion assay, Saadia Karim for sharing her expertise in *in vivo* imaging, Despoina Natsiou for her contribution to immunofluorescent staining experiments and Louise King for her contribution to the urothelial cell measurements.

Furthermore, I would like to thank our collaborators for helpful discussions and expertise: Prof Cathy Mendelsohn and Dr Ekaterina Batourina from Columbia University in New York, USA, for the warm welcome in their lab and for sharing their expertise on organotypic slice culture; Dr David Adams and Dr Louise van der Weiden from the Sanger Institute in Cambridge, UK, for contributing to the Sleeping Beauty project with sequencing and insertional sites analysis; Dr Theodorus van der Kwast at the Princess Margaret Cancer Centre, Toronto, Canada, and Dr Bas van Rhijn at the National Cancer Institute, Amsterdam, Netherlands, for their contribution to TMA analysis; Prof Margaret Knowles and Dr Darren Tomlinson at the Leeds Institute of Molecular Medicine, Leeds, UK, for their contribution to the generation of the Tg(UroII-hFGFR3IIIbS249C) mouse line; Dr Paul Timpson at the Garvan Institute, Sydney, Australia, for sharing his

expertise on the Collagen-I invasion assay; Dr Sioban Fraser from the Southern General Hospital, Glasgow, UK, for pathological analysis of the *UroIICre Fgfr3^{+ / K644E} Pten^{flox / flox}* model and the carcinogen-induced tumour models.

I gratefully acknowledge the funding sources that made my PhD work possible. My PhD studies were funded by the Beatson Institute for Cancer Research (BICR) as part of Cancer Research UK (CRUK), the University of Glasgow (GU), and the Medical Research council (MRC). I would also like to thank the Medical Research council (MRC) for a Centenary Award in 2012 of £22,188, which enabled me to carry out adenovirus-mediated *in vivo* gene transfer and organotypic invasion assays.

Finally, I would like to thank my family and friends for great support and encouragement from abroad throughout the three (and a bit) years of my PhD. Many thanks to friends and colleagues in Glasgow for giving some necessary distraction during the course of research, and who have become very close friends of mine.

Mona Foth

April 2014

Author's declaration

I declare that, except where explicit reference is made to the contribution of others, that this dissertation is the result of my own work and has not been submitted for any other degree at the University of Glasgow or any other institution.

Mona Foth

April 2014

Abbreviations

AdCre	AdenoCre
APC	Adenomatous Polyposis Coli
B-cat	β -Catenin
BSA	Bovine serum albumin
cDNA	Complementary DNA
CGH	Comparative genomic hybridisation
CIS	Carcinoma <i>in situ</i>
CK	Cytokeratin
CMV	Cytomegalovirus
CRUK	Cancer Research UK
CT	Computerised tomography
DNA	Desoxyribonucleic acid
E11	Embryonic day 11
eGFP	Enhanced green fluorescent protein
EGF	Epidermal growth factor
EGFR	Epidermal growth factor receptor
ERK	Extracellular signal regulated kinase
ES cells	Embryonic stem cells
FACS	Fluorescence-activated cell sorting
FANFT	N-(4,5-nitro-2-furyl-2-thiazolyl)-formamide
FGF	Fibroblast growth factor
FGFR3	Fibroblast growth factor receptor 3
GAB1	GRB2-associated-binding protein 1
GRB2	Growth factor receptor-bound protein 2
GCE	GFP-Cre-ERT2
gDNA	Genomic DNA
GDNF	Glial cell line-derived neurotrophic factor

GFP	Green fluorescent protein
GSTM1	glutathione S-transferase mu 1
H&E	Hematoxylin and eosin
HGF	Hepatocyte growth factor
HLA	Human leukocyte antigen
HRAS	Harvey rat sarcoma viral oncogene homolog
IHC	Immunohistochemistry
ISUP	International Society of Urologic Pathology
ITR	Inverted terminal repeat
IVIS	<i>In vivo</i> imaging system
JAK	Janus protein tyrosine kinase
KGF	Keratinocyte growth factor
LiCl	Lithium chloride
LOH	Loss of heterozygosity
LSL	Lox stop lox
MAPK	Mitogen-activated protein kinase
MDM2	Mouse double minute 2
MMTV	Mouse mammary tumour virus
MNU	N-methyl-N-nitrosurea
mRNA	Messenger RNA
mTOR	Mammalian target of rapamycin
NAT2	N-acetyltransferase
Neo	Neomycin resistance gene
OH-BBN	N-butyl-N-(4-hydroxybutyl) nitrosamine
PAH	Polycyclic aromatic hydrocarbon
PCR	Polymerase chain reaction
PFU	Plaque-forming unit
PIP3	Phosphatidylinositol (3,4,5)-triphosphate

PI3K	Phosphatidylinositol 3-kinase
PIK3CA	Phosphatidylinositol-4,5-bisphosphate 3-kinase, catalytic subunit alpha
PTEN	Phosphatase and tensin homolog
PUNLMP	Papillary urothelial neoplasms of low-malignant potential
RA	Retinoic acid
RB	Retinoblastoma protein
RFP	Red fluorescent protein
RNA	Ribonucleic acid
RTK	Receptor tyrosine kinase
SB	Sleeping Beauty
SHH	Sonic hedgehog
SMA	Smooth muscle actin
SOS	Son of sevenless
STAT3	Signal transducer and activator of transcription 3
SV40	Simian virus 40
Tg	Transgene, transgenic
TGF	Transforming growth factor, Tumour growth factor
TK	Tyrosine kinase
TMA	Tissue microarray
TNM	Tumour-Node-Metastasis
TURBT	Trans-urethral resection of bladder tumours
UroIICre	Uroplakin II Cre
WHO	World Health Organisation
WNT1	Wingless-int1
X-gal	5-Bromo-4-chloro-3-indolyl- β -D-galactopyranoside
YFP	Yellow fluorescent protein
Z/EG	lac Z/enhanced green fluorescent protein
ZEB1	Zinc finger E-box-binding homeobox 1

Chapter 1

Introduction

1.1 The Bladder

In order to study bladder cancer initiation, progression and invasion, it is essential to understand the normal function of the healthy bladder as part of the urinary system, as well as the composition and function of the urothelium, the tissue from which urothelial cell carcinoma emerges.

The mammalian urinary system comprises kidneys, ureters, bladder and urethra. Anatomically, the bladder is composed of the dome, which is the roof of the bladder reaching laterally down to the two ureters, and the funnel-shaped trigone reaching from the ureters down to the bladder neck that connects to the urethra (Figure 1-1).

The bladder, a hollow muscular organ, is composed of a so-called 'detrusor muscle' made of smooth muscles fibres covered in perivesical fat layers. Below the muscular coat, a layer of fibrous connective tissue interlaces with the urothelium, the inside layer of the bladder that faces the lumen. The connective tissue (also called stroma, submucosa or lamina propria) contains blood and lymphatic vessels, nerves and occasional glands.

As a storage organ, the bladder can hold between 400 to 600ml of urine for about five hours. During this time the urothelium is continuously in contact with the urine and with any toxins or tumourigenic agents that may be dissolved therein.

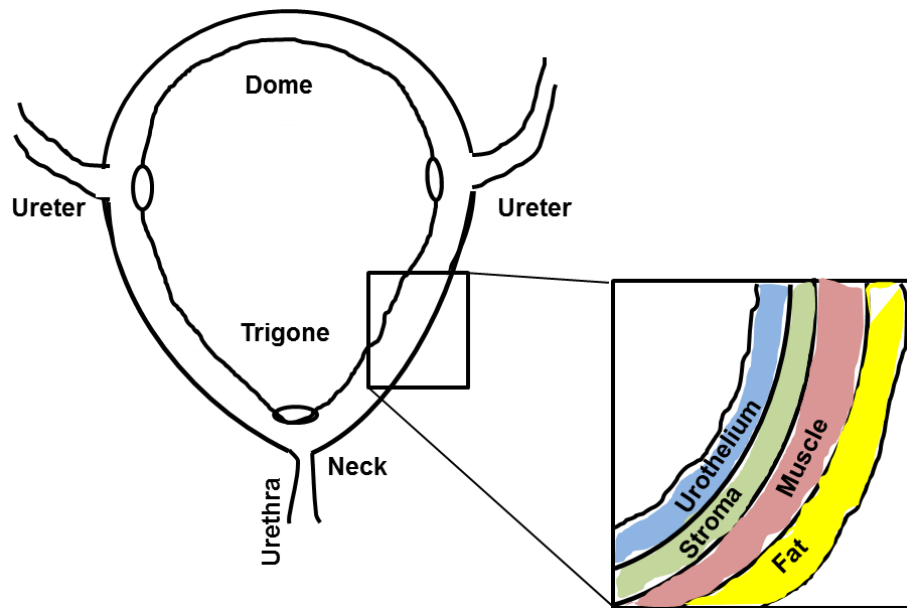


Figure 1-1: Anatomy of the normal bladder

Two ureters connect the kidneys to the bladder that is composed of dome and trigone. The neck is the area that connects the trigone to the urethra. The bladder wall (insert) is composed of urothelium, stroma, muscle and fat (inside to outside).

1.1.1 The Urothelium

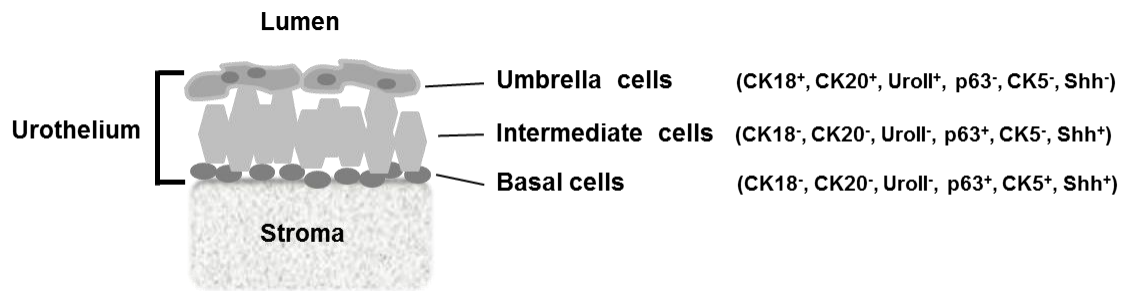
The urothelium is also called transitional cell epithelium, due the fact that it can stretch out into a single layer when storing the urine, and contract back upon releasing it. The urothelium is comprised of a sheet of extracellular matrix rich in collagen-IV and laminin that separates the stroma from the urothelium (Brown et al., 2006).

The human urothelium consists of four to seven cell layers, including a single basal cell layer, multiple intermediate cell layers, as well as a single umbrella cell layer facing the lumen. The murine urothelium has a similar composition, but comprises only three of these cell type layers in total (Figure 1-2).

Basal cells are small round-shaped cells that line up along the basement membrane. They are characterised by the expression of Cytokeratin-5 (CK5), p63, and Sonic hedgehog (Shh) (Castillo-Martin et al., 2010, Gandhi et al., 2013, Shin et al., 2011, Karni-Schmidt et al., 2011). The same studies report that basal cells are negative for Cytokeratin-18 (CK18), Cytokeratin-20 (CK20) and Uroplakins.

Intermediate cells are oriented perpendicular to umbrella and basal cells and can stretch into 1-4 layers. They express p63, Shh, and occasionally Uroplakins, but rarely CK5 (Castillo-Martin et al., 2010, Gandhi et al., 2013, Shin et al., 2011).

Umbrella cells are the terminally differentiated cell type in the urothelium that are facing the lumen. They are often binucleated and present morphologically with a stretched shape, covering the intermediate cell layer in an umbrella-like manner. Umbrella cells are marked by the expression of CK18 and CK20, which are absent in other layers (Castillo-Martin et al., 2010, Veranic et al., 2004). Umbrella cells also express Uroplakins (Kong, 2004, Gandhi et al., 2013), which are involved in the assembly of a protective barrier against urine, the apical plaques (Khandelwal et al., 2009). Expression of p63, Shh and CK5 is absent in umbrella cells (Castillo-Martin et al., 2010, Gandhi et al., 2013, Shin et al., 2011, Karni-Schmidt et al., 2011).

**Figure 1-2: Normal mouse urothelium**

Mouse urothelium consisting of three cell layers is characterised by the expression of different proteins. Umbrella cells express CK18, CK20 and Uro11, intermediate cells express p63 and Shh, basal cells express p63, Shh and CK5.

1.1.2 Urothelial lineage and stem cells

The question of urothelial lineage by which umbrella, intermediate and basal cells are generated has been debated for a long time and still remains controversial (Castillo-Martin et al., 2010, Khandelwal et al., 2009).

The adult urothelium is a quiescent epithelium with a proliferation rate of 0.02-0.05% in human and 0.1-1% in mice (Stewart et al., 1980). The turnover time is estimated to be 3-6 months (Khandelwal et al., 2009). However, upon chemical or mechanical injury the urothelium can rapidly regenerate (Khandelwal et al., 2009, Shin et al., 2011), suggesting the presence of urothelial stem cells.

Stem cells are unspecialised cells that have the ability to self-renew and to differentiate into several cell types (Weiner, 2008). In other epithelia such as the epidermis, there are populations of stem cells which are characterised as slowly cycling *in vivo* but showing a high proliferative potential *in vitro* (Morris and Potten, 1994). Elegant experiments have used these properties of slow turnover and long-term residence in tissue to characterise these cells. Labelling retaining studies first using BrdU, tritiated thymidine or EdU, and more latterly through the use of eGFP-tagged histone 2B (H2B-eGFP) allowed the visualisation and purification of these cells *in vivo* (Tumbar, 2004, Barker et al., 2007, Kurzrock et al., 2008).

Unlike in many other organs, stem cells in the bladder have not been unambiguously identified. For a long time it had been assumed that urothelial stem cells reside exclusively in the basal cell compartment (Kurzrock et al., 2008, Gaisa et al., 2011, Shin et al., 2011, Chan et al., 2009b).

Much effort has been made in order to narrow down urothelial stem cells within the basal cell compartment using marker expression studies and lineage tracing. It has been suggested that 10% of the basal cells could represent candidate stem cells, which show long-term regenerative potential and retain BrdU label one year after its administration (Kurzrock et al., 2008).

Furthermore, it was suggested that p63-expressing cells are the stem cells of the urothelium and that these are able to regenerate basal, intermediate and

umbrella (Pignon et al., 2013). However, it has been shown that p63 and its isoforms are also expressed in intermediate cells (Karni-Schmidt et al., 2011), which therefore does not limit urothelial progenitor cells to reside in the basal cell compartment.

Another study reported the expression of secreted protein Shh in a subpopulation of CK5-positive basal cells, which are capable of regenerating all cell types within the urothelium (Shin et al., 2011). CK5-expressing basal cells are undetectable in the urothelium between E11 and E14 when progenitor potential is high, and they form *after* umbrella and intermediate cells (Gandhi et al., 2013).

Recently, a new model of urothelial regeneration was suggested where at least two urothelial progenitor populations exist within the Shh-expressing population (Gandhi et al., 2013). The study describes fate-mapping in the urothelium upon chemical injury, where it was shown that CK5-positive cells do not generate umbrella cells. The study strongly suggested that lineage-tagged umbrella cells are descendants of intermediate cells, and it was therefore speculated that umbrella and intermediate cells arise from a separate lineage in the adult urothelium. The research group identified a second progenitor population, namely P-cells, which are a transient in the embryonic urothelium between day E11 and E13 and are marked by the expression of Foxa2, p63, Shh and Uroplakin. Fate-mapping suggested that P-cells are the progenitors of intermediate cells, which are present in the embryonic and adult urothelium. It remained unclear in the study where CK5-positive basal cells arise from and whether umbrella cells derive directly from P-cells or from P-cell-descendent intermediate cells.

The study by Gandhi was supported by previous immunohistochemical characterisation of the mouse urothelium using layer-specific markers, which suggested that umbrella cells do not differentiate from basal to intermediate cells, but constitute a different cell lineage (Castillo-Martin et al., 2010, Karni-Schmidt et al., 2011). The proposed model from the Castillo-Martin and Karni-Schmidt protein expression studies was that a urothelial progenitor or stem cell population gives rise to two separate cell lineages with distinct expression profiles, namely basal/intermediate and umbrella cells.

Taken together, further studies are necessary in order to clearly identify urothelial stem cells and to better understand urothelial generation and development. Expansion of such studies into mechanisms of cancer cell transformation could help to shed light on bladder cancer initiation and progression. Furthermore, better understanding of urothelial stem cells and their exact location would be of great benefit to the generation of mouse models of bladder cancer, where the availability of a reliable stem cell targeting Cre is still a limitation. Thus we will be examining the recombination efficiency of an established promoter-driven UroplakinIII-Cre as well as of a novel technique using adenoviral Cre delivery to the urothelium.

1.2 Bladder cancer

1.2.1 Epidemiology

Bladder cancer is the 5th most common and the 9th most lethal cancer in the UK (Parkin et al., 2005), Cancer Research UK statistics, 2013). According to Cancer Research UK statistics 2013, about 10,300 people were diagnosed in 2010 in the UK, which is about 28 people per day. Worldwide, it is estimated that 383,000 new cases are diagnosed per year. Generally, bladder cancer occurs in people aged 65 and over. Overall more men than women are affected, with bladder cancer being the 4th most common cancer in men in the UK and the 11th most common cancer in UK women (Cancer Research UK statistics, 2013). Between the mid-1970s and the 1990s male bladder cancer incidence rates increased, while female rates were lower but followed the same pattern. Bladder cancer is still prevalent in males, although both rates have decreased since the 1990s (Cancer Research UK statistics, 2013).

1.2.2 Causes

The principal risk factor of bladder cancer is smoking, which is estimated to account for 35% of the cases in the UK per year (Brennan et al., 2000, Wallerand et al., 2005)(Cancer Research UK statistics, 2013). Smoking is also associated with high stage and high grade urothelial tumours (Wallerand et al., 2005). Furthermore, occupational exposure to chemical carcinogens such as polycyclic aromatic hydrocarbons (PAHs), diesel exhausts, and aromatic amines is linked to a considerable number of bladder cancers as well (Kogevinas et al., 2003).

Although familial cases of bladder cancer are relatively rare, the risk is 2-fold higher in first degree relatives of bladder cancer patients (Burger et al., 2013). Inherited genetic factors such as N-acetyltransferase (NAT2), glutathione S-transferase mu 1 (GSTM1) and a sequence variant on 4p16.3 are associated with genetic predisposition (Garcia-Closas et al., 2005). In Africa and the Middle East a large number of bladder cancers are caused by schistosomiasis, a parasitic disease (Cancer Research UK statistics, 2013).

1.2.3 Types of bladder cancer

Urothelial cell carcinoma is the most common type of bladder cancer (90%) in the Western world (Cancer Research UK statistics, 2013). Urothelial cell carcinoma develops from the innermost layer of the bladder wall, the urothelium (Chapter 1.1.1). Urothelial cell carcinoma can be of non-invasive or muscle invasive nature (Chapter 1.2.10).

Squamous cell carcinoma accounts for 5% of the UK bladder cancers (Cancer Research UK statistics, 2013). This type of bladder cancer presents with a stratified skin-like tissue architecture. Squamous cell carcinoma is more common in developing countries in Africa and the Middle East, where it is linked to the infectious disease schistosomiasis (bilharzia). Squamous cell carcinoma of the bladder is also linked to chronic inflammation resulting from indwelling catheters, urinary calculi and urinary outflow obstruction (Cancer Research UK statistics, 2013).

Other rare types of bladder cancer include adenocarcinoma, which accounts for 1-2% of all bladder tumours and develops from mucus-producing glandular cells (Cancer Research UK statistics, 2013). Another rare type is soft tissue sarcoma, which originates in the detrusor muscle of the bladder (Cancer Research UK statistics, 2013).

1.2.4 Symptoms

The most common symptom of bladder cancer is blood in the urine (haematuria) seen in 80% of bladder cancer patients (Cancer Research UK statistics, 2013). Haematuria is usually not painful. Other symptoms can include frequency and urgency of passing urine.

1.2.5 Diagnosis

Bladder cancer is mostly diagnosed by examination of the bladder lining using cystoscopy, where a tube with optic cables is inserted through the urethra under (local or) general anaesthesia. Tissue samples taken (biopsies) are taken from normal and abnormal looking areas. Moreover, a computerised tomography (CT) scan can be performed to examine the whole urinary tract. Blood and urine tests for early detection of bladder cancer are in development where hormone levels or ratios of specific proteins such as Bladder Tumour Antigen (BTA), Nuclear Matrix Protein 22 (NMP-22) or Mini Chromosome Maintenance 5 (MCM5) are analysed.

1.2.6 Treatment

Depending on the stage and behaviour of the bladder tumour, the treatment for each patient is managed differently.

Superficial early bladder cancer can be removed by trans-urethral resection of the bladder tumour (TURBT) followed by regular cystoscopic surveillance. Adjuvant immunotherapy (intravesical instillation) is often given in form of Bacillus Calmette-Guerin (BCG) to stimulate the immune system and lower the chances of recurrence and progression (Babjuk et al., 2008). The exact mechanism by which BCG is effective is still unclear.

Invasive bladder tumours can often only be treated by removing parts or the entire bladder by radical cystectomy. Alternatively, radiotherapy can save the bladder from being removed, but this treatment requires daily presence in the hospital for 6 weeks to receive the treatment, and it can cause bowel inflammation as a side effect. Neoadjuvant chemotherapy (intravenous) is often given before the surgery, and can be used in combination with radiotherapy to aid these treatments. Chemotherapy is often based on a Cisplatin-containing drug combination, such as Gemcitabine/Cisplatin (GC) or Methotrexate/Vinblastine/ Doxorubicin (Adriamycin)/Cisplatin (MVAC) (Niegisch et al., 2013). The current standard care for metastatic disease, GC, shows a 49% response rate in the patients (von der Maase et al., 2005). Cisplatin acts by forming crosslinks to the DNA, leading to irreparable DNA damage that triggers cell death through

the apoptotic pathway (Bambury and Rosenberg, 2013). Gemcitabine is pyrimidine analogue that is integrated into the DNA during replication, leading to faulty nucleosides, and therefore triggering apoptosis (von der Maase et al., 2000).

Bladder cancer is one of the most expensive cancers of all to treat (Sangar et al., 2005). This is partly due to the intensive treatments that are necessary in case of an invasive tumour. Moreover, non-invasive tumours tend to recur frequently and therefore require repeated follow-up surveillance.

1.2.7 Prognosis

According to Cancer Research UK statistics 2013, about 80 to 90% of patients with non-invasive bladder cancer can live for more than 5 years. The prognosis for patients with muscle-invasive disease is less favourable, with only 50% survival at 5 years. Once the disease has become metastatic, the average survival drops to 12-18 months.

1.2.8 Pathology of urothelial cell carcinoma

1.2.8.1 Grading and staging

Based on the growth pattern of urothelial tumours, four diagnostic categories are described (flat, exophytic papillary, endophytic, and invasive) (Montironi et al., 2008).

Flat lesions show unaltered thickness of the urothelium, but are more characterised by atypic cellular features such as mitotic figures and loss of polarity. Flat lesions can present features such as reactive (inflammatory) atypia, dysplasia, or carcinoma *in situ* (CIS).

Exophytic papillary neoplasms include papilloma, PUNLMP, and low- and high-grade papillary carcinoma. These growths are characterised by a central fibrovascular core. Endophytic lesions, such as inverted papilloma, show features that are similar to exophytic papilloma; however, without the presence of a

central fibrovascular core. Invasive neoplasms exhibit lamina propria invasion and tumour cell infiltration into the detrusor muscle.

When diagnosing a cancer and its anatomical progression, the tumour stage is generally determined using the Tumour-Node-Metastasis (TNM) classification system.

The T stage is used to describe how far the cancer has grown (Figure 1-3). Carcinoma in situ (CIS) is an early high-grade but superficial lesion in the urothelium. Ta describes a superficial papillary tumour that is restricted to the urothelium. T1 cancers are tumours that have broken through the basement membrane and grown into the lamina propria (stroma). T2 cancers have invaded further into the detrusor muscle. T3 cancers show invasion into the adipose tissue surrounding the bladder wall. T4 stage describes invasion into neighbouring organs.

The N stage describes four stages of lymph node infiltration by the growing tumour. N0 denotes no lymph node invasion; N1 indicates cells in one lymph node in the pelvic area; N2 in more than one lymph node in the pelvis; and N3 in one or more lymph nodes in the groin or other parts of the body.

The M stage describes cancer spread into distant organs (M1 if positive, M0 if absent). Frequent sites of metastatic spread from a primary bladder tumour are the abdominal lymph nodes, the bones (pelvis and spine), lung and liver (Shinagare et al., 2011, Punyavoravut and Nelson, 1999).

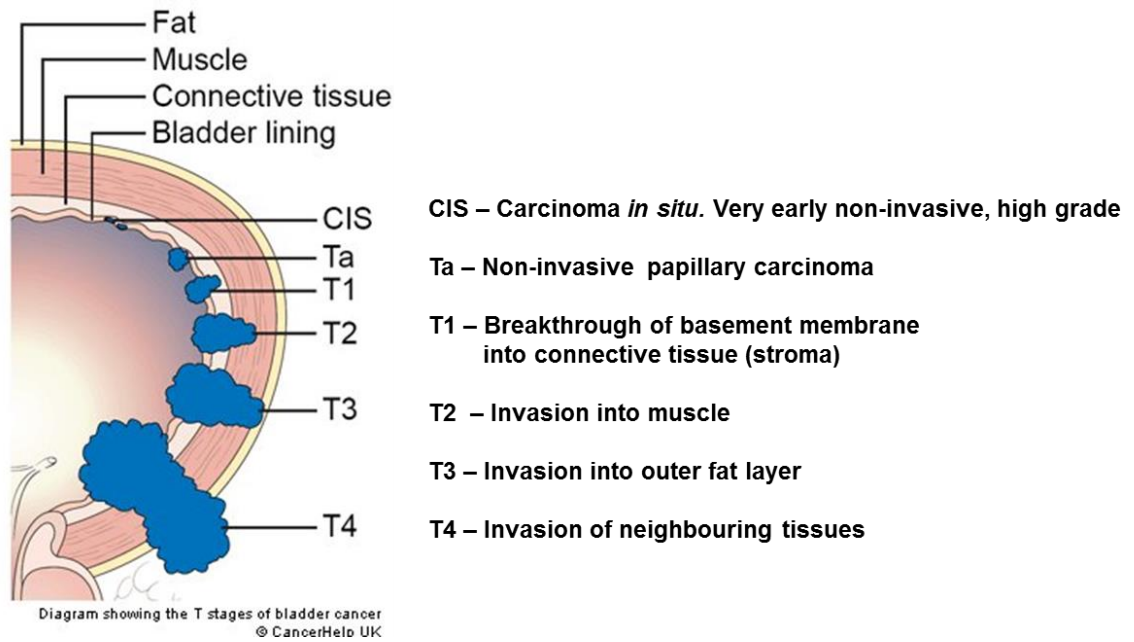


Figure 1-3: Staging of bladder cancer

Diagram showing the T stages of bladder cancer. T stages are classified as high-grade non-invasive lesion called carcinoma *in situ* (CIS), non-invasive papillary carcinoma (Ta), breakthrough of basement membrane with tumour cells in connective tissue (T1), invasion into muscle (T2), invasion into fat layer (T3) and invasion of neighbouring tissues (T4). Source: Cancer Research UK, 2013, <http://www.cancerresearchuk.org/cancer-help/type/bladder-cancer/treatment/bladder-cancer-stage-and-grade>

Grading of a cancer is determined upon microscopic examination of the biopsy sample. Low-grade cancers usually consist of cells that are normal looking and well differentiated and are associated with relatively slow growth, whereas high-grade cancers show high heterogeneity, poor differentiation and a tendency to grow quickly and progress.

Non-invasive urothelial tumours were classified in 1973 by the World Health Organisation (WHO) and the International Society of Urologic Pathology (ISUP) as urothelial papilloma, tumours of grade 1 (G1; well differentiated), grade 2 (G2; moderately differentiated) or grade 3 (G3; poorly differentiated) (Table 1-1).

In 2004 the WHO/ISUP made an attempt to re-classify early bladder tumours in order to improve their recognition and to provide better correlation of the neoplastic lesions with their cellular behaviour. Neoplasms were classified as urothelial papilloma, papillary urothelial neoplasms of low-malignant potential (PUNLMP), low-grade papillary urothelial carcinoma and high-grade urothelial carcinoma (Table 1-1).

Although the 2004 system was meant to replace the urological cancer classification of 1973, the old system is still being used by many pathologists, since it has been validated in terms of prognosis and patient outcome (Chen et al., 2012).

Table 1-1: WHO classification of urinary tumours in 1973 and 2004

WHO classification in 1973 and 2004	
WHO 1973	<ul style="list-style-type: none"> • Urothelial papilloma • Grade 1: Well differentiated • Grade 2: moderately differentiated • Grade 3: poorly differentiated
WHO 2004	<ul style="list-style-type: none"> • Urothelial papilloma • Papillary urothelial neoplasm of low-malignant potential (PUNLMP) • Low-grade papillary urothelial carcinoma • High-grade papillary urothelial carcinoma

1.2.8.2 Multifocality of urothelial tumours

Urothelial cell carcinoma typically presents with multifocal lesions (Habuchi, 2005). These individual tumours within the same tissue can be of similar or completely different stage, grade and site. Two basic mechanisms of how these multifocal lesions arise have been debated (Hafner et al., 2002). The multiple tumours may either arise independently by separate genetic events or they can be of monoclonal origin.

The majority of the reports have been suggesting a monoclonal origin of the multiple lesions, where one progenitor cell is transformed initially (Sidransky et al., 1992, Takahashi et al., 1998, Jones et al., 2005, Hartmann et al., 2000, Denzinger et al., 2006, Simon et al., 2001). Cells can subsequently undergo intraluminal spread using the urine to distribute and to implant at a different site within the bladder. Alternatively, they may reach other regions by intraepithelial migration, a process in which malignant cells spread throughout the urothelial lining.

The second theory, which is also called “field effect” or “field cancerisation”, is supported by a number of studies, where the multiple tumours show indications of oligoclonal origin (Hafner et al., 2001, Spruck et al., 1994, Stoehr et al., 2000). According to this concept individual cells acquire different mutations over time, and tumour lesions arise and develop independently.

It needs to be kept in mind that the two clonality concepts are not mutually exclusive. The correct classification of multifocal urothelial tumours, however, is of clinical importance in terms of prognosis as well as on deciding on the most suitable treatment.

1.2.9 Genetics behind bladder cancer

Genomic analysis such as by fluorescence in situ hybridisation (FISH), comparative genomic hybridisation (CGH) and sequencing techniques indicates a number of genes that are commonly deleted or mutated in bladder tumours (Knowles, 2008, Al Hussain and Akhtar, 2013) (Table 1-2).

Genome-wide alterations, such as copy number changes or deletions of whole chromosomes, chromosome arms, and individual loci on chromosome arms, are frequent events in both non-invasive and invasive bladder cancer (Knowles, 2008). Bladder tumours also frequently present with activation of major signalling pathways involving cell cycle regulating genes, genes involved in cell communication or transcriptional regulators.

1.2.9.1 Genome-wide alterations

Alterations in chromosome 9 (9p, 9q) are found in more than 50% of all bladder tumours of all grades and stages (Cairns et al., 1993), suggesting that this may be one of the earliest events in bladder cancer development (Kallioniemi et al., 1995). Partial deletions of chromosome 9 are found in 35-65% of non-invasive bladder tumours (Blaveri et al., 2005, Simoneau et al., 2000), suggesting the presence of tumour suppressor genes in this genomic region. Chromosome 9 contains an estimate of 800 to 900 genes (Humphray et al., 2004). A specific region on chromosome 9, 9p21-22, referred to as *CDKN2A* encoding for p16/INK4A and p14/ARF is frequently deleted in bladder cancer (Cairns et al., 1994). However, the value of p16 as a prognostic biomarker in bladder cancer is still not entirely clear (Friedrich et al., 2001). Although it is not entirely clear which genes exactly are responsible for cancer relapse, chromosome 9 deletions are also associated with recurrence of non-invasive papillary bladder tumours (Simoneau et al., 2000). Loss of heterozygosity (LOH) of chromosome 10 is a frequent event in advanced tumours (Kagan et al., 1998, Cappellen et al., 1997). Chromosome 10 harbours the tumour suppressor gene *PTEN*, which is frequently deleted in bladder cancer and associated with a higher tumour grade (Aveyard et al., 1999).

1.2.9.2 Changes in genes related to the p53 pathway and cell cycle

Alterations in genes that are involved in the regulation of p53 function, including *TP53*, *p21*, and *RB1* are highly associated with advanced and muscle-invasive tumours (Sidransky et al., 1991, Stein et al., 1998, Cairns et al., 1991). *MDM2*, a negative p53 regulator is often found overexpressed in non-invasive tumours (Habuchi et al., 1994, Lianes et al., 1994).

TP53 deletion is found in up to 70% of muscle-invasive bladder cancers (Sidransky et al., 1991, Lu et al., 2002). p53 is a nuclear phosphoprotein, which is encoded by the *TP53* gene (Vogelstein et al., 2000). The transcription factor p53 acts as a major tumour suppressor and gate keeper at the G1/S checkpoint of cell cycle. Nuclear accumulation of p53 protein can be an indication of *TP53* mutation, which is associated with greater risk of muscle-invasive disease and reduced survival (Esrig et al., 1994). Loss of wild type *TP53* in tumour cells may help to escape growth control (Sidransky et al., 1991).

TP53 mutations, such as point mutations and frameshift mutations, are also frequent events (~70%) in bladder cancer, resulting in functionally silent, missense, or dominant-negative forms of p53 protein (Habuchi et al., 1994). There are about six hotspot mutations in *TP53* that lead to a dominant-negative form of p53 protein function (Greenblatt et al., 1994). An example is *R175H*, a gain-of-function missense mutation which strongly promotes tumour formation and metastatic spread *in vivo* (Liu et al., 2000). Mutant p53 may provide a growth advantage to tumour cells (Sidransky et al., 1991).

LOH of the tumour suppressor 'Retinoblastoma protein' (RB) is found in 37% of muscle-invasive bladder tumours (Cairns et al., 1991). Encoded by the *RB1* gene the RB protein functions as a regulator of the cell cycle at the G1/S phase and as a recruiter of chromatin remodelling enzymes and transcription factors (Classon and Harlow, 2002). RB also regulates p53 activity through mouse double minute 2 homolog (*MDM2*) activation (Hsieh et al., 1999). During the G1 phase of the cell cycle, cyclin-dependent kinases (CDKs) phosphorylate and thereby inactivate RB. Not only loss of function but also phospho-RB (pRB) overexpression and hyperphosphorylation has been reported in bladder cancer (Chatterjee et al., 2004).

Loss of p21 (CIP1/WAF1) expression in patients with muscle-invasive bladder cancer has been shown to be an indicator of tumour progression (Stein et al., 1998). p21 is a cyclin-dependent kinase inhibitor protein that is encoded by the *CDKN1A* gene. p21 is a direct target of p53 and regulates cell cycle progression at the G1/S phase (el-Deiry et al., 1993). Loss of p21 was also strongly associated with higher recurrence and decreased overall survival (Stein et al., 1998), supporting a generally protective function of p21 against disease progression. However, in carcinoma *in situ* patients, p21 expression on its own, as well as co-expressed with p53, was associated with recurrence, progression and mortality (Shariat et al., 2003), suggesting a context-dependent role of p21 in bladder cancer.

The mouse double minute 2 homolog (MDM2) has been found overexpressed in about 30% of non-invasive tumours (Habuchi et al., 1994, Lianes et al., 1994), and is mutually exclusive in the relationship with *TP53* mutations (Network, 2014). *MDM2* encodes for an E3 ubiquitin-protein ligase that targets p53 protein for proteasomal degradation.

1.2.9.3 Activation of tyrosine kinase receptors

The fibroblast growth factor receptor 3 (*FGFR3*) is found mutated in 60-80% of non-invasive bladder cancers (Billerey et al., 2001, Cappellen et al., 1999, Tomlinson et al., 2007a, van Rhijn et al., 2012). *FGFR3* is a tyrosine kinase receptor for FGFs, which stimulates both the RAS/MAPK and the PI3K/AKT pathways and triggers a range of cellular processes such as cell growth and division during development (Bottcher, 2005, Goetz and Mohammadi, 2013). In muscle-invasive disease, *FGFR3* is found mutated in 0-30% of the cases (Billerey et al., 2001); however wild type receptor overexpression has been found in 54% of muscle-invasive tumours (Tomlinson et al., 2007a). A recent attempt to re-classify urothelial cell carcinomas primarily based on molecular features has revealed that *FGFR3* mutations and overexpression are associated with a subgroup of muscle-invasive bladder cancer with significantly poor prognosis (Sjodahl et al., 2012). In a recent study with focus on gene cooperation, *FGFR3* mutations were predominantly found alone (65%) (Juanpere et al., 2012). *FGFR3* and *HRAS* mutations have been shown to be mutually exclusive events in bladder

cancer, possibly due to redundant activation of downstream signalling (Kompier et al., 2010, Jebar et al., 2005, Juanpere et al., 2012).

The epidermal growth factor receptor (EGFR; ERBB-1; HER1) is often found overexpressed in up to 50% of human invasive carcinomas (Colquhoun and Mellon, 2002). EGFR is a tyrosine kinase receptor for ligands including EGF and TGF- α , which stimulate both the RAS/MAPK and the PI3K/AKT pathways and leading to DNA synthesis, cell proliferation and angiogenesis (Oda et al., 2005). Interestingly, it has been shown that the EGFR pathway is upregulated upon FGFR3 inhibition, which constitutes a resistance mechanism to receptor inhibition (Herrera-Abreu et al., 2013). In the same study EGFR dominated the downstream signalling through repression of mutant FGFR3 expression. It was speculated that FGFR3 may initiate cancer development until at some point increased EGFR signalling dominates and represses FGFR signalling (Herrera-Abreu et al., 2013).

1.2.9.4 Changes in genes related to the MAPK/ERK pathway

Activated MAPK/ERK signalling is implicated to be involved in bladder cancer (Kompier et al., 2010, Billerey et al., 2001). Hyperactive MAPK/ERK signalling is not only triggered by activated tyrosine kinase receptor signalling, but can also be caused by mutations in the rat sarcoma viral oncogene homolog (*RAS*). Harvey-RAS (*HRAS*) was the first oncogene isolated from a human bladder cancer cell line (Reddy et al., 1982). *HRAS* is a GTPase that is involved in regulating cell division in response to growth factor stimulation (Campbell et al., 1998). Point mutations in the *HRAS* gene can lead to constitutive activation of the GTPase protein and increased MAPK/ERK signalling, and thereby inducing uncontrolled cell division. *HRAS* is found mutated in non-invasive and invasive bladder cancer at a frequency that strongly varies between the different studies (15-40%) (Jebar et al., 2005, Knowles and Williamson, 1993, Fitzgerald et al., 1995, Ooi et al., 1994, Czerniak et al., 1992).

1.2.9.5 Changes in genes related to the PI3K/AKT pathway

The Phosphatidylinositol 3-kinase (PI3K)/AKT pathway is implicated to be involved in bladder cancer with a large number of tumours showing mutations in *PIK3CA* or *AKT1* or deletion of the tumour suppressor gene *PTEN* (Wu et al.,

2004, Knowles et al., 2009, Askham et al., 2010, Juanpere et al., 2012, Duenas et al., 2013).

PI3K is an enzyme that leads to AKT pathway activation by catalysing the production of Phosphatidylinositol (3,4,5)-triphosphate (PIP3), the substrate of the Phosphatase and tensin homolog (PTEN) (Maehama and Dixon, 1998). A catalytic subunit of PI3K, *PIK3CA*, is mutated in 15-25% of non-invasive tumours, leading to a significant proliferative advantage through increased lipid kinase activity and constitutive AKT activation (Lopez-Knowles et al., 2006, Askham et al., 2010, Ross et al., 2013, Juanpere et al., 2012, Knowles et al., 2009, Kompier et al., 2010). In non-invasive tumours, *PIK3CA* mutation was associated with reduced recurrence (Duenas et al., 2013). In invasive bladder cancer cell lines, inhibition of PI3K has been shown to reduce the invasive capacity (Wu et al., 2004). Co-occurrence of *FGFR3* and *PIK3CA* mutations was found in urothelial cell carcinoma across all stages and grades (Lopez-Knowles et al., 2006, Kompier et al., 2010, Duenas et al., 2013). On the other hand, *PIK3CA* and *AKT1* mutations have been shown to be mutually exclusive, possibly due to redundant activation of downstream signalling (Juanpere et al., 2012).

Loss of heterozygosity (LOH) of *PTEN* has been found in 30% of invasive tumours (Aveyard et al., 1999, Cappellen et al., 1997, Cairns et al., 1998). *PTEN* is a well-known negative regulator of the AKT/PI3K pathway. *PTEN* inhibits the PI3K-AKT pathway by dephosphorylating PIP3, the product of PI3K (Maehama and Dixon, 1998). *PTEN* is located on chromosome 10, a chromosome that is also frequently affected by LOH in advanced tumours (Kagan et al., 1998, Cappellen et al., 1997, Dahia, 2000). Point mutations or homozygous deletion of *PTEN* have been found in 14-23% of invasive tumours (Wang et al., 2000, Cairns et al., 1998).

1.2.9.6 Changes in genes related to the WNT pathway

The WNT pathway controls many events during development and regulates homeostasis in adult tissues (Reya and Clevers, 2005). Deregulation of WNT signalling can occur upon mutations in multiple components of the pathway, for example through LOH of the Adenomatous polyposis coli (*APC*) gene, which has been reported in 50% of bladder tumours (Bohm et al., 1997). Expression of β -

catenin has also been shown to be dysregulated in urothelial cell carcinoma (Zhu et al., 2000, Garcia del Muro et al., 2000, Nakopoulou et al., 2000).

Table 1-2: Common genetic alterations in urothelial tumours

	Gene	Frequency	Reference
Non-invasive tumours	FGFR3	60-80%	Billerey et al., 2001; van Rhijn et al., 2012
	9p, 9q	35-65%	Blaveri et al., 2005
	MDM2	30%	Hambuchi et al., 1994; Lianes et al., 1994
	PI3K (PIK3CA)	15-25%	Lopez-Knowles et al., 2006; Knowles et al., 2009
	HRAS	15%	Jebar et al., 2005; Fitzgerald et al., 1995; Knowles and Williamson, 1993, Ooi et al., 1994
Invasive tumours	TP53	70%	Hambuchi et al., 1994; Sidransky et al., 1991
	RB1	37%	Cairns et al., 1991
	PTEN	17-30%	Aveyard et al., 1999; Cappellen et al., 1997; Cairns et al., 1998; Wang et al., 2000
	9p, 9q	17-30%	Blaveri et al., 2005
	FGFR3	0-30%	Billerey et al., 2001; van Rhijn et al., 2001; Zieger et al., 2005
	HRAS	15%	Jebar et al., 2005; Fitzgerald et al., 1995; Knowles and Williamson, 1993, Ooi et al., 1994

1.2.10 Model of two independent pathways of bladder cancer progression

Based on histopathological and genomic analysis, a model of two independent pathogenesis pathways has been suggested, which could result in two different forms of urothelial cell carcinoma (Figure 1-1, adapted from (Knowles, 2008)).

According to the model, seventy percent of all urothelial cell carcinomas constitute non-invasive papillary tumours (Ta and T1), which are assumed to develop from a hyperplastic urothelium. Seventy percent of these papillary non-invasive tumours have a low potential to progress (Ta), but high potential to reoccur after removal. Thirty percent of the non-invasive tumours present with a higher grade and show breakthrough of cancer cells beyond the basement membrane into the connective tissue (T1), which are potentially life threatening. Non-invasive papillary carcinomas can progress to a higher grade; however, whether high-grade non-invasive lesions can stage progress to an invasive lesion is still a subject of investigation (Sylvester et al., 2006, Zieger et al., 2000, Herr, 2000, Cheng et al., 1999, Leblanc et al., 1999). In contrast, thirty percent of all urothelial cell carcinomas constitute muscle-invasive tumours (T2), which are assumed to develop from a dysplastic urothelium or a carcinoma *in situ* (CIS). CIS is regarded as the precursor of invasive bladder carcinoma, which mostly present as flat lesions with a high potential to progress and to metastasise.

Genomic analysis supports the model of two independent pathogenesis pathways since non-invasive and invasive tumours generally harbour different sets of mutations (Knowles, 2008). Alterations in chromosome 9 (9p, 9q) are found in more than 50% of all bladder tumours of all grades and stages (Cairns et al., 1993) (Chapter 1.2.8). Mutations in *RAS* are frequent events of both pathways as well (Jebar et al., 2005). Prominently, *FGFR3* is found mutated in 60-80% of non-invasive bladder cancer (Billerey et al., 2001). On the other hand, invasive bladder carcinomas often carry *TP53* and *RB* mutations. Analysis of gene cooperation and mutual exclusivity of certain genetic changes further support the two-pathway model. In a recent study with focus on gene cooperation, *PIK3CA* was mostly found co-mutated with *FGFR3* or *KRAS* (35%) (Juanpere et al.,

2012). On the other hand, mutual exclusivity has been found regarding *FGFR3* and *TP53* mutations (Bakkar et al., 2003, van Rhijn et al., 2004).

Most recently, invasive bladder tumours have been subcategorised into basal-, luminal-, and p53-like tumours based on their immunohistochemical expression pattern (Choi et al., 2014). The subtypes also showed distinct clinical outcome in regards to their growth behaviour and resistance to chemotherapy (Choi et al., 2014, Sjobahl et al., 2012)(see also Introduction to Chapter 5).

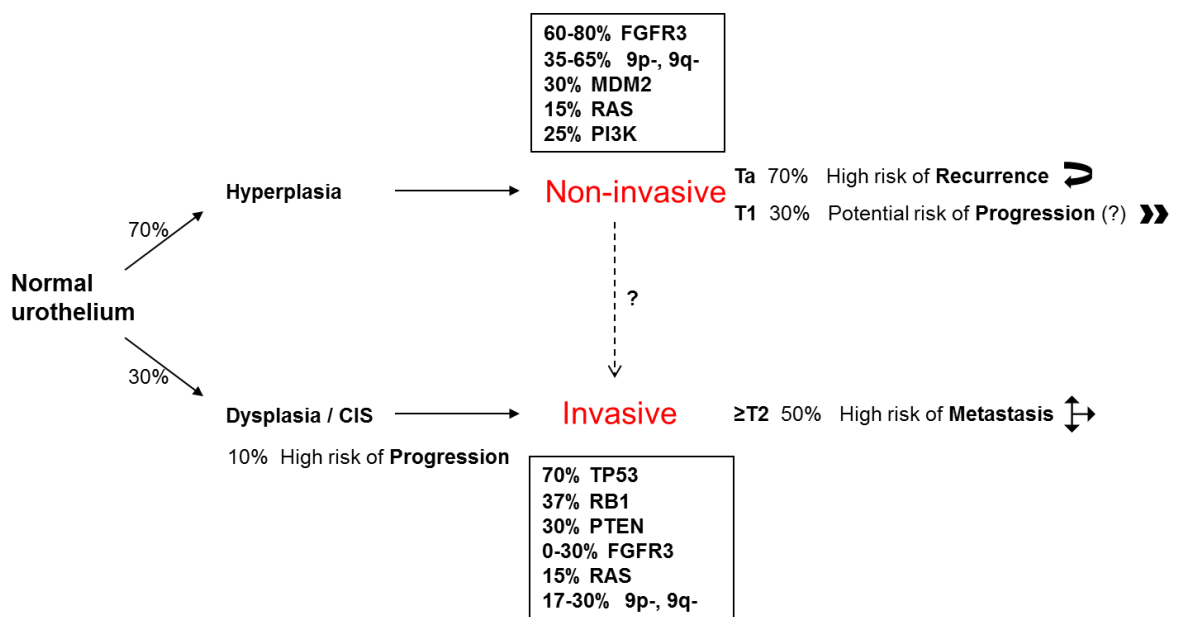


Figure 1-4: Current model of bladder cancer progression in two independent pathways

Non-invasive tumours (Ta, T1) arise from a hyperplastic urothelium and frequently present with alterations in *FGFR3*, *chromosome 9*, *MDM2*, *RAS* and *PI3K*. Invasive tumours (≥T2) arise from a dysplastic urothelium or carcinoma *in situ* (CIS) and frequently present with alterations in *TP53*, *RB1* and *PTEN*. Adapted from (Knowles, 2008)

1.3 Fibroblast Growth Factor Receptors (FGFRs)

Fibroblast growth factor receptors (FGFRs) are tyrosine kinase receptors that mediate the effects of Fibroblast Growth Factors (FGFs) (Goetz and Mohammadi, 2013). FGFRs are involved in a range of cellular processes such as cell division and differentiation, vascularisation and wound healing by stimulation of both the RAS/ Mitogen-Activated Protein Kinase (MAPK) and the Phosphatidylinositide-3 Kinase (PI3K)/AKT pathway (Bottcher, 2005).

The FGFR family consists of five receptors (FGFR1-FGFR5) that comprise several alternative splicing isoforms, which can bind 18 different FGF ligands (Wesche et al., 2011). FGFR1 is known to bind FGF1 (acidic-FGF, aFGF), FGF2 (basic-FGF, bFGF), FGF3, FGF4, FGF5, FGF6, FGF8 and FGF10; FGFR2 can additionally bind FGF7 and FGF9 (Powers et al., 2000). FGFR3 is known to be activated by FGF1, FGF2, FGF8, FGF9, and FGF18; and FGFR4 can bind to FGF 1, FGF 2, FGF 4, FGF 6, FGF8 and FGF 9 (Powers et al., 2000, Davidson et al., 2005). A fifth member of the FGFR family, FGFR5, has been identified, which in contrast to FGFR1-4 lacks a cytoplasmic tyrosine kinase domain (Sleeman et al., 2001, Kim et al., 2001).

FGF receptors are located at the cell surface, and are composed of an extracellular domain to receive FGF signals, a transmembrane domain, and an intracellular domain that mediates signal transmission into the nucleus (Figure 1-5). The extracellular domain (ligand binding domain) of each monomer consists of three immunoglobulin (Ig)-like domains (Ig I, Ig II and Ig III) (Wesche et al., 2011). The Ig II and III domains generally bind to the secreted FGF ligands. The transmembrane domain comprises a single helix structure, which anchors the receptor to the cell membrane. The intracellular domain (signal transmitting domain) is composed of two tyrosine kinase domains, TK1 and TK2.

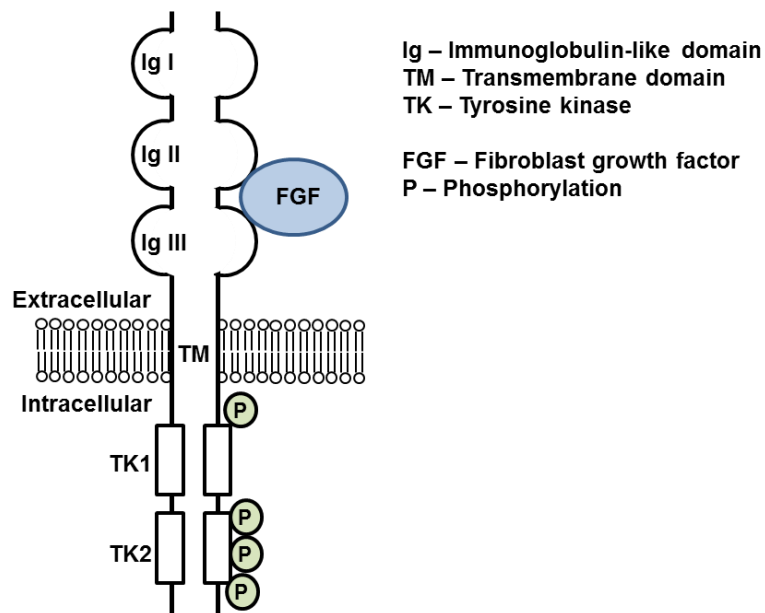


Figure 1-5: Fibroblast Growth Factor Receptor (FGFR)

The extracellular domain of FGFR3 is composed of three immunoglobulin (Ig)-like domains that bind to FGF ligands. The transmembrane domain comprises a single helix structure. The intracellular domain is composed of two tyrosine kinase (TK) domains to transmit the signal. Adapted from (Iyer and Milowsky, 2012)

Based on immunohistochemistry, FGFRs are expressed in many tissues with a distinct spatial pattern (Hughes, 1997). High levels of FGFR1 are seen in the skin, heart, lung, kidney and ureter. FGFR2 is expressed in the prostate and stomach. FGFR3 is expression is seen in the appendix, colon, liver and cervix. FGFR4 expression is seen in the liver, kidney, ureter and some vasculature tissues (Hughes, 1997).

In the normal bladder, expression of FGFR1 at the protein level is prominently seen in the urothelium but not in the detrusor muscle (Hughes, 1997). FGFR2 mRNA and protein levels are exclusively detectable in the urothelial compartment but not in the submucosa or muscle, based on semi-quantitative RT-PCR and immunohistochemistry respectively (Diez de Medina et al., 1997). Expression of FGFR3 is generally low or undetectable by Western blotting and immunohistochemical analysis of tissue microarray (Gomez-Roman et al., 2005, Tomlinson et al., 2007a). FGFR4 expression is detected in the urothelium and in the muscle (Hughes, 1997).

FGFs such as FGF2 (bFGF) are expressed at higher levels in mesenchymal bladder tissue rather than in epithelial cells like the urothelium (Cheng et al., 2013).

1.3.1 Downstream signalling

FGF-mediated receptor kinase activity stimulates major signalling pathways such as the RAS/MAPK, PI3K/AKT and the JAK/STAT pathway, and thereby promotes a range of cellular processes including cell growth and division, vascularisation, wound healing, and embryonic development (Bottcher, 2005).

Upon binding of an FGF molecule to the Ig-like region in the extracellular domain, the receptor dimerises and undergoes a conformational change that allows transphosphorylation of the tyrosine kinase domains of the intracellular part of the receptor (Brooks et al., 2012). The phosphorylated residues recruit adaptor proteins such as Phospholipase-C gamma (PLC- γ) or FGFR substrate 2 (FRS2), which help form a complex composed of Son of sevenless (SOS), Growth factor receptor-bound protein 2 (GRB2) and GRB2-associated-binding protein 1 (GAB1) (Wesche et al., 2011).

The phosphorylated complex can activate the RAS/MAPK via phosphorylated GRB2/SOS (Figure 1-6) (Hart et al., 2001). PI3K/AKT activation is mediated by GRB2/GAB1 interaction with PI3K (Hart et al., 2001). FGFR can also activate the STAT pathway by direct interaction with Proline-rich tyrosine kinase 2 (PYK2) or indirectly through Janus-family kinase (JAK) activation (Hart et al., 2000). Furthermore, it has been shown that FGF receptor signalling can also activate Src kinases (Cunningham et al., 2010, Sandilands et al., 2007).

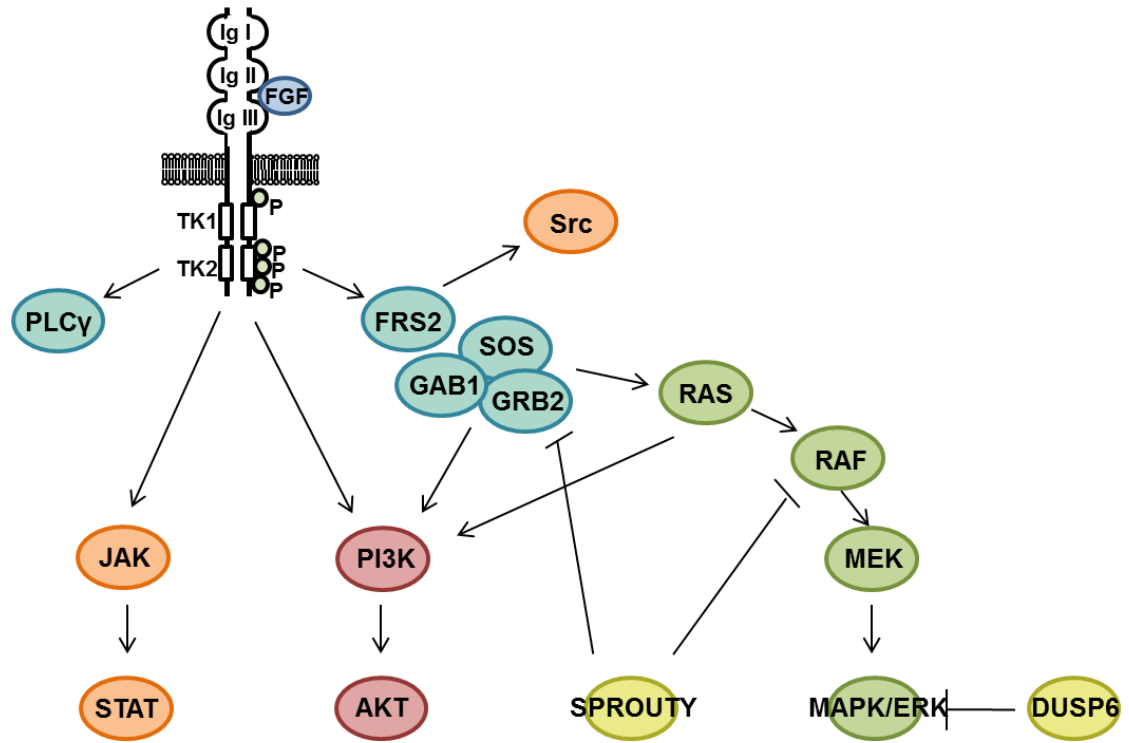


Figure 1-6: Fibroblast growth factor receptor signalling

FGFR phosphorylates adapter proteins such as PLC- γ or FRS2/GAB1/SOS/GRB2 (blue), which stimulate RAS/MAPK (green), PI3K/AKT (red), and Src or JAK/STAT (orange) pathways. Negative regulators of FGFR signalling are Sprouty2 and Dusp6 (yellow). Adapted from (Iyer and Milowsky, 2012, Bottcher, 2005, Ahmad et al., 2012a)

1.3.2 Negative regulation of FGFRs

FGFR signalling can be regulated in the extracellular space, and at the transmembrane level, as well as within the cell.

Well-known negative regulators of FGFR signalling are Sprouty (SPRY) family members, which disrupt downstream signalling by binding to GRB2 or RAF (Figure 1-6) (Hacohen et al., 1998). Furthermore, MAPK phosphatase 3 (MKP3; DUSP6) and 'Similar to FGF' (SEF) proteins can compete for binding sites or directly inhibit downstream signalling by dephosphorylation (Kovalenko et al., 2003, Li et al., 2007).

FGFR gene expression can be transcriptionally regulated by certain microRNAs. For example, mir-99, which is found downregulated in various human cancers, targets FGFR3 at the post-transcriptional level for its degradation (Oneyama et al., 2011, Catto et al., 2009, Kang et al., 2012).

1.3.3 FGFRs in cancer

Mutations in *FGFR* or receptor overexpression have been implicated to play a role in several cancer types, including multiple myeloma, cervical, prostate, breast, lung, gastric cancer and melanoma (Ahmad et al., 2012a, Wesche et al., 2011, Turner and Grose, 2010).

FGFR1 amplification is found in 17% of squamous cell carcinoma (Freier et al., 2007), 21% of lung adenocarcinoma (Dutt et al., 2011), and in up to 10% of breast cancer (Jacquemier et al., 1994). *FGFR1* overexpression has also been shown to play a role in tumorigenesis of the prostate (Sahadevan et al., 2007). Interestingly, overexpression of *FGFR1* is also found in urothelial cell carcinoma across all stages and grades (Tomlinson et al., 2009).

FGFR2 is found amplified in 10% of gastric cancers (Jang et al., 2001, Kunii et al., 2008) and 12% of endometrial cancers (Pollock et al., 2007). Overexpression of *FGFR2* has also been shown to increase the susceptibility to breast cancer (Meier et al., 2008), indicating similar oncogenic properties to *FGFR1* and 3. On the other hand, *FGFR2* has also been suggested to act as a tumour suppressor, since expression of the receptor was found downregulated in a number of cancer

types, including bladder, liver, salivary glands, prostate and melanoma (Amann et al., 2010, Diez de Medina et al., 1997, Naimi et al., 2002, Gartside et al., 2009). It is currently unclear whether FGFR2 is a tumorigenesis promoting or suppressing factor, or whether it may exhibit those opposite characteristics in a context-dependent manner (Ahmad et al., 2012a).

FGFR3 mutations have been identified in several cancer types, including multiple myeloma, cervical and bladder cancer (Chesi, 2001, Cappellen et al., 1999, Billerey et al., 2001). The functional role of *FGFR3* mutation in tumour formation was first demonstrated multiple myeloma (Chesi, 2001), skin hyperplasia in transgenic mice overexpressing mutant *FGFR3* (Logie, 2005), induction of transformation of transfected cell lines (Bernard-Pierrot et al., 2006) and in xenograft models (Qing et al., 2009, Bernard-Pierrot et al., 2006). The role of *FGFR3* in bladder cancer is discussed in more detail in (Chapter 1.3.4.1).

FGFR4 is mutated in 7-8% of soft tissue sarcoma (Taylor et al., 2009) and has been described as a potential driver of tumour growth in human breast tissue (Roidl et al., 2010). Overexpression of *FGFR4* has also been shown to play a role in tumorigenesis of the prostate (Murphy et al., 2010, Sahadevan et al., 2007).

Moreover, high levels of FGF expression have been detected in several cancers, including FGF3, FGF8 and FGF10 in breast carcinoma (Theodorou et al., 2004, Naidu et al., 2001, Marsh et al., 1999). Elevated levels of FGF2 are found in bladder cancer (Marzioni et al., 2009, Cheng et al., 2013). Upregulation of FGF1, FGF2, FGF6, FGF7, FGF8 and FGF9 levels are detectable in prostate cancer (Kwabi-Addo et al., 2004).

Taken together, the reports on genetic mutations and altered expression levels of FGFs and their receptors indicate a major role for FGF signalling in the development of a number of cancers.

1.3.4 Fibroblast growth factor receptor 3 (FGFR3)

FGFR3 is well-known to play a vital role in bone development and growth (Bottcher, 2005). Activating *FGFR3* mutations in the germ line can cause several forms of dwarfism, such as hypochondroplasia, achondroplasia and thanatophoric dysplasia and malformation of the cerebral cortex (Laederich and Horton, 2012, Iwata and Hevner, 2009, Iwata et al., 2000). In mice it has been shown that loss of FGFR3 leads to a neonatally lethal form of dwarfism (Colvin et al., 1996).

Tissue-specific alternative splicing events give rise to two major FGFR3 isoforms, which differ in their Ig-like domains (Ig III) but share the same structure in their tyrosine kinase domains (Chellaiah et al., 1994). Isoforms IIIb and IIIc therefore vary in their ligand-receptor binding specificity (Chellaiah et al., 1994, Miki et al., 1992). FGFR3IIIb for example shows higher affinity for FGF1 (aFGF) and FGF7 (KGF), but a lower affinity for FGF8 and FGF9, while FGFR3IIIc binds FGF1, FGF2, FGF4, FGF8 and FGF9 (Chellaiah et al., 1994, Ahmad et al., 2012a). The FGFR3IIIb splice variant appears to be expressed in epithelial lineages whereas FGFR3IIIc is predominantly expressed in fibroblastic cells (Scotet and Houssaint, 1995).

Based on quantitative RT-PCR, FGFR3 is 20 times higher expressed than any other FGFR in the urothelium (Tomlinson et al., 2005). FGFR3 mRNA levels were higher in epithelial cells, namely the urothelium, of the normal non-neoplastic bladder (Cheng et al., 2013).

1.3.4.1 FGFR3 in bladder cancer

Activating *FGFR3* mutations and overexpression of the wild type receptor are two major mechanisms which are associated with urothelial tumourigenesis (Iyer and Milowsky, 2012). Enhanced receptor signalling poses a proliferation and survival advantage to urothelial cells (di Martino et al., 2009). Around 80% of non-invasive and more than 50% of invasive urothelial cell carcinomas present with alterations in FGFR3 signalling either by mutation, overexpression or both (Iyer and Milowsky, 2012).

1.3.4.2 *FGFR3* mutation

FGFR3 mutations are found in 60-80% of non-invasive urothelial cell carcinoma (Billerey et al., 2001, Cappellen et al., 1999, Tomlinson et al., 2007a, van Rhijn et al., 2012). Muscle-invasive tumours of high grade carry *FGFR3* mutations in only 10-15% of the cases (Billerey et al., 2001). *FGFR3* wild type tumours are generally associated with higher grade and higher stage compared to tumours with *FGFR3* mutation (Bernard-Pierrot et al., 2006).

Presence of an *FGFR3* mutation in bladder cancer patients has been linked to favourable patient prognosis, as it is associated with low grade/stage pTa tumours (van Rhijn et al., 2012, Billerey et al., 2001, Hernandez et al., 2006).

Previous studies have shown association between *FGFR3* mutation in non-invasive papillary tumours of low grade with a higher risk of recurrence (Hernandez et al., 2006, Hernandez et al., 2005). Non-invasive papillary tumours of high grade, on the other hand, were not associated with recurrence or progression in patients (Hernandez et al., 2006, Hernandez et al., 2005). However, in a more recent study, no association was found between *FGFR3* mutational status and recurrence, progression or muscle invasion (Ploussard et al., 2011).

FGFR3 mutations in urothelial cell carcinoma can occur at different codons in the extracellular domain, the transmembrane domain, or the cytoplasmic tyrosine kinase domain, which can cause various changes in the receptor and aberrant signalling (Tomlinson et al., 2007a, di Martino et al., 2009).

Common *FGFR3* mutations are S249C (~66%) and R248C (~10%) leading to changes in the extracellular domain; Y373/375C (~15%) and G370/372C (~4%) occurring in the transmembrane domain; and K650/K652E (<2%) altering the cytoplasmic tyrosine kinase domain (Tomlinson et al., 2007a, Hernandez et al., 2006, Bernard-Pierrot et al., 2006) (Figure 1-7).

The most frequent mutation in *FGFR3*, S249C, accounts for ~66% of human non-invasive urothelial cell carcinoma with *FGFR3* mutant status (Tomlinson et al., 2007a, Duenas et al., 2013, Bernard-Pierrot et al., 2006). S249C is a point

mutation leading to a serine to cysteine exchange at position 249 in the linker region between the extracellular immunoglobulin-like domains Ig2 and Ig3 (d'Avis et al., 1998, Adar et al., 2002). *S249C* mutation triggers kinase activation through constitutive receptor dimerisation as a result of a higher level of disulfide bond formation in a completely ligand-independent manner (d'Avis et al., 1998, di Martino et al., 2009).

A less frequent mutation (<2%) in *FGFR3*, *K650E* or *K652E*, leads to highly activated receptor signalling (Naski et al., 1996, Tomlinson et al., 2007a). *K650E* constitutes a point mutation in the tyrosine kinase (TK) domain, leading to a lysine to glutamic acid exchange at position 650 in the TK activation loop (Tavormina et al., 1995). *K650E* mutation causes a conformational change in the receptor which favours autophosphorylation (Naski et al., 1996). *K650E* mutant receptor signalling shows increased mitogenic activity, which is partially ligand-independent, meaning it can be further enhanced by FGF binding (Naski et al., 1996).

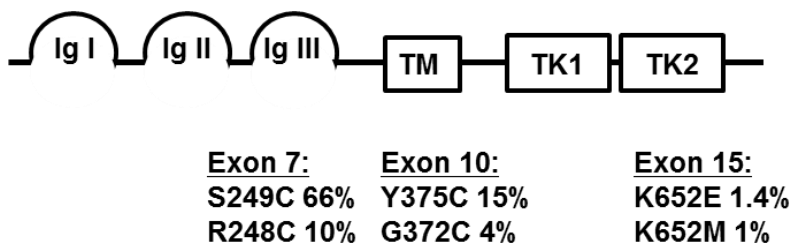


Figure 1-7: Mutations in Fibroblast growth factor receptor 3 (FGFR3)

Common *FGFR3* mutations are found in the immunoglobulin (Ig)-like domain (*S249C*, *R248C*), in the transmembrane domain (*Y375C*, *G372C*), and in the tyrosine kinase domain (*K652E*, *K652M*). Adapted from (Iyer and Milowsky, 2012)

1.3.4.3 FGFR3 overexpression

Overexpression of FGFR3 protein is also frequently found in urothelial cell carcinoma; however between the reports there is variation in terms of stage/grade association. For example, one study reported overexpression of FGFR3 protein in 49% of the bladder tumours, but no statistically significant stage or grade association was found (Matsumoto et al., 2004).

In bladder carcinomas with unknown *FGFR3* mutation status, elevated FGFR3 expression was associated with non-invasive tumours of low-grade and early stage (Mhaweche-Fauceglia et al., 2006, Tomlinson et al., 2007a). Another group reported 73% of non-invasive papillary carcinomas with unknown mutation status showed FGFR3 overexpression across all stages (Gomez-Roman et al., 2005).

When FGFR3 expression levels were examined in relation to *FGFR3* mutation status, correlation between receptor overexpression and presence of *FGFR3* mutation was indeed demonstrated, but the study lacked information on stage or grade of these tumours (Bernard-Pierrot et al., 2006).

A later study confirmed that bladder carcinomas with known *FGFR3* mutation are associated with FGFR3 overexpression, with 85% of the tumours showing strong FGFR3 expression (Tomlinson et al., 2007a). These tumours were predominantly non-invasive papillary carcinomas of low grade and early stage, demonstrating for the first time correlation between *FGFR3* mutation, receptor overexpression, and low grade/early stage association.

On the other hand, the same study also reported overexpression of FGFR3 in 42% of carcinomas with non-mutated wild type receptor, with the majority being high-grade muscle-invasive tumours (Tomlinson et al., 2007a).

Given the high frequency activating *FGFR3* mutations and overexpression of the wild type receptor in bladder cancer, it would be essential to further elucidate the functional importance of the receptor signalling in the urothelium and urothelial tumours. We will address this by using two different mouse models harbouring murine *Fgfr3* K644E or human *FGFR3* S249C mutation.

1.3.4.4 FGFR3 downregulation

Interestingly, two studies have also reported tumour suppressive properties of FGFR3. In one, FGFR3 protein expression was downregulated in colorectal cancer (Sonvilla et al., 2010). In a second study, FGFR3 overexpression had tumour suppressive effects on pancreatic cancer (PDAC) cell lines (Lafitte et al., 2013). Interestingly, there is association between FGFR3 loss and tumour stage in high-grade urothelial bladder cancers (Billerey et al., 2001, Tomlinson et al., 2007a, van Rhijn et al., 2012). Although yet unclear, it is possible that FGFR3 can either promote or suppress tumour development or progression in a context-dependent manner.

1.3.5 FGFR as a target of therapy

Inhibitors of FGF signalling have increasingly been developed to target many types of cancer (Brooks et al., 2012, Liang et al., 2013). Inhibition of FGFR has been suggested as a therapeutic option in urothelial cell carcinoma (Lamont et al., 2011, Tomlinson et al., 2007b). Several novel drugs against FGFRs including monoclonal antibodies, small-molecule inhibitors as well as ligand traps have been developed and show effectiveness in cell lines and xenograft models. An advantage of monoclonal antibodies is that they can be designed to specifically target one single type of FGFR; therefore, the dose-level can be maximised. Small-molecule inhibitors on the other hand cross-inhibit all FGFRs. A disadvantage of pan-FGFR3 inhibition is that this can cause more side-effects in the patient such as nausea or diarrhoea due to the involvement of FGFR pathways in phosphate and vitamin D homeostasis (Brooks et al., 2012).

R3Mab is a monoclonal antibody against wild type and mutant forms of FGFR3IIIb and IIIc, which has been shown to exhibit anti-tumour activity against bladder carcinoma and multiple myeloma xenografts in mice (Qing et al., 2009). R3Mab prevents FGF-binding as well as receptor dimerisation by inducing a conformational change to the receptor (Qing et al., 2009). NVP-BGJ398 is a small-molecule inhibitor of pan-FGFR (FGFR 1, 2 and 3) which showed significant inhibition of angiogenesis, tumour cell proliferation, and induction of tumour cell death in bladder cancer xenografts that overexpress wild type FGFR3 (Guagnano et al., 2011). NVP-BGJ398 prevents receptor phosphorylation and can have cytostatic or cytotoxic properties in a cell-dependent manner (Guagnano et

al., 2011). AZD4547, also a small-molecule inhibitor of pan-FGFR (FGFR 1, 2 and 3), showed anti-tumour activity in FGFR-overexpressing tumour cell lines including acute myeloid leukemia, breast cancer and multiple myeloma (Gavine et al., 2012). Similarly to NVP-BGJ398, AZD4547 prevents receptor phosphorylation and can have cytostatic or cytotoxic properties in a cell-dependent manner (Gavine et al., 2012). All of the named drugs are currently being used in clinical trials (Brooks et al., 2012, Liang et al., 2013).

However, it needs to be kept in mind that the role of FGFR3 as a promoter or suppressor of tumourigenesis is not entirely elucidated and may be context-dependent (Chapter 1.3.4.4.). FGFR3-targeted therapy therefore needs to be considered individually with caution.

A major limitation to the clinical development of FGFR inhibitors is the resistance mechanisms of tumours against FGFR3-targeted therapy. Inhibition of the FGFR3 pathway using parallel siRNA screens has been shown to trigger EGFR pathway activation as an escape mechanism (Herrera-Abreu et al., 2013). EGFR dominated the downstream signalling through repression of mutant FGFR3 expression. A reciprocal relationship was shown between FGFR and EGFR, demonstrated by upregulation of EGFR following FGFR inhibition and FGFR upregulation following EGFR inhibition. It was speculated that FGFR3 may initiate cancer development until at some point increased EGFR signalling dominates and represses FGFR signalling (Herrera-Abreu et al., 2013). Activation of the alternative receptor was capable of partially compensating for loss of the drug-targeted receptor tyrosine kinase signalling, which therefore constitutes a resistance mechanism that is of major clinical relevance in cancers where EGFR or FGFR are targeted. Another possible mechanism of acquired resistance to FGFR inhibition is the emergence of a second mutation site in *FGFR3* as shown recently (Chell et al., 2013). In this study, human multiple myeloma cell lines with drug resistance to AZ4547 were generated. Sequencing then revealed the emergence of *FGFR3 V555M* as a gatekeeper mutation to evade FGFR3 inhibition (Chell et al., 2013). Similarly, FGFR3-dependent malignant melanoma cell lines have shown to gain resistance to NVP-BGJ398 (pan-FGFR) small-molecule inhibition by acquiring *BRAF^{V600E}* or *KRAS* mutation (Guagnano et al., 2012).

For a translational benefit, further studies of the FGFR3 signalling pathway and its inhibitors are therefore essential and will aid the development of therapies for both non muscle-invasive and muscle-invasive bladder cancer with deregulation of FGF signalling.

1.4 Modelling bladder cancer *in vivo* and *in vitro*

The progress of medical research relies on the generation and use of suitable animal models. Therefore, different strategies have been employed to induce bladder tumorigenesis using approaches such as xenografts, carcinogen-induced models as well as genetically engineered mouse (GEM) models (Chan et al., 2009a). The incidence of spontaneous bladder tumours in mice is very low (<1 %) and is therefore not suitable as an investigational strategy (Oliveira et al., 2006). Experimental models of urothelial cell carcinoma also include cell culture of human primary tumour cells or bladder cancer cell lines for investigation *in vitro*. Cell culture provides the opportunity to analyse cancer initiation and progression, as well as the effectiveness of therapeutic drugs in a controlled environment.

1.4.1 Cell culture

Non-invasive human bladder cancer cell lines with superficial papillary characteristics include RT112, 97-7 and Ku-7 (Table 1-3). RT112 is derived from a non-invasive papillary urothelial cell carcinoma of histological grade 2 (G2) in a female Caucasian (ATCC, American Type Culture Collection). RT112 overexpresses *FGFR3* with no detectable point mutations (Qing et al., 2009). 97-7 is derived from a non-invasive urothelial cell carcinoma of histological grade 2-3 (G2-3) in a female Caucasian, and carries an *FGFR3 S249C* mutation (Qing et al., 2009). Ku-7 is derived from a superficial papillary carcinoma of low grade with no detectable *FGFR3* mutation (COSMIC, Catalogue of Somatic Mutations in Cancer database 2013).

Invasive human bladder cancer cell lines with advanced stage and aggressive growth behaviour include T24, EJ138, RT4, KU-19-19 and UM-UC3 (Table 1-3). T24 is derived from an invasive urothelial cell carcinoma of grade 3 (G3) in a female Caucasian and carries a homozygous mutation in *HRAS* and *TP53* (COSMIC, 2013). EJ138 is in fact T24 (or sometimes referred to as MGH-U1), which has been shown by isoenzyme analysis and HLA profiles (O'Toole et al., 1983). RT4 is derived from a well-differentiated grade 1 (G1) but muscle-invasive urothelial cell carcinoma in a male Caucasian, and carries a homozygous mutation in *CDKN2A* and *TSC1* (ATCC and COSMIC, 2013). RT4 overexpresses *FGFR3* with no

detectable point mutations (Qing et al., 2009). Ku-19-19 is derived from a metastatic bladder carcinoma in a male Caucasian, and carries a *KDM6A* mutation (COSMIC, 2013). UM-UC3 is derived from a muscle-invasive bladder carcinoma in a male Caucasian, and carries a *KRAS*, *TP53*, *CDKN2A* and *PTEN* mutation (ATCC).

Table 1-3: Human bladder cancer cell lines

Human bladder cancer cell lines		
Non-invasive	• RT112	<i>FGFR3</i> overexpression
	• 97-7	<i>FGFR3</i> S249C mutation
	• Ku-7	<i>FGFR3</i> wild type
Invasive	• T24	<i>HRAS</i> and <i>TP53</i> mutation
	• EJ138	<i>HRAS</i> and <i>TP53</i> mutation
	• RT4	<i>CDKN2A</i> and <i>TSC1</i> mutation, <i>FGFR3</i> overexpression
	• Ku-19-19	<i>KDM6A</i> mutation
	• UM-UC3	<i>KRAS</i> , <i>TP53</i> , <i>CDKN2A</i> and <i>PTEN</i> mutation

Furthermore, artificially transformed urothelial cell lines have been developed from stably transduced Normal human urothelial (NHU) cells or immortalised Normal human urothelial cells (TERT-NHUC) carrying mutation constructs, such as *FGFR3IIIb* (Bernard-Pierrot et al., 2006, di Martino et al., 2009). The advantage of these cell constructs is that the effect of a single specific mutation on normal urothelial cells can be analysed. Furthermore, potential inhibitors can be easily tested against stable expression levels of the specific construct. However, the artificial settings may not fully reflect the natural urothelial or tumour cell environment of a human bladder.

There are two murine cell lines that are frequently used today, namely MB49 and MBT2 (Loskog et al., 2005). MB49 originated from a 7,12-dimethylbenz[a]anthracene (DMBA)-induced tumour in a male C57BL/6 mouse that carries a *Kras*

mutation (Summerhayes and Franks, 1979). MBT2 is derived from a N-(4,5-nitro-2-furyl-2-thiazolyl)-formamide (FANFT)-induced bladder tumour in C3H mice that carries *p53* deficiency (Rikenbase, Japan, 2013)

1.4.2 Orthotopic models

Since cell culture cannot model the stroma and the complex microenvironment of a tissue or a tumour *in vitro*, techniques have been developed to inject cancer cells into living hosts by subcutaneous grafting or orthotopic injection directly into the organ. Therefore, in the case of bladder cancer, orthotopic models involve the implantation of primary tumour cells or cell lines directly into the urinary bladder of mice by catheterisation or laparotomy.

Orthotopic models are divided in two categories, namely xenograft and syngeneic models. In orthotopic xenograft models, human bladder cancer cells are implanted into nude mice. Human cell lines include KU7, KU19, T24 and UM-UC3, which resulted in tumour formation (Watanabe et al., 2000, Jurczok et al., 2008). A disadvantage of a xenograft model is that the immune response of the host cannot be assessed, which plays an important role in regulating tumour growth. In orthotopic syngeneic models, murine bladder cancer cells are implanted into immunocompetent mice (Summerhayes and Franks, 1979, Gunther et al., 1999). The disadvantage of syngeneic models is that the introduced cancer cells are of murine origin that may not fully reflect human neoplasms, and that the resulting tumours tend to grow fast.

Further limitations of orthotopic models are that they may differ from the original tumour in terms of morphology, growth behaviour and signalling characteristics, since cell lines in culture can acquire additional mutations over time and therefore undergo functional changes (Gabriel et al., 2007). Furthermore, the instillation procedure can be challenging as it involves either catheterisation of female mice or surgical laparotomy, both of which require general anaesthesia. Moreover, the tumour “take” rate in mice can vary from 30-100%, depending on the cell line, genetic background of the mice, and pre-treatment conditioning (Chan et al., 2009a).

1.4.3 Carcinogen-induced models

Over the past 30 years, much effort has been made to model invasive urothelial cell carcinoma in mice using bladder-specific carcinogens (Becci et al., 1981, Ohtani et al., 1986, McCormick et al., 1981).

Three chemicals have been shown to be most effective, namely FANFT (N-(4,5-nitro-2-furyl-2-thiazolyl)-formamide), MNU (N-methyl-N-nitrosurea), and OH-BBN (N-butyl-N-(4-hydroxybutyl) nitrosamine) (Oliveira et al., 2006). FANFT is a nitrofuran, which induces invasive and metastatic bladder neoplasms that often exhibit squamous cell transformation (Soloway, 1977, Cohen et al., 1976). However, administration of FANFT via the diet requires 8-11 months for tumour induction and progression (Erturk et al., 1970). MNU is an alkylating agent that transfers methyl groups to nucleobases, which can generate derivatives such as 6-O-methylguanine that can provoke transition mutations (PubChem Compound NCBI, 2014). MNU can trigger tumourigenesis of the urothelium upon a single dose via catheterisation (Kunze et al., 1989, Steinberg et al., 1991). For health and safety reasons, FANFT and MNU have been widely replaced by OH-BBN, which is derived from tobacco smoke, and which has now become one of the most well studied bladder carcinogens in mice (Becci et al., 1981, Ohtani et al., 1986).

Although OH-BBN is administered systemically by gavage or in drinking water, it induces tumourigenesis specifically in the urothelium (Becci et al., 1981, Ohtani et al., 1986, McCormick et al., 1981, He et al., 2012). The reason for bladder-specificity is not entirely clear, but it is speculated that this may be due to prolonged exposure in the bladder, presence (or absence) of metabolic enzymes that activate (or detoxify) OH-BBN in the bladder as compared to other organs, or lower DNA repair capacity of urothelial cells compared to non-urothelial cells (He et al., 2012).

OH-BBN causes different histological lesions in mouse and rat bladder models. In rats, OH-BBN administration promotes mainly superficial non-invasive tumours (Fukushima et al., 1976, Dunois-Larde et al., 2005). In mice, OH-BBN-induced tumours present with similar histology to advanced human urothelial cell carcinoma (Becci et al., 1981, McCormick et al., 1981, Ohtani et al., 1986). They

are generally of highly invasive nature and often show a mixed histology with features of both urothelial cell carcinoma and squamous cell differentiation (Becci et al., 1981, McCormick et al., 1981, Yamamoto et al., 1998). Similar to observations in human bladder cancer, OH-BBN causes clonally independent multifocal urothelial tumours in the same bladder (Yamamoto et al., 1998). Within these, an individual tumour generally originates from the same precursor cell and is therefore monoclonal (Yamamoto et al., 1998).

OH-BBN tumours also show a similar molecular profile that is comparable to invasive human bladder tumours (Williams et al., 2008). Strikingly, *TP53* mutations are frequent events (~80%) in OH-BBN-induced invasive carcinomas (Ogawa et al., 1998, Yamamoto et al., 1997, Yamamoto et al., 1995). Mutations in the *Hras* gene were reported to be low (Ogawa et al., 1998, Yamamoto et al., 1995). Consistent with the genetic profile of human invasive bladder carcinomas, activating *FGFR3* mutations are a rare event in invasive tumours induced by OH-BBN in mice (Billerey et al., 2001, Dunois-Larde et al., 2005).

Analysis of gene expression in OH-BBN-induced tumours showed differential expression of cell cycle regulating genes such as p53, and signalling pathways involving RAS, EGFR, TGF- β (el-Marjou et al., 2000, Yao et al., 2004). In human invasive carcinomas EGFR is found overexpressed in up to 50% of the tumours (Colquhoun and Mellon, 2002). Similarly, in invasive OH-BBN-induced mouse tumours, EGFR is frequently found overexpressed (el-Marjou et al., 2000, Yao et al., 2004).

Overall, mouse models of chemically induced bladder cancer are excellent models to investigate the mechanisms of urinary bladder carcinogenesis, since they promote tumourigenesis in a bladder-specific fashion and recapitulate tumour development in well-defined stages from carcinoma *in situ* (CIS) to invasive carcinoma. However, tumour induction and progression in carcinogen-induced models can take as long as 8-14 months. Furthermore, the experiments require adequate health and safety regulations for the involved staff.

1.4.4 Genetically engineered models

Genetically engineered mice (GEM) have significantly advanced the understanding of urothelial cell carcinoma at the molecular level over the past 20 years (Frese and Tuveson, 2007). GEM include transgenic mice, knock-in and knock-out mice, as well as a variety of genetic modification tools to achieve tissue-specificity and/or temporal induction of the genetic modification (Frese and Tuveson, 2007).

1.4.4.1 Generation of GEM

Transgenic mice are generated by pronuclear injection, by which foreign homologous DNA is injected into the pronucleus of a zygote that is subsequently transplanted into a foster female (Gordon and Ruddle, 1981). Transgene integration, however, takes place in a random manner. Thus, the integration site, copy number and integration pattern are usually not predictable.

Endogenous GEM such as knockin and knockout mice are generated by targeted recombination via embryonic stem (ES) cell injection. In this procedure, embryonic stem cells are isolated from a blastocyst and cultured *in vitro*. A plasmid with the gene of interest is introduced into the ES cells by electroporation where the sequence integrates into the host genome by homologous recombination. Recombined cell clones are then selected against a toxin to which they are resistant through a resistance gene introduced by the plasmid. Successfully recombined and selected ES cells are injected into a blastocyst and subsequently implanted into a pseudopregnant foster female (Capecchi, 1994). Replacement by the artificial construct can lead to complete disruption of the endogenous gene in the case of a targeted tumour suppressor, or to mutant protein expression at physiological levels in the case of an introduced oncogenic mutation.

Constitutive knockouts present the introduced genetic modification in all cells of the body. A variety of conditional modification tools have been engineered in order to achieve tissue-specificity or time-specific gene alteration, for example the Cre/loxP recombination technology or the inducible CreER-T system (Nagy, 2000).

The Cre/loxP system utilises the Cre recombinase enzyme, which targets two specific sequences *loxP* sequences placed before and after the gene of interest in order to excise it from its original location (Nagy, 2000). The CreER-T system is used to generate inducible knockins and knockouts in order to control temporal activity. The system is based on a fusion protein of CMV/Cre with a mutant ligand-binding domain of the estrogen receptor (ER). Therefore, Cre expression can specifically be activated by treatment with tamoxifen, an ER antagonist, providing a time-specific switch between a wild type and a mutant state.

1.4.4.2 Cre promoters

The expression of the gene of interest can be modulated by the nature of the promoter that controls Cre expression. For example, constitutive GEM can be generated using a ubiquitous promoter for Cre expression, whereas conditional GEM carry a tissue-specific promoter to express Cre in only one specific cell type.

In order to express Cre recombinase in the bladder, a number of tissue-specific promoters have been employed. The Uroplakin II (UroII) promoter is one of the most frequently used promoters of transgene expression in the urinary bladder. UroplakinII is expressed in mice in umbrella and intermediate cells (Choi et al., 2009, Lin et al., 1995, Kong, 2004) from embryonic day 16 (E16) (Oottamasathien et al., 2007). The UroII promoter has been used to promote the expression of Cre enzyme for loxP-specific gene targeting in knockin and knockout models (Ahmad et al., 2012b). Furthermore, the UroII promoter has been used to directly promote the expression of oncogenes such as *SV40T*, *Hras* and *Egfr* without the use of Cre recombinase expression (Zhang et al., 1999, Zhang et al., 2001, Cheng et al., 2002).

Recently, it was found that the original promoter contained a region of UroII that was oppositely inserted, which may result in a differential expression pattern of Uroplakin. Therefore, a modified Uroplakin II promoter has been cloned to express Cre (*UPKII Cre*) with the correct insertion (Ayala de la Pena et al., 2011). This new UPKII Cre promoter has shown differences in the effects of Cre-mediated recombination in the bladder compared to the original UroII Cre

promoter. For example, mice expressing *SV40T* under the UPKII promoter developed CIS only (Ayala de la Pena et al., 2011), while *SV40T* under the UroII Cre promoter resulted in muscle-invasive bladder cancer (Grippio and Sandgren, 2000, Zhang et al., 1999).

Other Cre drivers in the urothelium include the fatty acid-binding protein (*Fabp*) promoter, which drives Cre expression in all cell layers of the urothelium as well as in the renal calyces and pelvis, ureters, and small intestinal and colonic epithelium (Saam and Gordon, 1999, Tsuruta, 2006). Shh-Cre is primarily active in a subgroup of urothelial basal cells; but it is also expressed in the prostate (Shin et al., 2011). CK5-and $\Delta\text{Np}63\text{-Cre}$ have been used to drive the expression of the recombinase in the urothelium (Pignon et al., 2013, Gandhi et al., 2013). However, CK5 and p63 are also commonly expressed in the skin (Di Como et al., 2002, Moll et al., 2008). A relatively novel technique has been developed to deliver Cre recombinase to the urothelium using a Cre-expressing adenovirus (AdenoCre; AdCre) (Puzio-Kuter et al., 2009). In contrast to promoter-based Cre expression, AdenoCre allows transduction and recombination of a specific number of cells (see also Introduction to Chapter 6).

1.4.4.3 Advantages and disadvantages of GEM

The advantages of GEM are that candidate tumour suppressor genes or oncogenes can be deleted or mutated singly or in combination, constitutively or conditionally, and thereby model the conditions of known cancer signalling pathways. On the other hand, tumours of GEM models often show less heterogeneity than is generally found in human tumours (Ahmad et al., 2012b). Secondly, the cancer cell of origin may not be the same as in the humans since the location of tumourigenesis strongly depends on the promoter that is used. Furthermore, due to the fact that only a small number of candidate mutations are introduced, GEM models may not represent the full spectrum of mutations and genome-wide alterations that are seen in human tumours. Finally, GEM models often have long latency and incomplete penetrance. Furthermore, depending on the nature of the promoter that is used, the introduced constructs may be expressed at non-physiological levels (Ahmad et al., 2012b).

1.4.4.4 Human bladder cancer genetics in mice

***Fgfr3* models**

Given the preponderance of *FGFR3* mutations in urothelial cell carcinoma, a number of attempts have been made to model this event in the mice. Surprisingly, as yet these attempts have failed to produce a mouse model of tumorigenesis that recapitulates human tumorigenesis. Much of this study will be investigating why this is the case and how we could generate models that develop tumours driven by *FGFR3*.

It has been shown in mice that *Fgfr3 K644E* mutation alone under the control of Uroplakin II promoter to drive Cre expression in the urothelium (*UroIIcre Fgfr3^{+/K644E}*) did not result in urothelial tumorigenesis by 18 months (Ahmad et al., 2011c), indicating that mutant *FGFR3* alone it is insufficient to drive urothelial tumorigenesis.

Fgfr3 mutation in combination with *Kras* activation under the control of *UroIIcre* (*UroIIcre Fgfr3^{+/K644E} Kras^{+/G12D}*) also failed to produce tumours by 12 months (Ahmad et al., 2011c), indicating that *FGFR3* and *KRAS* do not cooperate in driving urothelial tumorigenesis. This result supports the finding that *FGFR3* and *HRAS* are unlikely to occur together in human bladder tumours (Jebar et al., 2005). However, *UroIIcre Fgfr3^{+/K644E} Kras^{+/G12D}* mice developed skin papilloma due to unexpected UroII promoter activity in the skin (Ahmad et al., 2011c), indicating a functional role of activated *FGFR3* signalling in contributing to tumorigenesis.

Similarly, *Fgfr3* mutation in combination with β -catenin activation (*UroIIcre Fgfr3^{+/K644E} β -catenin^{+/exon3}*) did not result in urothelial tumorigenesis (Ahmad et al., 2011c). However, these mice developed lung carcinoma due to UroII promoter activity in the lung. These results support that *FGFR3* plays a functional role in tumorigenesis in the presence of cooperating mutations in a tissue-specific fashion.

One potential reason why these studies did not observe urothelial cancer could be that they were using an *Fgfr3 K644E* mutation that is relatively uncommon in bladder cancer. Thus in this study we will assess whether the most common

FGFR3 mutation in bladder cancer, *S249C*, might be more tumour promoting in this system.

***Egfr* models**

The effect of other receptor tyrosine kinases such as EGFR that stimulate the RAS/MAPK pathway in a similar manner as *FGFR3* has extensively been investigated in the mouse bladder.

Overexpression of EGFR using the *Uroll* promoter (*Uroll EGFR⁺*) has been shown to produce urothelial hyperplasia in mice around 10 months of age, without progression to carcinoma (Cheng et al., 2002).

EGFR activation in combination with HRAS activation (*Uroll EGFR⁺ Hras^{Q61L}*) did not promote neoplastic progression of the hyperplastic urothelium by 10 months (Cheng et al., 2002). However, EGFR activation in combination with SV40T overexpression (*Uroll EGFR⁺ SV40T⁺*) promoted the development of high-grade bladder carcinomas by 10 months (Cheng et al., 2002), indicating that activated EGF receptor tyrosine kinase signalling functionally contributes to tumourigenesis in the presence of cooperating mutations.

***Hras* models**

Aberrant signalling through RAS/MAPK as a major signalling pathway downstream of *FGFR3* has been implicated to play a role in urothelial cancer. In mice, HRAS activation with low copy number (1-2 copies) under the control of the *Uroll* promoter (*Uroll Hras^{Q61L}*) led to urothelial hyperproliferation by 10 months and low-grade non-invasive urothelial carcinoma formation between 12-26 months (Zhang et al., 2001). Similar observations were made in mice with high copy number (30-48 copies) where mice presented low-grade non-invasive urothelial carcinoma already by 5 months of age (Zhang et al., 2001). This finding was supported by another study using the same mouse model (*Uroll Hras^{Q61L}*), where homozygous *Hras* hyperactivation led to urothelial hyperplasia with progression to low-grade superficial papillary bladder tumours by 6 months in 100% of the cases (Mo et al., 2007). However, the very same model (*Uroll Hras^{Q61L}*) used by our group showed urothelial hyperplasia, but no tumour formation was observed

by 12 months (Ahmad et al., 2011b). This could be due to different mouse genetic background or different animal units.

HRAS activation in combination with β -catenin activation under the control of *UroII*Cre (*UroII*Cre *Hras*^{Q61L} β -catenin^{exon3/exon3}) resulted in low-grade, non-invasive urothelial carcinoma (Ahmad et al., 2011b). HRAS activation in combination with *p53* deletion (*UroII*Cre *Hras*⁺ *p53*^{flox/flox}) resulted in superficial low-grade papillary tumours or high-grade tumours in 30% of the mice by 3-6 months (Gao et al., 2004). HRAS activation in combination with EGFR activation (*UroII* *Hras*^{Q61L} *EGFR*⁺) resulted in urothelial hyperplasia without indication of tumour formation by 10 months (Cheng et al., 2002).

Given that *Hras* in combination with cooperating mutations is a potent driver of urothelial tumourigenesis, we will investigate the effect of RAS/MAPK activation through *Hras* G12V mutation and relevant cooperating mutations in an AdenoCre-induced mouse model and in a Sleeping Beauty insertional mutagenesis mouse model.

***p53* models**

A dominant-negative *p53* truncation mutation expressed under the *UroII* promoter in mice (*UroII* *p53*^{dom.neg.}), leading to disruption of endogenous *p53* protein function in the urothelium, has been shown to produce hyperplasia and dysplasia without progression to carcinoma by 20 months (Gao et al., 2004). Similar results were obtained when *p53* was homozygously deleted under the control of a modified UroplakinIII-Cre promoter (*UPKIII*Cre *p53*^{flox/flox}), where the mice failed to form urothelial tumours (Ayala de la Pena et al., 2011). Likewise, using an AdenoCre-driven mouse model of *p53* deletion (AdCre *p53*^{flox/flox}), no urothelial abnormalities were observed (Puzio-Kuter et al., 2009).

However, *p53* inactivation in combination with homozygous *Pten* deletion using AdenoCre (AdCre *p53*^{flox/flox} *Pten*^{flox/flox}) led to formation of CIS or invasive bladder tumours with 100% penetrance by 6 months including metastasis in 60% of the cases by 4-6 months (Puzio-Kuter et al., 2009). *p53* deletion in combination with HRAS activation (*UroII*Cre *p53*^{flox/flox} *Hras*⁺) resulted in

superficial low-grade papillary tumours or high-grade tumours in 30% of the mice by 3-6 months (Gao et al., 2004).

Rb models

Deletion of *Rb1* using the *UroII*Cre promoter in mice (*UroII*Cre *Rb1*^{flox/flox}) has been shown to promote apoptosis, but failed to produce urothelial cell carcinoma (He et al., 2009).

Rb1 deletion in combination with *p53* inactivation under the control of *UroII*Cre (*UroII*Cre *Rb1*^{flox/flox}) resulted in urothelial hyperplasia with nuclear abnormalities in 10-20% of the cases without progression to carcinoma by 28 months (He et al., 2009). Similarly, using the AdenoCre promoter, *Rb1* deletion in combination with *Pten* deletion (AdCre *Rb1*^{flox/flox} *Pten*^{flox/flox}) or *p53* inactivation (AdCre *Rb1*^{flox/flox} *p53*^{flox/flox}) did not promote carcinoma formation (Puzio-Kuter et al., 2009).

SV40 T models

The Simian vacuolating virus 40 (SV40) is a polyomavirus (DNA virus) that can integrate into infected host cells and potentially induce tumours (Ali and DeCaprio, 2001). Through expression of large T antigen, SV40 can suppress p53 and pRB protein function (Ali and DeCaprio, 2001), which makes it a useful experimental tool to assess the effect of inactivation of the two key tumour suppressors in mice.

SV40 T antigen overexpression under the control of *UroII*Cre (*UroII* SV40T⁺) using a low copy number results in severe urothelial dysplasia followed by CIS formation (Zhang et al., 1999). Using a high copy number of the transgene, *UroII* SV40T⁺ mice presented with invasive, metastatic bladder cancer (Cheng et al., 2002). Interestingly, a follow-up study using the same model reported that the majority of CIS eventually evolved into high-grade, superficial papillary tumours before a small fraction of them advanced to invasive and metastatic cancer (Cheng et al., 2003). SV40 expression under the Cytokeratin 19 (CK19) promoter (*CK19* SV40T⁺) resulted in CIS followed by highly invasive bladder tumours by 12 weeks of age, as well as 20% of the mice developing metastasis to the lungs at 12 weeks (Grippe and Sandgren, 2000). Papillary lesions were not observed in

this model. Expression of SV40 under the control of a modified Uroplakin II promoter (*UPKII SV40T⁺*) resulted in CIS at one week after birth (Ayala de la Pena et al., 2011). However, muscle invasion and metastasis was an infrequent event in this model.

SV40 T antigen overexpression in combination with EGFR overexpression (*UroII EGFR⁺ SV40T⁺*) promoted the development of high-grade bladder carcinomas in mice by 10 months (Cheng et al., 2002). Given that SV40T targets many pathways, this could suggest that in mice multiple hits are required to transform the quiescent bladder epithelium into bona fide urothelial tumours. Thus in this study we combine a number of events with *FGFR3* mutation to assess whether this can provoke urothelial carcinogenesis.

***Pten* models**

Homozygous *Pten* deletion under the control of *UroII*Cre in mice (*UroII*Cre *Pten^{flox/flox}*) did not lead to any abnormal urothelial phenotype (Ahmad et al., 2011a). Similarly, using the AdenoCre promoter, homozygous *Pten* deletion (AdCre *Pten^{flox/flox}*) did not lead to any urothelial abnormalities (Puzio-Kuter et al., 2009).

However, using the *Fabp* promoter to drive Cre expression in all layers of the urothelium, along with intestinal epithelium (*Fabp*Cre *Pten^{flox/flox}*), homozygous *Pten* deletion resulted in urothelial hyperplasia by 6 weeks and high-grade muscle-invasive carcinoma formation in 22% of cases by 13 months of age (Yoo et al., 2006). Another study using the same mouse model (*Fabp*Cre *Pten^{flox/flox}*) reported hyperplasia by 2 months and the development of non-invasive bladder tumours in 10% of cases by 10 months (Tsuruta, 2006). This inconsistency between studies is still unclear but could represent different cell populations targeted by the different Cre promoters, mouse genetic background or even different animal units.

Pten deletion in combination with β -catenin activation under the control of *UroII*Cre (*UroII*Cre *β -catenin^{+ / exon3} Pten^{flox/flox}*) resulted in low-grade non-invasive urothelial carcinoma (Ahmad et al., 2011a). Homozygous *Pten* inactivation in combination with *p53* deletion using AdenoCre (AdCre *p53^{flox/flox} Pten^{flox/flox}*) led

to formation of CIS or invasive bladder tumours with 100% penetrance by 6 months including metastasis in 60% of the cases by 4-6 months (Puzio-Kuter et al., 2009).

Given that loss of PTEN appears to be able to contribute to urothelial tumourigenesis, we will use a model with *Pten* deletion as an experimental tool to assess the effects of PI3K-AKT activation in the presence of *Fgfr3* mutation in the urothelium.

Wnt models

β -catenin activation under the control of the *UroII*Cre promoter (*UroII*Cre β -catenin^{exon3/exon3}) has been shown to produce localised hyperproliferative lesions in the bladder epithelium by 3 months without progression to carcinoma (Ahmad et al., 2011a).

β -catenin activation in combination with *Pten* deletion (*UroII*Cre β -catenin^{+ / exon3} *Pten*^{fllox/fllox}) resulted in low-grade, non-invasive urothelial carcinoma (Ahmad et al., 2011a). Similarly, β -catenin activation in combination with HRAS activation (*UroII*Cre β -catenin^{exon3/exon3} *Hras*^{Q61L}) resulted in low-grade, non-invasive urothelial carcinoma (Ahmad et al., 2011b).

1.5 Aims of the study

Bladder cancer poses a major health issue worldwide that causes considerable morbidity and mortality due to ineffective or lacking therapeutic strategies. It is therefore essential to better understand the disease process and the molecular changes and mechanisms behind bladder cancer formation and progression in order to develop novel therapy approaches. Alterations in FGFR3 signalling are frequently found in bladder cancer, either by mutation, overexpression or both. However, there are open questions that urgently need to be addressed, such as the functional role of FGFR3 in cancer initiation, invasion and progression of tumours, as well as the exact mechanism of FGFR3-dependent tumourigenesis as a valuable step towards the discovery of novel therapeutic targets.

The overall aim of this study is to examine the role of *FGFR3* mutation in bladder cancer initiation and progression by using mouse models.

The following 4 objectives were addressed:

- I. **To investigate the role of FGFR3 in non-invasive bladder cancer.** This first experiment was based on our previous findings that *Fgfr3* mutation alone is insufficient to drive tumourigenesis in the urothelium (Ahmad et al., 2011c), suggesting that a cooperating mutation may be obligatory for FGFR3-dependent tumorigenesis. We found an indication that increased PI3K/AKT signalling may be required for tumour formation in the bladder. Hypothesising that the putative cooperating mutation is a regulator of PI3K/AKT signalling, we targeted a candidate gene, *Pten*, to test the synergistic effects of FGFR3 and PI3K-AKT signalling activation in the bladder (Chapter 3).
- II. **To identify mutations that cooperate with FGFR3, PTEN, or RAS in promoting urothelial tumourigenesis.** It has been shown in mouse models that *Fgfr3*, *Pten* and *Ras* are unable to drive urothelial tumourigenesis when mutated individually. It would therefore be important to test their potential to cooperate with a second, randomly introduced mutation that can be identified and validated. This unbiased screening approach could also help to identify novel mutations that play an important role in

bladder cancer. Hypothesising that *Fgfr3*, *Pten*, and *Hras* are fundamentally able to promote cancer formation in the presence of cooperating mutations, we generated mice with these mutations in conjunction with transposable “Sleeping Beauty” elements. (Chapter 4).

- III. **To investigate the role of *FGFR3* mutation in tumour progression and invasion.** Alterations in *FGFR3* signalling either by mutation or overexpression are found in 50% of invasive bladder tumours. However, it is unclear whether *FGFR3* activation can actively promote tumour progression, or whether it is acquired during the evolution of the cancer without functional contribution to its progression. To address whether an *FGFR3* mutation can predispose urothelial cells to tumourigenesis, and to evaluate its role in tumour progression in established tumours, we subjected *Fgfr3*-mutant and *Wild type* mice to a bladder-specific carcinogen, N-butyl-N-(hydroxybutyl)-nitrosamine (OH-BBN). We compared the effect of two different point mutations in *Fgfr3*, as well as the effect of *Pten* deletion and *Fgfr3-Pten* double mutation in the invasive tumours (Chapter 5).
- IV. **To establish techniques in order to generate and assess invasive bladder tumours.** The progress of anti-cancer drug development relies on the generation and use of suitable animal models, as well as on the essential techniques to analyse and assess the effect of the therapy. We therefore first aimed to generate an invasive bladder cancer model with metastatic potential, in which recombination is promoted in a spatially and temporally controlled fashion using a Cre-expressing adenovirus. In order to then detect and monitor tumour development and progression in the living animals, we tested fluorescent imaging and ultrasound imaging in the mouse bladder. Furthermore, with the aim to assess cell transformation, migration and response to drug treatment, we tested essential *ex vivo* techniques and assays (Chapter 6).

Chapter 2

Materials and Methods

2.1 Mice

All mice were maintained under non-barrier conditions and given a standard diet (CRM (E) expanded diet from Special Diets Services; Cat no 801730) and water *ad libitum*.

The Biological Services department at the Beatson Institute provided animal husbandry including setting up matings, weaning pups, and tail tipping for genotyping.

Mice were sacrificed using an approved schedule 1 procedure. All experiments were carried out with the Personal Licence 60/12893 in accordance with the Project Licence 60/4271 under the UK Home Office guidelines.

2.1.1 Mouse lines and genotyping alleles

Mouse lines used throughout the project are indicated in (Table 2-1).

DNA extraction from tail tips and genotyping by PCR was performed by Transnetyx, USA, (<http://www.transnetyx.com/>). The company uses a method based on real time PCR and DNA hybridisation to detect the presence or absence of alleles in the DNA.

Table 2-1: Mouse lines and genotyping alleles

Allele	Reference	Transnetyx probes
<i>UrollCre</i>	Mo et al., 2005	Cre (+/-)
<i>Fgfr3^{+ / K644Eneo}</i>	Iwata et al., 2000	Fgfr3-2 Mut (+/+, +/-, -/-)
<i>Tg(Uroll-hFGFR3IIIbS249C)</i>	Generated in collaboration by T. Iwata, M. Knowles, D. Tomlinson (unpublished)	hFgfr3-1 Tg (+/-)
<i>Pten^{flox/flox}</i>	Lesche et al., 2002	PTEN LoxP (+/-) PTEN WT (+/-)
<i>Hras^{+ / G12V}</i>	Provided by K. Haigis, MGH Boston	Hras1-3 FL (+/-) Hras1-3 WT (+/-)
<i>T2/Onc3</i>	Dupuy et al., 2009	T3Onc-1 Tg (+/-)
<i>RosaSBase^{LSL}</i>	Dupuy et al., 2009	UREN-27 KI (+/-) ROSA WT (+/-)
<i>B-catenin^{exon3/exon3}</i>	Harada et al., 1999	DBC-1 KO (+/-) DBC-1 WT (+/-)
<i>p53^{flox/flox}</i>	Jonkers et al., 2001	p53Flox Mut (+/-) p53Flox WT (+/-)
<i>p53^{R172H/R172H}</i>	Olive et al., 2004	Trp53-1 Mut (+/+, +/-, -/-)
RFP	Luche et al., 2007	tdRFP (+/-)
Z/EG	Novak et al., 2000	LAC Z (+/-) eGFP (+/-)

2.1.2 Genetic background of mice

UrollCre transgenic mice were originally on FVB/N background (Mo et al., 2005). *Tg(Uroll-hFGFR3IIIbS249C)* transgenic mice were on C57/CBA mixed background (Chapter 2.3). The background of all other mice was C57Bl/6.

2.2 Sleeping Beauty mutagenesis

Bladders were gently emptied of urine. Tissues were generally snap-frozen in liquid nitrogen immediately after collection and stored at -80C until further preparation.

2.2.1 T2/Onc3 excision PCR assay

Excision of the *T2/Onc3* transposon in the *UroIIICreFgfr3^{+ /K644E} RosaSBase^{LSL} T2/Onc3* bladder was assessed by PCR (Collier et al., 2005). Bladders and tail tips were thawed on ice, and genomic DNA was extracted using the QIAamp DNA Mini kit (Qiagen). PCR products were visualised in a 1.5% agarose gel containing ethidium bromide.

T2/Onc3 excision PCR primers and PCR conditions were as follows (Table 2-2 and Table 2-3):

Table 2-2: T2/Onc3 excision PCR primers

Primer	Sequence (5' - 3')
Forward	TGTGCTGCAAGGCGATTA
Reverse	ACCATGATTACGCCAAGC

Table 2-3: T2/Onc3 excision PCR conditions

T2/Onc3 PCR	Temperature	Time
Initial denaturation	94 C	2 min
-----	40 cycles	-----
Denaturation	94 C	30 sec
Annealing	55 C	30 sec
Elongation	72 C	2 min 30 sec
Final elongation	72 C	5 min

2.2.2 Splinkerette PCR and Sequencing

Splinkerette PCR was performed to amplify transposon junctions from genomic DNA of mice carrying transposon insertions.

Genomic DNA was extracted from snap frozen mouse bladders and tails using DNeasy kit (Qiagen). Splinkerette PCR, sequencing and bioinformatics analysis was performed by Dr Louise Van Der Weyden and Dr David J. Adams at the Sanger Institute (Cambridge, UK) as previously described (Uren et al., 2009). See also Introduction to Chapter 4.

2.3 Generation of Tg(UroII-hFGFR3IIIbS249C)

The vector design was performed by Dr Tomoko Iwata (University of Glasgow), Dr Darren Tomlinson (LIMM, Leeds, UK) and Prof Margaret Knowles (LIMM, Leeds, UK).

A pGEM-T vector (Promega) was used containing a multiple cloning site (MCS) for EcoRI, SpeI, Sall, and NotI (Figure 1-1). The MCS was cloned into pGEM digested with NcoI and SacI. The UroplakinII (UroII) fragment of 2.5kb was released from a vector supplied by Robert Weeks (Dunedin, New Zealand) using EcoRI and SpeI,

and ligated into the same sites in the pGEM MCS. Human *FGFR3IIIb* cDNA was mutated at position 249 and at the stop codon. The clones contained restriction sites for *Sall* at the 5' end and *NotI* at the 3' end of the gene for ease of cloning into pGEM-Uroll. A poly-A sequence was added 156 bp after the 3' end of the *FGFR3* gene. The resulting pGEM-Uroll-hFGFR3IIIb-S249C construct contained 10,294 bp and was fully sequenced.

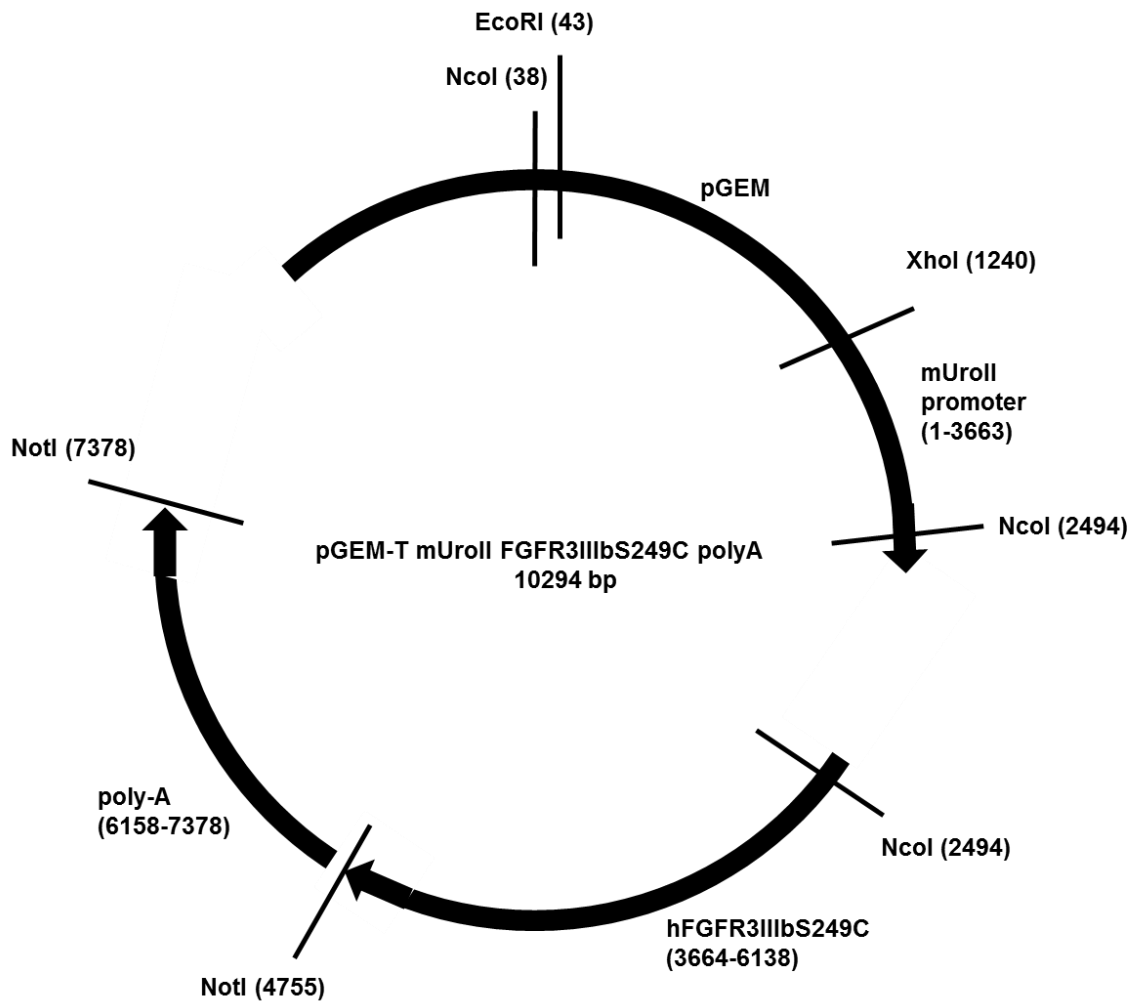


Figure 2-1: Tg(Uroll-hFGFR3IIIbS249C) vector map

Schematic representation of pGEM-T vector containing murine UroplakinII promoter and human *FGFR3IIIb* cDNA with *S249C* mutation.

In order to test the expression level of the construct, three human bladder cancer cell lines (VMCUB-1, VMCUB-3 and UMUC-3) were transfected with pGEM-UroII-hFGFR3IIb-S249C or the empty vector. RNA was extracted and an RT-PCR was performed to determine FGFR3 expression levels. A 1.8-fold increase in FGFR3 expression was detected in cells with the full construct compared to control cells containing the empty vector (Dr Darren Tomlinson, data not shown).

Transgenic animals were generated by pronuclear injection of the pGEM-UroII-hFGFR3IIb-S249C vector construct. Mouse studs and donors were on C57/CBA F1 background. Tg(UroII-hFGFR3IIbS249C) transgenic mice were therefore on C57/CBA F2 mixed background and further crossed with C57Bl/6. The presence of the transgene in the offspring was confirmed in two mice by sequencing (Dr Tomoko Iwata, data not shown).

Presence of the *FGFR3* S249C mutation in Tg(UroII-hFGFR3IIbS249C) bladders was assessed by PCR. PCR primers and conditions are indicated in (Table 2-4 and Table 2-5). Tail tips were thawed on ice, and genomic DNA was extracted using the QIAamp DNA Mini kit (Qiagen). PCR products were visualised in a 1.5% agarose gel containing ethidium bromide.

Amplified PCR product of Tg(UroII-hFGFR3IIbS249C) was extracted from 1.5% agarose gels using the QIAquick PCR purification kit (Qiagen #28104). Sequencing was done by the Beatson Sequencing Service (AB Applied Biosystems, 3130XL).

Table 2-4: Tg(UroII-hFGFR3IIbS249C) PCR primers

Primer	Sequence (5' - 3')
hFGFR3 6F	TGTGCTGCAAGGCGATTA
mFgfr3 R6903	CTGAGGATGCCTGCATACAC

Table 2-5: *FGFR3* S249C PCR conditions

S249C PCR	Temperature	Time
Initial denaturation	94 C	2 min
-----	35 cycles	-----
Denaturation	94 C	30 sec
Annealing	55 C	30 sec
Elongation	72 C	30 sec
Final elongation	72 C	5 min

2.4 OH-BBN treatment

Mice were administered 0.05% w/v N-butyl-N-(4-hydroxybutyl) nitrosamine (OH-BBN, TCI UK #B0938) in drinking water, which was prepared freshly three times a week. Two different lengths of treatment were performed. In one, animals were treated for 10 weeks with OH-BBN followed by 10 weeks of regular water (further called “10+10 weeks”). In the other, animals were subjected to 20 weeks continuously of OH-BBN (further called “20 weeks”). Animals were sacrificed at different time points during the procedure or when 20 weeks were completed.

2.5 Virus injections

Cre-expressing Adenovirus and Lentivirus (Feline Immunodeficiency Virus) was injected into the bladder upon laparotomy as previously described (Table 2-6) (Puzio-Kuter et al., 2009, Seager et al., 2010).

2.5.1 Virus preparation

Virus was mixed with 10% Hexadimethrine bromide (Polybrene, Sigma #107689-10G) and kept on ice until injection.

Table 2-6: Cre viruses

Virus	ID	Titer stock (pfu/ml)	Source
AdenoCre	Ad5CMVCre	2×10^{11}	Vector Core Facility Iowa, USA
	Ad5CMVCre-eGFP	1×10^{11}	
LentiCre	FIVCMVCre-eGFPVSVG	2×10^8	Vector Core Facility Iowa, USA

2.5.2 Anaesthesia

Mice were anaesthetised using 2-chloro-2-(difluoromethoxy)-1,1,1-trifluoroethane (Isoflurane-Vet 100% w/w Inhalation Vapour, Liquid, Merial Animal Health Ltd., UK) through a Key Fill Vapouriser 5% connected to medical air and an active scavenging unit (Vet Tech Solutions). Isoflurane was supplied at level 4 to put the mouse asleep. During the procedure, mice were maintained at level 2.

2.5.3 Surgical procedure

The lower abdomen was shaved, and a small incision was made to expose the bladder (Figure 2-2). The bladder was emptied of urine using a 0.5ml syringe (BD Micro Fine 0.5ml 29G x 12.7mm). The virus was orthotopically instilled via a second syringe. The bladder was let sink back into the abdomen, and the incision was closed with suture (Coated Vicryl Suture, 4/0 Violet 45cm, 17mm 3/8Circle Taper Point Needle, MidMeds UK#W9074) and wound clips (Clay Adams Clips, Vet Tech solutions #IN015A). Animals were monitored for recovery.

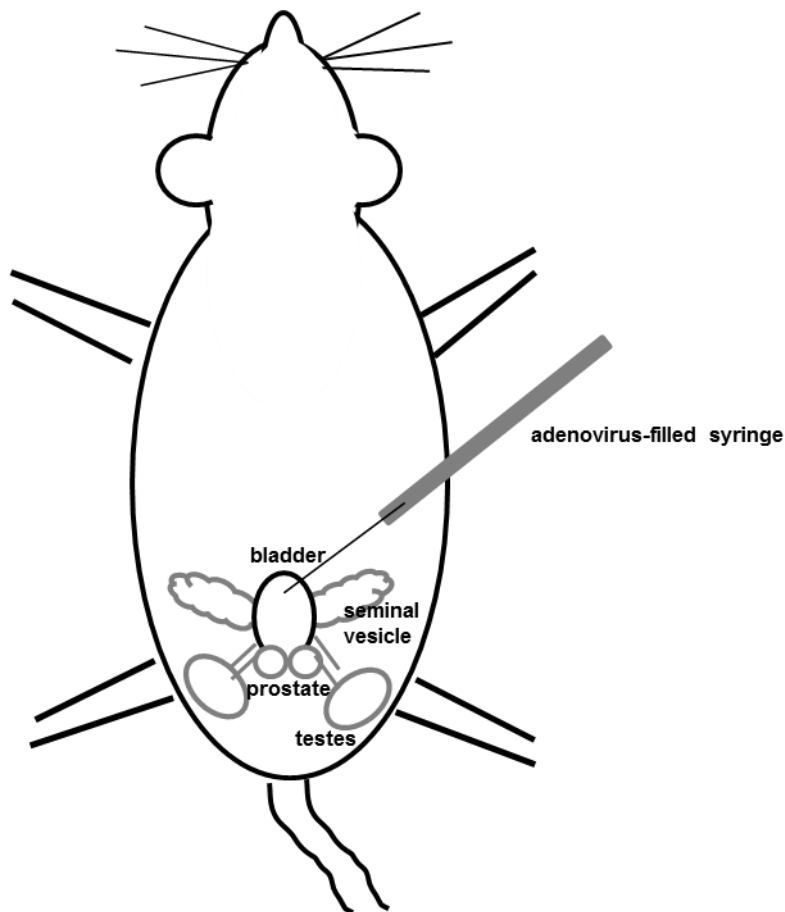


Figure 2-2: Virus injection into mouse bladder

Schematic representation of the urinary tract that is exposed upon laparotomy. Adenovirus is injected into the emptied bladder using a syringe. Adapted from (Seager et al., 2010)

2.6 Live imaging

Prior to live imaging, mice were either anaesthetised (Chapter 2.5.2) or sacrificed before the procedure.

2.6.1 Fluorescent imaging

The abdominal area of mice was shaved using an electric hair trimmer. Mice were scanned by IVIS Spectrum (Perkin Elmer). Filter-pair imaging with epi-illumination was used. mCherry (red channel) was used with excitation wavelength at 587 nm and emission at 610 nm. GFP (green channel) was used with excitation at 465 nm and emission at 520 nm. The field of view was set at 13.3 cm. The focus of subject height was set at 1.5 cm. Auto settings were used for exposure and photo acquisition. Pictures were analysed using Photoshop software (Adobe Photoshop CS2).

2.6.2 Ultrasound scanning

Hair in the abdominal region was removed using depilatory cream (Nair). Ultrasound gel (Henleys Medical, salt-free) was applied to the abdomen, and the animal was tape-secured to a heated (40 C) ultrasound platform. Bladders were then imaged by ultrasound (Vevo 770, Visualsonics Inc., 25MHz transducer) and photos were converted to JPEG format using OsiriX software (OsiriX 5.7 32-bit, Geneva, Switzerland) and analysed using ImageJ software (NIH, Bethesda, USA).

2.7 Tissue harvest and fixation

Bladders were gently emptied of urine and placed in 10% formalin for overnight fixation. Fixed bladders were embedded in paraffin by the Beatson Histology Service with the bladder dome facing up and the trigone down. Alternatively for X-Gal staining, formalin-fixed bladders were transferred into 10%, 20%, and 30% sucrose in PBS, OCT-embedded with the bladder dome facing up and the trigone down, and frozen in liquid nitrogen. Paraffin or OCT-frozen sections were cut starting from the trigone side of the bladder.

2.8 Histology

Haematoxylin and eosin (H&E) and PAS staining (Leica Microsystems staining solutions #3803812 and #03800E) was performed on 4 μm paraffin-embedded sections by the Beatson histology Service (Table 2-7).

X-Gal staining (K1465-01, Invitrogen Life Technologies, UK) was performed on 10 μm formalin-fixed OCT-embedded frozen sections by the Beatson histology Service (Table 2-7).

Table 2-7: Processing methods for histological staining

Embedding	Staining
Paraffin	Haematoxylin and Eosin (H&E)
	Periodic acid Schiff (PAS)
OCT/frozen	X-gal

2.9 Immunohistochemistry

Routine immunohistochemistry was performed by the Beatson histology service (Caspase-3, E-Cadherin, GFP, Ki67, Pten, pAKT, pERK, p21, p63, SMA, β -catenin). Immunofluorescent staining experiments were greatly supported by Despoina Natsiou (University of Glasgow).

The specificity of each antibody has been carefully examined at the outset of the experiments at the Histology Services of the Beatson Institute for Cancer Research and by myself. Ki67, Caspase-3, E-cadherin, pERK, pAKT, p-mTOR, PTEN and p21, are routinely used in the Institute and validated in multiple tissue/cancer types. For pERK we have performed an experiment with p-Erk1/2 antibody (Cell Signaling, #4370; 1:100) together with the Blocking Peptide specific to this antibody (Cell Signaling, #1150; 1:50, as directed by the manufacturer's instructions). CK5, CK18, Uroplakin II and p63 have been

optimised for bladder tissue: positive and negative control slides were added to each experiment as appropriate. As an internal control, we evaluated negative staining in the areas that are not supposed to be stained within the same sections together with the presence of staining in the intended tissue/cellular components.

Slides were dewaxed in xylene for 2x5min, and rehydrated in 100%, 95% and 70% ethanol with a final step in PBS.

To reduce endogenous peroxidase activity, samples were incubated in 0.3% H₂O₂ in distilled water for 20 min.

Antigen retrieval was routinely performed in 0.01M citric acid (pH 6) in a boiling waterbath for 20-30 minutes. For β -catenin immunostaining, retrieval was performed for 50 min. For CK5, CK18 and Uroll immunostaining, retrieval was performed in a pressure cooker inside a microwave with open lid for 15 min and with closed lid for 4 minutes at full power. Slides were then allowed to cool down for 20 min at room temperature. 1M citric acid was made up by 105.07g in 500 ml (no pH adjustment); 5ml of 1M solution were used to make 500ml of 0.01M citric acid to be pH adjusted by NaOH.

To prevent endogenous staining, non-specific sites were blocked with 5% normal goat serum in PBS for 1 hour. Incubation with primary antibody was performed overnight at 4°C (Table 2-8).

Signals were subsequently visualised by chromogenic or fluorescent procedure.

Table 2-8: Primary antibodies

Primary antibody	Company	Catalogue number	Concentration
B-catenin, C19220	BD Transduction Labs	610154	1:1000
Caspase-3, ASP-175	Cell Signaling	9661	1:50
CK5	Abcam	ab24647	1:500
CK18	Progen	61028	1:10
pan-CK, AE1/AE3	Thermo	MS-343	1:100
E-cadherin , Clone-36	BD Transduction Labs	61081	1:300
Fascin	Sigma	HPA005723	1:150
FGFR3, C-15	Santa Cruz	sc-123	1:40
FGFR3, B-9	Santa Cruz	sc-13121	1:300
GFP	Abgent	AM1009a	1:25
Ki67, SP6	Thermo	RM-9106	1:100
Pten	Cell Signaling	9559	1:50
pAKT1/2 (Ser473)	Cell Signaling	4060	1:50
pERK1/2	Cell Signaling	9101	1:100
pmTOR (S2448)	Cell Signaling	2976	1:30
p21, M19	Santa Cruz	sc-471	1:400
p53	Vector Labs	VP-P956	1:150
p63	Santa Cruz	sc-8431	1:1000
RFP	Rockland	600-401-379	1:200
Smooth muscle actin (SMA)	Sigma Aldrich	A-2547	1:25,000
Sox9	Millipore	AB-5535	1:500
Uroll	Santa Cruz	sc15178	1:50
γ H2aX	Cell Signaling	9718	1:50
ZEB1	Novus Biologicals	NBP1-05987	1:100

2.9.1 Chromogenic signals

Biotinylated secondary antibody (Table 2-9) was applied for 2 hours at room temperature, followed by the ABC Elite Standard kit (Vector Labs, PK-6100) for signal enhancement for 1 hour at room temperature. Sections were incubated with 3,3'-Diaminobenzidine (DAB; K3468, Dako) until colour development. Sections were subsequently counterstained with haematoxylin, dehydrated in 100%, 95% and 70% ethanol with a final incubation in xylene for 5 minutes, and mounted with DPX (Distyrene, Plasticizer, Xylene) mounting media.

Table 2-9: Biotinylated secondary antibodies

Biotinylated secondary antibody	Host	Company	Catalogue number	Concentration
Anti-Rabbit IgG	Goat	Vector Labs	BA-1000	1:200
Anti-Rat IgG	Goat	Vector Labs	BA-9401	1:200
Anti-Mouse IgG	Goat	Vector Labs	BA-9200	1:200

2.9.2 Fluorescent signals

Following fluorescent antibody incubation (Table 2-10), sections were incubated with 4',6-diamidino-2-phenylindole (DAPI; 1:1000) and mounted with Vectashield (Vector Labs, H-1000).

Table 2-10: Fluorescent secondary antibodies

Fluorescent secondary antibody	Wave length	Company	Catalogue number	Concentration
Alexa Fluor Goat Anti-Mouse IgG ₁	488 (green)	Invitrogen	A-21121	1:200
Alexa Fluor Goat Anti-Rabbit IgG	594 (red)	Invitrogen	A-11012	1:200

2.9.3 Scanning of slides

Slides were scanned by Nanozoomer slide scanner (Hamamastu) and analysed by SlidePath Digital Image Hub (Leica Biosystems).

2.10 Microscopy

Pictures of chromogenic staining were taken by Axio Imager light microscope (Zeiss A1). Pictures of fluorescent staining were taken by Zeiss upright confocal microscope (Zeiss 710). IHC staining was examined in the minimum of n=3 per genotype.

2.11 Measurements of urothelial thickness

Three representative photos were taken for each H&E stained section at 40x magnification. Urothelial thickness was measured in 25-30 μm intervals at random fashion using ImageJ software (NIH, Bethesda, USA). Each picture contained 20-50 measurements. The mean value of the thickness was initially calculated per sample, and was then subsequently used to determine the mean value per genotype as presented in the results.

2.12 Measurements of urothelial cell size

To determine the cell size, IHC with E-cadherin was performed by the Beatson Histology Service. Measurement of urothelial cell size was performed by Louise King (University of Glasgow).

Three representative photos were taken for each tissue section at 40x magnification. Each cell was marked around the cell membrane and the areas were quantified using ImageJ. The sizes of fifteen cells each layer were measured per layer per sample.

2.13 Human tissue microarray (TMA)

TMA staining of clinical specimen was performed by Dr Tomoko Iwata (University of Glasgow) and the Beatson Histology Service. TMA scoring was performed by Dr Theo van der Kwast (UHN, Toronto, Canada) and Dr Bas van Rhijn (NCI, Amsterdam, Netherlands).

The medical-ethical committee of the University Health Network, Toronto (02-0515-C and 08-0263-T) and the Research Ethics Board (REB), Canada, approved the work with human tissue and to extract clinical data.

66 samples of T1 urothelial tumours of low- and high-grade according to WHO 2004 classification system, and G2 and G3 according to WHO 1973 classification system were subjected to immunohistochemistry for pmTOR and FGFR3 (B9). TMA sections were scored according to the 4 point scale (0=negative, 1=faint, 2=intermediate, 3=strong/intense) and the 2 point scale (0= normal, 1=overexpression).

2.14 Statistics

Statistics were performed using SPSS software (SPSS Statistics Version 19, IBM). For thickness, cell size, proliferation, and apoptosis experiments we used the Kruskal-Wallis test for non-parametric distribution of data in order to define overall significance across multiple categories (genotypes). The Mann-Whitney test was subsequently used to analyse individual significance between the genotypes. For human tissue micro array (TMA) analysis and frequency analysis of histological features in OH-BBN-induced tumours we used Pearson Chi-Square test.

2.15 Cell and tissue culture

2.15.1 Preparation of cell stocks

Cells were harvested at 70-80% confluency, frozen in the specific growth media (Table 2-11) containing 10% DMSO, and stored at -80°C. For reconstitution, cells in cryovials (Starlab, Milton Keynes, UK) were thawed in a 37°C water bath, washed with PBS or growth media, resuspended in Matrigel and subsequently seeded.

2.15.2 Cell counting

Cells were counted using either a haemocytometer (Marienfeld, Neubauer-improved) for absolute numbers or by a cell counter (Roche, Casy Innovatis) for relative cell numbers. For cell counts in the haemocytometer, single cells were mixed 1:1 with Trypan blue. A 10µl aliquot was then applied to the haemocytometer chamber. Cells in the 4 x 16 squares were counted using a light microscope with phase contrast. The number of cells was then calculated by multiplying the total cell number of all 4 squares by the Trypan blue dilution factor (2), which results in the number of cells x 10⁴/ml. For the automated cell counter, cell pellets were resuspended in 5-10ml PBS. 400µl of the suspension was mixed with 19.6ml of Casiton solution (Roche). The automated cell counter displays the number of cells/ml.

2.15.3 Culture of human cell line EJ138

A liquid nitrogen stock of EJ138 at passage 34 was obtained from the Radiation Oncology group, University of Glasgow. EJ138 was maintained in DMEM with 2mM of L-Glutamine, 10% FBS and 1% of Penicillin-Streptomycin without addition of growth factors. Cell culture dishes were incubated at 37°C under 5% CO₂, and the media was changed three times a week. Cells were counted and seeded on Collagen-I matrices (Chapter 2.15.6).

2.15.4 Primary cell culture from mouse bladder

Bladders were harvested and placed in cold PBS until preparation of the culture. To generate single cells, bladders were inverted and the urothelium or tumorous

tissue was scraped off using a scalpel. Cell clumps were manually broken down using a pipette.

After washing with PBS, the cell pellet was incubated for 20-30 min in 1ml TrypLE (Gibco, Invitrogen) containing 10 μ l (0.8 μ g/ml) recombinant DNase I (Roche) and 100 μ l DNase I reaction buffer (Roche). Cells were washed in PBS and filtered through a 70 μ m cell strainer (BD Falcon, 70 μ m yellow). Cells were then used for Matrigel culture or Collagen-I invasion assay.

2.15.5 Matrigel culture and colony formation assay

Single cells were counted and seeded in approximately 25 μ l Matrigel droplets (BD Biosciences, #356231) in 24-well plates and covered with either ADF media (Table 2-11) supplemented with growth factors (Table 2-12).

Cells were resuspended in Matrigel at a known concentration and droplets of the mixture were seeded in 24-well plates. After allowing the Matrigel droplets to solidify for a few minutes at 37°C, 0.5ml of ADF growth media (Table 2-11) supplemented with growth factors (Table 2-12) was added per well. Plates were incubated at 37°C under 5% CO₂, and the media was changed three times a week.

Colonies were counted using a light microscope with phase contrast at 10x magnification.

To passage the cells, colonies in the Matrigel were resuspended into single cells using a 1000 μ l pipette tip; cells were washed 2-3 times with PBS, counted and re-seeded.

2.15.6 Collagen-I invasion assay

Invasion into an organotypic matrix containing human fibroblasts from skin explants and Collagen-I from rat tails has been described previously (Timpson et al., 2011).

Single cells at a known concentration in 1ml DMEM media were seeded onto Collagen-I matrices containing either normal human fibroblasts (NHF) (Timpson et al., 2011) or telomerase-immortalised fibroblasts (red TIFF) (Munro et al., 2001). Cells were allowed to attach to the matrix for 3-4 days.

Matrices were then transferred onto grids with an air-media interface. Cells were allowed to invade for 14 days with DMEM media being changed every other day. Matrices were cut in halves and fixed in 4% PFA overnight. H&E staining as well as immunohistochemistry was performed on 4 µm-thick paraffin-embedded sections.

2.15.7 Organotypic slice culture

Organotypic slice culture of the bladder was performed as previously described (Batourina et al., 2012).

Bladders or bladder tumours were cut into 2-3mm slices using dissecting scissors (Straight 7mm blades, Coherent Vannas #500086) under a dissection microscope. Duplicate slices were placed with the urothelium facing down on membrane culture inserts (Millipore #PICMORG50) in glass bottom dishes (In Vitro Scientific #D35-20-1-N) containing basal conditional media (Table 2-11) supplemented with recombinant rat glial cell line-derived neurotrophic factor (rGDNF), human hepatocyte growth factor (hHGF), and human keratinocyte growth factor (hKGF, also known as FGF7) (Table 2-12). Explants were covered with a drop of sterile mineral oil (Sigma-Aldrich # M5904).

Cultures were maintained at 37°C with 5% CO₂ concentration. Basal conditional medium was changed three times a week.

2.15.8 Tamoxifen induction of organotypic slice culture

Organotypic slice cultures were induced by addition of 1 μ M 4-Hydroxytamoxifen solution or for controls using 1.2 μ l 100% ethanol. 5mg of 4-OH-Tamoxifen powder (Sigma, H7904-25mg) was resuspended in 2.5ml 100% ethanol to produce a 5mM stock solution. 1 μ l of the 4-OH-Tamoxifen stock solution was added per 10ml media. The organotypic slices were then incubated at 37°C in 5% CO₂ atmosphere for 20hrs before the culturing media was changed and new growth factors were added.

2.15.9 R3Mab treatment of organotypic slice culture

Organotypic slice explants were subjected to 10nM R3Mab (Genentech, MFGR1877s) or 10nM control antibody (Genentech, gD 5237) every other day for 4 days in basal conditional media. Slices were placed in 4% PFA overnight, paraffin-embedded and processed for histological staining.

Table 2-11: Media components

Media	Components	Company and cat no	Stock conc.	Final conc	Volume to add
DMEM (500ml)	Dulbecco's Modified Eagles Medium (DMEM)	Gibco Invitrogen, #11995-073	100%	88%	440ml
	L-Glutamine	Gibco Invitrogen, #25030-081	200mM	2mM	5ml
	Foetal Bovine Serum (FBS)	Sigma, #A9647	100%	10%	50ml
	Penicillin-Streptomycin	Gibco Invitrogen, #215140-148	100%	1%	5ml
ADF (50ml)	Advanced DMEM/F12 (ADF)	Gibco Invitrogen, #12634-028	100%	76%	46.5ml
	Foetal Bovine Serum (FBS)	Sigma, #A9647	100%	0.1%	0.5ml
	L-Glutamine	Gibco Invitrogen, #25030-081	200mM	2mM	0.5ml
	HEPES	Gibco Invitrogen, #15630-056	1M	10mM	0.5ml
	Penicillin-Streptomycin	Gibco Invitrogen, #215140-148	100%	1%	0.5ml
	N2	Gibco Invitrogen, #17502-048	100%	1%	0.5ml
	B27	Gibco Invitrogen, #12587-010	100%	2%	1ml
Basal conditional (50ml)	Dulbecco's Modified Eagles Medium (DMEM)	Gibco Invitrogen, #11995-073	100%	79%	42ml
	L-Glutamine	Gibco Invitrogen, #25030-081	200mM	4mM	1ml
	Foetal Bovine Serum (FBS)	Sigma, #A9647	100%	10%	5ml
	Insulin-Transferrin-Selenite (ITS)	Gibco Invitrogen, #51300-044	100%	1% ~5ug/ml	0.5ml
	Penicillin-Streptomycin	Gibco Invitrogen, #215140-148	100%	1%	0.5ml
	All-trans Retinoic acid (RA)	Sigma-Aldrich, #R2625-50MG	10mM	0.2uM	1ml

Table 2-12: Growth factors

Media	Growth factors	Company and cat no	Stock conc.	Final conc	Dilution
ADF	hKGF/FGF7	Peprotech, #100-19-B	1ug/ml	20ng/ml	1:50
	hFGF16	Peprotech, #100-29-A	1ug/ml	20ng/ml	1:50
	mShh	Peprotech, #315-22-A	1ug/ml	50ng/ml	1:20
	hTGF- α	Peprotech, #100-16-A	1ug/ml	25ng/ml	1:40
	hEGF	Peprotech, #AF-100-15	1ug/ml	50ng/ml	1:20
Basal conditional	rGDNF	RD Systems, #512-GF	100ug/ml	100ng/ml	1:1000
	hHGF	RD Systems, #294-HGN	50ug/ml	100ng/ml	1:500
	hKGF/FGF7	Peprotech, #100-19-B	100ug/ml	100ng/ml	1:1000

Chapter 3

The role of FGFR3 in non-invasive bladder cancer

3.1 Introduction

In order to study the functional role of FGFR3 activation in bladder tumourigenesis, we have previously generated a mouse model in which *Fgfr3* *K644E*, a constitutively active form of FGFR3 (Iwata et al., 2000), is conditionally expressed in the urothelium by placing Cre recombinase expression under the Uroplakin II (UroII) promoter (*UroII*Cre *Fgfr3*^{+/K644E}) (Ahmad et al., 2011c). These mice did not develop bladder cancer at 18 months, suggesting that cooperating mutations are required for FGFR3 to drive tumourigenesis in the bladder. In the same study in combination with *K-Ras* or *B-Catenin*, *Fgfr3* activation caused tumours in the skin and in the lungs, respectively, suggesting that FGFR3 is able to induce tumourigenesis in the presence of cooperating mutations (*UroII*Cre *Fgfr3*^{+/K644E}*Kras*^{+/G12D} and *UroII*Cre *Fgfr3*^{+/K644E} β -*catenin*^{+/exon3}). It was observed that the PI3K/AKT pathway was highly upregulated in these lung tumours, while it remained unchanged in the bladder of mice with the same genotype (Ahmad et al., 2011c). This could indicate that increased PI3K/AKT signalling may be required for tumour formation in the bladder.

In human bladder tumours, mutations in *FGFR3* and PI3K/AKT pathway genes and their activation are strongly co-associated (Lopez-Knowles et al., 2006, Kompier et al., 2010, Duenas et al., 2013). A catalytic subunit of PI3K, *PIK3CA*, is frequently mutated in non-invasive urothelial cell carcinoma, leading to a significant proliferative advantage through increased lipid kinase activity and constitutive AKT activation (Lopez-Knowles et al., 2006, Askham et al., 2010, Ross et al., 2013). FGFR3 signalling can activate the PI3K/AKT pathway by phosphorylated GRB2/GAB1 interaction with PI3K (Hart et al., 2001).

The PI3K/AKT pathway is involved in a range of cellular processes such as proliferation, apoptosis, survival and migration by controlling the expression of a range of proteins including Bcl-2-associated X (Bax), nuclear factor kappa-light-chain-enhancer of activated B cells (NF- κ B), mouse double minute 2 homolog (MDM2) and mammalian target of rapamycin (mTOR) (Fresno Vara et al., 2004). mTOR has been shown to be a candidate for effective therapeutic targeting (Ahmad et al., 2011a, Puzio-Kuter et al., 2009). Furthermore, PI3K/AKT signalling increases the expression of cell-cycle regulating genes such as p21 by suppressing GSK3B and activating mTOR (Yohn et al., 2011). p21 was previously

shown to be up-regulated in the mouse urothelium in which *Pten* is deleted (Yoo et al., 2006).

In this chapter we aimed to test the synergistic effects of FGFR3 and PI3K-AKT signalling activation. At the time of planning and initiating the experiments, a mouse model with activating *Pi3k* mutation was unavailable. Therefore we used a mouse line with *Pten* deletion as an experimental tool to assess the effects of PI3K-AKT activation in the presence of *Fgfr3* mutation in the urothelium.

3.2 Establishment of the *UroIIcre Fgfr3^{+ /K644E} Pten^{flox/flox}* mouse model

3.2.1 Generation of the cohorts

We generated cohorts of *UroIIcre Fgfr3^{+ /K644E}* (n=25), *UroIIcre Pten^{flox/flox}* (n=20) and *UroIIcre Fgfr3^{+ /K644E} Pten^{flox/flox}* (n=24) and examined bladders at 5-18 months (Table 3-1). Some animals were euthanised due to causes unrelated to changes in the bladder, including infection or lymphoma. Mice were also sacrificed due to skin rash on the back owing to UroIIcre recombination in the epidermis (Ahmad et al., 2011c).

The term “Control” used throughout Chapter 3, as opposed to “Wild type” in other chapters refers to mice of C57Bl/6 (n=7) and mice with presence of T2/Onc3 (n=4), which does not lead to any abnormal bladder phenotype by itself.

Table 3-1: Summary of mouse cohorts with *Fgfr3* and *Pten* mutation

Genotype	n	Age at time of analysis	Non-bladder related deaths	Increased urothelial thickness	Cellular abnormalities
<i>Control</i>	11	10-18 months	None	None	None
<i>UroIIcre Fgfr3^{+ /K644E}</i>	25	5-15 months	n=2 (8%)	None	None
<i>UroIIcre Pten^{flox/flox}</i>	20	9-18 months	n=4 (20%)	n=12 (60%)	None
<i>UroIIcre Fgfr3^{+ /K644E} Pten^{flox/flox}</i>	24	11-18 months	n=4 (17%)	n=20 (83%)	n=20 (83%)
<i>UroIIcre Fgfr3^{K644E /K644E} Pten^{flox/flox}</i>	3	10-12 months	None	n=2 (66%)	n=2 (66%)

3.2.2 FGFR3 and PTEN protein expression

Protein levels of the targeted genes were assessed by immunohistochemistry in n=3 samples per genotype (Figure 3-1). We detected similar levels and patterns of FGFR3 protein expression in the urothelium of *Control* (A) and *Uro11Cre Fgfr3^{+ /K644E}* (C) as we have reported previously (Ahmad et al., 2011c). FGFR3 levels were also similar in *Uro11Cre Pten^{flox/flox}* (E) and *Uro11Cre Fgfr3^{+ /K644E} Pten^{flox/flox}* (G), indicating that FGFR3 expression was neither influenced by *Fgfr3* mutation nor deletion of *Pten*.

Levels of PTEN protein were similarly low in *Control* (B) and *Uro11Cre Fgfr3^{+ /K644E}* (D), indicating that PTEN expression is unaltered in the presence of *Fgfr3 K644E* mutation. Knockdown of *Pten* expression in the urothelium of *Uro11Cre Pten^{flox/flox}* was considered as successful (F).

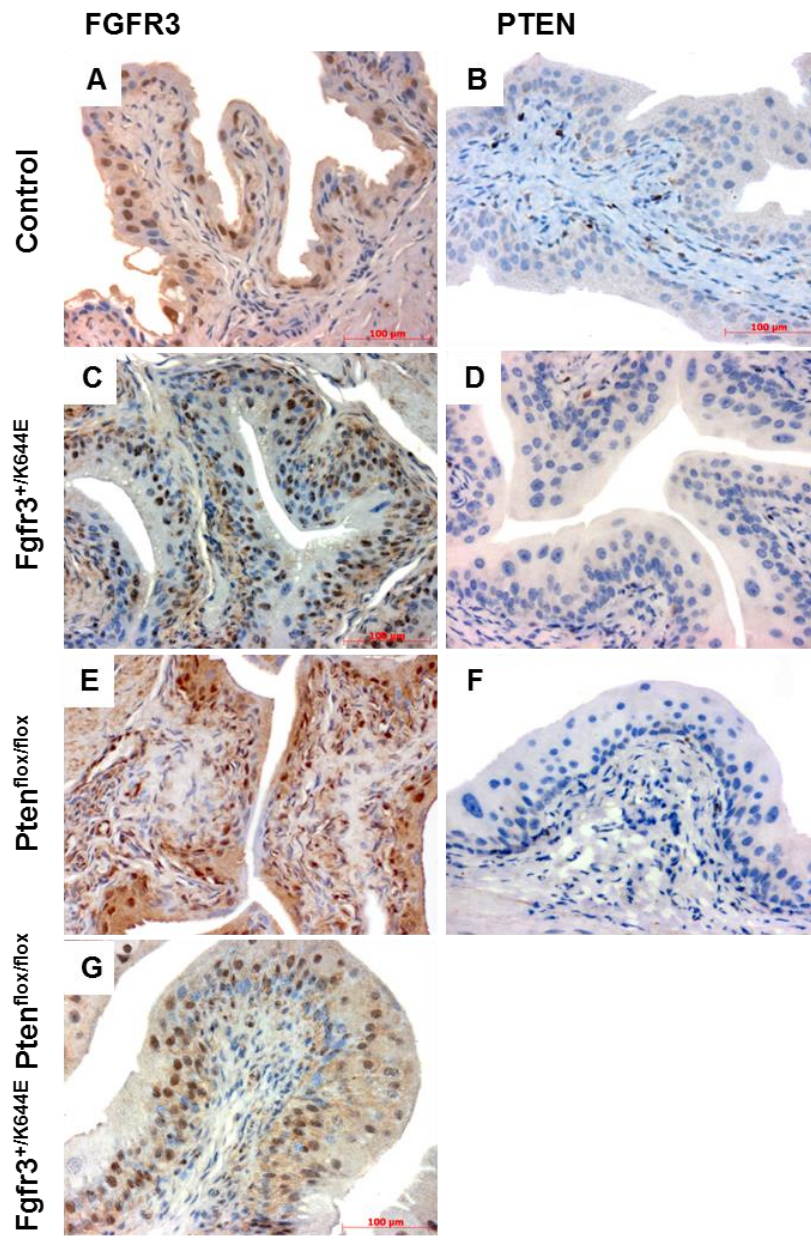


Figure 3-1: FGFR3 and PTEN expression in the *Uro11Cre Fgfr3*^{+/K644E} *Pten*^{flox/flox} urothelium
 Immunohistochemistry for FGFR3 in bladders of Control (A), *Uro11Cre Fgfr3*^{+/K644E} (C), *Uro11Cre Pten*^{flox/flox} (E) and *Uro11Cre Fgfr3*^{+/K644E} *Pten*^{flox/flox} (G). Immunohistochemistry for PTEN in bladders of Control (B), *Uro11Cre Fgfr3*^{+/K644E} (D), and *Uro11Cre Pten*^{flox/flox} (F). Scale bar represents 100 µm (A-G).

3.2.3 Recombination under the UroIICre promoter

Cre-dependent recombination in the urothelium under the UroII promoter was assessed by X-gal staining and GFP expression using Z/EG reporter mice (Figure 3-2).

In the presence of the *UroIICre* allele, cells with a GFP-positive nucleus were observed in the majority of umbrella and intermediate cells, whereas basal cells showed fewer cells with GFP-positivity (A). Successful recombination was confirmed with only little X-gal staining remaining in some of the umbrella cells of the urothelium in *UroIICre Z/EG* (B), which is most likely an artefact since similar staining is seen in *Z/EG* (C).

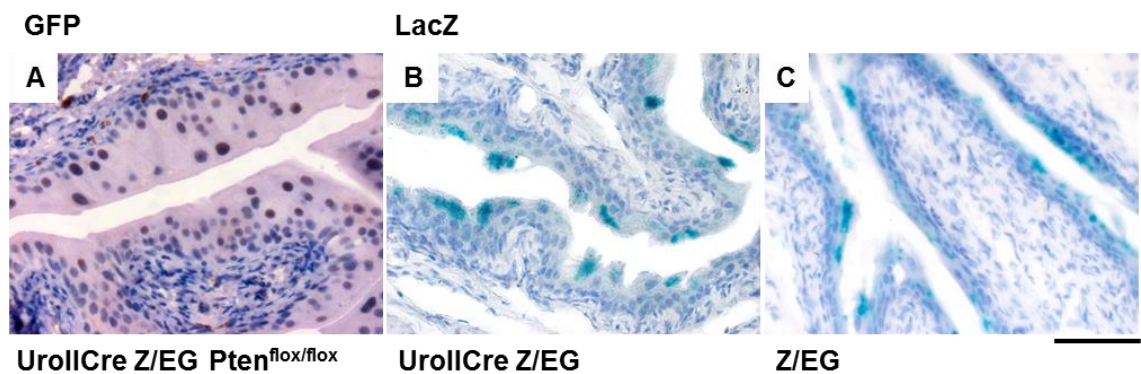


Figure 3-2: Recombination in the urothelium under UroIICre

Paraffin sections of *UroIICre Z/EG Pten^{flox/flox}* stained by GFP (A). Frozen sections of *UroIICre Z/EG* (B) and *Z/EG* only (C) with X-gal staining. Scale bar represents 100 μ m (A-C).

3.3 Increased thickness of the *Uro11Cre Fgfr3^{+ /K644E} Pten^{flox/flox}* urothelium

To see the effect of *Pten* deletion together with *Fgfr3* mutation in the urothelium, we analysed H&E-stained sections of *Wild type* (Control), *Uro11Cre Fgfr3^{+ /K644E}*, *Uro11Cre Pten^{flox/flox}*, and *Uro11Cre Fgfr3^{+ /K644E} Pten^{flox/flox}* (Figure 3-3).

The *Uro11Cre Fgfr3^{+ /K644E}* urothelium (n=25) (b, f) appeared similar to that of *Control* (n=11) (a, e) in regards to the morphology of the three layers, namely umbrella, intermediate and basal cells (e, *insert*). A mild increase in urothelial thickness was observed in *Uro11Cre Pten^{flox/flox}* (n=12 out of 20, 60%) (c, g). Furthermore, we observed a severe increase in thickness in the urothelium of *Uro11Cre Fgfr3^{+ /K644E} Pten^{flox/flox}* bladders (n=20 out of 24, 83%) (d, h) compared to *Control*.

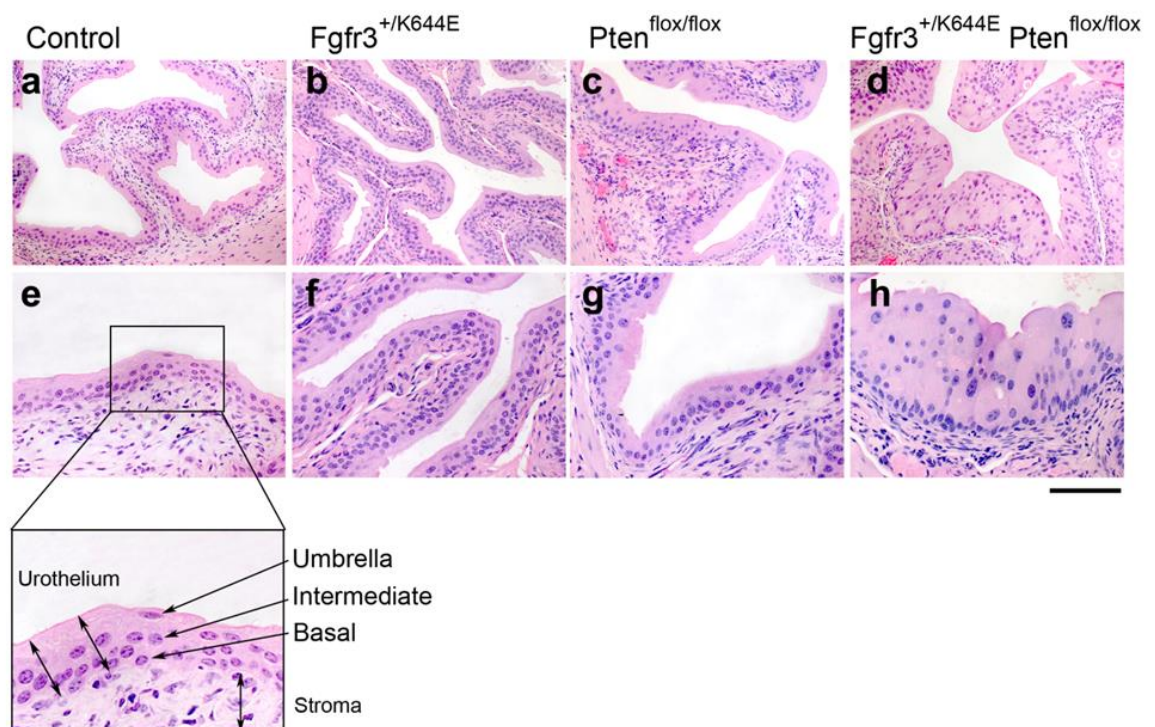


Figure 3-3: Increased thickness of the *Uro11Cre Fgfr3^{+ /K644E} Pten^{flox/flox}* urothelium by H&E
 Representative H&E sections of *Control* (a, e), *Uro11Cre Fgfr3^{+ /K644E}* (b, f), *Uro11Cre Pten^{flox/flox}* (c, g), and *Uro11Cre Fgfr3^{+ /K644E} Pten^{flox/flox}* (d, h) at low (a-d) and high magnification (e-h). Scale bar represents 200 μ m in panel a-d and 100 μ m in panel e-h.

We have quantified the changes in urothelial thickness in mice aged to 11-18 months. Consistent with our previous observations (Ahmad et al., 2011c, Ahmad et al., 2011a), we found no significant difference in urothelial thickness between *UroIIcre Fgfr3^{+ /K644E}* and *Control*, or between *UroIIcre Pten^{flox/flox}* and *Control* (Figure 3-4). There was no significant difference when *UroIIcre Fgfr3^{+ /K644E}* and *UroIIcre Pten^{flox/flox}* were compared. However, urothelial thickness was significantly increased when both mutations were present in *UroIIcre Fgfr3^{+ /K644E} Pten^{flox/flox}* (n=13) compared to either *UroIIcre Fgfr3^{+ /K644E}* (n=9) (p=0.00005, Mann-Whitney test) and *UroIIcre Pten^{flox/flox}* (n=7) (p=0.00049), suggesting that this increase is owing to the cooperation of *Fgfr3* and *Pten* mutation.

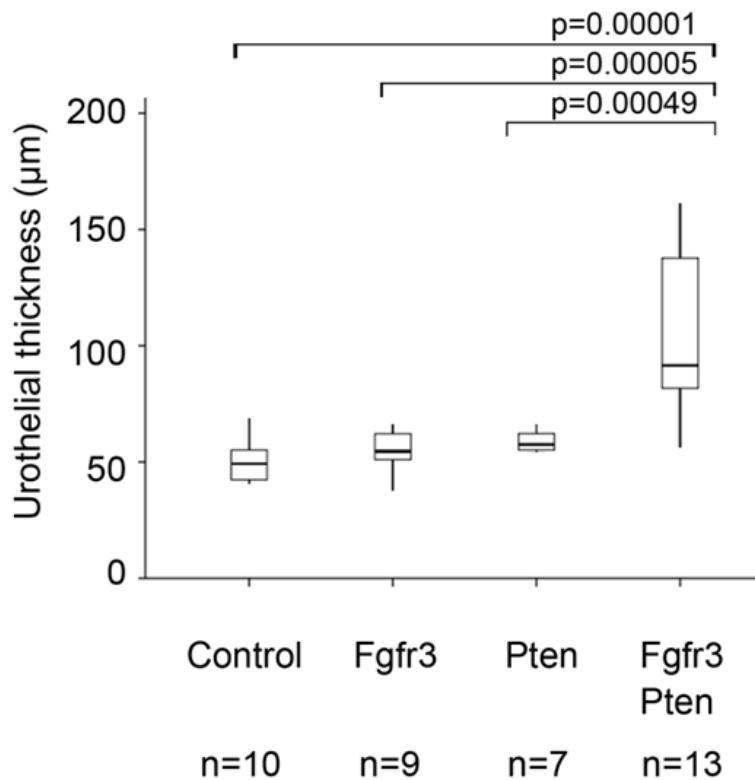


Figure 3-4: Quantification of thickness in *UroIIcre Fgfr3^{+ /K644E} Pten^{flox/flox}* urothelium
 Thickness of the urothelium in *Control*, *UroIIcre Fgfr3^{+ /K644E}* (Fgfr3), *UroIIcre Pten^{flox/flox}* (Pten) and *UroIIcre Fgfr3^{+ /K644E} Pten^{flox/flox}* (Fgfr3 Pten).

We have also analysed the effect of homozygous mutation in *Fgfr3* (*UroIIcre Fgfr3^{K644E/K644E}*) (Figure 3-5). The urothelium of *UroIIcre Fgfr3^{K644E/K644E}* mice indeed showed thickening (n=11 out of 12) (A, B). Furthermore, mice with double homozygous mutations in *Fgfr3* and *Pten* (*UroIIcre Fgfr3^{K644E/K644E} Pten^{flox/flox}*) revealed a similar phenotype to that of *UroIIcre Fgfr3^{K644E/K644E}* *Pten^{flox/flox}* (n=2 out of 3) (C, D).

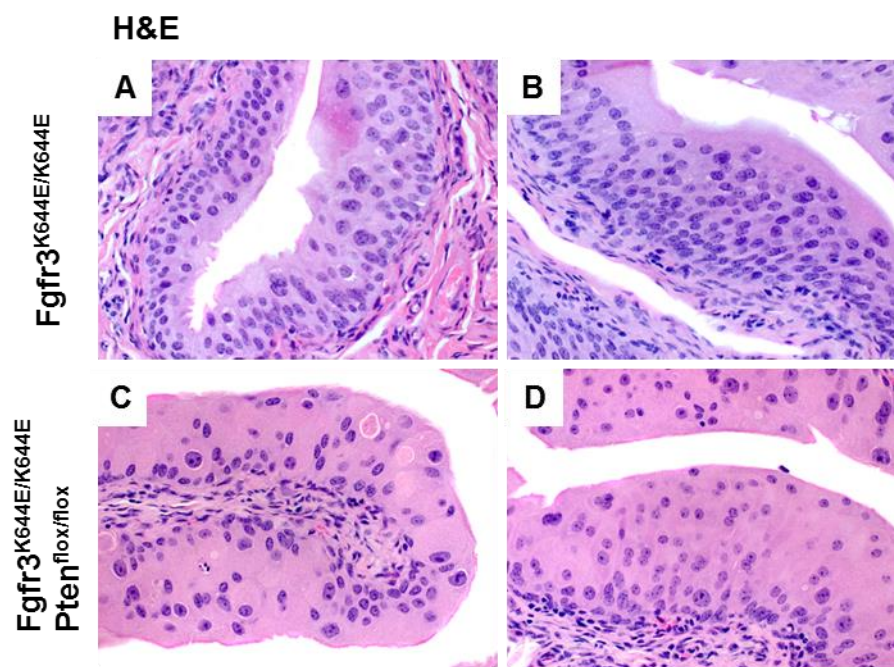


Figure 3-5: Thickening of the urothelium in *UroIIcre Fgfr3^{K644E/K644E}* and *UroIIcre Fgfr3^{K644E/K644E} Pten^{flox/flox}*
 Representative H&E sections of bladders of *UroIIcre Fgfr3^{K644E/K644E}* (A, B) and *UroIIcre Fgfr3^{K644E/K644E} Pten^{flox/flox}* (C, D). Scale bar represents 100 μ m (A-D).

3.4 Abnormal morphology of *UroIIcre Fgfr3^{+ /K644E} Pten^{flox/flox}* urothelium

Next we examined the appearance of the urothelia more closely (Figure 3-6).

In addition to increased urothelial thickness, several abnormal features in cellular morphology were observed in *UroIIcre Fgfr3^{+ /K644E} Pten^{flox/flox}*, including vacuolisation (arrow in c), condensed cellular appearance (circled in e), enlargement of cells and nuclei (arrow heads in e, f), and loss of orientation (mis-localisation of umbrella, intermediate and basal cells).

High glycogen levels were detected in vacuoles observed in *UroIIcre Fgfr3^{+ /K644E} Pten^{flox/flox}* by Periodic acid-Schiff (PAS) staining (n=3) (g).

At least one of these cellular features were observed in the majority of *UroIIcre Fgfr3^{+ /K644E} Pten^{flox/flox}* bladders (n=20, 83%), while none of these abnormal features were present in *Control* (n=11) (a, d), *UroIIcre Fgfr3^{+ /K644E}* (n=25) or *UroIIcre Pten^{flox/flox}* urothelium (n=20).

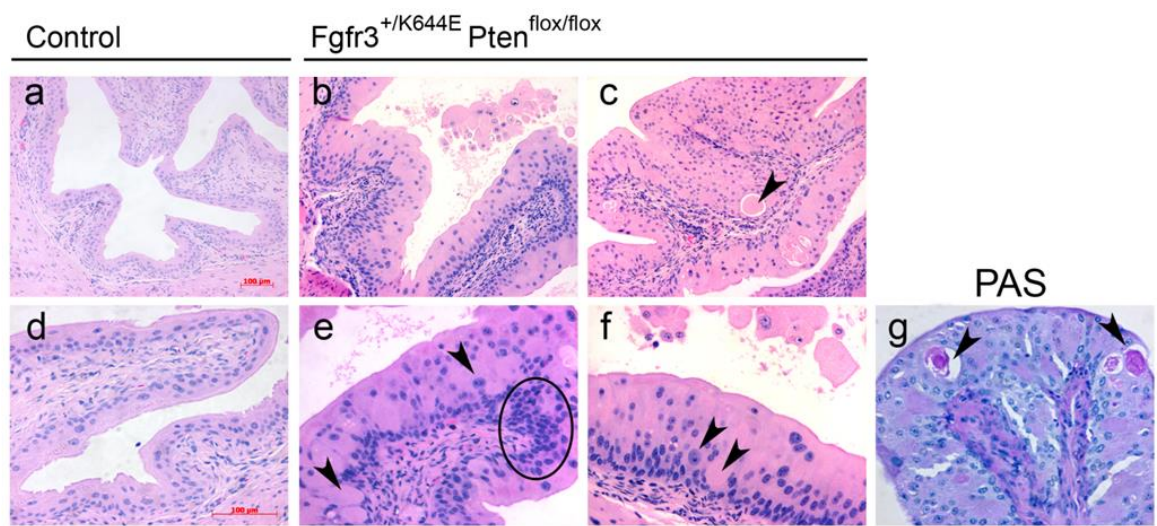


Figure 3-6: Abnormal morphology of the *UroIIcre Fgfr3^{+ /K644E} Pten^{flox/flox}* urothelium
 Representative H&E sections of *Control* (a, d) and *UroIIcre Fgfr3^{+ /K644E} Pten^{flox/flox}* (b, c, e, f). Scale bar represents 200 μ m in panel a-c and 100 μ m in d-g.

3.5 Differential expression of layer-specific markers

In order to see whether the abnormal phenotype is caused by a change in urothelial cell identities, the bladders were stained with urothelial markers well-established in mice (Figure 3-7).

UroplakinII (UroII) is a marker for umbrella and some intermediate cells (Kong, 2004), while Cytokeratin 5 (CK5) is expressed in basal cells of the normal urothelium (Shin et al., 2011, Castillo-Martin et al., 2010) (a, b).

However, in the *UroII*Cre *Fgfr3*^{+/*K644E*} *Pten*^{flox/flox} urothelium, UroII-positive cells were present in deeper layers close to the submucosa, while CK5 expression was absent in some parts of the innermost layers of the urothelium, showing an inverse expression pattern (e, f, i, j).

Furthermore, p63, which is normally present in the nuclei of basal and intermediate cells (Castillo-Martin et al., 2010) (c), showed a disorganised expression pattern (g, k).

Double staining of CK18, an alternative marker of umbrella cells in mice (Castillo-Martin et al., 2010), together with CK5 clearly showed the abnormal localisation of CK18-positive cells deep in the urothelium of *UroII*Cre *Fgfr3*^{+/*K644E*} *Pten*^{flox/flox} (h, l), indicating abnormal differentiation of urothelial cells in *UroII*Cre *Fgfr3*^{+/*K644E*} *Pten*^{flox/flox}.

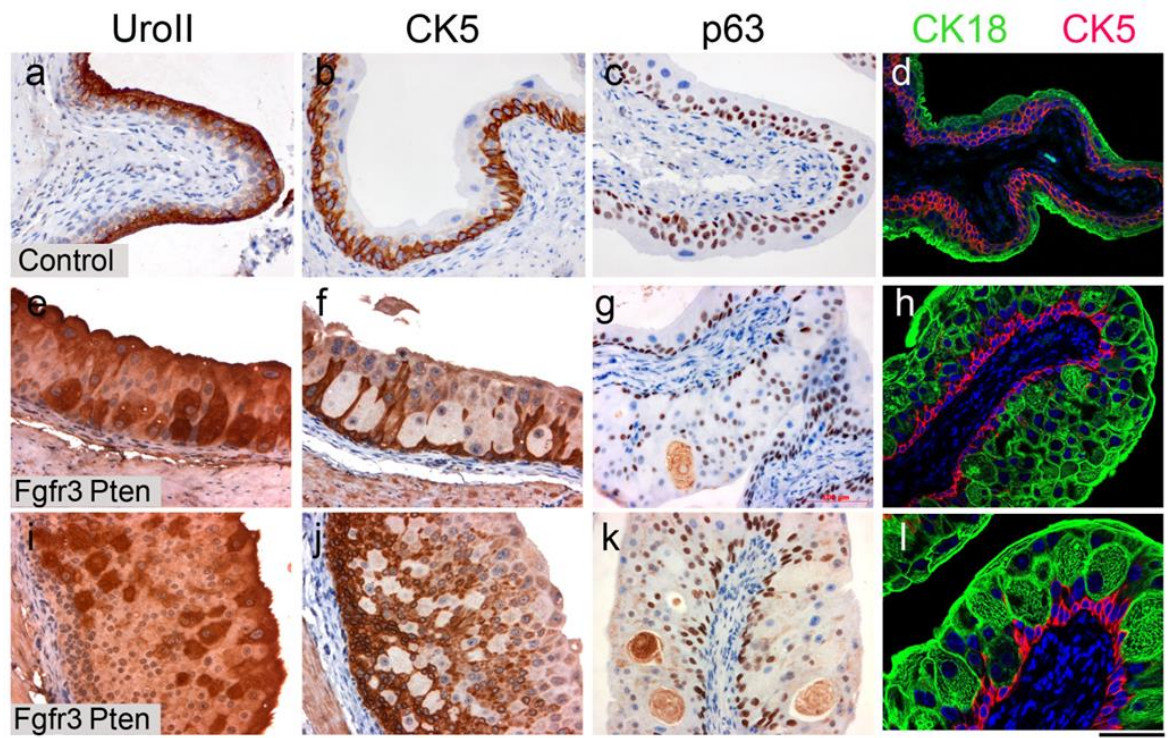


Figure 3-7: Abnormal cellular identity in the *Uro11Cre Fgfr3^{+/K644E} Pten^{flox/flox}* urothelium
 Immunohistochemistry for UroplakinII (a, e, i), CK5 (b, f, j and d, h, l), p63 (c, g, k), CK18 (d, h, l), and double staining with CK18 (green) and CK5 (red) (d, h, l) in *Control* (a-d) and *Uro11Cre Fgfr3^{+/K644E} Pten^{flox/flox}* bladders (e-l). Scale bar represents 200 μ m in a-d and 100 μ m in e-l.

3.6 Increase in the size of intermediate cells in *UroIICre Fgfr3^{+ /K644E} Pten^{flox/flox}* urothelium

The increase in the urothelial thickness can be caused by deregulation of cell size and/or cell number.

We first addressed whether these were due to changes in cell size, and if so, whether the cell size change was seen in specific urothelial cell populations (Figure 3-8). An example of E-cadherin staining is shown in *UroIICre Fgfr3^{+ /K644E} Pten^{flox/flox}* bladder (a), in which cells are lined in red for the measurement of surface area.

No significant difference in cell size was observed in the innermost basal and outermost umbrella layers among the cohorts (b, d). In contrast, in the intermediate layer (between the inner and outermost layers), while *Fgfr3* mutation alone did not influence the cell size (*UroIICre Fgfr3^{+ /K644E}*, n=5), *Pten* mutation alone (*UroIICre Pten^{flox/flox}*, n=6) increased the cell size compared to *Control* (n=5, p=0.017, Mann-Whitney test) (c). Furthermore, the presence of both *Fgfr3* and *Pten* mutations (*UroIICre Fgfr3^{+ /K644E} Pten^{flox/flox}* urothelia, n=10) further increased the cell size comparing to *Fgfr3* mutation alone (p=0.001), as well as to *Pten* alone (p=0.016), suggesting that the *Fgfr3* mutation cooperates with the *Pten* loss to further increase the cell size.

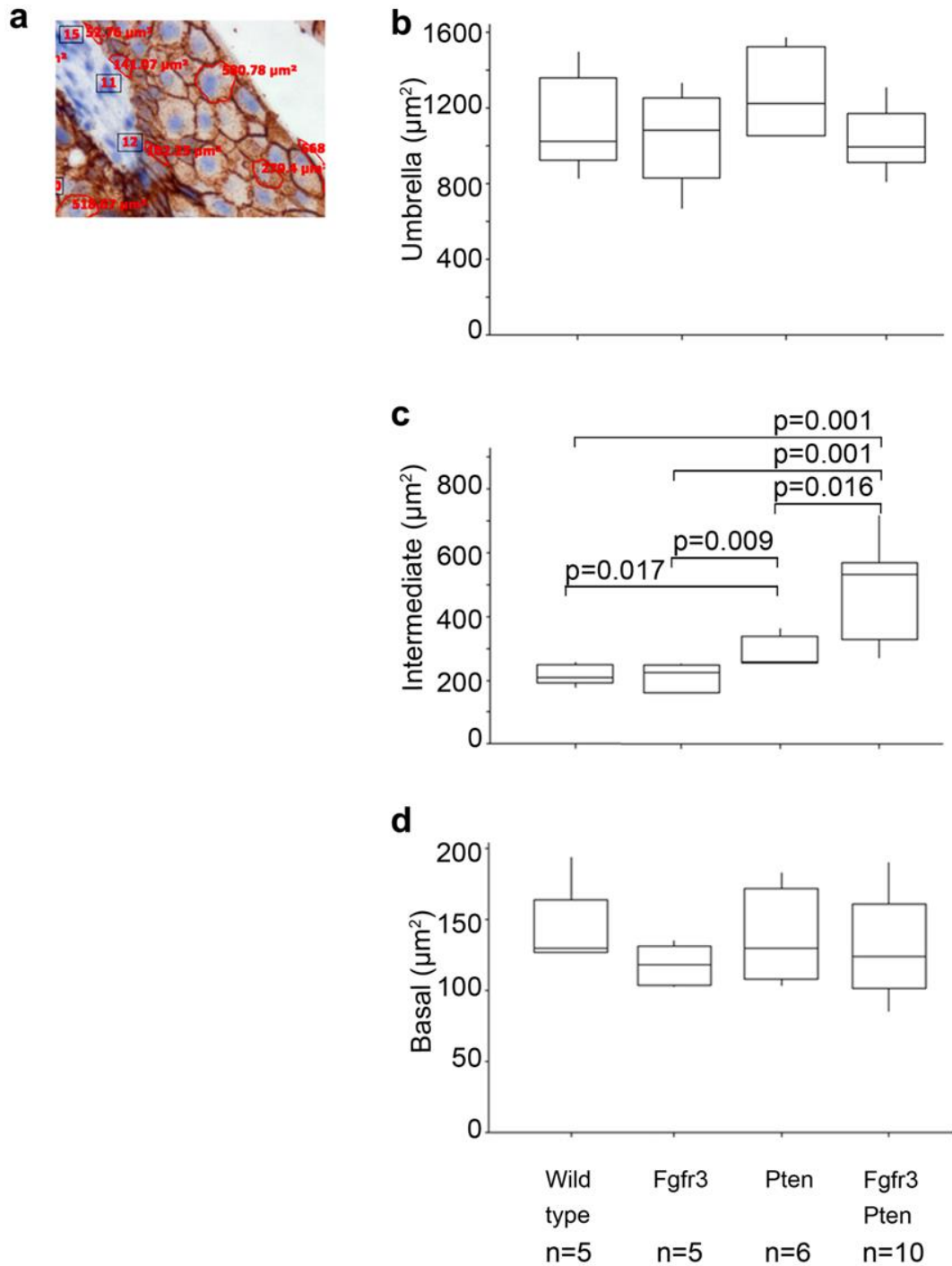


Figure 3-8: Differential effects of *Fgfr3* and *Pten* mutations in regulation of cell size in the urothelium

Example of cell surface measurement on E-cadherin-stained section (a). The sizes of umbrella (b), intermediate (c) and basal cells (d) among the different genotypes.

3.7 Increased proliferation in *UroIICre Fgfr3^{+ /K644E} Pten^{flox/flox}* urothelium

Next we examined the proliferation in the urothelium by Ki67 immunohistochemistry (Figure 3-9). Albeit in a relatively small number of cells, Ki67 positivity was identified in all layers of the urothelium, including umbrella cells (a) (Castillo-Martin et al., 2010).

Taken all layers together, a significant increase in Ki67-positive cells was seen in the presence of both *Fgfr3* and *Pten* mutation (*UroIICre Fgfr3^{+ /K644E} Pten^{flox/flox}*, n=9, p=0.004), as well as in the presence of *Pten* mutation only (*UroIICre Pten^{flox/flox}*, n=6, p=0.009, Mann-Whitney test), compared to *Fgfr3* mutation only (*UroIICre Fgfr3^{+ /K644E}*, n=5) (c). This indicates that cell proliferation was increased due to *Pten* loss.

Similar effects were observed in the outermost umbrella and intermediate layer (d, e), while no significant changes were seen in the innermost basal layer (f).

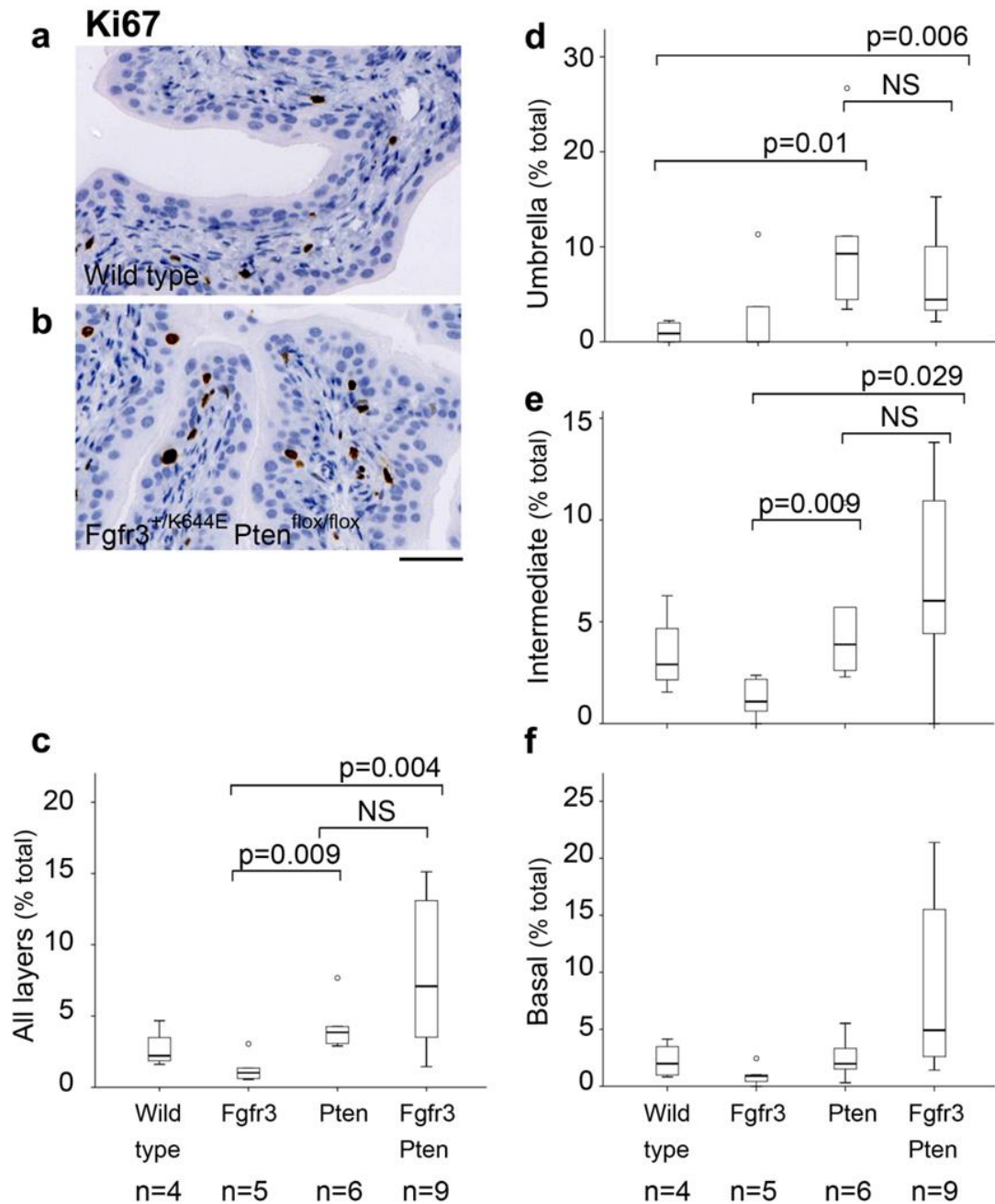


Figure 3-9: Differential effects of *Fgfr3* and *Pten* mutations in regulation of proliferation in the urothelium

Ki67 -stained sections of Wild type (a) and *UroIIICre Fgfr3^{+/K644E} Pten^{flox/flox}* (b). Proliferation in all layers (c), umbrella (d), intermediate (e) and basal cells (f) among the different genotypes. Scale bar represents 100 μ m in panel a-b.

3.8 Increased apoptosis in the *Uro11Cre Fgfr3^{+K644E}* urothelium

We have also examined apoptotic events (Figure 3-10). Very few apoptotic events were observed in the urothelium of all cohorts including *Control* (a) and *Uro11Cre Fgfr3^{+K644E} Pten^{flox/flox}* urothelium (b).

Overall, apoptosis was significantly increased when both *Fgfr3* and *Pten* mutations were present (*Uro11Cre Fgfr3^{+K644E} Pten^{flox/flox}*, n=10) or *Fgfr3* mutation alone (*Uro11Cre Fgfr3^{+K644E}*, n=5) compared to *Uro11Cre Pten^{flox/flox}* (p=0.004 and 0.032, respectively, Mann-Whitney test) (c). As there was no additional increase with both mutations together comparing to *Fgfr3* mutation alone, the increase in the apoptosis is likely to be owing to the *Fgfr3* mutation. Similar effects were observed in the outermost umbrella and intermediate cell layers (d, e).

In contrast, in the innermost basal cell layer, apoptotic events were increased when *Pten* mutation was present (*Uro11Cre Pten^{flox/flox}*, n=5) (f). However, the overall small number of apoptotic cells in the basal layer made the interpretation of results difficult.

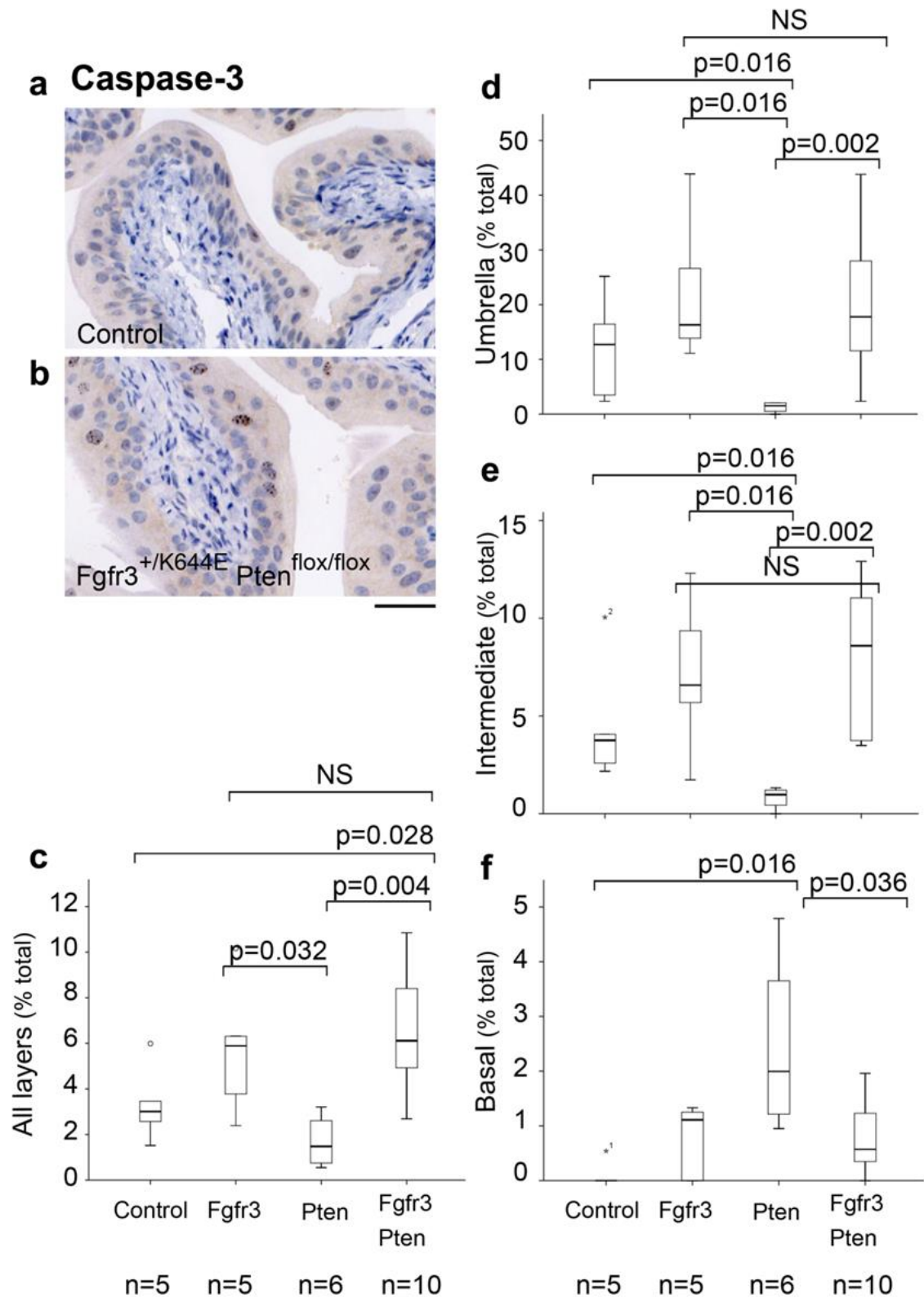


Figure 3-10: Increased apoptosis in the *UroIIcre Fgfr3*^{+/K644E} *Pten*^{flox/flox} urothelium
 Caspase-3-stained sections of Wild type (a) and *UroIIcre Fgfr3*^{+/K644E} *Pten*^{flox/flox} (b). Apoptosis in all layers (c), umbrella (d), intermediate (e) and basal cells (f) among the different genotypes. Scale bar represents 100 μ m in panel a-b.

3.9 Changes in MAPK/AKT signalling and cell cycle regulation

To examine underlying mechanisms leading to the observed phenotype, we addressed how *Fgfr3* and *Pten* mutations altered their downstream signalling cascades. The activation of MAPK and PI3K-AKT pathways were characterised in the bladder using antibodies that recognise the phosphorylated forms of ERK1/2 (pERK1/2) and AKT (Ser473) (pAKT), respectively (Figure 3-11).

In *Controls*, phosphorylated ERK1/2 (pERK1/2) was observed in a cell-specific fashion in the urothelium, however not limited to a particular layer (n=9) (a). Staining was similar in *UroIIcre Fgfr3^{+ /K644E}* (n=9) and *UroIIcre Pten^{fllox/fllox}* (n=9) (d, g). In contrast, in *UroIIcre Fgfr3^{+ /K644E} Pten^{fllox/fllox}* samples (n=9/12, 75%) pERK1/2 was seen in all layers in a cell-specific fashion (j), which resembles the overall pattern of UroII and CK5 staining (Figure 3-7).

Phosphorylated AKT (Ser473) (pAKT) was absent in *Control* (n=3), *UroIIcre Fgfr3^{+ /K644E}* (n=6) and *UroIIcre Pten^{fllox/fllox}* (n=7) (Figure 3-11 b, e, h), but up-regulated in 55% of *UroIIcre Fgfr3^{+ /K644E} Pten^{fllox/fllox}* samples (n=6/11, k).

p21 was present most abundantly in the outermost umbrella layer in *Control* (n=3) (c), and this remained similar in *UroIIcre Fgfr3^{+ /K644E}* (n=3) and *UroIIcre Pten^{fllox/fllox}* (n=3) (f, i). However, in *UroIIcre Fgfr3^{+ /K644E} Pten^{fllox/fllox}* urothelium (n=4), p21 was expressed throughout all urothelial layers (l). This p21 upregulation appeared to have coincided with the overall up-regulation of PI3K-AKT signalling (k).

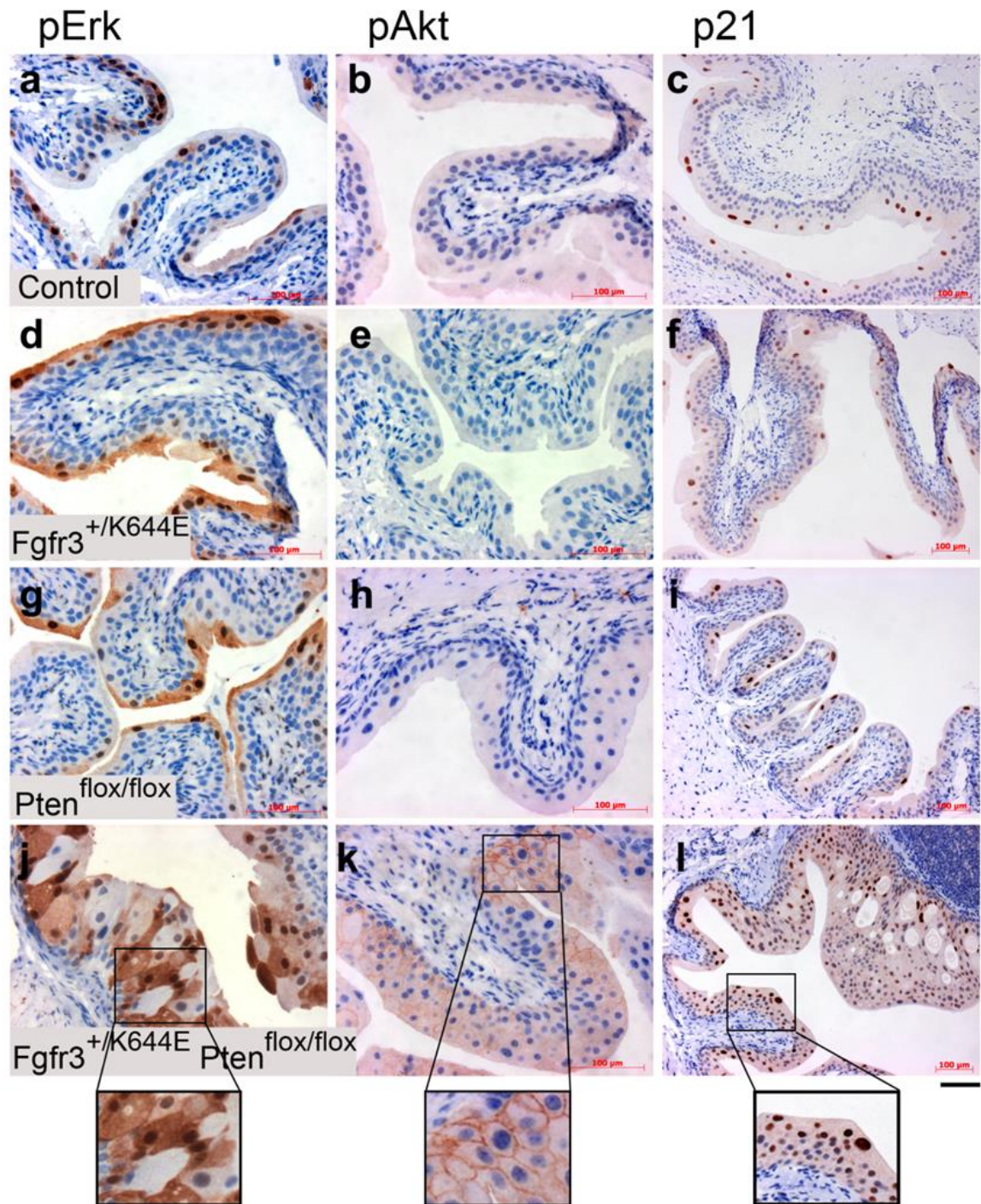


Figure 3-11: Deregulation of downstream signalling and cell cycle arrest in the *Uro11Cre Fgfr3^{+/K644E} Pten^{flox/flox}* urothelium

Immunohistochemistry for phosphorylated ERK (pERK) (a, d, g, j), phosphorylated AKT (pAKT) (b, e, h, k) and p21 (c, f, i, l) on *Control* (a-c), *Uro11Cre Fgfr3^{+/K644E}* (d-f), *Uro11Cre Pten^{flox/flox}* (g-i), and *Uro11Cre Fgfr3^{+/K644E} Pten^{flox/flox}* bladders (j-l). Scale bar represents 50 μm in a, b, d, e, g, h, j, k, and 100 μm in c, f, i, l.

3.10 Analysis of pathway association between FGFR3 and AKT signalling by tissue microarray (TMA)

In order to address whether PI3K-AKT signalling is functionally associated with FGFR3 activation in human non-muscle invasive bladder cancer, we evaluated the levels of FGFR3 protein expression and the phosphorylated form of mTOR, p-mTOR (S2448) in 66 T1 urothelial tumours on tissue microarray platform. TMA was performed by Dr Theodorus van der Kwast and Dr Bas van Rhijn at the Princess Margaret Hospital in Toronto, Canada.

Immunohistochemistry staining intensity of FGFR3 and p-mTOR on the TMA was categorised using the 4-point scale: strong (blue), intermediate (green), faint (yellow) and negative (white) (Figure 3-12). FGFR3 and p-mTOR levels were then analysed for correlation. An increase in intermediate FGFR3 expression (green) was associated with increased level of p-mTOR ($p=0.014$, Pearson Chi-Square test). This may indicate presence of synergy of FGFR3 and PI3K-AKT pathways. The decrease in strong expression of FGFR3 (blue) was statistically not significant ($p=0.101$).

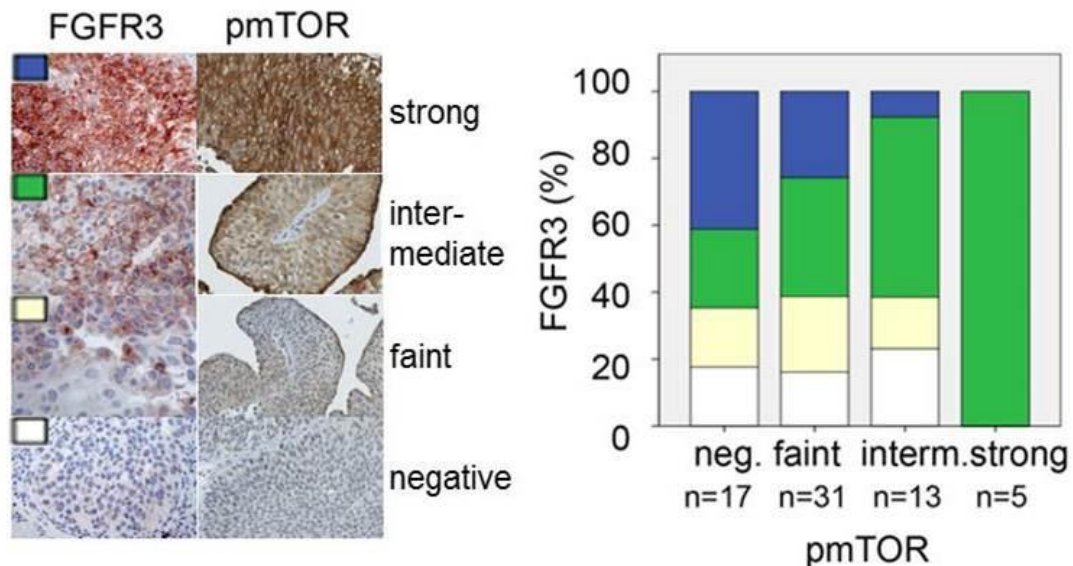


Figure 3-12: Tissue microarray analysis of FGFR3 and p-mTOR expression levels in T1 urothelial tumours

Immunohistochemistry staining on human non-invasive T1 tumours was categorised as strong (blue), intermediate (green), faint (yellow) and negative (white). Right panel shows correlation between increased FGFR3 expression (green) and increased level of p-mTOR.

Similar trends were observed when the levels were characterised in each tumour grade (Figure 3-13). The increasing trend of intermediate expression of FGFR3 (green) along the increased p-mTOR level was not statistically significant in non-invasive low-grade (a) and high-grade (b) papillary urothelial carcinoma according to WHO 2004 classification system, and G2 (c) and G3 (d) according to WHO 1973 classification system ($p=0.579$, 0.056 , 0.124 , and 0.058 , in a-d, respectively). This may be due to the low number of available samples indicated.

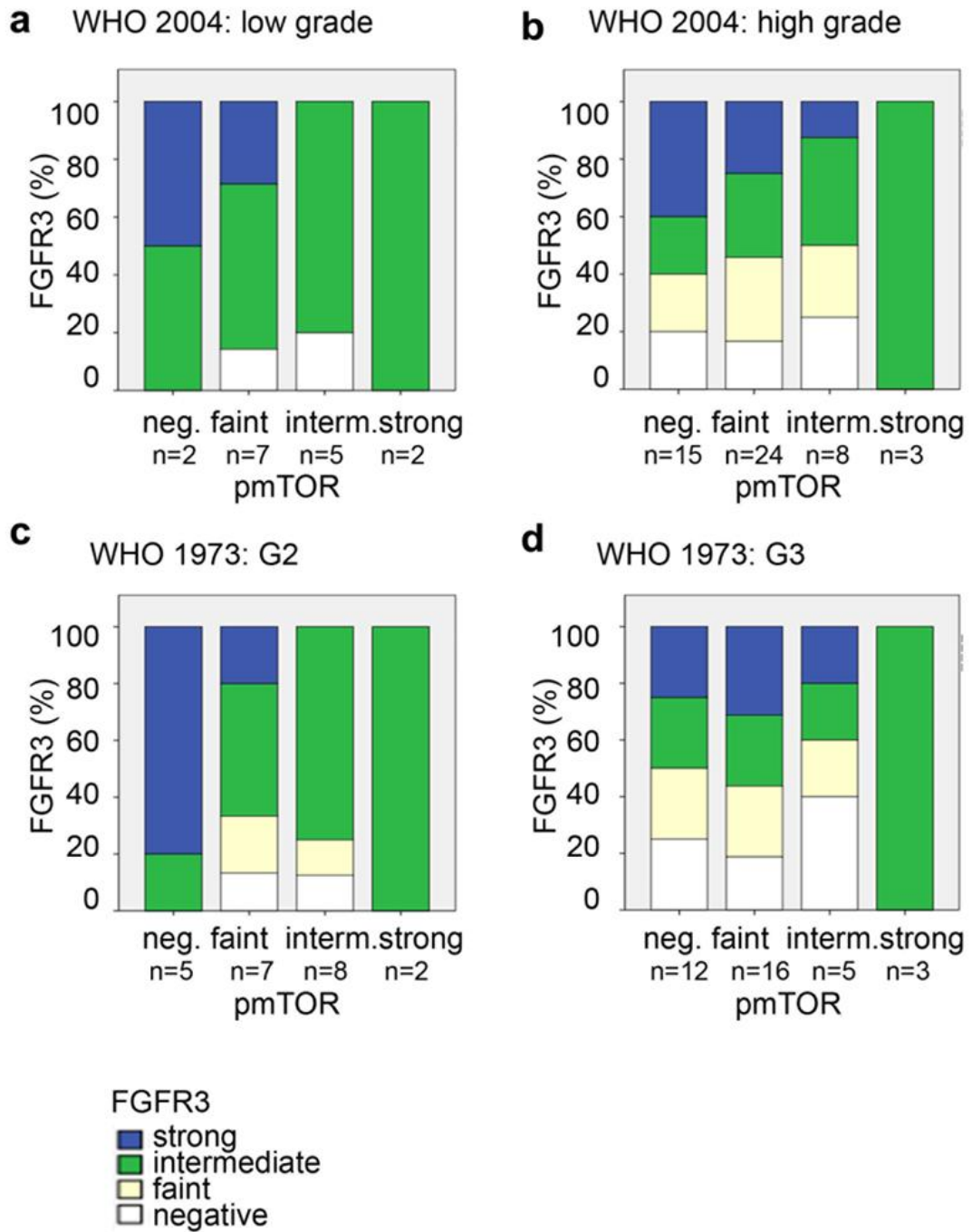


Figure 3-13: Tissue microarray analysis of FGFR3 and p-mTOR expression levels according to tumour grade

Non-invasive low-grade (a) and high-grade (b) papillary urothelial carcinoma according to WHO 2004 classification system, and G2 (c) and G3 (d) according to WHO 1973 classification system

3.11 Discussion

The present study provides functional evidence that supports that upregulation of FGFR3 signalling together with that of PI3K-AKT signalling plays a role in the initiation of urothelial tumourigenesis. Furthermore, this chapter demonstrates that *Fgfr3* and *Pten* mutations cooperatively promote morphological changes of the urothelium, while not when mutated individually.

3.11.1 The *UroII*Cre *Fgfr3*^{+/K644E} *Pten*^{flox/flox} model

The current model carries a *K644E* mutation in *Fgfr3*. *In vitro*, this mutation promotes strongly enhanced signalling through a conformational change in the receptor that favours autophosphorylation (Naski et al., 1996). Additionally, its kinase activity can be further enhanced by FGF binding (Naski et al., 1996). However, *K644E* mutation is only found in less than 2% of human non-invasive bladder cancers. Although the kinase domain mutations such as *K644E* are less common compared to *S249C* in humans (Tomlinson et al., 2007a, Duenas et al., 2013, Bernard-Pierrot et al., 2006), this mouse line offers several advantages as an experimental model, namely because the Cre-Lox construct enables the expression of mutant *Fgfr3* in a urothelium-specific fashion and the mutation is highly activating, thus maximising the chance of a detectable phenotype. However, our model did not show increased FGFR3 signalling in the bladder *in vivo*.

3.11.2 *UroII*Cre recombination

Recombination analysis in the urothelium Z/EG reporter mice indicated that UroplakinII-Cre (*UroII*Cre) predominantly recombines in umbrella and intermediate cells but less extensively in basal cells (Figure 3-2). The original reference reported recombination in all three layers; however, it seemed to predominantly occur in umbrella and intermediate cells as indicated by their lacZ staining (Mo et al., 2005). This is in accordance with our results where lacZ staining was predominantly observed in umbrella and intermediate cells. Moreover, the thickening of the intermediate cell layer in *UroII*Cre *Fgfr3*^{+/K644E} *Pten*^{flox/flox} accompanied by cellular abnormalities further supports that *UroII*Cre recombination predominantly occurs in the intermediate cell layer. If the cancer cell of origin of urothelial cell carcinoma naturally resides in the basal cell

compartment, it is possible that it is not recombined under *UroIICre* and the mutations of interest are not introduced in the correct cells to initiate tumourigenesis. This may be supported by the fact that our animal model failed to develop bladder tumours by 18 months. To further determine the exact location of recombination it would be useful to cross the *UroIICre* to a *Rosa26 tdRFP* reporter mouse line (Luche et al., 2007), where recombination events can be visualised by RFP immunohistochemistry.

3.11.3 Urothelial thickening

Mild urothelial thickening was observed in 60% of mice with *Pten* deletion, although this increase was statistically not significant upon quantification (Figure 3-4). Previously it was reported that loss of *Pten* under the control of the *FabpCre* promoter leads to urothelial hyperplasia (Tsuruta, 2006, Yoo et al., 2006). Moreover, using the *UroIICre* promoter, *Pten* loss in combination with hyperactivated β -Catenin even leads to the development of urothelial papillary carcinomas (Ahmad et al., 2011a). *Pten* loss with *p53* deletion using adenoviral Cre delivery led to high-grade muscle-invasive bladder cancer (Puzio-Kuter et al., 2009). In our current study, hyperplasia was not observed following *Pten* loss. This is consistent with the observations in previous studies by our group (Ahmad et al., 2011a) and others (Puzio-Kuter et al., 2009).

In contrast to the mild urothelial thickening observed in mice with homozygous *Pten* deletion, mice with homozygous mutation in *Fgfr3* showed strong increase in urothelial thickness, emphasising the potent effect of activated FGFR3 signalling (Figure 3-4).

Mice heterozygous for *Fgfr3* mutation and homozygous for *Pten* deletion showed a statistically significant increase in urothelial thickness, but not when *Fgfr3* or *Pten* were singly mutated, suggesting that this increase is owing to the cooperation of *Fgfr3* and *Pten* mutation (Figure 3-3 and Figure 3-4). The urothelium of these mice showed global hypertrophy with several cellular characteristics indicative of abnormal differentiation, which was overall similar to the histopathology seen in urothelial papilloma in humans.

Although mice with *Fgfr3* mutation and *Pten* deletion showed a thickened urothelium with increased proliferation, it did not produce tumours in the animal model up to 18 months. This indicates that pathogenesis caused by FGFR3 and PI3K-AKT signalling pathway mutations are unlikely to progress unless further mutations occur that overcome the intact cell cycle inhibitor machinery. In humans, *FGFR3* mutations are highly associated with non-muscle-invasive bladder cancer with better clinical outcome (Billerey et al., 2001, van Rhijn et al., 2002).

3.11.4 Abnormal urothelial differentiation

Significantly, while the papillary structures with fibro-vascular cores seen in human non-muscle-invasive bladder cancer were not observed, the urothelium of *Uro11Cre Fgfr3^{+ / K644E} Pten^{flox / flox}* did demonstrate several morphological abnormalities that may reflect pathogenesis in humans. These included increased urothelial thickness, caused by an increase in cell size and cell proliferation, and loss of polarity (Figure 3-6 and Figure 3-7). These histopathological features are comparable to hyperplasia and dysplasia, regarded as early stages in the putative model of bladder cancer pathogenesis in humans.

This functional cooperation was also reflected by the atypical expression of layer-specific markers indicating abnormal differentiation and/or maturation of cells in the *Uro11Cre Fgfr3^{+ / K644E} Pten^{flox / flox}* urothelium (Figure 3-7). UroplakinIII-positive cells were present in deeper layers close to the submucosa, while CK5 was absent in some parts of the deeper layers of the urothelium, showing an inverse expression pattern. Double staining with CK18 together with CK5 clearly showed the abnormal localisation of umbrella cells deep in the urothelium of *Uro11Cre Fgfr3^{+ / K644E} Pten^{flox / flox}*, indicating abnormal differentiation and/or maturation of cells as an effect of *Fgfr3* and *Pten* mutation in combination. A recent study *in vitro* showed similar large, vacuolated and flattened cell morphology and increased proliferation of Normal Human Urothelial (NHU) cells stably expressing hotspot *PI3KCA* mutations (Ross et al., 2013). Despite the difference that these effects solely resulted from *PI3KCA* activation *in vitro*, the findings are supportive of our observations in mice. This may reflect the

complexity of signalling events leading to tumourigenesis *in vivo*, in which multiple gene mutations and epigenetic events are likely to be required.

3.11.5 Cell size and cell number

The increase in intermediate cell size was observed owing to both *Fgfr3* and *Pten* mutations in combination, whereas that of cell proliferation was mainly an effect of *Pten* deletion (Figure 3-8 and Figure 3-9). These results indicate that *Fgfr3* and *Pten* mutation cooperatively caused urothelial hypertrophy, while *Pten* contributed to hyperplasia in the *UroIICre Fgfr3^{+K644E} Pten^{flox/flox}* urothelium. The effects of *Fgfr3* and *Pten* mutations were cell-type specific, particularly in intermediate and umbrella cell layers. The basal cell layer was not significantly affected in this model.

3.11.6 Changes in downstream signalling

Cooperation of *Fgfr3* and *Pten* mutations seem to have resulted in deregulation of the MAPK pathway in the double mutant, which may correlate with abnormal differentiation and/or maturation of urothelial cells, indicating the local involvement of the MAPK pathway in pathogenesis through regulation of cell differentiation (Figure 3-11).

The observed p21 upregulation appeared to have coincided with the overall up-regulation of PI3K-AKT signalling, which is in accordance with the evidence *in vitro* that activation of PI3K-AKT pathway up-regulates p21 (Yohn et al., 2011). The elucidation of precise causal mechanisms, however, requires further studies.

Furthermore, up-regulation of pAKT was observed when both *Fgfr3* and *Pten* mutations together, and not in single mutants (Figure 3-11). In humans, a higher pAKT level was found in 50% bladder tumours, independent of stage/grade and is associated with the presence of mutations, including *PIK3CA*, *FGFR3*, and both together (Juanpere et al., 2012).

Potential cooperation of the FGFR3 and the AKT pathways was further supported by a TMA of human T1 samples where an increase in expression of FGFR3 protein was correlated with increased level of p-mTOR (Figure 3-12). Activation of PI3K-

AKT downstream protein, mTOR, is confirmed to be strongly associated with pAKT (Korkolopoulou et al., 2012). Relationship between FGFR3 overexpression and p-mTOR is relatively unstudied and one report showed no statistical association (Korkolopoulou et al., 2012). However, in the current study, although the number of analysed T1 bladder samples was small, we were able to show association of the intermediate level of FGFR3 overexpression with increased p-mTOR (Figure 3-12 and Figure 3-13). In humans, *PIK3CA* mutations were also found in normal urothelium, indicating that it is an early event (Duenas et al., 2013).

Further work would include a larger clinical cohort to establish whether concurrent *FGFR3* mutation and p-mTOR activation confers a better prognosis in non-muscle-invasive bladder cancer patients.

3.11.7 Limitations of the model

There are several differences between the nature of our mouse model in relationship to human bladder cancer that may limit the direct interpretation. Firstly, although we used *Pten* loss as an experimental tool in this study, in humans, occurrence of *FGFR3* mutations are associated with non-invasive bladder cancer while *PTEN* loss with muscle-invasive tumours, and therefore little overlap is expected (Askham et al., 2010, Knowles, 2008). *FGFR3* mutations and loss of heterozygosity in *PTEN* are found together only in a small number of cases of TaG1, T1G2, and T2G3 (Askham et al., 2010). Statistically, *PTEN* loss was not associated with upregulation of pAKT in clinical bladder cancer specimen (Askham et al., 2010). However, in the absence of available mouse lines with *Pi3kca* mutations, we turned to a model that enables conditional *Pten* deletion (Tsuruta, 2006, Yoo et al., 2006). PTEN is a well-known inhibitor of PI3K-AKT signalling and it was shown that its deletion resulted in pAKT upregulation in bladder tumours in mice (Ahmad et al., 2011a). Secondly, a study of clinical specimens reported that 85% of tumours with *FGFR3* mutations also overexpressed FGFR3 protein (Tomlinson et al., 2007a). In contrast, changes in FGFR3 protein level were not apparent in our model (Figure 3-1). This could be due to the expected low level of endogenous protein expressed in the mouse urothelium. The mechanism of *Fgfr3* mutations leading to an increased protein level is unclear; however *in vitro* studies showed that impaired lysosomal

degradation of FGFR3 protein was caused by mutations, increasing the stability of FGFR3 mutant protein in the plasma membrane (Cho et al., 2004).

3.11.8 Future plans

Considering that *Fgfr3* in combination with other mutations can induce substantial architectural and cellular changes in the urothelium, it would be interesting to identify potential other cooperating mutations that drive urothelial tumourigenesis together with activated FGFR3. Particularly, it would be interesting to analyse the effect of *Pi3k* mutation in combination with *Fgfr3*, and whether the result is comparable to our current model where *Pten* deletion is utilised to activate AKT signalling.

3.11.9 Conclusion

Altogether, our study demonstrated that *Fgfr3* and *Pten* mutations cooperatively promote morphological changes of the urothelium, but not when mutated individually. Furthermore, this study provides functional evidence that supports that upregulation of FGFR3 signalling plays a causative role in urothelial pathogenesis of non-invasive bladder cancer together with upregulated PI3K-AKT signalling.

Chapter 4

Search for cooperating genes by Sleeping Beauty mutagenesis

4.1 Introduction

The Sleeping Beauty (SB) system is a method to screen functional genes by insertional mutagenesis (Dupuy et al., 2005, Dupuy et al., 2009). The SB system is based on transposon excision by a transposase and subsequent reintegration into a random location in the genome (“cut and paste”), which can either lead to a gain-of-function event or to interruption of the reading frame and therefore silencing of a gene (Copeland and Jenkins, 2010). Transposon-derived sequences are common components (40%) of the human and mouse genome, which demonstrates the importance of transposition in the context of evolution (Lander et al., 2001, Waterston et al., 2002).

Sleeping Beauty transposons belong to the group of Tc1/mariner transposable elements that were initially isolated from salmonid fish species (Ivics et al., 1997). Thereafter, great effort has been made to genetically improve these transposable elements in order to generate a powerful tool for forward genetic screens, and for generating novel phenotypes in mice in a less time-consuming and less technically challenging manner in contrast to vector-based gene-trap approaches with ES cells.

The SB transposase is encoded by the Cre-inducible *RosaSBase^{LSL}* allele, which allows tissue-restricted expression of the enzyme (Dupuy et al., 2009). The *T2/Onc3* transposon concatemer on the other hand contains ~200 copies of the SB transposon (Dupuy, 2005). The SB transposase recognises two imperfect terminal sequences called “inverted repeats” up- and downstream of each individual transposon (*T2/Onc3*), excises it from its concatemer and reintegrates about 40-50% of the mobilised *T2/Onc3s* into another place in the genome in a random fashion (Copeland and Jenkins, 2010). *T2/Onc3* is equipped with a bi-directional polyA (pA) sequence that allows integration in either orientation. Furthermore, due to the presence of splice donor and splice acceptor sequences in *T2/Onc3*, the transposon integration can promote expression of an oncogene or terminate transcription of a tumour suppressor gene along with neutral mutations resulting from integration into non-functional sites within the genome (Dupuy et al., 2005, Collier et al., 2005). 90% of all insertions lead to a gain-of-function effect (Copeland and Jenkins, 2010).

The frequency of SB transposition in somatic cells varies greatly in a tissue-dependent manner (5-30 events per cell type) (Collier et al., 2005, Dupuy et al., 2005). In the mouse germline 1-2 transpositions occur per animal born (Dupuy et al., 2001). *T2/Onc3* can continuously be re-mobilised into subsequent locations. It generally leaves a footprint of about five nucleotides at its previous insertion site, and can therefore potentially still interrupt the reading frame of a gene after its departure, even though this event remains undetected by splinkerette PCR (Copeland and Jenkins, 2010).

Splinkerette PCR is an assay in which transposon junctions are amplified from genomic DNA of mice carrying transposon insertions. Following restriction enzyme digestion, DNA fragments are ligated to a linker sequence (“splinkerette”). After a clean-up digestion reaction to remove DNA segments with splinkerette adapters on both ends of the fragment, a primary PCR with splinkerette-specific primers is performed. Thereafter, a secondary nested PCR is performed using the primary PCR product. Secondary PCR products are visualised by agarose electrophoresis, purified from the gel, and cloned into a vector (“TOPO-shotgun cloning”). TOPO-shotgun cloning is a de-multiplexing step for the pool of different splinkerette-PCR products that have resulted from the multiple SB transposition events in the tissue of interest. Ligation products are transformed into bacterial cells and amplified in 96-well plates for subsequent capillary read sequencing.

Although generally the entire genome is accessible to SB transposition (Collier et al., 2005), it has been reported that 50-80% of the SB germline transpositions show preference in the site of relocation, which is particularly near the original location (“local hopping” (Carlson et al., 2003). A lower frequency of local hopping has been reported in ES cells (Liang et al., 2009) and various somatic cell types (Collier et al., 2005, Starr et al., 2009, Dupuy et al., 2005).

The SB system has been established in tissues such as the liver (Keng et al., 2009), gastrointestinal tract (March et al., 2011, Starr et al., 2009), pancreas (Mann et al., 2012), hematopoietic system (Dupuy et al., 2005), soft tissue (Collier et al., 2005), mouse embryonic stem cells (Luo et al., 1998) and in the germline (Dupuy et al., 2001). SB has also been shown to carry on its insertional mutagenesis activity in metastatic lesions (Dupuy et al., 2009, Keng et al., 2009,

Mann et al., 2012). However, Sleeping Beauty has not been tested in the bladder yet.

In this chapter we aimed to identify genes that cooperate with *Fgfr3* or *Pten* to promote tumourigenesis using an unbiased screening approach. More specifically, we sought to elucidate whether *Fgfr3* *K644E* mutation is fundamentally able to drive urothelial cell carcinoma in the presence of SB-induced mutations. Furthermore, since our previous results indicated functional cooperation between *Fgfr3* and *Pten* mutation (Chapter 3), we sought to investigate whether insertional mutagenesis may support these data. We hypothesised that *Fgfr3* mutation may be identified among the common insertional sites in sequenced *Pten*-mutant Sleeping Beauty tumours; and that *Pten* inactivation may be found in *Fgfr3*-mutant SB tumours.

In addition, we sought to identify genes that can cooperate with a strongly activating *Hras* mutation to promote bladder cancer. *HRAS* is found mutated at variable frequencies in different reports on human bladder cancer, ranging from 6-70% (Czerniak et al., 1992, Jebar et al., 2005, Fitzgerald et al., 1995). However, it may not be the sole initiator (Knowles and Williamson, 1993, Ahmad et al., 2011b), indicating that a second mutation may be required. In mice, *Hras* mutation is known to cause low-grade non-invasive bladder cancer either by itself (Zhang et al., 2001, Mo et al., 2007) or together with activated WNT signalling (Ahmad et al., 2011b), as well as high-grade invasive urothelial cell carcinoma in combination with *p53* inactivation (Gao et al., 2004).

Experimentally, we approached the question of gene cooperation by generating Sleeping Beauty mouse cohorts that carried an additional *Fgfr3*, *Pten* or *Hras* mutation. We intended to sequence any resulting SB-induced tumours for the common insertional sites in order to reveal the genetic alterations that cooperatively promoted tumourigenesis.

4.2 Sleeping Beauty mutagenesis in the urothelium of *Uro11Cre Fgfr3^{+ / K644E}*

We generated a cohort of n=29 mice in which heterozygous *K644E* mutation in *Fgfr3* is combined with the transposase allele *RosaSBase^{LSL}* and the transposon donor *T2/Onc3* (Dupuy et al., 2009) in the urothelium, *Uro11Cre Fgfr3^{+ / K644E} RosaSBase^{LSL} T2/Onc3* (Table 4-1). We also generated a cohort of mice with Sleeping Beauty elements only, *Uro11Cre RosaSBase^{LSL} T2/Onc3* (n=10), as well as a cohort with homozygous *Fgfr3* mutation, *Uro11Cre Fgfr3^{K644E / K644E} RosaSBase^{LSL} T2/Onc3* (n=18). None of the mice showed clinical signs of bladder tumours by 8-21 months.

Table 4-1: Sleeping Beauty mouse cohorts with *Fgfr3* mutation

**Uro11Cre Fgfr3^{K644E / K644E} RosaSBase^{LSL} T2/Onc3* mice were sacrificed at the time where kyphosis became prevalent. This phenotype is due to a low-level of FGFR3 expression in the presence of homozygous *Fgfr3^{K644Eneo}* allele (Li et al., 1999, Iwata et al., 2000, Deng et al., 1996). **The increase in urothelial thickness observed in *Uro11Cre Fgfr3^{K644E / K644E} RosaSBase^{LSL} T2/Onc3* was milder comparing to those in *Uro11Cre Fgfr3^{+ / K644E} Pten^{flx/flx}*.

Genotype	n	Age at time of analysis	Increased urothelial thickness	Cellular abnormalities
<i>Uro11Cre RosaSBase^{LSL}T2/Onc3</i>	10	6-18 months	None	None
<i>Uro11Cre Fgfr3^{+ / K644E} RosaSBase^{LSL}T2/Onc3</i>	29	11-21 months	None	None
<i>Uro11Cre Fgfr3^{K644E / K644E} RosaSBase^{LSL}T2/Onc3</i>	18	8-14 months*	n=7 (39%)**	None

We evaluated whether Sleeping Beauty transposon excision had occurred in the bladder by T2/Onc3 PCR assay (Figure 4-1).

Successful mobilisation of the transposon (225 bp) from its concatemer form (2.2 kb) was confirmed in all of ten tested samples of *UroIIICre Fgfr3^{+ / K644E} RosaSBase^{LSL} T2/Onc3*. DNA extract from the tail, where transposon jumping is not expected to occur, was used as negative control (lane: Tail), while colon crypt cells, in which successful transposition had been confirmed previously (unpublished), was used as a positive control (lane: Crypt).

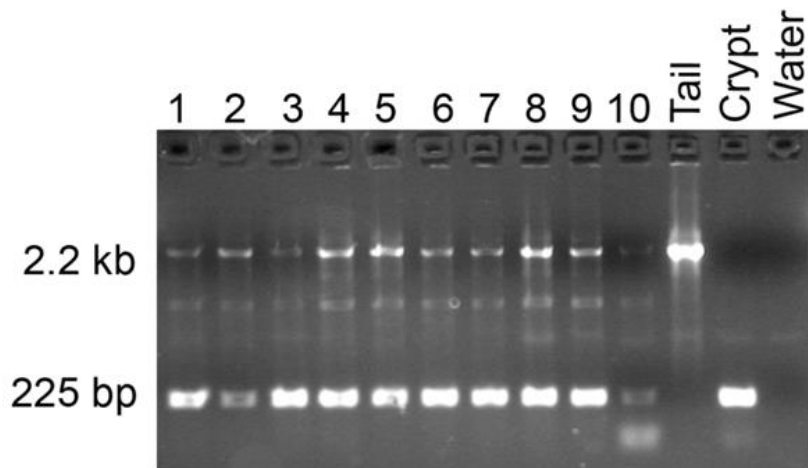


Figure 4-1: T2/Onc3 excision PCR

1.5% agarose gel showing mobilisation of transposon (225 bp) in *UroIIICre Fgfr3^{+ / K644E} RosaSBase^{LSL} T2/Onc3* T2/Onc3 samples (lanes: 1-10) and controls (lanes: tail, crypt, water).

We analysed the urothelial appearance in *Uro11Cre Fgfr3^{+/K644E} RosaSBase^{LSL} T2/Onc3* (*Fgfr3^{+/K644E} SB⁺*, n=29) and *Uro11Cre Fgfr3^{K644E/K644E} RosaSBase^{LSL} T2/Onc3* (*Fgfr3^{K644E/K644E} SB⁺*, n=18) at 18 months (Figure 4-2).

Fgfr3^{+/K644E} SB⁺ mice retained a histologically normal urothelial appearance (B), similar to control mice with SB transposase and transposon (*Uro11Cre RosaSBase^{LSL} T2/Onc3* (*SB⁺*, n=10) (A).

Fgfr3^{K644E/K644E} SB⁺ mice were sacrificed at an average of 12 months for kyphosis. The kyphosis phenotype is similar to that of *Fgfr3* knockout mice caused by the homozygous effects of the knock-in allele (*Fgfr3^{+/K644Eneo}*) in reducing transcription of FGFR3 in the full body (Li et al., 1999, Iwata et al., 2000).

More than half of the *Fgfr3^{K644E/K644E} SB⁺* cohort (61%, n=11 out of 18) retained histologically normal urothelial appearance. However, 39% (n=7 out of 18) of the mice showed mild hyperplasia (D), similar to that in *Uro11Cre Fgfr3^{K644E/K644E}* (*Fgfr3^{K644E/K644E}*, n=10) (C, and Figure 3-5 A, B), but milder than *Uro11Cre Fgfr3^{+/K644E} Pten^{flox/flox}* (Figure 3-3 h).

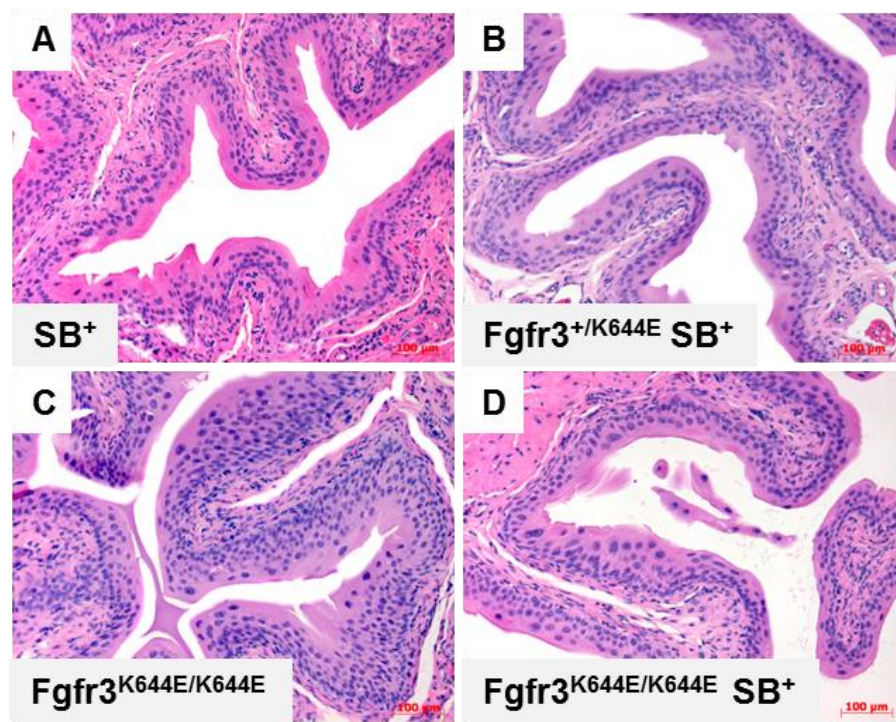


Figure 4-2: Sleeping Beauty insertional mutagenesis in the presence of *Fgfr3* mutation
 Representative H&E sections of *Uro11Cre RosaSBase^{LSL} T2/Onc3* (*SB⁺*) (A), *Uro11Cre Fgfr3^{+/K644E} RosaSBase^{LSL} T2/Onc3* (*Fgfr3^{+/K644E} SB⁺*) (B), *Uro11Cre Fgfr3^{K644E/K644E}* (*Fgfr3^{K644E/K644E}*) (C) and *Uro11Cre Fgfr3^{K644E/K644E} RosaSBase^{LSL} T2/Onc3* (*Fgfr3^{K644E/K644E} SB⁺*) (D). Scale bar represents 100 µm in A-D.

4.3 Sleeping Beauty mutagenesis in the urothelium of *UroIICre Pten^{flox/flox}*

We generated a cohort of n=20 mice in which homozygous *Pten* deletion combined with the transposase allele *RosaSBase^{LSL}* and the transposon donor *T2/Onc3* (Table 4-2). One *UroIICre Pten^{flox/flox} RosaSBase^{LSL} T2/Onc3* animal out of n=20 (5%) developed a tumour.

Table 4-2: Sleeping Beauty mouse cohorts with *Pten* mutation

Genotype	n	Age at time of analysis	Increased urothelial thickness	Cellular abnormalities	Tumour
<i>UroIICre RosaSBase^{LSL}T2/Onc3</i> (as in Table 4-1)	10	6-18 months	None	None	None
<i>UroIICre Pten^{flox/flox} RosaSBase^{LSL}T2/Onc3</i>	20	6-17 months	n=9 (45%)	n=9 (45%)	n=1 (5%)

Histologically, the bladder tumour in *UroIICre Pten^{flox/flox} RosaSBase^{LSL} T2/Onc3* ($Pten^{flox/flox}$ SB⁺) was superficial and of low grade (n=1) (Figure 4-3 A). Furthermore, in 45% (n=9 out of 20) of *Pten^{flox/flox} SB⁺*, a global hypertrophic phenotype was observed (B), similar to *UroIICre Fgfr3^{+K644E} Pten^{flox/flox}* (Figure 3-3 h).

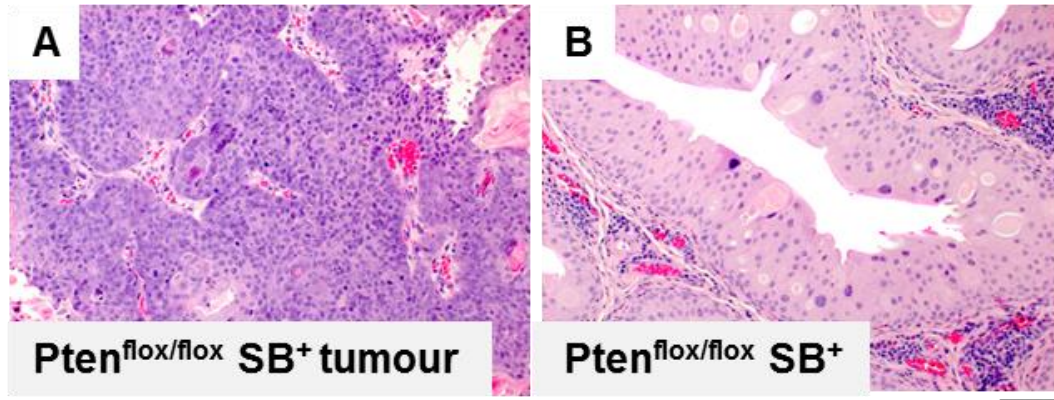


Figure 4-3: Sleeping Beauty insertional mutagenesis in the presence of *Pten* mutation
Representative H&E sections of a *UroIICre Pten^{flox/flox} RosaSBase^{LSL} T2/Onc3* tumour ($Pten^{flox/flox}$ SB⁺ tumour, n=1) (A) and *UroIICre Pten^{flox/flox} RosaSBase^{LSL} T2/Onc3* urothelium ($Pten^{flox/flox}$ SB⁺, n=9) (B). Scale bar represents 100 μ m in A-B.

The similarity of urothelial phenotype in *Pten*^{flox/flox} *SB*⁺ and *Uro11Cre Fgfr3*^{+ /K644E} *Pten*^{flox/flox} led us to the hypothesis that the SB mutagenesis may have targeted the *Fgfr3* gene or caused gene alterations leading to similar downstream effects. We therefore assessed FGFR3 expression by immunohistochemistry (Figure 4-4).

The relative level of FGFR3 protein in *Pten*^{flox/flox} *SB*⁺ bladders (B) was unchanged compared to the *SB*⁺ control (A) (n=5 each), indicating that other genes may have been targeted in the mutagenesis.

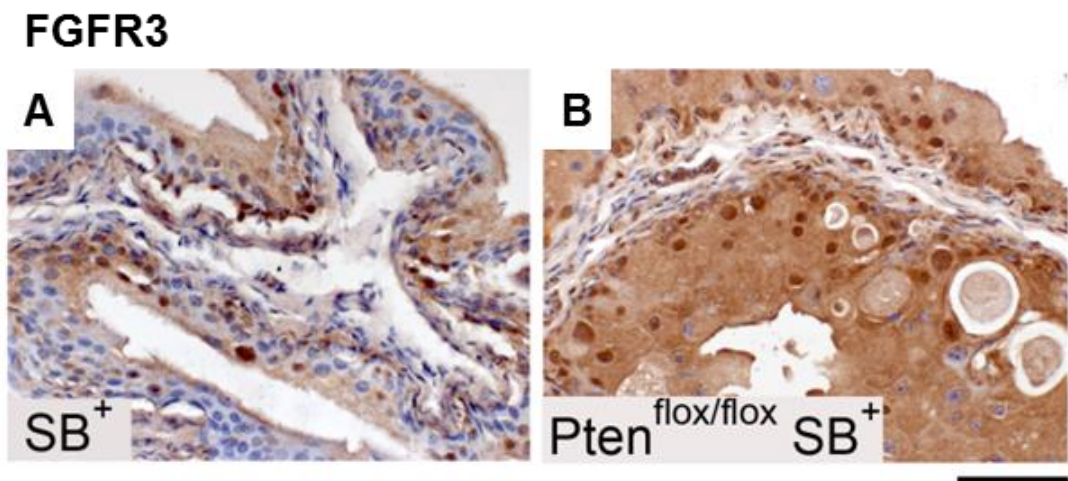


Figure 4-4: FGFR3 expression in *Uro11Cre Pten*^{flox/flox} *SB*⁺ urothelium
Immunohistochemistry for FGFR3 in bladders of *Uro11Cre RosaSBase*^{LSL} *T2/Onc3* (*SB*⁺) (A) and *Uro11Cre Pten*^{flox/flox} *RosaSBase*^{LSL} *T2/Onc3* (*Pten*^{flox/flox} *SB*⁺) (B). Scale bar represents 100 μ m in A-B.

Since *Fgfr3* was not likely a direct target, we tested by immunohistochemistry in n=3 samples each whether the MAPK or the AKT pathway had generally been affected by the SB mutagenesis (Figure 4-5 and Figure 4-6).

Similar to *UroIIcre Fgfr3^{+ /K644E} Pten^{flox/flox}* (Figure 3-11 j), phosphorylated ERK was observed in a cell-specific fashion in the urothelium of *Pten^{flox/flox} SB⁺* (Figure 4-5 H), while its level remained low in *UroIIcre RosaSBase^{LSL} T2/Onc3* (*SB⁺*), *UroIIcre Fgfr3^{+ /K644E} RosaSBase^{LSL} T2/Onc3* (*Fgfr3^{+ /K644E} SB⁺*), and in the tumour of *Pten^{flox/flox} SB⁺* (B, E, K).

Expression of p21 was restricted to umbrella cells in *SB⁺* (C) and *Fgfr3^{+ /K644E} SB⁺* (F). In contrast, p21-positive cells were scattered in all layers of the *Pten^{flox/flox} SB⁺* urothelium (I), however, less extensive than in *UroIIcre Fgfr3^{+ /K644E} Pten^{flox/flox}* (Figure 3-11 l). Increased numbers of p21-positive cells were observed in the tumour developed in *Pten^{flox/flox} SB⁺* (Figure 4-5 L).

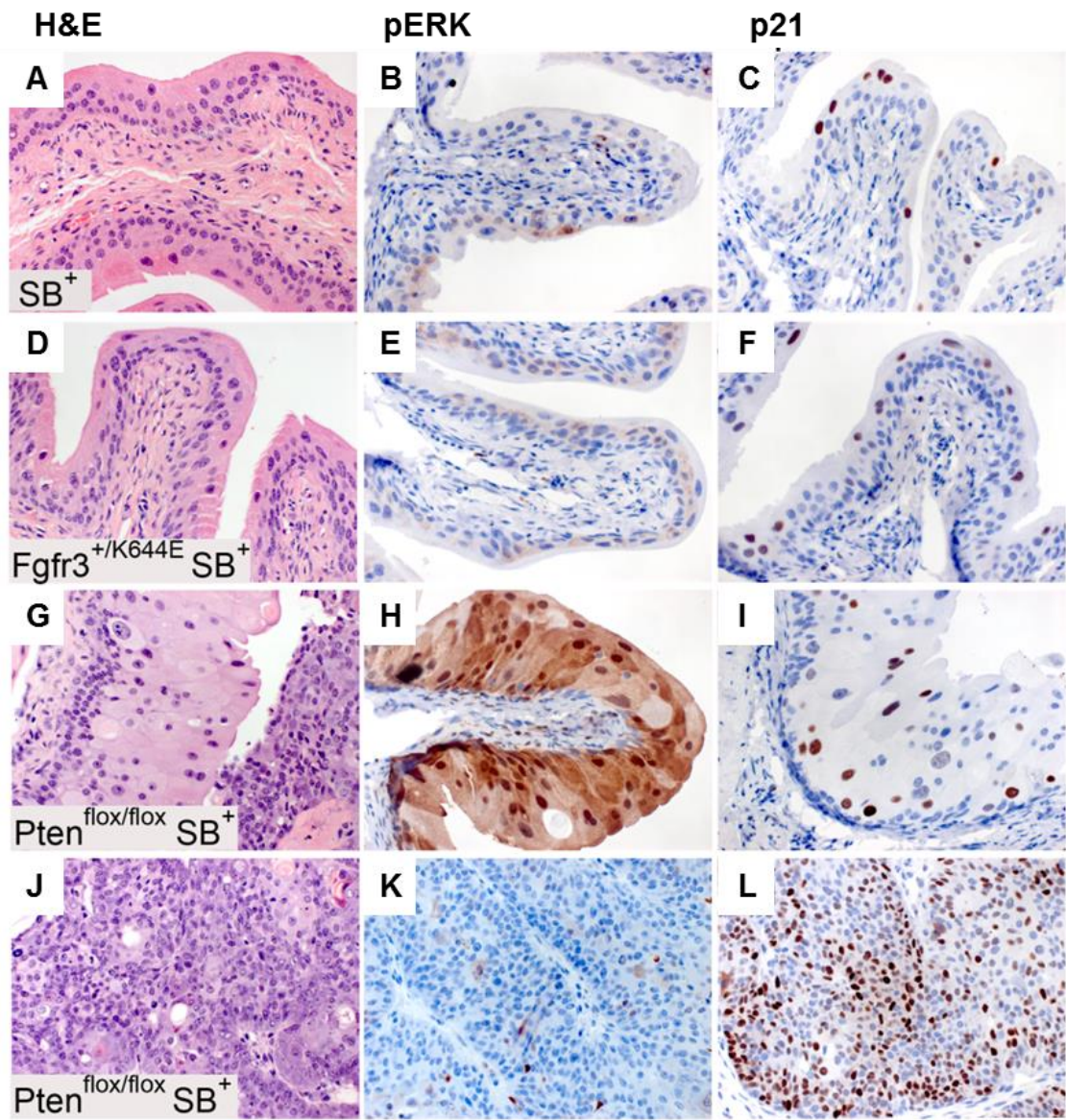


Figure 4-5: Sleeping Beauty insertional mutagenesis in the presence of *Fgfr3* and *Pten* mutation

Representative H&E sections of *Uro11Cre RosaSBBase^{L/SL} T2/Onc3(SB⁺)* (A), *Uro11Cre Fgfr3^{+/K644E} RosaSBBase^{L/SL} T2/Onc3(Fgfr3^{+/K644E} SB⁺)* (D) and *Uro11Cre Pten^{flox/flox} RosaSBBase^{L/SL} T2/Onc3(Pten^{flox/flox} SB⁺)* (G, J). Immunohistochemistry for pERK (B, E, H, K), and p21 (C, F, I, L) in bladders of SB⁺ (B, C), Fgfr3^{+/K644E} SB⁺ (E, F) and Pten^{flox/flox} SB⁺ (H, I, K, L). Scale bar represents 100 μ m in A-L.

Phospho-AKT was up-regulated in the *Pten*^{flox/flox} *SB*⁺ tumour (Figure 4-6 D). However, unlike *UroIIcre Fgfr3*^{+/K644E} *Pten*^{flox/flox} (Figure 3-11 k), its level remained low in the *Pten*^{flox/flox} *SB*⁺ urothelium (n=3) (Figure 4-6 C). Phospho-AKT levels were similarly low in the urothelium of *SB*⁺ (n=3) (A) and *Fgfr3*^{+/K644E} *SB*⁺ (B).

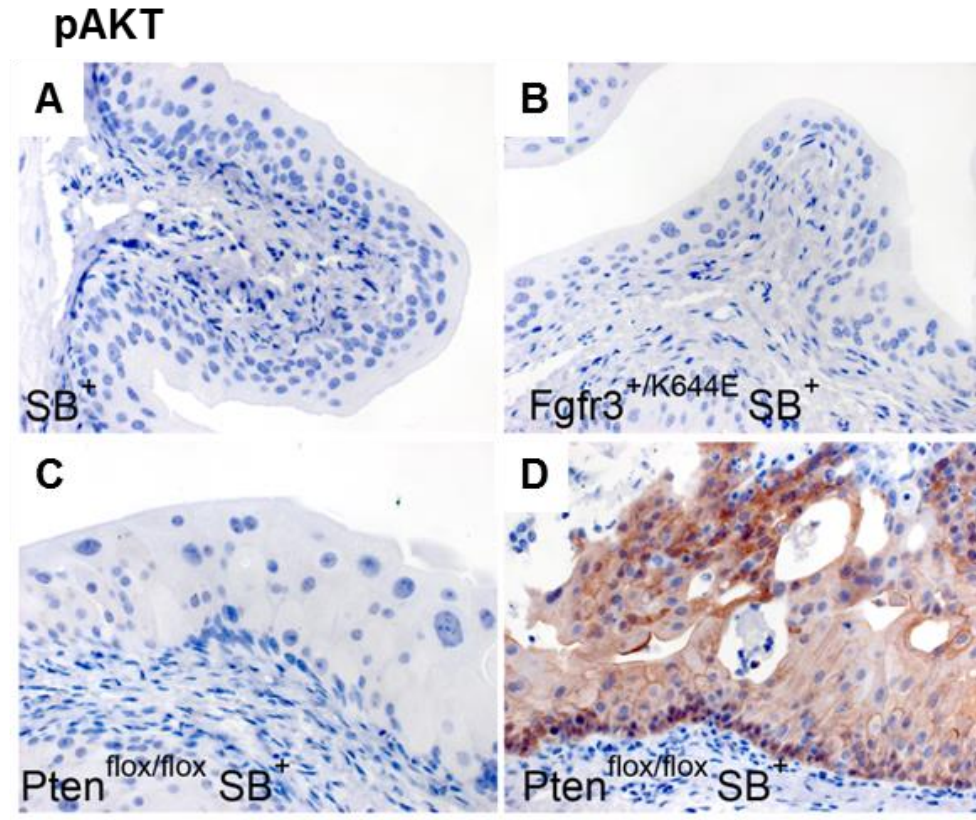


Figure 4-6: Upregulation of pAKT in the *Pten*^{flox/flox} *SB*⁺ tumour

Immunohistochemistry for pAKT in bladders of *UroIIcre RosaSBBase*^{LSL} *T2/Onc3*(*SB*⁺) (A) *UroIIcre Fgfr3*^{+/K644E} *RosaSBBase*^{LSL} *T2/Onc3*(*Fgfr3*^{+/K644E} *SB*⁺) (B) and *UroIIcre Pten*^{flox/flox} *RosaSBBase*^{LSL} *T2/Onc3*(*Pten*^{flox/flox} *SB*⁺) (C, D). Scale bar represents 100 μm in A-D.

Next, we performed splinkerette PCR and subsequent sequencing to analyse common insertion sites in hyperplastic bladders (n=8) as well as in the tumour (n=1) of *Pten*^{flox/flox} *SB*⁺ mice (Table 4-3). Splinkerette PCR, sequencing and bioinformatics analysis were performed by Dr Louise van der Weyden and Dr David J. Adams at the Sanger Institute in Cambridge, UK.

We were unable to obtain information on individual samples, such as the genetic changes in the tumour itself. However, the tumour sample was included in the analysis of the most common insertional sites in *Pten*^{flox/flox} *SB*⁺ bladders. Although the number of analysed samples was small, we observed transposon insertions in a number of known cancer driver genes, which include transcriptional regulators *Ep400* (Samuelson et al., 2005) and *Asxl2* (Katoh, 2013) and the known drivers of epithelial- mesenchymal transition (EMT), *Cadherin1* (*Cdh1*) and *Notch1*. While interactions between FGF signalling with *Ep400* and *Asxl2* have not been reported so far, regulation of EMT by FGF signalling is documented (Katoh and Nakagama, 2013), supporting that *Fgfr3* and *Pten* cooperation may merge at the signalling downstream, leading to the apparent *Pten*^{flox/flox} *SB*⁺ urothelial phenotype.

Table 4-3: Common insertional sites in *UroII*Cre *Pten*^{flox/flox} *SB*⁺
The top four genes in *UroII*Cre *Pten*^{flox/flox} *SB*⁺ urothelium.

Gene	Chromosome	Function
<i>Ep400</i>	5	Transcriptional activation
<i>Cdh1</i>	8	Cell adhesion
<i>Notch1</i>	2	Development and cell differentiation
<i>Asxl2</i>	12	Zinc finger

4.4 Sleeping Beauty mutagenesis in the urothelium of *UroIICre Hras^{+ /G12V}*

We generated a cohort of n=16 Sleeping Beauty mice carrying a strongly activating *Hras* G12V mutation combined with the transposase allele *RosaSBase^{LSL}* and the transposon donor *T2/Onc3* (Table 4-4).

In order to test whether enhanced MAPK signalling can promote tumourigenesis in the mouse urothelium by adding an activating *Fgfr3* mutation to the HRAS-hyperactivated bladder, we also generated a cohort of n=5 *UroIICre Fgfr3^{+ /K644E} Hras^{+ /G12V}* animals combined with the Sleeping Beauty elements (Table 4-4).

None of the *Hras* mutant mice or *Fgfr3-Hras* mutant mice with the Sleeping Beauty elements showed clinical signs of bladder tumours by 18 months.

Table 4-4: Sleeping Beauty mouse cohorts with *Hras* mutation

Genotype	n	Age at time of analysis	Increased urothelial thickness	Cellular abnormalities
<i>UroIICre Hras^{+ /G12V}</i>	16	12 months	None	None
<i>UroIICre Fgfr3^{+ /K644E} Hras^{+ /G12V}</i>	15	12 months	None	None
<i>UroIICre RosaSBase^{LSL}T2/Onc3</i> (as in Table 4-1)	10	6-18 months	None	None
<i>UroIICre Hras^{+ /G12V} RosaSBase^{LSL}T2/Onc3</i>	16	6-18 months	n=7 (44%)	None
<i>UroIICre Fgfr3^{+ /K644E} Hras^{+ /G12V} RosaSBase^{LSL}T2/Onc3</i>	5	7-18 months	None	None

We then analysed the histological appearance of the Sleeping Beauty urothelia with *Hras* and *Fgfr3-Hras* mutation and the ones of *Hras* and *Fgfr3-Hras* controls without Sleeping Beauty elements (Figure 4-7).

UroIIcre Hras^{+/*G12V*} controls alone did not show gross urothelial abnormalities apart from mild hyperplasia at 12 months of age (*Hras*^{+/*G12V*}, n=16, A). Similar observations were made in mice with *Hras* mutation and the additional SB elements, *UroIIcre Hras*^{+/*G12V*} *RosaSBase*^{LSL} *T2/Onc3* (*Hras*^{+/*G12V*} SB⁺, n=16, B).

A normal urothelial phenotype and occasionally mild hyperplasia was present in *UroIIcre Fgfr3*^{+/*K644E*} *Hras*^{+/*G12V*} animals at 12 months (*Fgfr3 Hras*, n=15, C). Additional SB elements did not produce any abnormal urothelial phenotype in *UroIIcre Fgfr3*^{+/*K644E*} *Hras*^{+/*G12V*} *RosaSBase*^{LSL} *T2/Onc3* either (*Fgfr3 Hras SB*⁺, n=3 at 18 months, n=2 at 7 months, D).

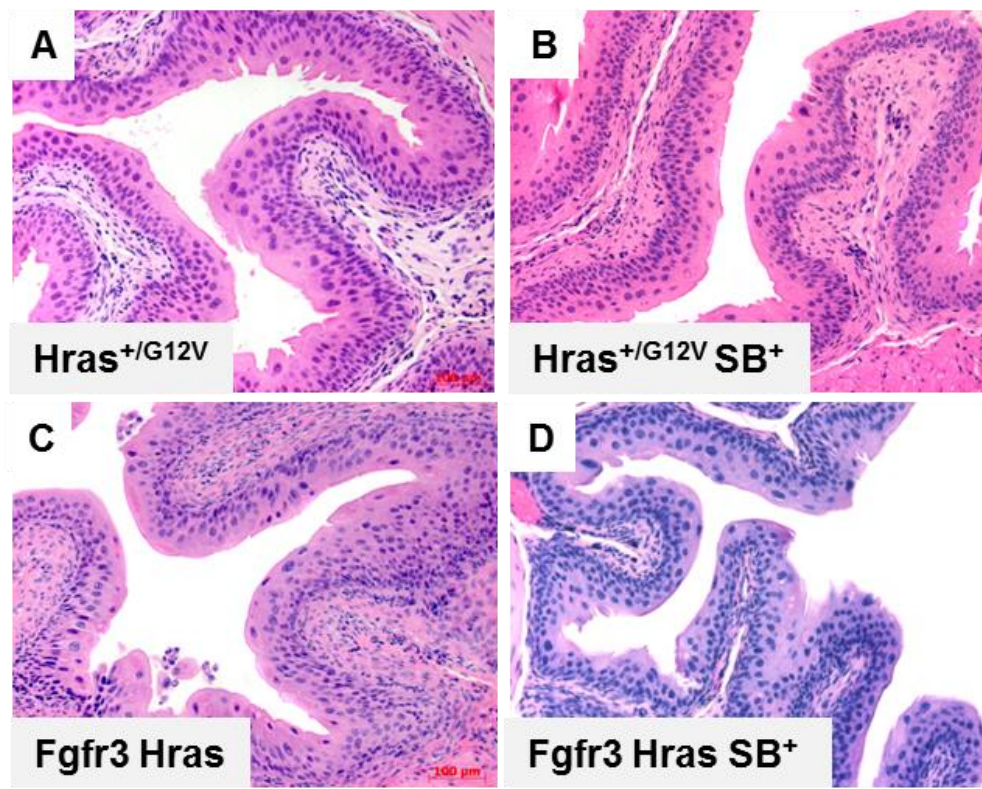


Figure 4-7: Sleeping Beauty insertional mutagenesis in the presence of *Hras* mutation and/or in combination with *Fgfr3* mutation

Representative H&E sections of *UroIIcre Hras*^{+/*G12V*} (*Hras*^{+/*G12V*}) (A), *UroIIcre Hras*^{+/*G12V*} *RosaSBase*^{LSL} *T2/Onc3* (*Hras*^{+/*G12V*} SB⁺) (B), *UroIIcre Fgfr3*^{+/*K644E*} *Hras*^{+/*G12V*} (*Fgfr3 Hras*) (C), and *UroIIcre Fgfr3*^{+/*K644E*} *Hras*^{+/*G12V*} *RosaSBase*^{LSL} *T2/Onc3* (*Fgfr3 Hras SB*⁺) (D). Scale bar represents 100 μm in A-D.

4.5 Discussion

The aim of this chapter was to identify mutations that cooperate with *FGFR3*, *PTEN*, or *RAS* mutation in promoting urothelial tumourigenesis an unbiased fashion. We have therefore performed Sleeping Beauty (SB) insertional mutagenesis. This unbiased screening approach was also intended to identify novel mutations that play an important role in urothelial tumourigenesis.

4.5.1 SB in *Uro11Cre Fgfr3^{+/K644E}*

We generated a cohort of n=29 mice in which a heterozygous *Fgfr3 K644E* mutation is introduced together with transposable Sleeping Beauty (SB) elements. SB controls presented a histologically normal urothelium that were indistinguishable from *Wild type* bladders. None of the *Uro11Cre Fgfr3^{+/K644E} SB⁺* mice showed clinical signs of bladder tumours, but a histologically normal urothelial appearance, suggesting that a second mutation by SB mutagenesis alongside *Fgfr3* was insufficient to cause bladder tumours.

Nor did a homozygous mutation in *Fgfr3*, *Fgfr3^{K644E/K644E} SB⁺*, promote tumourigenesis (Figure 4-2). It could be hypothesised that an additional mutation in combination with *Fgfr3 K644E* is generally insufficient for tumourigenesis to occur, indicating that *Fgfr3* may require more than one additional mutation in order to successfully transform urothelial cells.

In anticipation of potential gene cooperation with *Pten*, the lack of hypertrophic phenotype in *Fgfr3^{+/K644E} SB⁺*, as observed in *Uro11Cre Fgfr3^{+/K644E} Pten^{flox/flox}* (Chapter 3) is likely to be due to the low probability of homozygous targeting that would be required for *Pten* loss to take effect.

4.5.2 SB in *Uro11Cre Pten^{flox/flox}*

We also performed the SB mutagenesis in the presence of *Pten* mutation (n=20), where one *Uro11Cre Pten^{flox/flox} SB⁺* animal (5%) developed a bladder tumour. In 45% (n=9) we observed global hypertrophy (Figure 4-3), phenocopying the changes that we previously observed in *Uro11Cre Fgfr3^{+/K644E} Pten^{flox/flox}* urothelia (Chapter 3). Immunohistochemistry indicated that FGFR3 is unlikely a direct co-operator with *Pten* deletion in the SB model. However, it could be involved at

the level of its downstream signalling, particularly that of the MAPK-pathway (Figure 4-5), which was indicated in the hypertrophic urothelium that has led to similar downstream effects.

Hypertrophic *UroII*Cre *Pten*^{flox/flox} *SB*⁺ bladders were sequenced in collaboration with the Sanger Institute. We identified four frequently disrupted genes in these hypertrophic bladders, which include transcriptional regulators (*Ep400*, *Asx12*), and drivers of EMT (*Cdh1* and *Notch1*). FGF signalling to Notch1 and Wnt cascades are able to regulate EMT (Kato and Nakagama, 2013), which further supports that FGFR3 and PTEN signalling may merge downstream. It is possible that the transposon excision has left footprints that are not detected by splinkerette PCR, but that do lead to a loss-of function mutation.

4.5.3 Identification of cooperating mutations in SB-induced *UroII*Cre *Pten*^{flox/flox} tumours

Although FGFR3 was unlikely to be the direct co-operator with *Pten* deletion in the SB model, involvement at the level of its downstream signalling, particularly in the MAPK pathway was indicated in the hypertrophic regions. We identified four frequently disrupted genes in these hypertrophic bladders by splinkerette PCR and sequencing, which include transcriptional regulators (*Ep400*, *Asx12*), and drivers of EMT (*Cdh1* and *Notch1*) (Table 4-3).

Ep400 is a chromatin-remodelling factor that is associated with cellular transformation by Adenoviral E1A (Chan et al., 2005). Ep400 complex interaction has been found with adenoviral E1A, Simian vacuolating virus 40 (SV40), myc, p53 and p21 (Chan et al., 2005). By regulating p53/p21 transcription, Ep400 controls cellular senescence and apoptosis (Chan et al., 2005, Samuelson et al., 2005). With regards to cancer, decreased Ep400 expression was shown to be associated with advanced tumour stage and higher grade of malignancy in renal cell carcinoma (Macher-Goeppinger et al., 2013). The role of Ep400 in the bladder has not been reported so far.

ASXL family members are epigenetic scaffolding protein involved in transcriptional regulation through PRC2, BAP1 and/or NHR complexes (Kato, 2013). ASXL2 promotes adipocytic differentiation by upregulating transcription

of the fatty acid binding protein 4 (*Fabp4*) (Katoh, 2013). Truncation of *ASXL2* occurs in prostate, pancreatic and breast cancer (Katoh, 2013). A potential role of *ASXL2* in the bladder has not been reported to date.

Cadherins are involved in cell-cell adhesion, determination of cell polarity and differentiation (Berx and van Roy, 2009). Cadherin 1 (*Cdh1*, or E-Cadherin) binds to p120-catenin and β -catenin (Berx and van Roy, 2009). Loss of *Cdh1* is associated with cancer cell motility and constitutes a marker of EMT (Berx and van Roy, 2009). E-cadherin is repressed by other EMT indicator proteins such as Snail, ZEB2 and Slug (Berx and van Roy, 2009).

Notch1 is a transmembrane receptor that regulates an evolutionarily conserved intercellular signalling pathway that controls differentiation, survival, proliferation, and cell-to-cell interactions (Allenspach et al., 2002). Upregulated Notch signalling through overexpression of Notch-ligand Jagged2 in bladder carcinoma cell lines was associated with invasion and metastasis (Li et al., 2013).

4.5.4 SB in *UroII*Cre *Hras*^{+/*G12V*}

We also performed the SB mutagenesis in the presence of *Hras* mutation (n=16). *UroII*Cre *Hras*^{+/*G12V*} *SB*⁺ showed a normal urothelial phenotype apart from mild hyperplasia at 12 months of age. An additional *Fgfr3* mutation to further enhance MAPK signalling in combination with *Hras* mutation in the presence of the SB elements did not result in any abnormal urothelial phenotype either.

4.5.5 SB as an insertional mutagenesis tool in the bladder

The PCR assay confirmed successful excision of the T2/Onc3 transposon from the concatemer in all tested samples (Figure 4-1). However, it should be noted that this assay does not address transposon re-integration. Furthermore, the assay does not reveal potentially altered expression patterns of the transposase in terms of time and location.

The fact that mice carrying a strongly activating *Hras* mutation did not develop tumours at any stage (Figure 4-7) indicates that Sleeping Beauty is a rather inefficient tool for the analysis of the urothelium in contrast to other organs

(Keng et al., 2009, Starr et al., 2009, March et al., 2011). Neither did the combination of *Fgfr3* and *Hras* mutation with SB mutagenesis lead to urothelial pathogenesis (Figure 4-7).

An explanation for the inefficiency of SB in the urothelium could be the low proliferation rate of the mouse bladder (0.1-1%) (Stewart et al., 1980), which likely results in only few transposition and insertional mutagenesis events. In our experimental settings it is possible that tumour initiation may not have occurred in the relatively small number of cohort samples that underwent the SB experiment (n=29), considering that n=60-100 mice were used for SB mutagenesis in other organs with tumourigenesis occurring in 70-100% of the animals (Starr et al., 2009, Keng et al., 2009, Dupuy et al., 2009). Another possible explanation for the inefficient outcome of the SB screening could be that bladder cells in comparison to other somatic cell types may express certain host factors (e.g. DNA-bending proteins; (Zayed et al., 2003) at insufficient levels, which are required for transposition. Moreover, Sleeping Beauty can potentially miss small genetic loci such as miRNAs, which may influence bladder tumourigenesis. The role of miRNAs in bladder tumourigenesis has recently become a subject of investigation (Guancial et al., 2014a).

4.5.6 Future work

For future analysis of cooperating mutations in bladder cancer it may be of interest to test other insertional mutagenesis systems. An alternative to Sleeping Beauty that has been shown to mobilise transposable elements even with better efficiency in somatic cells (up to 300 times) is the Piggy Bac insertional mutagenesis system (Liang et al., 2009, Cadinanos and Bradley, 2007). Piggy Bac (PB) is also based on transposon integration, but displays higher transposition efficiency as well as no indication of local hopping (Ding et al., 2005, Liang et al., 2009). PB carries an inducible ERT2 domain, which allows the transposition to be turned off in the absence of tamoxifen after the tumours are initiated (Cadinanos and Bradley, 2007). However, similar to SB, the low proliferation rate of the bladder may as well lower the chances of obtaining sufficient results when screening for gene cooperation. Furthermore, the type of mutation that is induced by PB may be similar to the SB system, where 90% of all insertions represent gain-of-function mutations (Copeland and Jenkins, 2010).

4.5.7 Conclusion

Altogether, no direct association between *Fgfr3* and *Pten* mutations was found in urothelial tumours despite confirmation of successful transposon excision. However, the SB system itself may constitute a tool of questionable efficiency in the bladder since even a strongly activating *Hras* mutation in conjunction with SB was unable to induce urothelial tumourigenesis and *Pten* deletion together with Sleeping Beauty only produced one single bladder tumour. We therefore decided to move to another system to increase mutations within the bladder to cooperate with FGFR3 with a relevant mutational spectrum.

Chapter 5

The role of FGFR3 in tumour progression and invasion

5.1 Introduction

Carcinogen-induced bladder tumour models have been studied in order to investigate the effect of specific genetic alterations on malignant progression such as loss of *p53*, activation of Signal transducer and activator of transcription 3 (*Stat3*), as well as deficiency of *Secreted protein acidic and rich in cysteine* (*Sparc*) or *p21* (Ho et al., 2012, Tsuruta, 2006, Said et al., 2013, Ozaki et al., 1998). Heterozygous *p53* knockout mice showed increased susceptibility to urothelial tumour formation upon OH-BBN exposure compared to carcinogen-treated *Wild type* controls, emphasising the role of *p53* as a tumour suppressor (Ozaki et al., 1998). Loss of *SPARC*, a protein whose role in bladder physiology and tumourigenesis had been unclear and conflicting, was shown to accelerate bladder carcinogenesis and progression compared to *Wild type* litter mates (Said et al., 2013). *Stat3* activation in the urothelium promoted the development of invasive bladder cancer through the carcinoma *in situ* (CIS) pathway as opposed to *Wild type* mice that frequently developed urothelial hyperplasia and non-invasive cancer (Ho et al., 2012).

Presence of an *FGFR3* mutation in bladder cancer patients has been linked to favourable patient prognosis, as it is associated with low grade/stage pTa tumours (van Rhijn et al., 2012, Billerey et al., 2001, Hernandez et al., 2006). On the other hand, FGFRs have also been implicated in the regulation of epithelial-to-mesenchymal transition (EMT), invasion, and formation of distant metastasis in bladder cancer cell lines (Tomlinson et al., 2012, Cheng et al., 2013, Billottet et al., 2008, Savagner et al., 1994, Chaffer et al., 2006). *FGFR3* *wild type* receptor overexpression has been found in 42% of muscle-invasive tumours (Tomlinson et al., 2007a). Mutations in *FGFR3* are found in 10-15% of high grade invasive neoplasms (Billerey et al., 2001). Therefore, in total more than 50% of invasive urothelial cell carcinomas present with alterations in *FGFR3* signalling either by mutation, overexpression or both (Iyer and Milowsky, 2012). However, the mechanistic role of *FGFR3* in muscle-invasive bladder cancer is still not entirely clear. A recent attempt to re-classify urothelial cell carcinomas primarily based on molecular features has revealed a subgroup of muscle-invasive bladder cancer that present with *FGFR3* mutations and overexpression, which was associated with significantly poor prognosis (Sjodahl et al., 2012). *p63*-positivity has been identified as an indicator of progression and lethality in

muscle-invasive bladder cancer (Choi et al., 2012, Karni-Schmidt et al., 2011). Interestingly, p63 has been shown to be capable of inducing *FGFR3* transcription (Sayan et al., 2010). Moreover, FGFR3 expression appeared to directly correlate with p63 expression in a set of human bladder cancer cell lines (Cheng et al., 2013). Altogether, these observations imply a role of *FGFR3* mutation in tumour progression and invasion.

Recently, a study suggested subcategorising muscle-invasive bladder cancers into basal-, luminal-, and p53-like tumours (Choi et al., 2014). According to the results of a large number of tumours that were analysed, basal-like tumours are characterised by the expression of CK5, CK6, CK14, CD44, ZEB, Cadherin-3 (CDH3), Vimentin (VIM), MYC and EGFR and are associated with squamous differentiation. Luminal-like tumours were enriched with CK20, CD24, Forkhead box protein A1 (FOXA1), Trans-acting T-cell-specific transcription factor (GATA3), X-box binding protein 1 (XBP1), E-Cadherin and FGFR3. p53-like tumours expressed luminal biomarkers and an additional wild type p53 gene expression signature. p53-like tumours were associated with chemotherapy resistance. The basal-like subtype-associated expression of MYC, CD44, CK5, CK6 and CK14 has been shown to be widely controlled by the p63 isoform Δ Np63 in other tissues (Romano et al., 2009, Boldrup et al., 2007, Marquis et al., 2012). p63 expression was associated with progression of muscle-invasive tumours (Choi et al., 2012, Karni-Schmidt et al., 2011). *TP53* mutation frequencies were similar in all of the muscle-invasive subtypes (Choi et al., 2014).

Exposure to carcinogens often causes DNA damage, which can be lethal to the cell if not fully repaired (Roos and Kaina, 2006). Alternatively, it can lead to genomic instability promoting cancer formation (Lord and Ashworth, 2012). The induction of double-strand breaks activates the ATM/Chk2 DNA repair machinery leading to the phosphorylation of histone H2aX (γ H2aX) (Bartkova et al., 2005). γ H2aX has been shown to be expressed in rat bladders following OH-BBN treatment (Toyoda et al., 2013). γ H2aX has also been shown to be expressed in human non-invasive low-grade urothelial carcinoma (Cheung et al., 2009). Epithelial tumours progressing towards invasion often express proteins indicative of epithelial-to-mesenchymal-transition (EMT), such as Fascin, zinc finger E-box binding homeobox 1 (ZEB1), β -catenin, Sex Determining Region Y-Box 9 (Sox9) and E-cadherin (Schmalhofer et al., 2009, Thiery, 2002). Fascin has been

reported to be expressed in various stages of bladder tumours (Karasavvidou et al., 2008, Chen et al., 2012), and is often found at high levels in tumour cells where it marks the invasive edge (Karasavvidou et al., 2008, Tong et al., 2005). ZEB1, a zinc finger transcription factor, is another marker of EMT that is associated with tumour cell migration and invasion by regulating cell fate (Schmalhofer et al., 2009). β -catenin and Sox9 expression is associated with stemness/progenitor properties, cancer progression and invasiveness (Wang et al., 2008, Fodde and Brabletz, 2007). E-Cadherin expression is associated with loss of cell-cell adhesion in the process of malignant progression, stabilising the invasive mesenchymal phenotype (Schmalhofer et al., 2009). Nuclear accumulation of p53 protein can be an indication of *TP53* mutation, which is associated with greater risk of muscle-invasive disease and reduced survival (Esrig et al., 1994). p21 is a direct target of p53 and regulates cell cycle progression at the G1/S phase (el-Deiry et al., 1993). Loss of p21 (CIP1/WAF1) expression has been shown to be an indicator of bladder cancer progression, and it was strongly associated with higher recurrence and lower patient survival (Stein et al., 1998).

In this chapter, we aimed to investigate the role of FGFR3 in tumour progression and invasion *in vivo*. Based on our results in Chapter 3, we hypothesised that an *FGFR3* mutation can predispose urothelial cells to tumourigenesis. Moreover, based on two recent publications that *FGFR3* mutation is also found in a subset of muscle-invasive bladder tumours, we hypothesised that the receptor mutation can contribute to cancer progression. Experimentally, we approached the question of the role of *FGFR3* mutation in tumour progression by subjecting *Fgfr3*-mutant and *Wild type* mice to OH-BBN. Furthermore, we also analysed *Fgfr3-Pten* double mutation in OH-BBN-induced tumours.

We have based our previous *in vivo* experiments on an *Fgfr3 K644E* mutation, which leads to highly activated receptor signalling (Naski et al., 1996). However, the frequency of the human equivalent *FGFR3 K650E* is less than 2% of the *FGFR3* mutations in bladder cancer (Tomlinson et al., 2007a). In contrast, *FGFR3 S249C* accounts for ~66% of all *FGFR3* mutations in human non-invasive urothelial cell carcinoma (Tomlinson et al., 2007a, Duenas et al., 2013, Bernard-Pierrot et al., 2006). Therefore, it is possible that the two mutations have a differential oncogenic effect in the urothelium. This is supported by cell culture studies

where different *FGFR3* mutations caused different mechanisms of kinase activity affecting morphological transformation, cell proliferation, and anchorage-independent growth (Tomlinson et al., 2007a, di Martino et al., 2009). In order to resemble the conditions of human bladder cancer more closely, it would be of interest to analyse the effect of an *S249C* mutation in *FGFR3* in the urothelium. We therefore generated a transgenic line carrying Tg(UroII-hFGFR3IIIbS249C) construct to introduce a human *FGFR3 S249C* mutation to the murine urothelium. We then sought to compare two different point mutations in *FGFR3*, namely murine *Fgfr3 K644E* and human *FGFR3 S249C*, in the normal untreated urothelium as well their effect on tumour progression in established OH-BBN-induced neoplasms.

5.2 Generation of the Tg(UroII-hFGFR3IIIbS249C) mouse

The transgenic line Tg(UroII-hFGFR3IIIbS249C), which I will call *FGFR3-S249C* from now on, was generated by Dr T. Iwata (University of Glasgow), Prof M. Knowles (Leeds, UK) and Dr D. Tomlinson (Leeds, UK). The design of the vector and generation of the transgenic line is described in the Methods (Chapter 2.3). The line was rederived from frozen embryos that were thawed and implanted into pseudo pregnant C57Bl/6 mice. Following crosses were carried out on C57Bl/6 background.

Firstly, we confirmed the presence of the *S249C* mutation in *FGFR3* in the offspring (Figure 5-1).

A PCR assay was performed on isolated genomic DNA from mouse tail tips (A). A PCR product of 396 bp was detected in n=5 tested animals (lanes 1-5). Due to a DNA quality issue the assay failed to produce a clean band in one case (lane 6). Neg. ctrl. and Water were also included.

Sequencing of the product revealed a nucleotide exchange of cytosine to guanine (C -> G) (B, arrow). The sequence was compared against the NCBI whole human genome database using the BLAST search tool (Altschul et al., 1990), where a percentage of 99% identity was found in chromosome 4.

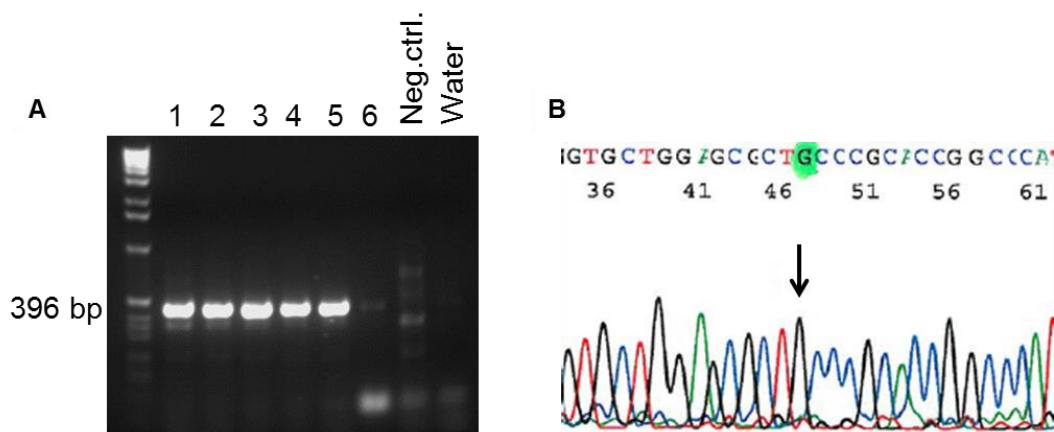


Figure 5-1: Establishment of the Tg(UroII-hFGFR3IIIbS249C) model
FGFR3 S249C point mutation detected in five animals by PCR (A) and by sequencing (B).

The five *FGFR3-S249C* mice that were positively tested for the *S249C* mutation were subsequently bred to C57Bl/6 mice in order to establish the line.

We also generated a cohort of *UroIIcre Tg(UroII-hFGFR3IIIbS249C) Pten^{flox/flox}*, further called *FGFR3-S249C Pten*, by intercrossing *FGFR3-S249C* with transgenic *UroIIcre* (Zhang et al., 1999) and mice homozygous for floxed *Pten* allele, *Pten^{flox/flox}* (Lesche et al., 2002). For comparison we used our previous mouse cohort with *Fgfr3 K644E* mutation, *UroIIcre Fgfr3^{+ /K644E}*, further called *Fgfr3-K644E* (Table 5-1).

FGFR3-S249C bladders were harvested at 6 months (n=3) and 12 months (n=6) of age. *FGFR3-S249C Pten* bladders were harvested at 9-12 months of age (n=10). Some animals were euthanised due to causes unrelated to changes in the bladder, including infection or pregnancy.

Table 5-1: Summary of mouse cohorts for *FGFR3-S249C* transgene analysis

Genotype	n	Age at time of analysis	Non-bladder related deaths	Increased urothelial thickness	Cellular abnormalities
<i>Control</i>	11	10-18 months	None	None	None
<i>UroIIcre Fgfr3^{+ /K644E}</i> (as in Table 3-1)	25	5-15 months	n=2 (8%)	None	None
<i>Tg(UroII-hFGFR3IIIbS249C)</i>	9	6-12 months	n=1 (16%)	None	None
<i>UroIIcre</i> <i>Tg(UroII-hFGFR3IIIbS249C)</i> <i>Pten^{flox/flox}</i>	10	10-12 months	n=1 (11%)	None	None

In order to examine the effect of *FGFR3 S249C* mutation in the bladder alone and in combination with *Pten* deletion, we analysed the appearance of the transgenic urothelia (Figure 5-2).

The urothelia of *Wild type* (n=11) (A) and *Fgfr3-K644E* (n=25) (D) appeared similar to *FGFR3-S249C* (n=9) (G) at 12 months of age. *FGFR3-S249C Pten* bladders did not show any histological abnormalities (n=10) (J) in contrast to *UroIIcre Fgfr3^{+/K644E} Pten^{flox/flox}* (Chapter 3), where severe morphological changes of the urothelium had been observed.

Proliferation was similarly low in *Wild type* (B), *Fgfr3-K644E* (E), *FGFR3-S249C* (H) and *FGFR3-S249C Pten* (K) in all layers of the urothelium.

Similar levels and patterns of FGFR3 protein expression were detected in the urothelium of *Wild type* (C), *Fgfr3-K644E* (F) and *FGFR3-S249C* (I), indicating that FGFR3 expression was not influenced by the nature of the *Fgfr3* mutation. FGFR3 staining of *FGFR3-S249C Pten* urothelia was not available at the time of writing.

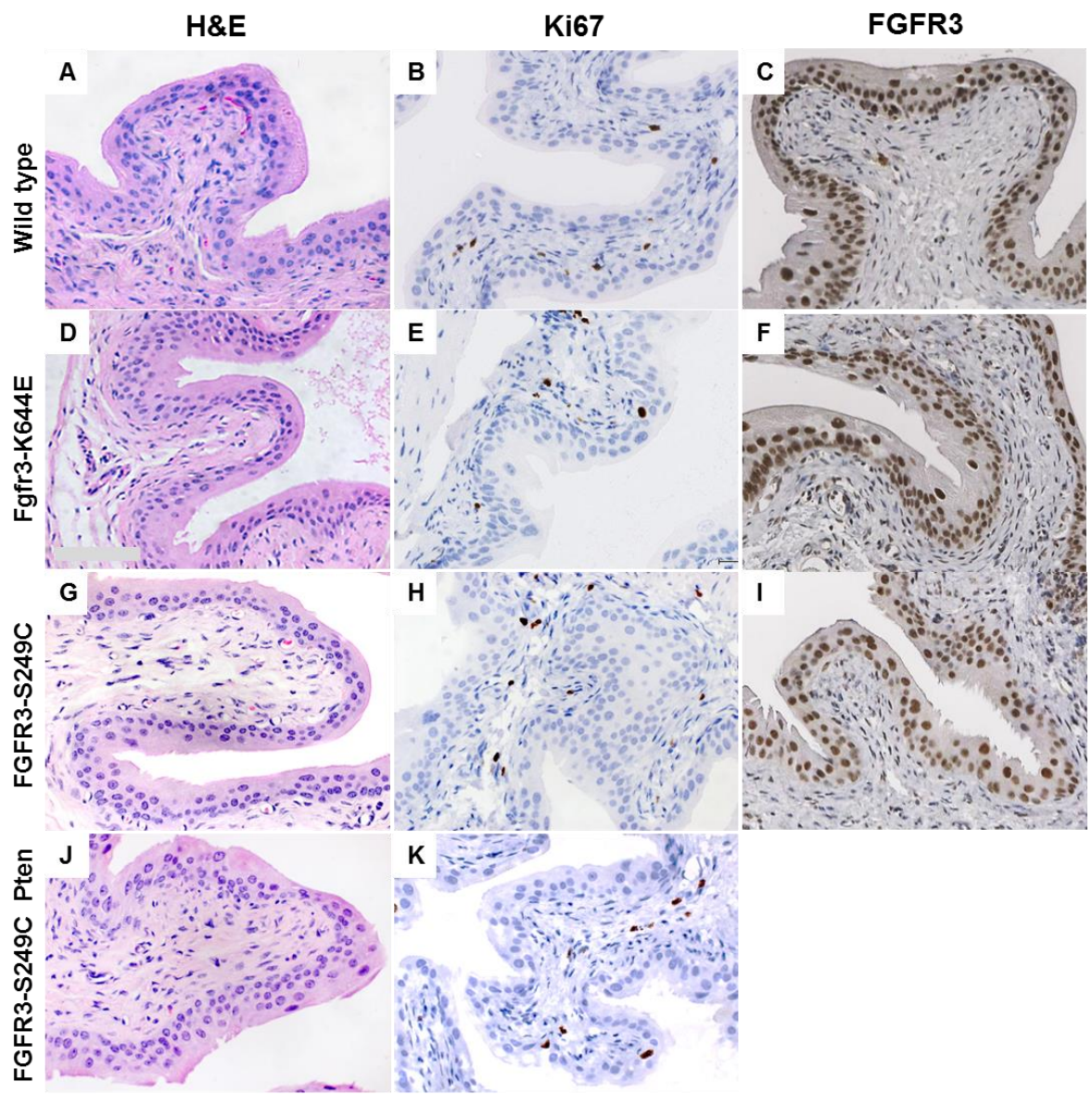


Figure 5-2: Urothelial appearance of *Wild type*, *Fgfr3-K644E*, *FGFR3-S249C* and *FGFR3-S249C Pten* at 12 months

Representative sections of *Wild type*, *UroIIcre Fgfr3^{+/K644E}*, *Tg(UroII-hFGFR3IIIbS249C)* and *UroIIcre Tg(UroII-hFGFR3IIIbS249C) Pten^{fllox/fllox}* stained by H&E (A, D, G, H), anti-Ki67 (B, E, H, K) and anti-FGFR3 (C, F, I). Scale bar represents 100 μ m (A-K).

5.3 Mouse cohorts that were subjected to OH-BBN

In order to evaluate the role of *FGFR3* S249C mutation in tumour progression, we subjected *FGFR3-S249C* mice as well as *Wild type* to 0.05% w/v N-butyl-N-(4-hydroxybutyl)-nitrosamine (OH-BBN) for 10 weeks followed by a period of 10 weeks with normal drinking water (further called “10+10 weeks”) (Table 5-2).

Furthermore, we generated cohorts of *Uro11Cre Pten^{flox/flox}* (*Pten*) and *FGFR3-S249C Pten^{flox/flox}* (*FGFR3-S249C Pten*). At the time of writing, no *Uro11Cre Fgfr3^{+K644E}* (*Fgfr3-K644E*) mice had been subjected to OH-BBN due to insufficient numbers.

Table 5-2: OH-BBN-treated mouse cohorts

Mice were subjected to 0.05% w/v N-butyl-N-(4-hydroxybutyl)-nitrosamine for 10 weeks, followed by 10 weeks of normal drinking water. Mice were sampled over a time course as indicated

Genotype	Age at start of treatment	n sampled at 2 weeks	n sampled at 6 weeks	n sampled at 10+2 weeks	n sampled at 10+10 weeks
<i>Wild type</i>	8-16 weeks	5	5	5	17
<i>Tg(Uro11-hFGFR3IIIbS249C)</i>	8-16 weeks	5	5	5	17
<i>Uro11Cre Pten^{flox/flox}</i>	8-16 weeks	None	None	5	16
<i>Uro11Cre Tg(Uro11-hFGFR3IIIbS249C) Pten^{flox/flox}</i>	8-16 weeks	None	None	None	19
<i>Uro11Cre Fgfr3^{+K644E} Pten^{flox/flox}</i>	8-16 weeks	None	None	None	7

5.4 **FGFR3 S249C** mutation increases sensitivity to tumourigenesis after long-term OH-BBN exposure

We compared the histological changes in the urothelium of *Wild type*, *FGFR3-S249C*, *UroIIcre Pten^{flox/flox} (Pten)*, *FGFR3-S249C Cre Pten^{flox/flox} (FGFR3-S249C Cre Pten)* and *UroIIcre Fgfr3^{+ /K644E} Pten^{flox/flox} (Fgfr3-K644E Pten)* subjected to 10 weeks of carcinogen exposure followed by 10 weeks of normal drinking water (“10+10”) (Figure 5-3). As an example of histological features of OH-BBN-treated urothelia at high magnification, *FGFR3-S249C* bladders are shown (Figure 5-4).

Based on their cell-morphological changes, tumours among all five cohorts seemed to be comparable in terms of grade and severity (Figure 5-3). Cell-morphological changes among all cohorts included the absence of umbrella cells in the urothelium, small nests with cellular atypia (Figure 5-3 C and H, black arrows).

While none of these abnormal features were seen in untreated *FGFR3-S249C* bladders (n=9) (Figure 5-4 A), we observed characteristics of advanced tumours in OH-BBN-treated bladders, including squamous cell transformation with keratinisation (Figure 5-3 C, red arrow, and (Figure 5-4 C, arrow), carcinoma *in situ* (CIS) with lobular appearance of the urothelium-stroma boundary cohorts (Figure 5-4 B, dotted line), and invasion through the basement membrane (Figure 5-3 G, black arrow and (Figure 5-4 D, arrow with dotted line).

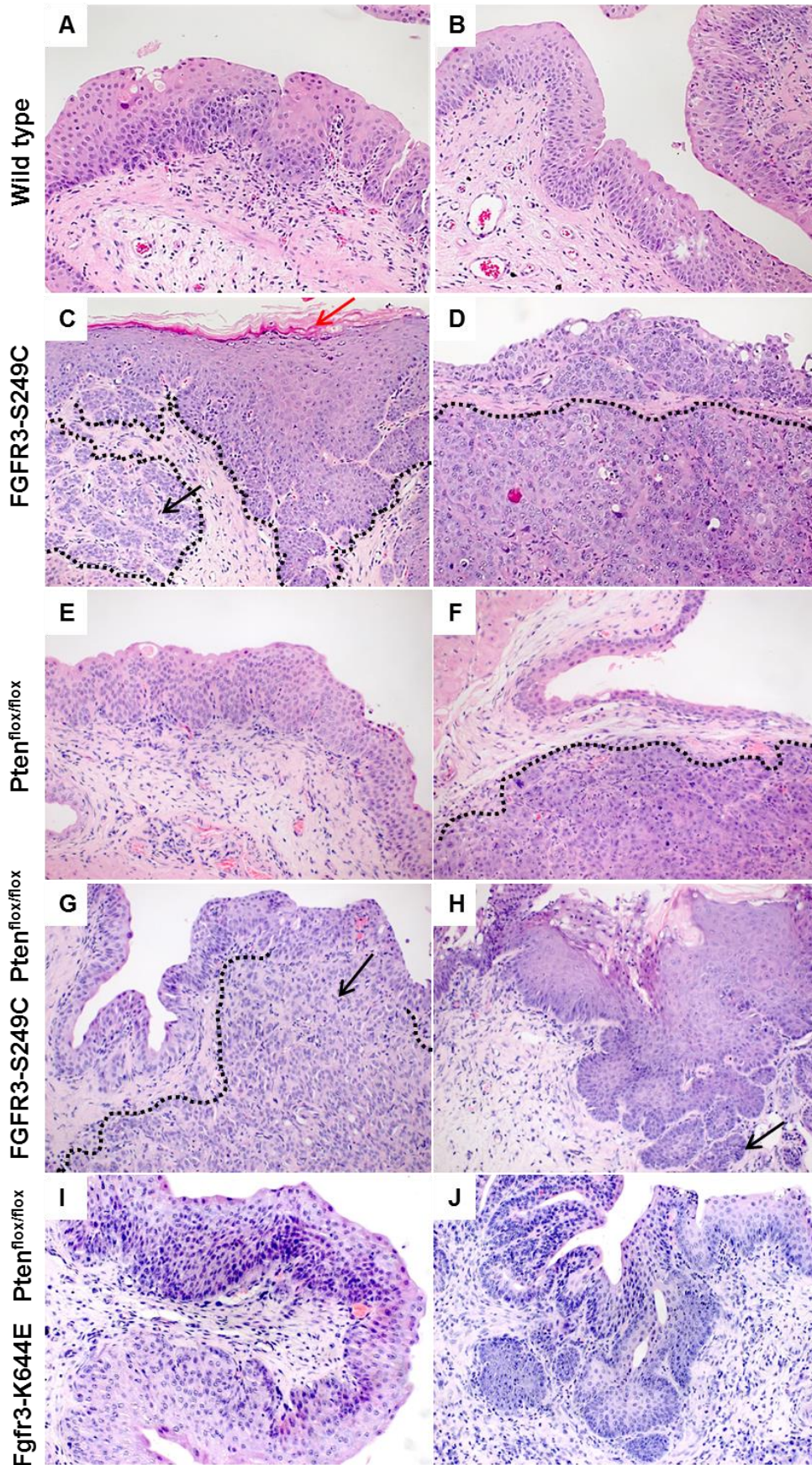


Figure 5-3: OH-BBN treated urothelia after 10+10 weeks

Two examples per genotype of *Wild type*, *FGFR3-S249C*, *Pten*, *FGFR3-S249C Pten* and *Fgfr3-K644E Pten* stained by H&E. Dotted lines represent invasive edge of tumour cells with neighbouring stroma. Scale bar represents 100 μ m (A-J).

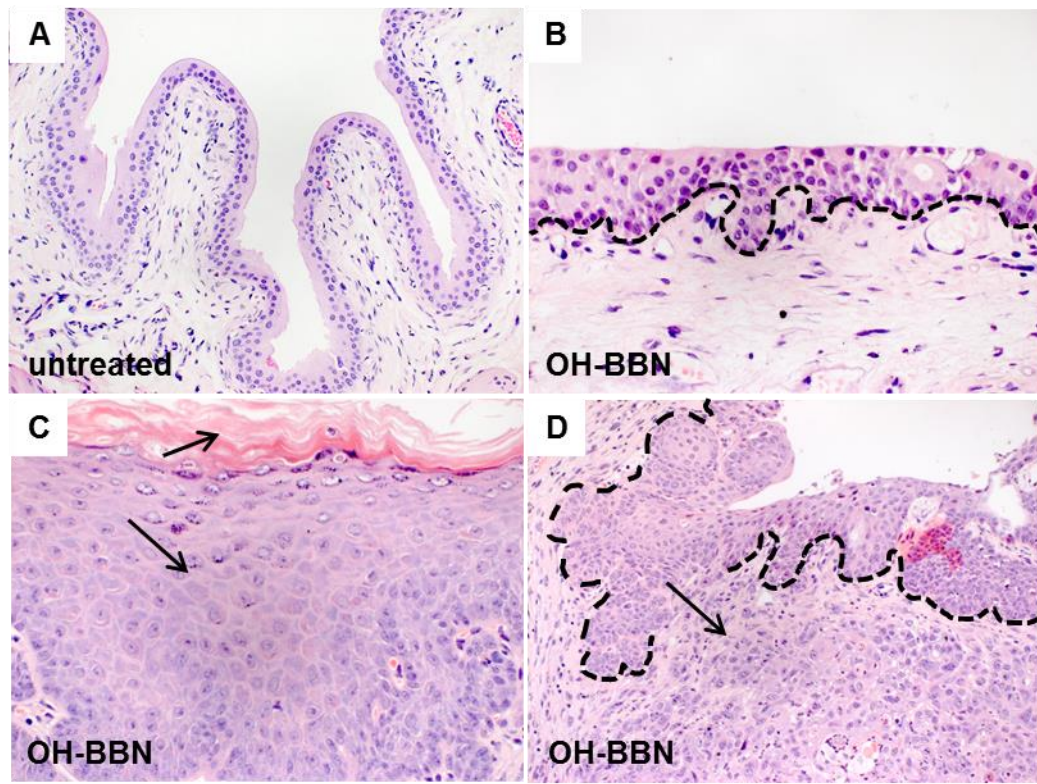


Figure 5-4: Abnormal features in *FGFR3-S249C* at high magnification upon OH-BBN treatment

Untreated *FGFR3-S249C* (A) and OH-BBN-treated *FGFR3-S249C* (B-D) sections stained by H&E showing CIS in the urothelium with lobulation (B), squamous cell transformation with keratinisation (C) and invasion through the basement membrane (D). Dotted line indicates basement membrane. Scale bar represents 100 μm in A, D and 50 μm in B, C.

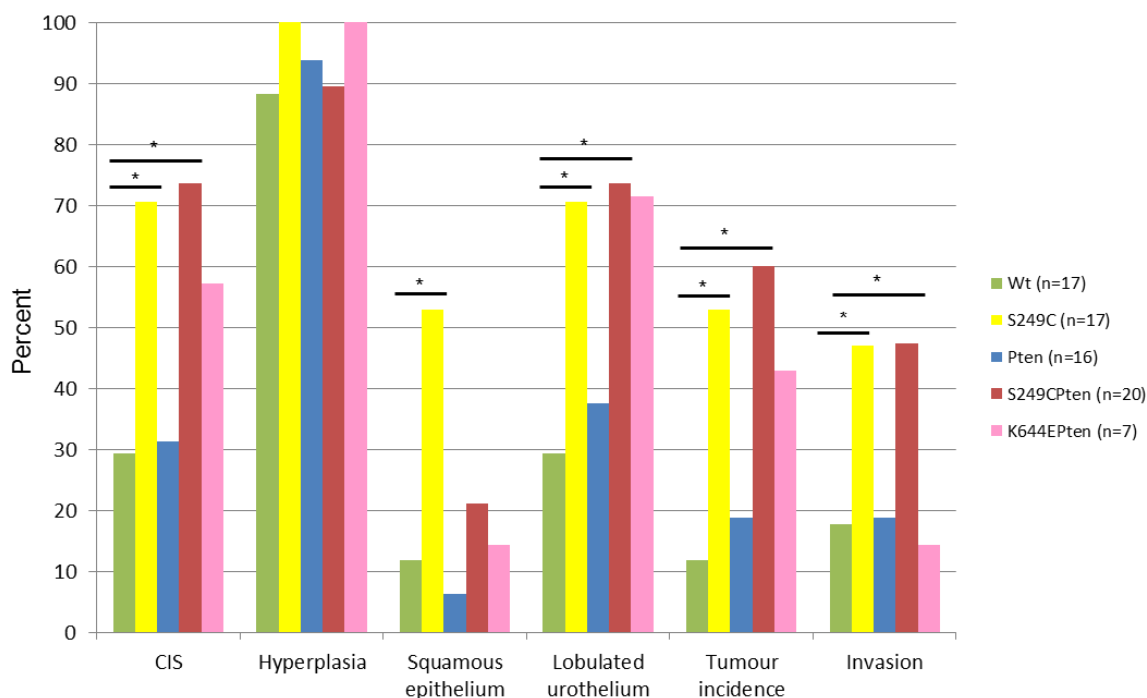
Next we scored the presence of carcinoma *in situ* (CIS), hyperplasia, keratinised squamous epithelium, lobulation of the urothelium-stroma boundary, tumour incidence and invasion in bladders of *Wild type* (n=17), *FGFR3-S249C* (n=17), *Pten* (n=16), *FGFR3-S249C Pten* (n=19) and *Fgfr3-K644E Pten* (n=7) after 10+10 weeks of OH-BBN exposure Table 5-3 and Figure 5-5).

A significantly higher incidence of CIS was observed in *FGFR3-S249C* (71%) and *FGFR3-S249C Pten* (74%) compared to *Wild type* (29%) (Pearson Chi-Square, $p=0.015$ and $p=0.018$ respectively). The incidence of CIS in *Fgfr3-K644E Pten* was also higher (57%), but did not reach significance compared to *Wild type*. Hyperplasia was observed in the majority of samples across all genotypes. Keratinising squamous metaplasia was significantly more frequent in *FGFR3-S249C* (53%) compared to *Wild type* (12%) ($p=0.026$). Lobulation of the urothelium-stroma boundary was more often seen in *FGFR3-S249C* (71%) ($p=0.038$), *FGFR3-S249C Pten* (74%) ($p=0.018$) and *Fgfr3-K644E Pten* (71%; NS) compared to *Wild type* (29%). Tumours occurred significantly more often in *FGFR3-S249C* (53%) ($p=0.026$), *FGFR3-S249C Pten* (60%) ($p=0.006$) and *Fgfr3-K644E Pten* (43%; NS) compared to *Wild type* (12%). Invasion was more often seen in *FGFR3-S249C* (47%) ($p=0.024$) and *FGFR3-S249C Pten* (47%) ($p=0.031$) compared to *Wild type* (12%). In *Fgfr3-K644E Pten* invasion was at a similar frequency (14%) compared to *Wild type* (12%).

Table 5-3: Histological changes of OH-BBN-treated mouse cohorts (“10+10 weeks”)

Mice were subjected to 0.05% w/v N-butyl-N-(4-hydroxybutyl)-nitrosamine for 10 weeks, followed by 10 weeks of normal drinking water. *Initially we generated n=20 *UrollCre Tg(Uroll-hFGFR3IIIbS249C) Pten^{flox/flox}* animals. One was found dead with a bladder tumour, which was not included into histological analysis with the other n=19. However, it was counted for “tumour incidence” with a total of 12 out of 20 animals.

Genotype	n	Carcinoma in situ (CIS)	Hyperplasia	Squamous epithelium	Lobulation	Tumour incidence	Invasion
<i>Wild type</i>	17	5 (29%)	15 (88%)	2 (12%)	5 (29%)	2 (12%)	2 (12%)
<i>Tg(Uroll-hFGFR3IIIbS249C)</i>	17	12 (71%)	17 (100%)	9 (53%)	12 (71%)	9 (53%)	8 (47%)
<i>UrollCre Pten^{flox/flox}</i>	16	5 (31%)	15 (94%)	1 (6%)	6 (38%)	3 (19%)	3 (19%)
<i>UrollCre Tg(Uroll-hFGFR3IIIbS249C) Pten^{flox/flox}</i>	19	14 (74%)	17 (89%)	4 (21%)	14 (74%)	12 out of 20 (60%)*	9 (47%)
<i>UrollCre Fgfr3^{+ / K644E} Pten^{flox/flox}</i>	7	4 (57%)	7 (100%)	1 (14%)	5 (71%)	3 (43%)	1 (14%)

**Figure 5-5: Frequency of histological features and tumour formation in OH-BBN-treated cohorts after 10+10 weeks**

Wild type (Wt, green), *FGFR3-S249C* (S249C, yellow), *UrollCre Pten^{flox/flox}* (Pten, blue), *FGFR3-S249C Pten^{flox/flox}* (S249CPten, red) and *Fgfr3-K644E Pten^{flox/flox}* (K644EPten, pink). CIS= Carcinoma *in situ*

5.5 *Fgfr3* K644E mutation increases sensitivity to tumourigenesis after long-term OH-BBN exposure

In order to examine the effects of *Fgfr3* mutation on malignant progression towards potential metastatic development, we subjected a small cohort of *UroIICre Fgfr3^{+K644E}* mice (*Fgfr3-K644E*, n=7) as well as *Controls* (n=6) to 0.05% w/v OH-BBN for 20 weeks continuously without a following water period (“20 weeks”) (Table 5-4 and Figure 5-6). We also generated cohorts of *UroIICre Pten^{flox/flox}* (*Pten*, n=7) and *UroIICre Fgfr3^{+K644E} Pten^{flox/flox}* (*Fgfr3-K644E Pten*, n=6) that were subjected to the same OH-BBN time schedule. At the time of writing, no *FGFR3-S249C* mice had been treated for 20 weeks continuously due to insufficient numbers.

It has to be noted that the mice in this experiment were 4-9 months older than the mice that were previously treated for 10+10 weeks, starting the treatment at 8-11 months of age. The term “*Control*” in this 20-weeks experiment as opposed to “*Wild type*” in other Chapters refers to mice of C57Bl/6 and mice with presence of T2/Onc3 which does not lead to any bladder phenotype by itself.

CIS was most frequently observed in *Wild type* (100%) and *Pten* (100%), compared to *Fgfr3-K644E* (86%) and *Fgfr3-K644E Pten* (67%). Hyperplasia was observed most frequently in *Fgfr3-K644E* (100%), *Pten* (100%) and *Fgfr3-K644E Pten* (100%), compared to *Wild type* (67%). Squamous transformation was more frequently seen in *Fgfr3-K644E* (86%), *Pten* (57%) and *Fgfr3-K644E Pten* (50%), compared to *Wild type* (33%). The difference in squamous cell transformation between *Fgfr3-K644E* and *Wild type* was statistically significant (p=0.029, Pearson Chi-Square test). Lobulation of the urothelium-stroma boundary was more often seen in *Fgfr3-K644E* (100%) and *Fgfr3-K644E Pten* (100%) compared to *Wild type* (50%) and *Pten* (86%). Tumours were more frequently seen in *Fgfr3-K644E* (71%) than in *Wild type* (33%), *Pten* (57%) and *Fgfr3-K644E Pten* (50%). Invasion was also more often seen in *Fgfr3-K644E* (71%) than in *Wild type* (17%), *Pten* (57%) and *Fgfr3-K644E Pten* (50%).

Apart from the incidence of squamous cell transformation, there was no significance in the distribution across the cohorts, which may be due to the small number of animals.

Table 5-4: Histological changes of OH-BBN-treated mouse cohorts (“20 weeks”)

Mice were subjected to 0.05% w/v N-butyl-N-(4-hydroxybutyl)-nitrosamine for 20 weeks continuously.

Genotype	n	Age at start of treatment	Carcinoma in situ (CIS)	Hyperplasia	Squamous epithelium	Lobulation	Tumour incidence	Invasion
Control	6	8 months	6 (100%)	4 (67%)	2 (33%)	3 (50%)	2 (33%)	1 (17%)
<i>UroIICre Fgfr3^{+/K644E}</i>	7	9-11 months	6 (86%)	7 (100%)	6 (86%)	7 (100%)	5 (71%)	5 (71%)
<i>UroIICre Pten^{flox/flox}</i>	7	6-11 months	7 (100%)	7 (100%)	4 (57%)	6 (86%)	4 (57%)	4 (57%)
<i>UroIICre Fgfr3^{+/K644E} Pten^{flox/flox}</i>	6	7-11 months	4 (67%)	6 (100%)	3 (50%)	6 (100%)	3 (50%)	3 (50%)

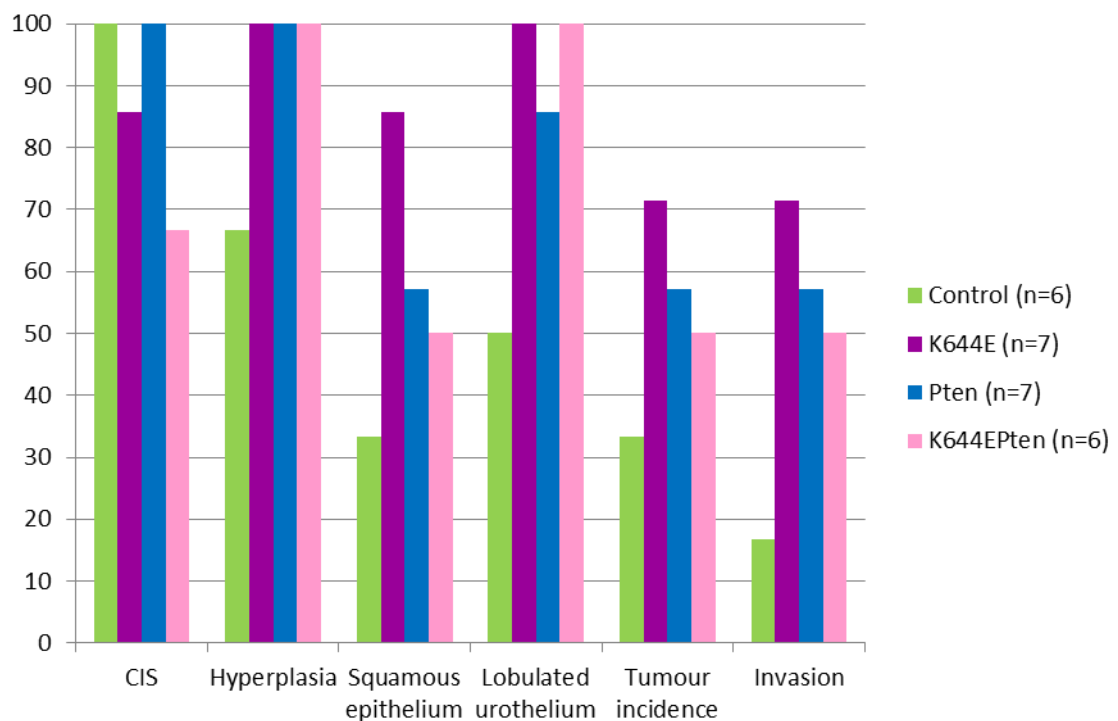


Figure 5-6: Frequency of histological features and tumour formation in OH-BBN-treated cohorts with *Fgfr3* K644E mutation after 20 weeks continuously

Control (green), *UroIICre Fgfr3^{+/K644E}* (purple), *UroIICre Pten^{flox/flox}* (blue), *UroIICre Fgfr3^{+/K644E} Pten^{flox/flox}* (pink). CIS= Carcinoma *in situ*

Next we examined proliferation, expression of cell cycle regulating genes, as well as expression of markers indicating epithelial-to mesenchymal transition (EMT) in OH-BBN-induced tumours. *Fgfr3-K644E* mutant bladders, with a high incidence of tumours, were used as an example (Figure 5-7).

Ki67 expression was seen at low levels in the untreated *Fgfr3-K644E* urothelium (A). Increased proliferation was typically found along the basal layer of cells of the transformed urothelium (B) as well as in the tumour mass (D).

p53 expression was low in untreated *Fgfr3-K644E* bladders(D). Following OH-BBN-induced DNA damage, p53 protein was elevated along the basal cell layer as well as in some of the intermediate cells (E). p53 expression had not been lost in most of the invading tumour cells; in fact it seemed to have accumulated in some regions of the tumours (F).

p21 expression was restricted to umbrella cells in untreated *Fgfr3-K644E* bladders (G). Following OH-BBN exposure, a fraction of p53-positive cells, in particular along the basal cell layer, was p21-positive (H). Invading tumour cells also expressed p21 (I, above black dotted line); however, the expression was less intense in areas with high p53 expression (I, between black and white dotted lines). This could indicate that the p53-antibody, particularly noticeable in (I), may have visualised regions with mutant p53 rather than wild type p53, which could explain the lack of p21 induction in those regions.

To visualise breakthrough of the basement membrane as well as the invasive edge, Fascin expression levels were analysed. In the untreated *Fgfr3-K644E* urothelium, Fascin was observed in basal and some intermediate cells (J). Fascin expression was seen along the lobulated urothelium-stroma boundary (K) and marked the invasive edge (L, arrow heads).

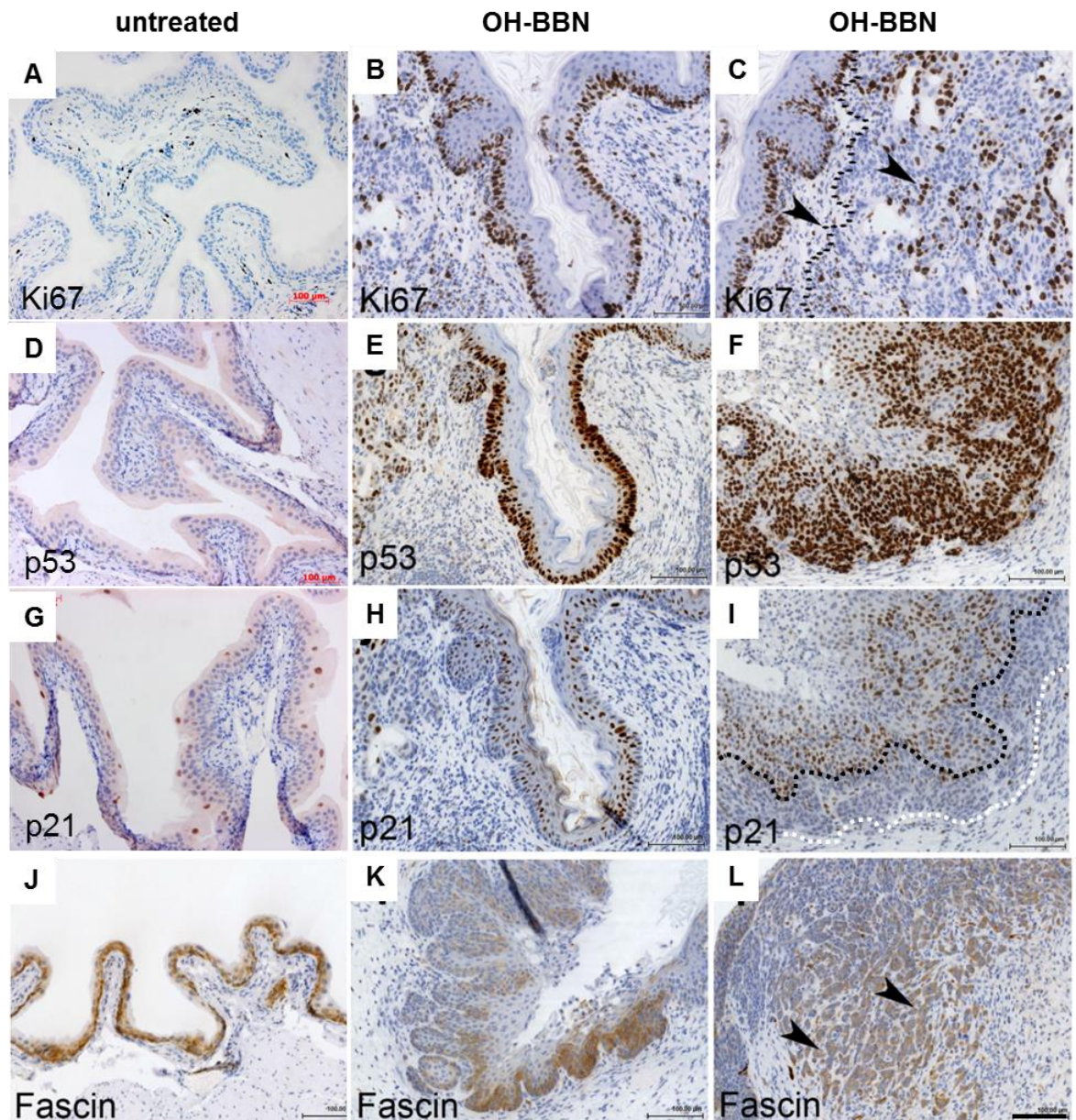


Figure 5-7: Abnormal protein expression in *Fgfr3-K644E* at high magnification after 20 weeks continuous OH-BBN treatment

Immunohistochemistry showing Ki67 (A-C), p53 (D-F) p21 (G-I) and Fascin (J-L) levels of untreated *Fgfr3-K644E* (A, D, G, J) and OH-BBN-treated *Fgfr3-K644E* bladders (B, C, E, F, H, I, K, L). Scale bar represents 100 μ m in A-L.

We further characterised the nature of the tumours by analysing the expression of urothelial layer-specific proteins as well as markers indicative of epithelial-mesenchymal transition (EMT) (Figure 5-8).

Expression of Cytokeratin 5 (CK5), which is normally expressed in basal cells (Castillo-Martin et al., 2010), was seen along the lobulated urothelium-stroma boundary as well as in invading tumour cells (a). Similarly, p63, which is normally expressed in basal and intermediate cells (Castillo-Martin et al., 2010), was seen along the basal layer and in tumour cells (b), indicating that these tumour cells could potentially be of basal cell origin.

Invading cells were also positive for β -catenin (c) and Sox9 (d), indicating that these cells had undergone a change in their genetic program. Loss of membranous E-Cadherin expression was observed in invading cells (e), indicating loss of cell-cell adhesion in the process of malignant progression (Schmalhofer et al., 2009). Invading cells were also positive for ZEB1 (f), further supporting that EMT had occurred.

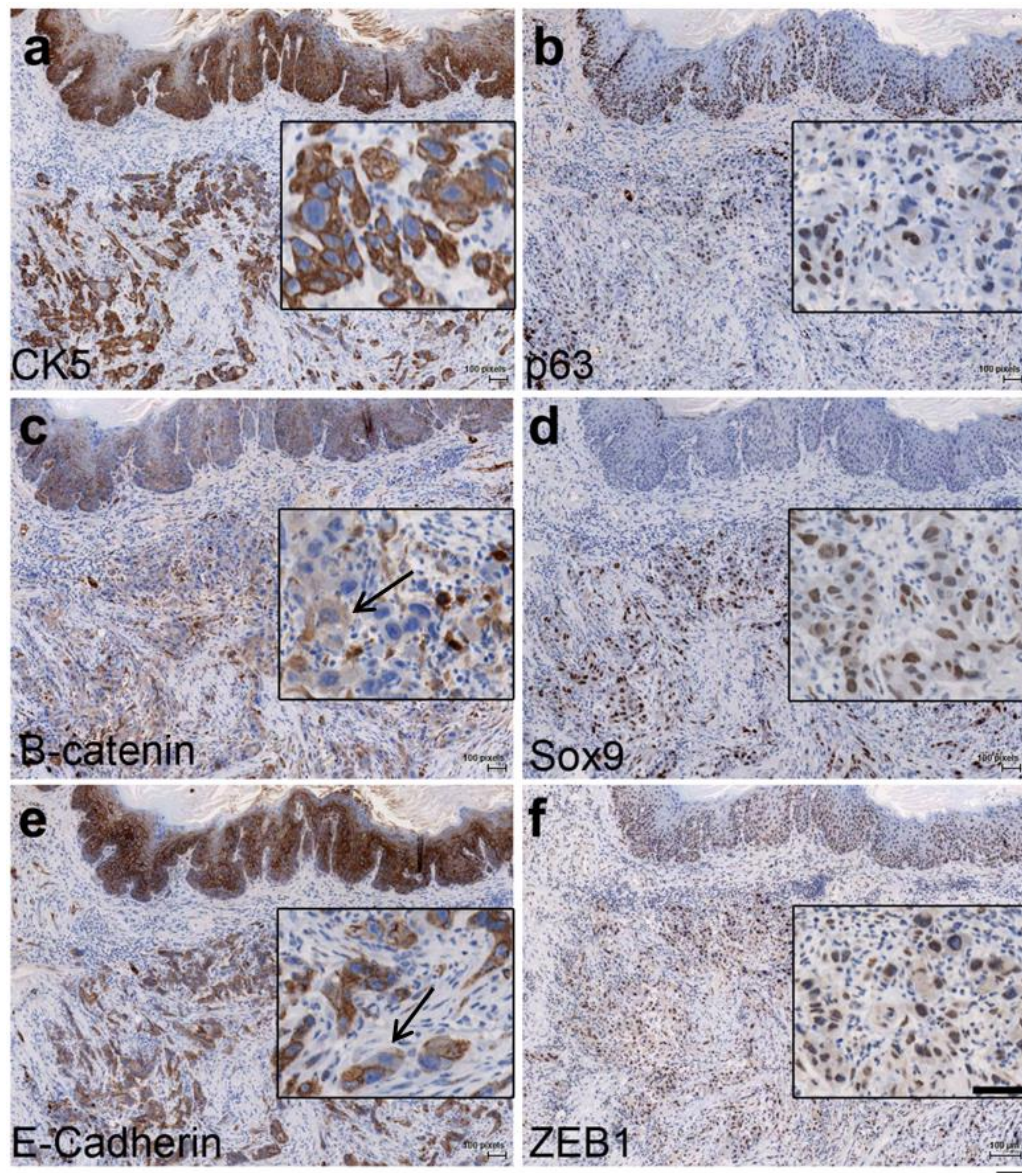


Figure 5-8: The effects of *Fgfr3* K644E mutation in tumour progression upon OH-BBN treatment

Representative sections of the bladders stained for CK5 (a), p63 (b), β -Catenin (c), Sox9 (d) E-Cadherin (e) and ZEB1 (f). Bottom scale bar represents 100 μ m in main pictures a-f. Insert scale bar (f) represents 50 μ m for magnified inserts a-f.

5.6 *FGFR3* S249C mutation promotes pre-neoplastic changes in a time course of OH-BBN exposure

To investigate the difference in tumourigenesis between *Wild type* and *FGFR3*-mutant bladders, we examined the histological changes in the urothelium in response to OH-BBN treatment in a time course over 20 weeks (Figure 5-9 and Figure 5-10).

Bladders of *Wild type* (n=5) and *FGFR3-S249C* (n=5) were compared at two weeks after starting the OH-BBN treatment (Figure 5-9, A and B respectively). Loss of polarity (A, arrows), cellular atypia and pleomorphism (B, circle) and hyperchromatic nuclei (B, arrows), was observed in all examined samples of both genotypes.

Similarly at 6 weeks of OH-BBN treatment all examined *Wild type* (n=5) (C) and *FGFR3-S249C* (n=5) (D) mice additionally displayed frequent mitoses (D, arrow) and dysplasia as indications of CIS in the urothelium.

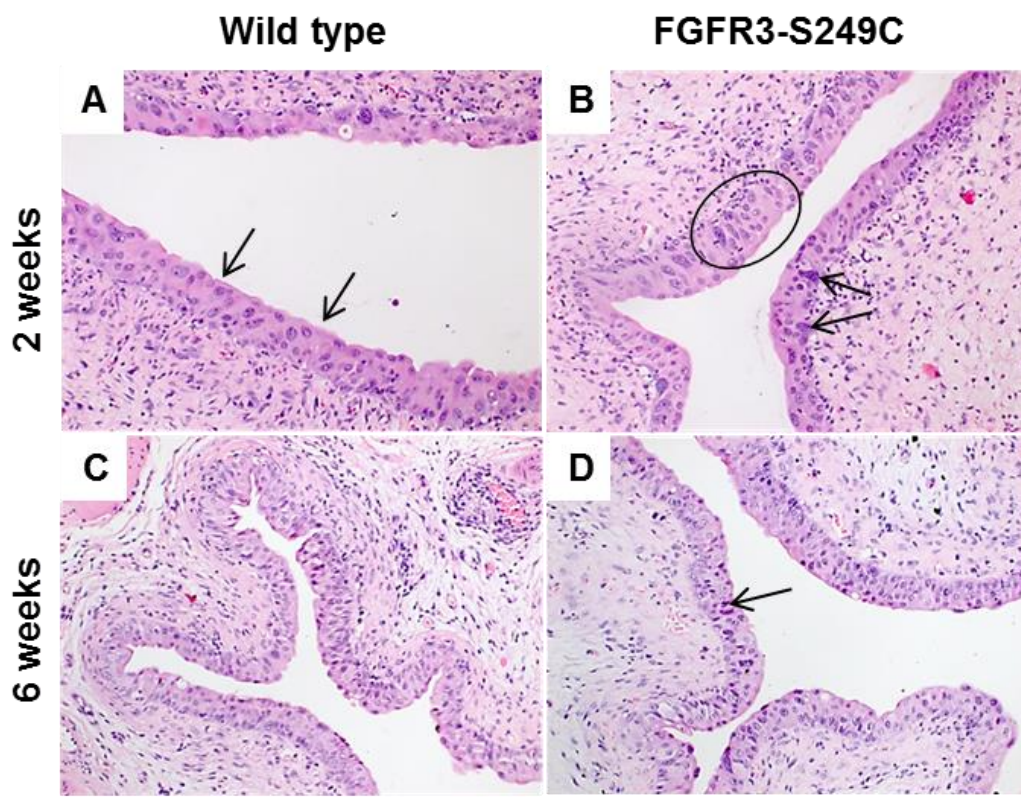


Figure 5-9: Histological changes of *Wild type* and *FGFR3-S249C* bladders after two and six weeks of OH-BBN exposure

Representative H&E sections of *Wild type* and *Tg(Uro11-hFGFR3IIIbS249C)*. Scale bar represents 100 μ m (A-D).

We continued the OH-BBN treatment up to a total of 10 weeks followed by additional 2 weeks of normal drinking water (“10+2 weeks”, Figure 5-10).

Additional features such as hyperplasia (A, B, arrows), squamous cell transformation (C, arrows), and lobulation of the urothelial-stroma boundary (A, B, C, dotted lines) were observed in samples of *Wild type* (n=5) (A), *FGFR3-S249C* (n=5) (B), as well as in *UroIIcre Pten^{flox/flox}* (n=5) (C).

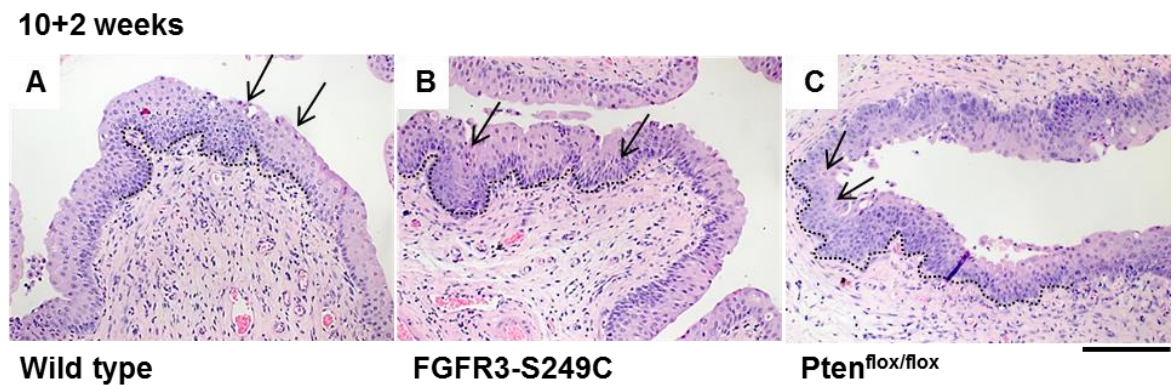


Figure 5-10: Histological changes of *Wild type*, *FGFR3-S249C* and *UroIIcre Pten^{flox/flox}* bladders after 10+2 weeks of OH-BBN exposure

Representative H&E sections of *Wild type* (n=5) and *Tg(UroII-hFGFR3IIIbS249C)* (n=5). Scale bar represents 100 μ m (A-C).

We then scored the presence of carcinoma *in situ* (CIS), hyperproliferation, keratinising squamous metaplasia, lobulation of the urothelium-stroma boundary, tumour incidence and invasion in bladders of *Wild type* (n=5), *FGFR3-S249C* (n=5) and *UroII-Cre Pten^{flox/flox} (Pten)* (n=5) at 10+2 weeks of OH-BBN exposure (Figure 5-11).

CIS was observed in all samples (n=5, 100%) of *Wild type* and *Pten*. *FGFR3-S249C* showed a decrease in CIS, with presence in only 60% of the samples. Hyperplasia was most frequently seen in *FGFR3-S249C* (n=5, 100%) compared to *Wild type* (n=2, 40%) and *Pten* (n=4, 80%). Squamous metaplasia was most frequently observed in *FGFR3-S249C* (n=3, 60%) compared to *Wild type* (n=1, 20%) and *Pten* (n=1, 20%). Lobulation of the urothelium-stroma boundary was also most frequently observed in *FGFR3-S249C* (n=3, 60%) compared to *Wild type* (n=2, 40%) and *Pten* (n=1, 20%). No tumours or signs of invasion were detectable in *Wild type*, *FGFR3-S249C* or *Pten* at 10+2 weeks of OH-BBN exposure.

The distribution was not statistically significant in any of the categories (Pearson Chi-Square test).

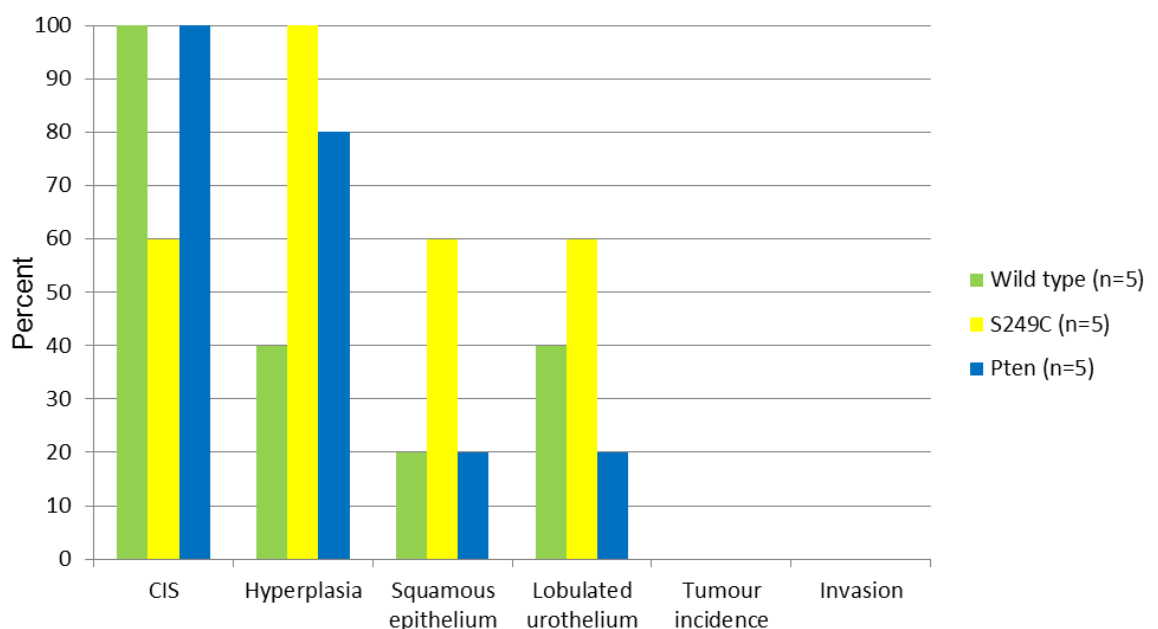


Figure 5-11: Frequency of histological features and tumour formation after 10+2 weeks OH-BBN-treated *Wild type* (green), *Tg(UroII-hFGFR3IIIbS249C)* (S249C, yellow) and *UroII-Cre Pten^{flox/flox} (Pten)* (Pten, blue). CIS= Carcinoma *in situ*

5.7 Analysis of DNA damage in *Wild type* and *FGFR3* mutants

We compared the DNA-damaging effect of OH-BBN on the urothelium of *Wild type* and *FGFR3-S249C* bladders in a time course over 20 weeks (Figure 5-12).

In the absence of carcinogen treatment, γ H2aX phosphorylation was seen in *Wild type* bladders (n=3 out of 3) (A) as well as in *FGFR3-S249C* bladders (n=3/3) (B) at low levels. In two out of three untreated *Wild type* samples (n=2/3), γ H2aX positivity was observed throughout all layers of the urothelium in (A). In untreated *FGFR3-S249C* bladders (n=3/3), γ H2aX phosphorylation was mainly observed in the umbrella cells, but not in intermediate or basal cells (B).

At two weeks of OH-BBN treatment, strong phosphorylation of γ H2aX was detected in *Wild type* (n=2/2) (C), as well as in *FGFR3-S249C* (n=2/3) (D), indicating a high incidence of double strand breaks.

Similarly, at six weeks of OH-BBN treatment, γ H2aX phosphorylation was seen at high levels in *Wild type* (n=3/3) (E), as well as in *FGFR3-S249C* (n=2/3) (F), which was overall comparable with the γ H2aX phosphorylation level at two weeks of OH-BBN exposure (C-D).

At ten weeks of OH-BBN exposure followed by two weeks of normal drinking water (10+2 weeks), a decrease in γ H2aX phosphorylation was observed in *Wild type* (n=2/3) (G), as well as in *FGFR3-S249C* (n=2/3) (H) compared to γ H2aX phosphorylation at two and six weeks (C-F). Cells that had undergone squamous transformation in *FGFR3-S249C* (n=1/3) were negative for γ H2aX (H, black arrow); whereas cells along the lobulated urothelium-stroma boundary were positive (H, red arrow).

At ten weeks of OH-BBN exposure followed by ten weeks of normal drinking water (10+10 weeks), two tumours had developed in *FGFR3-S249C*, which showed high levels of γ H2aX (J, red arrows, n=2/2). No tumours had developed in the *Wild type* cohort at this point, where therefore no comparison of γ H2aX phosphorylation levels could be made. In areas of *Wild type* samples that retained relatively normal urothelium, γ H2aX phosphorylation was present

(n=3/3) (I), however at much lower levels compared to *Wild type* samples at two- or six-weeks of treatment (C, E). *FGFR3-S249C* urothelia underwent more dramatic changes, such as hyperplasia or CIS with varying γ H2aX phosphorylation in each sample (n=3 total), which requires to be addressed in future experiments in order to generate conclusive data.

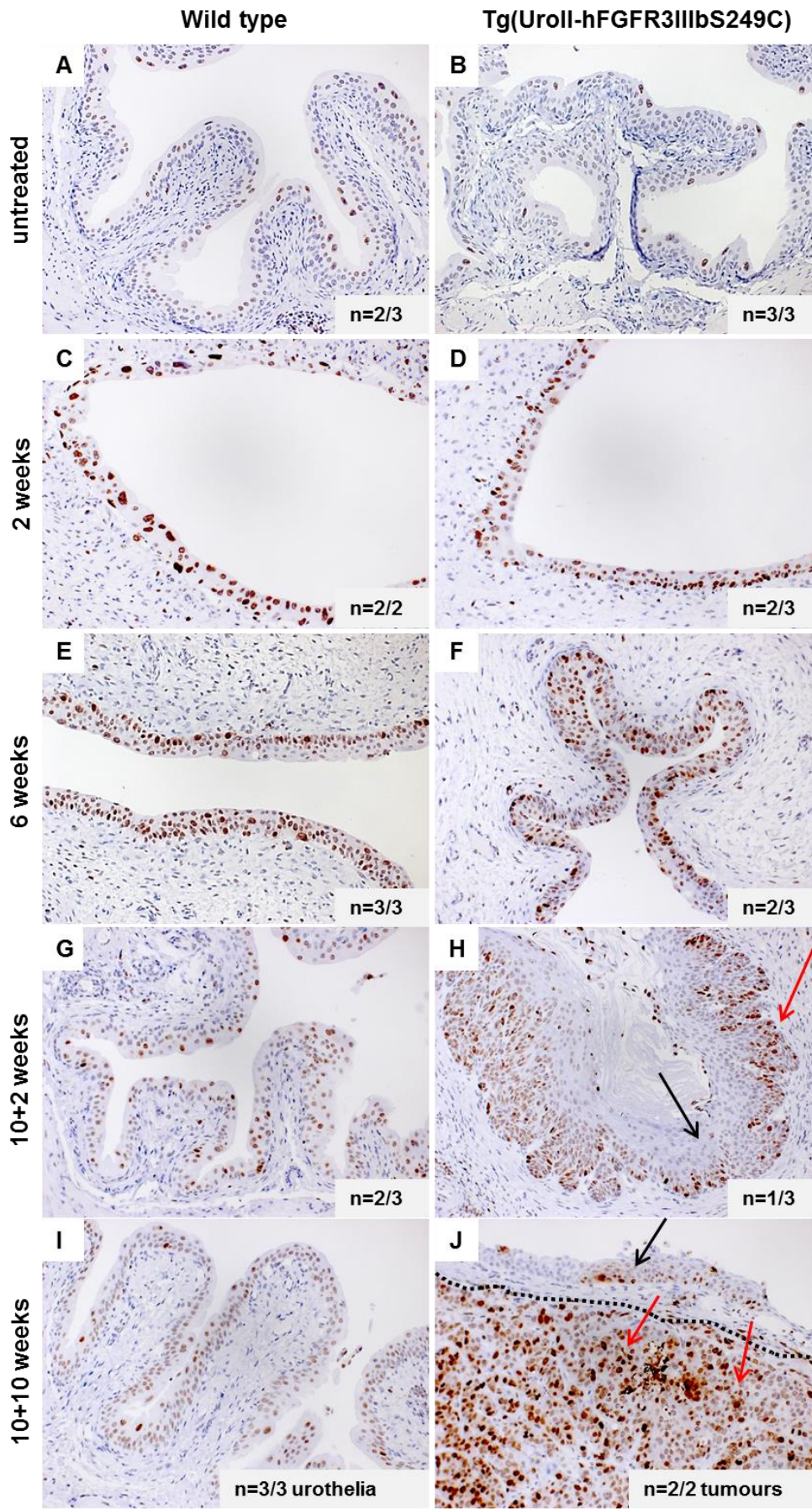


Figure 5-12: Double-strand breaks upon OH-BBN treatment

Immunohistochemistry for γ H2aX in bladders of *Wild type* (A, C, E, G, I) and *Tg(UroII-hFGFR3IIIbS249C)* (B, D, F, H, J). Scale bar represents 100 μ m (A-J).

5.8 Discussion

To address the question whether an *FGFR3* mutation could predispose urothelial cells to tumourigenesis, and to evaluate its role in tumour progression, we subjected *Fgfr3*- and *FGFR3*-mutant as well as *Wild type* mice to a bladder-specific carcinogen, N-butyl-N-(hydroxybutyl)-nitrosamine (OH-BBN). We compared two different point mutations in *Fgfr3* and *FGFR3*, as well as the effect of *Pten* deletion and *Fgfr3-Pten* double mutation in OH-BBN-induced tumours.

5.8.1 Tg(UroII-hFGFR3IIIbS249C) line

The generation of *FGFR3-S249C* transgenic mice revealed that mice carrying the *FGFR3-S249C* transgene retained a histologically normal urothelial appearance at 12 months (Figure 5-2), consistent with our observations with heterozygous *Fgfr3 K644E* knock-in mutation in the urothelium (Ahmad et al., 2011c). In the presence of either of the two *Fgfr3* mutations, the proliferation rate in the urothelium was similarly low as in *Wild type*. Furthermore, *FGFR3* expression levels were comparable between both genotypes and compared with *Wild type*. These results support our previous experiments, suggesting that *FGFR3* activation by itself is not able to induce urothelial pathogenesis.

In contrast to *UroIIcre Fgfr3^{+/K644E} Pten^{flox/flox}* bladders, where significant increase in urothelial thickness and severe cell-morphological changes were observed (Chapter 3), we did not see any urothelial abnormalities in *UroIIcre FGFR3-S249C Pten^{flox/flox}* bladders (Figure 5-3). *FGFR3-S249C Pten^{flox/flox}* urothelia showed no similarities to *UroIIcre Fgfr3^{+/K644E} Pten^{flox/flox}*, which suggests that activated FGFR-signalling with a *K644E* mutation is more potent than an *S249C* mutation to induce urothelial cell changes in a *Pten* deficient background in a non-tumour context.

In the comparison of the two *FGFR3* mutations, *S249C* and *K644E*, it needs to be noted that Tg(UroII-hFGFR3IIIbS249C) is a transgene (see Methods, Chapter 2.3), which is expressed in addition to endogenous *FGFR3* levels. *UroIIcre Fgfr3^{+/K644E}* on the other hand is a knock-in construct, generating a heterozygous activating mutation at the expense of one endogenous *Fgfr3* copy (Iwata et al., 2000,

Ahmad et al., 2011c). Furthermore, *FGFR3-S249C* generates human recombinant FGFR3 protein in the mouse bladder, whereas *UroIIICre Fgfr3^{+/K644E}* produces FGFR3 protein of murine origin. Both *S249C* and *K652E* have been shown to be able to transform NIH-3T3 cells, but to have no obvious effect on normal urothelial cells in culture (di Martino et al., 2009).

Although both *K644E* and *S249C* mutation lead to highly activated FGFR3 signalling, their mechanisms may be different and could explain the different urothelial phenotypes seen in our *in vivo* studies. *K644E* mutation leads to a conformational change in the receptor that favours autophosphorylation (Naski et al., 1996). It has been suggested that *K644E* mutation may therefore deregulate a mechanism for controlling the kinase activity (Naski et al., 1996), which may possibly result in differential downstream signalling activation. *S249C* on the other hand triggers constitutive receptor dimerisation as a result of a higher level of disulfide bond formation (d'Avis et al., 1998, di Martino et al., 2009). This may lead to a different shape of the FGFR3 protein and could affect receptor function or preference in binding to certain adapter proteins downstream.

S249C may be of greater clinical relevance since it accounts for ~66% of human non-invasive urothelial cell carcinoma with *FGFR3* mutant status (Tomlinson et al., 2007a, Duenas et al., 2013, Bernard-Pierrot et al., 2006).

5.8.2 *FGFR3* mutation increases sensitivity to tumourigenesis after OH-BBN exposure

In response to OH-BBN treatment, and regardless of the nature of additional genetically introduced mutations, the urothelia underwent a number of pre-neoplastic changes, such as loss of polarity, cellular atypia and pleomorphism, hyperchromatic nuclei, frequent mitoses and dysplasia as indications of carcinoma *in situ* (CIS) (Figure 5-4). Keratinising squamous metaplasia, which is considered rather a pre-neoplastic condition, is infrequently found in human bladder biopsies in the UK (Ahmad et al., 2008). However, it may pose a risk of malignant transformation to invasive bladder cancer (Guo et al., 2006). In fact, squamous cell transformation, which is a neoplastic condition, frequently co-occurs with urothelial cell carcinoma at an advanced stage at the time of

diagnosis, and it is associated with enhanced expression of EGFR and p53 (Guo et al., 2006).

Strikingly, after 10+10 weeks of OH-BBN treatment we found that *FGFR3 S249C* mutation can promote malignant progression in carcinogen-induced bladder tumours (Figure 5-3 and Figure 5-4). *FGFR3* mutated mice exhibited a 2.4-fold higher incidence of CIS and a 4.4-fold higher incidence of squamous cell transformation upon administration of OH-BBN compared to *Wild type* controls. They also showed a 4.4-fold higher incidence of tumour formation and 3.9-fold higher incidence of invasion. The urothelium showed characteristics of advanced tumours including breakthrough of the basement membrane and expression of Fascin (Karasavvidou et al., 2008). It is therefore possible that *FGFR3* mutation predisposes urothelial cells to tumourigenesis or acts as a tumour promoter in already established neoplasms. This could be of relevance to the prognosis of patients with a bladder tumour with *FGFR3* mutation, as FGFR3 signalling may provide a growth advantage to the cells and may drive progression of an existing tumour towards muscle invasion. In human invasive bladder cancer, wild type FGFR3 is frequently found overexpressed (Tomlinson et al., 2007a). However, we have not addressed FGFR3 expression levels in our carcinogen-induced mouse tumour model with *FGFR3* mutation.

Surprisingly, we observed a lower incidence of tumour formation and invasion as well as lower incidence of CIS and squamous metaplasia in *UroIIICre Pten^{flox/flox}* compared to *FGFR3-S249C*, suggesting that the presence of an *FGFR3 S249C* mutation promotes tumourigenesis upon OH-BBN exposure considerably more than *Pten* loss. In fact, the frequency of these features in *UroIIICre Pten^{flox/flox}* was overall similar to OH-BBN-treated *Wild type* mice. It is possible that MAPK activation may be more potent than Akt activation in order to promote progression of an existing tumour.

This was also supported by the fact that *FGFR3 S249C* in combination with *Pten* deletion (*FGFR3 S249C Pten^{flox/flox}*) had a higher incidence in tumour formation as well as CIS, squamous cell transformation, lobulation and invasion than *UroIIICre Pten^{flox/flox}* alone, emphasising the potent effect of *FGFR3 S249C* on malignant progression (Figure 5-5). A similar trend was observed for *Fgfr3 K644E* in combination with *Pten* deletion treated for 10+10 weeks (Figure 5-5).

Although not significant, these mice also showed a higher incidence of CIS and tumour formation compared to *Pten* only. These results indicate that an *Fgfr3* *K644E* mutation may have a similar effect towards malignant progression as *FGFR3* *S249C* in the presence of *Pten* deletion. However, at the time of writing there were no OH-BBN-treated *UroIIcre Fgfr3^{+K644E}* mice available for a direct comparison between *S249C* and *K644E* mutation upon OH-BBN treatment in tumour progression.

Using a treatment schedule where OH-BBN was administered for 20 weeks continuously, *Fgfr3* *K644E* also showed 2-fold increase in tumourigenesis, a 2.5-fold increase in squamous metaplasia and a 4-fold increase in invasion compared to *Wild type* (Figure 5-6). This result supports the suggestion that *Fgfr3* mutation is likely to play a role in carcinogen-induced bladder cancer in mice, and that *Fgfr3* mutation may be involved in promotion of squamous cell transformation as well as invasion. A similar trend was observed in *UroIIcre Pten^{flox/flox}* urothelia as well as both *Fgfr3* and *Pten* mutations in combination. It has to be noted that a longer OH-BBN protocol was used, the number of animals was too low for statistically solid conclusions, and that the mice in this experiment were older than the mice that were previously treated for 10+10 weeks. In a recent study, where *Secreted Protein Acidic and Rich in Cysteine (Sparc)*-deficient mice were treated for 25 weeks continuously with OH-BBN, mice showed decreased survival and accelerated urothelial pathology with metastasis to the lymph nodes and lungs (Said et al., 2013). It would be interesting to extend our current treatment protocol to a time where metastases occur in the animal model in order to investigate the effect of *FGFR3* mutation in late stages of cancer progression.

5.8.3 DNA damage response upon OH-BBN

Although no obvious phenotypic difference was evident by H&E staining between *Wild type* and *FGFR3* *S249C* mutant bladders, we examined the urothelia at the molecular level to see whether the sensitivity to DNA damage or the DNA repair machinery is altered in *FGFR3*-mutant cells (Figure 5-12). Due to the small number of samples no conclusive statement could be made. However, in two out of three untreated *Wild type* samples, γ H2aX positivity was observed throughout all layers of the urothelium, whereas in untreated *FGFR3-S249C* bladders, γ H2aX phosphorylation was mainly observed in the umbrella cells but not in

intermediate or basal cells in three out of three samples. Whether this indicates a possible difference between *Wild type* and *FGFR3 S249C* in frequency and location of urothelial cells carrying double strand breaks remains to be addressed in future experiments. It would also be interesting to include γ H2aX levels of *Fgfr3 K644E* mutant bladders in future analyses.

Upon carcinogen exposure, γ H2aX phosphorylation was the highest at 2-6 weeks of OH-BBN treatment in both *Wild type* and *FGFR3-S249C*. When the carcinogen was removed after 10 weeks of OH-BBN treatment and the mice were continued on normal drinking water, the bladders showed a mild decrease in γ H2aX phosphorylation in samples from 10+2 and 10+10 weeks. This may be due to elimination of cells with DNA damage alongside urothelial hyperproliferation, resulting in increased production of new cells with intact DNA. Interestingly, in other organs such as the intestine, cells with DNA damage are eliminated and renewed after 4-5 days (van der Flier and Clevers, 2009). In the bladder, presumably due to the slow turnover rate of the urothelium (Khandelwal et al., 2009), these cells were still present even 10 weeks after OH-BBN-induced DNA damage. Due to the difference in the number of tumours that had formed in *FGFR3 S249C* but not in *Wild type*, no comparison could be made in terms of expression level and pattern of γ H2aX in the tumour cells. Future experiments could also include Western blotting in order to examine γ H2aX phosphorylation levels; however the separation of the urothelium from the bladder wall in mice is technically challenging and the amount of cells is usually low or insufficient for protein extraction.

5.8.4 OH-BBN as a tool to induce invasive bladder cancer in mice

OH-BBN provides a reliable tool to induce urothelial cell carcinoma in mice, since it resembles human bladder cancer not only histologically, but also at a molecular level (Becci et al., 1981, Yao et al., 2004). They are generally of highly invasive nature and often show a mixed histology with features of both urothelial cell carcinoma and squamous cell differentiation (Becci et al., 1981). Molecularly, OH-BBN tumours frequently carry mutations in genes that regulate major signalling pathways such as p53, RAS, EGFR and TGF- β (Yao et al., 2004). Despite the fact of systemic distribution by administration through gavage or drinking water, the carcinogen appears to induce mutations in an organ-specific

manner (He et al., 2012). However, a limitation of carcinogen-induced mutagenesis is that the DNA damage occurs in a random fashion. Therefore, OH-BBN cannot induce specific DNA mutations, which may be desired in an experimental setting.

Exposure to chemical carcinogens is one of the risk factors of developing bladder cancer. It is estimated that more than one third of bladder tumours are associated with cigarette smoking (Parkin, 2011). Smoking appears to influence *p53* mutation status and is associated with invasive, high-grade bladder cancer (Wallerand et al., 2005). In contrast, *FGFR3* mutations are not associated with smoking and may result from endogenous DNA damage (Wallerand et al., 2005). Our data show that *FGFR3* does have an effect on progression of existing tumours in mice. It is possible that in humans *FGFR3* mutation as an early event may initially help the tumour to progress, and that it is lost later at a more advanced stage of the tumour.

5.8.5 Future work

Firstly, it would be interesting to confirm in a larger cohort of carcinogen-induced *Fgfr3*-mutant mice whether *Fgfr3 K644E* mutation has an effect similar to *FGFR3 S249C* in accelerating bladder tumour formation.

Secondly, further studies of the *FGFR3* signalling pathway are essential and will aid the development of therapies for both non muscle-invasive and muscle-invasive bladder cancer with deregulation of FGF signalling. For example, it would be essential to test the effect of *FGFR3* inhibitors on OH-BBN-induced *FGFR3-S249C* bladder tumours. This could be done *in vitro* and *in vivo*. FGF signalling inhibitors have been developed and applied in many cancer types (Brooks et al., 2012). Inhibition of *FGFR* has been suggested as a therapeutic option in urothelial cell carcinoma (Lamont et al., 2011, Tomlinson et al., 2007b, Network, 2014). Several novel drugs against *FGFRs* including R3Mab (Qing et al., 2009), BGJ398 (Guagnano et al., 2011) and AZD4547 (Gavine et al., 2012) have been shown to be effective in cell lines and xenograft models. For a translational benefit, further studies of the *FGFR3* signalling pathway and its inhibitors are therefore essential. However, it has to be kept in mind that

inhibition of the FGFR3 pathway may trigger EGFR activation (or other pathway activation) as an escape mechanism (Herrera-Abreu et al., 2013).

Lastly, it would be interesting to identify *FGFR3*-cooperating mutations that can promote tumour progression alongside FGFR3. This could be elucidated by exome sequencing of OH-BBN-induced tumours of *Fgfr3* mutant bladders, which would help to identify molecular events that occur together with *Fgfr3* mutation to drive urothelial cell carcinoma or potentially further aid progression.

5.8.6 Conclusion

Altogether, the present results demonstrate that an *FGFR3 S249C* mutation alone does not lead to tumourigenesis in the urothelium, similar to *Fgfr3 K644E* mutation alone. Differential effects between *K644E* and *S249C* on the cellular architecture were only apparent in combination with another mutation such as *Pten* deletion. Moreover, our results indicate that *FGFR3* can predispose urothelial cells to tumourigenesis or can even act as an active tumour promoter in already established neoplasms. This could be of relevance to the prognosis of patients with a high-grade bladder tumour with *FGFR3* mutation, as FGFR3 signalling may provide a growth advantage to the cells and may drive progression of an existing tumour towards muscle invasion.

Chapter 6

Technological improvement of an invasive bladder cancer model

6.1 Introduction

6.1.1 AdenoCre

Given that UroII^{Cre} recombination appeared to be missing the basal cells which have been a putative cell origin for urothelial cell carcinoma, we next wished to use a model where basal cells can be targeted. Moreover, due to UroplakinIII expression in other tissues, some of our previous UroII^{Cre} models had developed tumours in the skin and lung (Ahmad et al., 2011c). This may indicate a later cancer onset in the bladder and therefore require more specific recombination in a smaller number of urothelial cells to allow the emergence of bladder tumours.

Most urothelial Cre promoters, including the fatty acid-binding protein (Fabp), Sonic hedgehog (Shh), Cytokeratin 5 (CK5), p63 (Δ Np63) and Uroplakin-II (UroII) also drive the expression of the recombinase in other tissues. For example, the Fabp promoter drives Cre expression in all cell layers of the urothelium as well as in the renal calyces and pelvis, ureters, and small intestinal and colonic epithelium (Saam and Gordon, 1999, Tsuruta, 2006). Shh-Cre is primarily expressed in a subgroup of basal cells; but it is also expressed in the prostate (Shin et al., 2011). CK5- and Δ Np63-Cre have been used to drive the expression of the recombinase in the urothelium (Pignon et al., 2013, Gandhi et al., 2013). However, CK5 and p63 are also commonly expressed in the skin (Di Como et al., 2002, Moll et al., 2008).

At the time of our previous experiments (Chapters 3, 4 and 5) the UroplakinIII promoter was the best available option to drive Cre recombination in the urothelium. UroII^{Cre}-driven recombination to express *FGFR3* in combination with OH-BBN exposure, which specifically targets the bladder, resulted in invasive urothelial tumours (Chapter 5). However, OH-BBN acts on the entire bladder, which can potentially promote tumourigenesis in all exposed urothelial cells. The resulting tumours present with large and fast growth behaviour, which likely reach the pre-determined end point of the experiment before potential metastasis can occur. With the use of OH-BBN it is difficult to induce specific genetic mutations, because the carcinogen induces random DNA damage in all cells. Therefore, each of the resulting tumours is composed of a large set of

different mutations, leading to great variability of genetic profiles at the time of tumour examination.

An alternative method of Cre delivery to the tissue of interest involves the use of a recombinant Adenovirus (Anderson et al., 2000, Anton and Graham, 1995). Cre-recombinant Adenovirus type 5 (AdenoCre) is a viral vector that is replication-deficient due to deletion of the 0-9.2 map units, which include the left inverted terminal repeat (ITR) region, as well as transformation-deficient due to lack of the original E1a sequence (Anderson et al., 2000). In replacement of E1a, AdenoCre harbours the Cre transgene, which is controlled by a Cytomegalovirus (CMV) promoter (Anton and Graham, 1995). Since Adenoviruses do not integrate into the host genome, the expression of Cre is transient (Brody and Crystal, 1994).

Adenoviral gene transfer has successfully been used to transduce cells in culture (Hawley et al., 2010, Prost et al., 2001), as well as tissues *in vivo* such as the lung (Jackson, 2001), breast (Russell et al., 2003), uterus (Wang et al., 2006) and brain (Davidson et al., 1993).

AdenoCre has recently also been tested in the bladder, where the virus was orthotopically instilled via laparotomy or catheterisation (Puzio-Kuter et al., 2009, Yang et al., 2013). The work by Puzio-Kuter suggested that AdenoCre could target basal cells (Puzio-Kuter et al., 2009). The study further reported muscle-invasive tumours by six months with 100% penetrance in $p53^{flox/flox}$ $Pten^{flox/flox}$ mice (Puzio-Kuter et al., 2009). 60% of these tumours metastasised to lymph nodes and distant sites between 4-6 months. No tumours were observed in $p53$ or $Pten$ single mutants. Loss of either $p53$ or $Pten$ in combination with loss of Retinoblastoma protein (Rb) following AdenoCre injection did not result in tumour formation or a visibly abnormal urothelial phenotype (Puzio-Kuter et al., 2009). In a second study in which $p53^{flox/flox}$ $Kras^{+/LSLG12D}$ mice were orthotopically instilled with AdenoCre, bladders developed mild urothelial hyperplasia at six months but showed no evidence of tumour initiation (Yang et al., 2013).

In this chapter we aimed to generate an invasive bladder cancer model in which the effect of different gene combinations can be tested in a spatially and temporally controlled fashion. We therefore sought to replace UroIIcre-driven

recombination by AdenoCre delivery. AdenoCre infection not only allows bladder-restricted recombination (Puzio-Kuter et al., 2009, Seager et al., 2010) but also may enable recombination in a smaller number of cells that are individually surrounded by a normal tissue environment. Furthermore, we wished to assess whether these smaller lesions may allow models to survive longer and therefore tumours to have the potential to progress and eventually metastasise.

6.1.2 *In vivo* imaging

In the bladder, clinical signs of tumours such as a palpable mass or haematuria are generally present at late stages of the disease. Therefore, a number of non-invasive *in vivo* imaging techniques have been developed to detect tumours at early stages and to monitor disease progression as well as drug response. These include ultrasound, magnetic resonance imaging, computer tomography, and bioluminescent or fluorescent imaging (Lyons, 2005).

Ultrasound imaging has been used to detect tumours as small as 0.52 mm³ in an orthotopic bladder cancer model (Patel et al., 2010). Optimised micro-ultrasound with targeted contrast enhancement involves detection of a probe that has been inserted into the bladder via a catheter (Chan et al., 2011). Probes such as microbubbles coated with a monoclonal antibody against a target molecule can be detected and quantified. A drawback of ultrasound imaging techniques is the variability of the images acquired from the same tumour as well as motion artefacts resulting from breathing (Chan et al., 2009a).

Magnetic resonance imaging (MRI) provides the advantage of early tumour detection with high resolution (Kikuchi et al., 2003). However, image acquisition and processing is very costly and time consuming. MRI scanners are therefore not available at every institute.

Computer tomography (CT) is an x-ray-based technology that allows creating a 3-dimensional picture with high spatial resolution based on the density of the analysed tissue (Martiniova et al., 2010). Positron emission tomography (PET) is often used in combination with CT (CT-PET), where a biologically active molecule is introduced into the body to improve image acquisition. However, introduction of contrast-enhancing agents may trigger an immune response.

Furthermore, due to the high sensitivity of this technology, minor tissue abnormalities can lead to misinterpretations.

Bioluminescent imaging (BLI) is based on luciferase, an enzyme that converts substrates such as luciferin into light signals emitting between 500-620nm. Luciferase-transfected cancer cells can therefore easily be detected in orthotopic models; however, it is unclear whether luciferase may trigger an immune response in the animal and it gives no information on tumour anatomy (Henriquez et al., 2007).

Fluorescent imaging is based on genetically introduced reporters such as GFP or RFP (Lyons, 2005). An RFP signal can be detected between 570-620nm, whereas GFP is between 465-520nm. Fluorescent reporters can also be used in combination. However, this imaging method suffers from autofluorescence of abdominal hair and internal organs, and in the case of the bladder from the presence of urine.

With the aim to detect and monitor tumour development and progression in living animals, we tested fluorescent imaging and ultrasound imaging in the mouse bladder.

6.1.3 *In vitro* models

In vitro cell culture provides the opportunity to analyse cancer initiation and progression, as well as to test the effectiveness of therapeutic drugs in a controlled environment. *In vitro* approaches to investigate urothelial cell carcinoma include cell culture techniques of human and mouse primary tumour cells, bladder cancer cell lines, as well as organotypic cultures.

Sphere formation in a 3-dimensional (3D) environment such as in Matrigel has been described as an indication of self-renewal as characteristic of stem cells (Sato et al., 2009, Xin et al., 2007) and cancer stem cells (Nicolis, 2007). For example, the highly invasive human bladder cancer cell line T24 cultured on ultra-low attachment plates starts to form spherical colonies after 7 days as an indicator of stem cell behaviour (Zhang et al., 2012). Sphere formation has also been tested using cells from Stat3-activated bladder tumours in mice (Chen et

al., 2012). Furthermore, it was shown in normal mouse bladders that FACS-sorted Shh-expressing urothelial cells are capable of forming spheres in Matrigel (Shin et al., 2011). In contrast to monolayer cultures, it has been shown that 3D tumour sphere cultures match the *in vivo* response to chemotherapeutics better (Kim and Alexander, 2013), supporting the use of 3D culture systems.

Organotypic slice culture of the bladder has been described as a tool to analyse tissue development and the underlying signalling pathways in a well-defined environment (Batourina et al., 2012). The advantage of this culture technique is that the tumour can be kept in its original environment, surrounded by urothelium, connective tissue and striated muscle. The effect of therapeutic drugs on invasion in this *ex vivo* system has not been tested yet; however, the technique can potentially constitute useful assay.

With the aim to image invasive bladder cancer *in vivo*, and to assess transformation and cell migration we set out to establish essential *ex vivo* techniques and assays.

6.2 Establishment of techniques to generate and detect invasive bladder cancer in mice

6.2.1 Generation of mouse cohorts to test AdenoCre recombination efficiency

In order to test adenoviral Cre delivery to the mouse bladder we used RFP reporter mice (*Rosa26 tdRFP*) where recombined cells can be visualised upon successful AdenoCre transduction (Luche et al., 2007) (Table 6-1). As an alternative we used *Rosa26 lacZ* mice, where recombination can be traced by X-gal staining on frozen tissue. We also generated mice carrying one or two copies of an activating β -catenin mutation, β -catenin^{+/*exon3*} or β -catenin^{*exon3/exon3*} respectively, where recombination can be visualised by immunohistochemistry against β -catenin protein. This method has also been used in previous studies, where upregulation of nuclear β -catenin was demonstrated in β -catenin^{*exon3/exon3*} bladders under the control of *UroII*Cre (Ahmad et al., 2011a, Ahmad et al., 2011b).

Table 6-1: Summary of mice injected for recombination analysis

Mouse bladders were injected with 2×10^9 pfu Ad5CMVCre-eGFP with 10% Polybrene

Genotype	n	Age at injection (months)	Time post injection
<i>Wild type</i>	1	2	12 days
<i>Rosa26 tdRFP</i>	16	2-3	3-40 days
<i>Rosa26 LacZ</i>	3	6-7	21 days
<i>B-cat</i> ^{+/<i>exon3</i>} or <i>B-cat</i> ^{<i>exon3/exon3</i>}	8	2-7	12-30 days

6.2.2 Assessment of recombination

In order to analyse the location and frequency of AdenoCre recombination upon infection, as well as to establish an imaging technique by which disease progression can be monitored in living animals, we tested the IVIS Spectrum *in vivo* imaging system.

We instilled *Rosa26 tdRFP* (n=16) and a *Wild type* control (n=1) orthotopically with Ad5CMVCre-eGFP and imaged the mice after 12-40 days using the IVIS Spectrum (Figure 6-1). In the bladder, an AdenoCre dose of 1×10^9 pfu has been demonstrated to successfully generate tumours in a *p53^{flox/flox} Pten^{flox/flox}* background (Puzio-Kuter et al., 2009). We used an Ad5CMVCre-eGFP dose of 1×10^9 pfu in *Rosa26 tdRFP* (n=8), as well as 2×10^9 pfu in *Rosa26 tdRFP* (n=8) and *Wild type* (n=1).

An RFP (mCherry) signal between 587-610nm was expected from cells that have undergone recombination. A strong RFP signal was observed in the guts of *Wild type* (A, circled) as well as the reporter mice (B), a background signal which most likely results from alfalfa, a plant that is part of the rodent diet that the animals are commonly provided with at the Beatson animal unit. The bladders of *Wild type* and reporter mice (A, B, yellow arrows) emitted only a weak RFP signal. Due to high background fluorescence in the guts, and the weak signal from the bladders, the occurrence of recombination in the bladder could not be unambiguously determined. No difference was observed between AdenoCre-injected low-dose (1×10^9 pfu) and high-dose (2×10^9 pfu) mice based on fluorescent signal intensity using the IVIS spectrum (data not shown).

The transduction of cells by AdenoCre can be visualised through an *eGFP* reporter carried by the recombinant adenovirus (Ad5CMVCre-eGFP).

A GFP signal between 465-520nm was expected from AdenoCre-infected bladder cells. A strong GFP signal was observed in *Wild type* (C, yellow arrow) as well as the reporter mice (D, black arrows). However, this is likely to have resulted from urine that is autofluorescent. This is supported by the fact that a prominent spot of GFP-positive urine was seen in *Wild type* (C, white arrow).

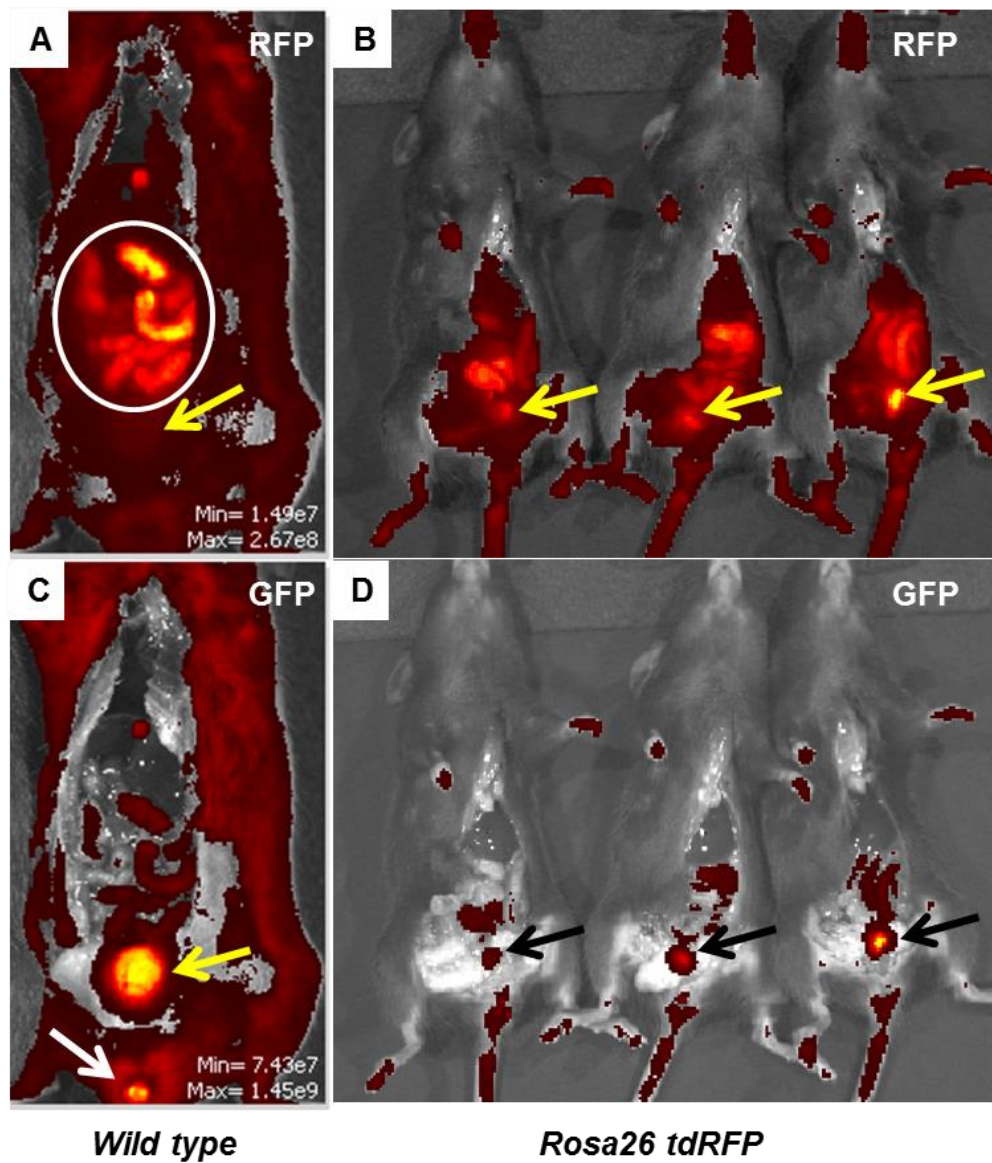


Figure 6-1: Cre recombination upon adenoviral transduction visualised by IVIS Spectrum
Wild type mouse (A, C) and three *Rosa26 tdRFP* expressing mice (B, D) imaged for RFP (A, B) and GFP (C, D) at 12 days after injection of 2×10^9 pfu Ad5CMVCre-eGFP.

Next we examined AdenoCre transduction and recombination in the urothelium at the cellular level (Figure 6-2). We first examined the expression of GFP and RFP to visualise the events of transduction and recombination, respectively, in the urothelium of *Rosa26 tdRFP* mice.

GFP expression was detected in a low number of urothelial cells located in the umbrella and intermediate layer of *Rosa26 tdRFP* reporter mouse bladders (A), indicating successful transduction of a small number of cells by AdenoCre.

RFP antibody staining showed broad unspecific positivity in the majority of cells in the urothelium (B). Some individual cells in the umbrella and intermediate layer occasionally showed stronger staining intensity (B, arrows), similar to the one observed in the GFP staining (A).

X-gal staining was performed on frozen sections from bladders carrying a lacZ reporter (n=3) (C). The majority of umbrella cells showed positive blue staining, indicating recombination to have occurred. However, as shown in (Figure 3-2), X-gal generally stains umbrella cells independently of a recombination event.

As an alternative to the RFP and lacZ reporter systems, we aimed to visualise AdenoCre recombination in *β-catenin^{exon3/exon3}* bladders using a *β-catenin* antibody. In our experiments, a small number of positive recombination events was observed in urothelial cells, along with broad recombination in a large number of cells in the stromal compartment (D, arrows).

Altogether, AdenoCre recombination was most effectively detected by nuclear *β-catenin* expression in the presence of a *β-catenin^{exon3/exon3}* activating mutation. GFP expression was generally low in the urothelium, and at times even absent in a full bladder section. Furthermore, GFP positivity only reveals successful transduction and not recombination. Therefore, GFP staining was only used in combination with other reporters in future experiments. Due to the non-specificity on the RFP antibody, no conclusions could be drawn on urothelial recombination, and therefore the staining was discontinued. Likewise, X-gal staining was discontinued in future experiments due to non-specific blue staining of umbrella cells. The exact percentage of successfully recombined cells could not be determined by immunohistochemistry.

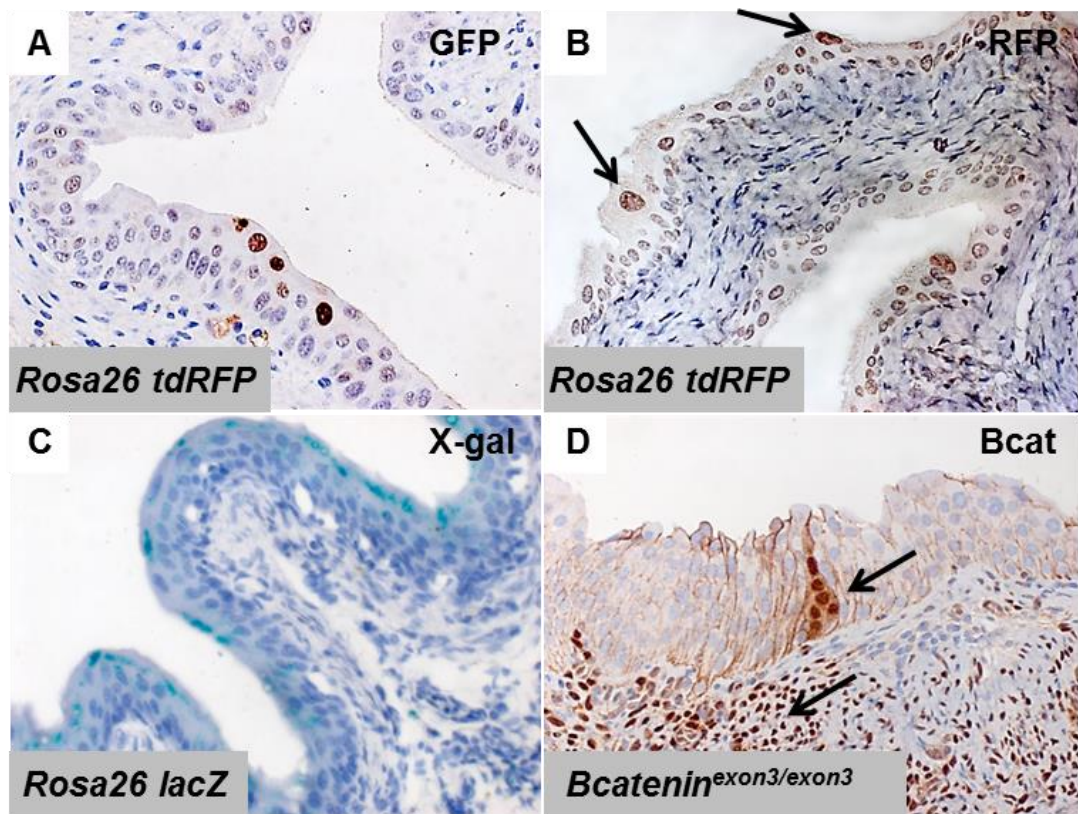


Figure 6-2: Cre recombination at cellular level upon high-dose AdenoCre transduction
Immunohistochemistry for GFP (A) and RFP (B) on bladder sections of *Rosa26 tdRFP*. X-gal staining on *Rosa26 lacZ* (C). Immunohistochemistry for β -catenin on *Bcatenin^{exon3/exon3}* bladder (D).

6.2.3 Monitoring tumour formation and progression *in vivo*

Although IVIS Spectrum has only been used to image healthy bladders of reporter mice, it seemed to provide an insufficient tool to monitor bladder tumours due to high level of background signal at two different wavelengths (Chapter 6.2.2). We therefore aimed to establish an alternative, the Vevo 770 Visualsonics ultrasound, as an imaging system for the bladder in order to monitor tumour progression in living animals.

To establish the methodology, we first aimed to image transgenic animals that were known to develop carcinoma in the bladder. In a previous study, we had generated mice with *β-catenin* and *Hras* activation, *UroIIcre β-catenin^{exon3/exon3} Hras^{Q61L}*, which reliably produced tumours by 8 months of age (Ahmad et al., 2011b). We then generated mice without *UroIIcre*, where AdenoCre was used to induce cell transformation, namely *β-catenin^{exon3/exon3} Hras^{G12V/G12V}* (Chapter 6.4). In contrast to the *H-Ras Q61L* overexpression model (Ahmad et al., 2011b), our *Hras G12V* cohort carries a homozygous knock-in mutation that allows expression of endogenous levels of oncogenic *Hras G12V*. Bladders were examined using ultrasound (Figure 6-3).

Injected *Wild type* bladders (n=1) and non-injected *Wild type* bladders (n=3) showed a normal bladder wall of approximately 0.3-0.4 mm in thickness (A). In AdenoCre-injected *β-catenin^{exon3/exon3} Hras^{G12V/G12V}* mice (n=6), we observed bladder wall thickening with an irregular surface towards the bladder lumen at 5.5 months post injection in all bladders (B).

Upon bladder wall thickening, tumours were monitored in n=4 mice over 14 weeks, all of which showed increasing growth. Shown as representative in (Figure 6-3), we observed a small exophytic tumour of 0.5 mm in diameter in the same animal at 8 months post injection (C, arrow). At 9 months post injection, the tumour had grown to a larger size, filling a considerable part of the bladder lumen (D). These results indicated that ultrasound imaging is likely to be sensitive enough to detect relatively small growths (≥ 0.5 mm) within the bladder.

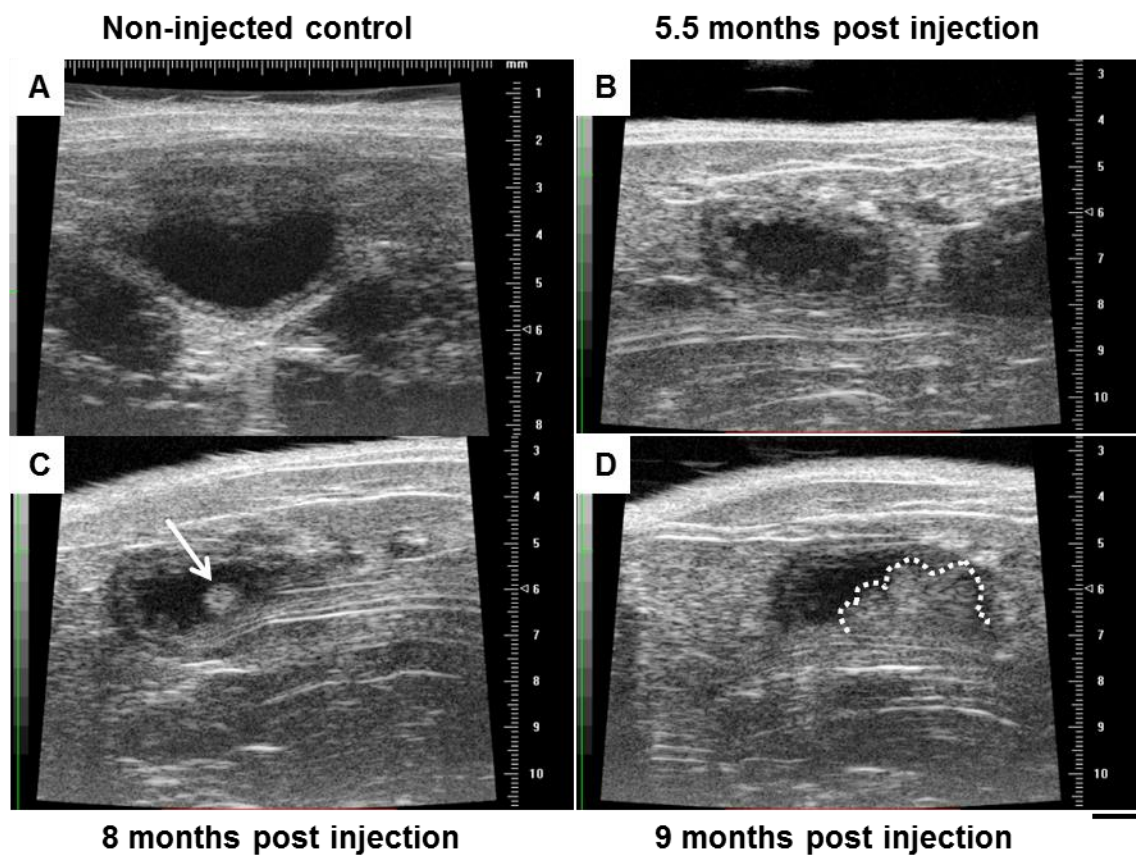


Figure 6-3: Monitoring of tumour progression using Vevo 770 Visualsonics ultrasound Bladders of non-injected *Wild type* (A) and AdenoCre-injected β -catenin^{exon3/exon3} *Hras*^{G12V/G12V} (B-D) at different stages post AdenoCre injection. Scale bar represents 1 mm (A-D).

6.3 Highly aggressive tumours in AdenoCre *p53 Pten* bladders

6.3.1 Tumours in AdenoCre *p53^{flox/flox} Pten^{flox/flox}* bladders

In order to develop a model that reliably produces muscle-invasive bladder tumours we generated mice with *p53* and *Pten* deficiency that are known to develop highly aggressive tumours by 6 months post AdenoCre injection (Puzio-Kuter et al., 2009)

Bladders of *p53^{flox/flox} Pten^{flox/flox}* mice at 2 months of age (n=5), were injected with 2×10^9 pfu of Ad5CMVCre (Table 6-2).

All injected mice developed pelvic tumours by 3.5 months post-injection (Chapter 6.6). One animal had to be killed due to the pelvic tumour formation at 2.8 months post injection in order to comply with the Home Office regulations. A second animal was killed at 2.8 months post injection due to adverse effects from a bladder tumour.

Table 6-2: Summary of *p53* and *Pten* deleted mice injected with AdenoCre

Mouse bladders were injected with 2×10^9 pfu Ad5CMVCre-eGFP with 10% Polybrene. Asterisks indicate cause of death or termination due to signs of illness

Genotype	ID	Time post injection	Non-urothelial tumours	Urothelial abnormalities (H&E)	Bladder tumour (H&E)	Tumour origin in muscle (IHC)
<i>p53^{flox/flox} Pten^{flox/flox}</i> (n=5)	1	2.8 months	Large pelvic tumour*	CIS, mitoses, pleomorphism	Yes	Yes
	2	2.8 months	Small pelvic tumour	CIS, mitoses, pleomorphism	Yes*	Yes
	3	3.5 months	Small pelvic tumour	CIS, mitoses, pleomorphism	Yes*	Yes
	4	3.5 months	Small pelvic tumour	CIS, mitoses, pleomorphism	Yes*	Yes
	5	3.5 months	Large pelvic tumour*	CIS, mitoses, pleomorphism	Yes	Yes

The other three double knockout mice were examined by ultrasound after 3.5 months (Figure 6-4). Large tumours were detected in all $p53^{flox/flox} Pten^{flox/flox}$ (n=3) (B, circled in white) unlike in non-injected *Wild type* controls (A).

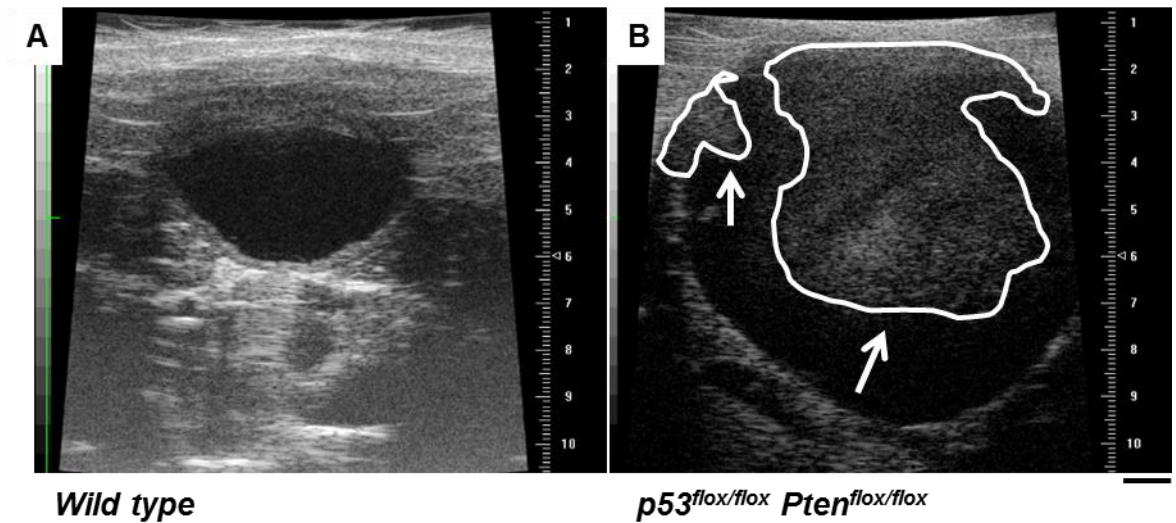


Figure 6-4: Ultrasound of AdenoCre $p53^{flox/flox} Pten^{flox/flox}$ bladders at 3.5 months post injection

Representative bladders of non-injected *Wild type* (A) and AdenoCre-injected $p53^{flox/flox} Pten^{flox/flox}$ (B). Scale bar represents 1 mm (A-B).

Following tumour detection via ultrasound imaging, bladders were harvested at 3.5 months post injection.

Upon examination of the H&E-stained sections, we observed characteristics of highly aggressive tumours in four out of five $p53^{flox/flox} Pten^{flox/flox}$ bladders (Figure 6-5). Bladders presented CIS in the urothelium (A, arrow). There was also a surrounding tumour mass; however this had no obvious connection to the urothelium (A, dotted line). Tumours displayed poorly differentiated cells with pleomorphism and frequent mitoses (B, arrows), invasion of cells into the bladder muscle (C, arrows and dotted line), as well as invasion into the “honeycomb”-shaped adipose tissue (D, arrows).

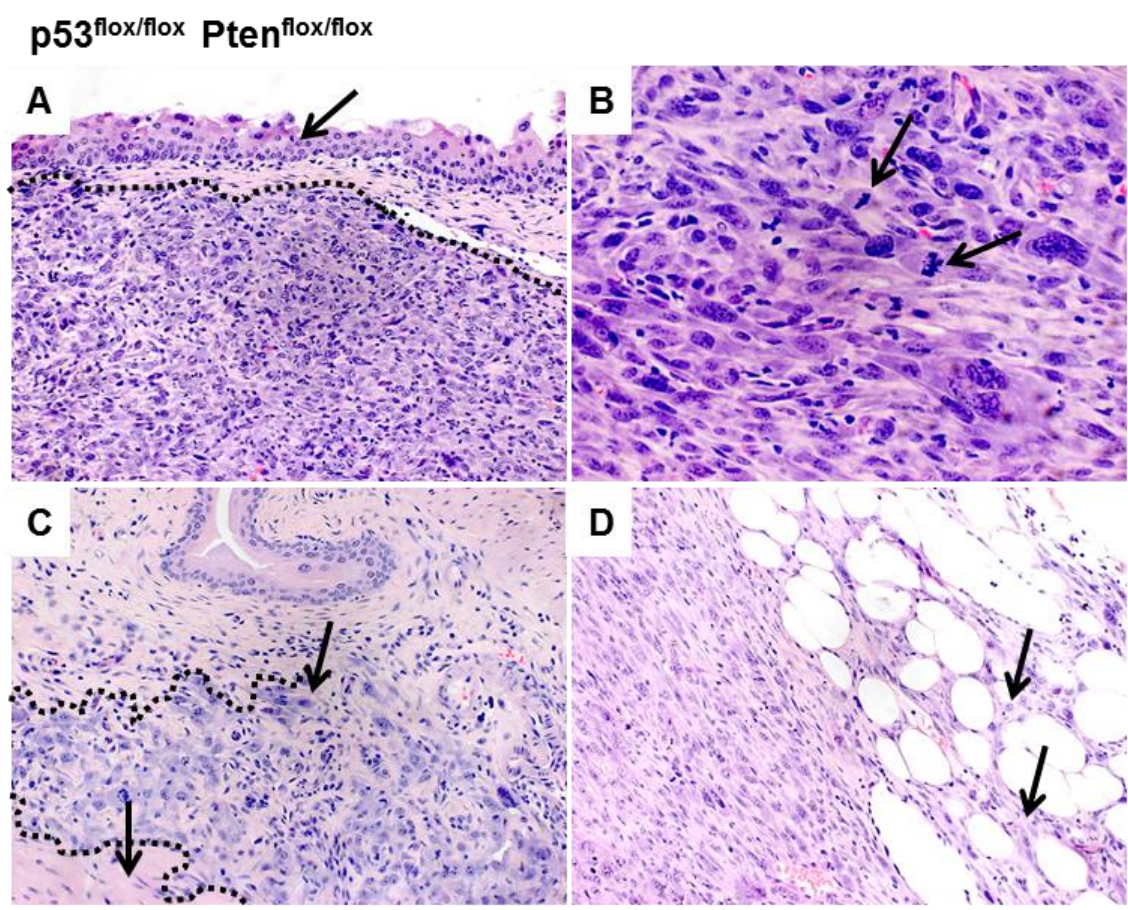


Figure 6-5: Histology of AdenoCre $p53^{flox/flox} Pten^{flox/flox}$ bladders at 3.5 months post injection
Representative bladder sections stained by H&E. Scale bar represents 100 μm in A, C, D, and 50 μm in B).

In order to further characterise the tumour type, we performed immunohistochemistry for the urothelial markers pan-cytokeratin (pan-CK) and p63 to determine the cell of origin, as well as immunohistochemistry for Fascin and Sox9 as indicators of invasion and stemness (Figure 6-6).

Pan-CK was strongly expressed in the urothelium of $p53^{flox/flox}$ $Pten^{flox/flox}$ bladders, but not in the underlying tumour cells, indicating a non-epithelial origin of the tumours (A, arrows; for orientation of tissue compare with H&E Figure 6-5 A). Similarly, p63 was exclusively present in the urothelium and absent in the tumour (B, arrows), further supporting non-epithelial origin of these tumours.

Fascin was expressed along the basal cells of the urothelium as shown before in Chapter 5 (Figure 5-7 J). Furthermore, it was widely expressed in the underlying tumour (C, arrows), indicating aggressive growth and potential for invasion (Karasavvidou et al., 2008). Sox9 was seen in a small number of cells within the tumour (D, arrows). This may indicate that these cells had undergone a change in their genetic program as Sox9 expression is associated with stemness/progenitor properties, cancer progression and invasiveness (Wang et al., 2008).

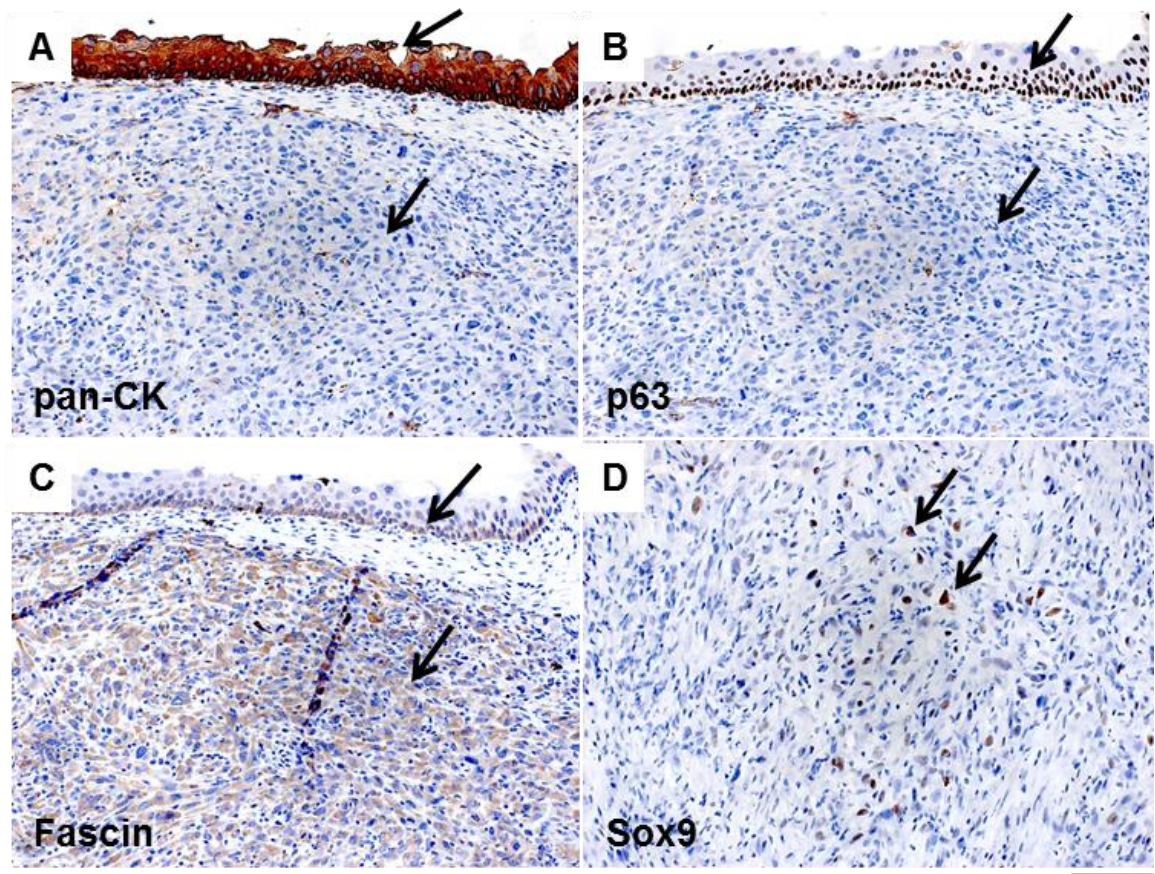


Figure 6-6: Immunohistochemistry of AdenoCre-induced $p53^{flox/flox}$ $Pten^{flox/flox}$ bladders at 3.5 months post injection

Immunohistochemistry for pan-CK (A), p63 (B), Fascin (C) and Sox9 (D) on representative bladder sections. Scale bar represents 100 μ m in A-D.

In order to confirm that the AdenoCre $p53^{flox/flox}$ $Pten^{flox/flox}$ tumours originated in the muscle and not in the urothelium, we performed immunohistochemistry for smooth muscle actin (SMA) (Kirsch et al., 2007) (Figure 6-7).

SMA was expressed in the normal bladder muscle (A, white arrow). SMA was strongly expressed in the tumour, supporting that the tumours originated in the smooth muscle of the bladder (A, black arrow, and B).

Based on our histology and immunohistochemistry results, our AdenoCre $p53^{flox/flox}$ $Pten^{flox/flox}$ tumours are different from the ones that were previously described in the same bladder cancer model (Puzio-Kuter et al., 2009). We suggest that these highly aggressive tumours in $p53^{flox/flox}$ $Pten^{flox/flox}$ originated in the muscle around the site of AdenoCre injection rather than from recombined urothelium.

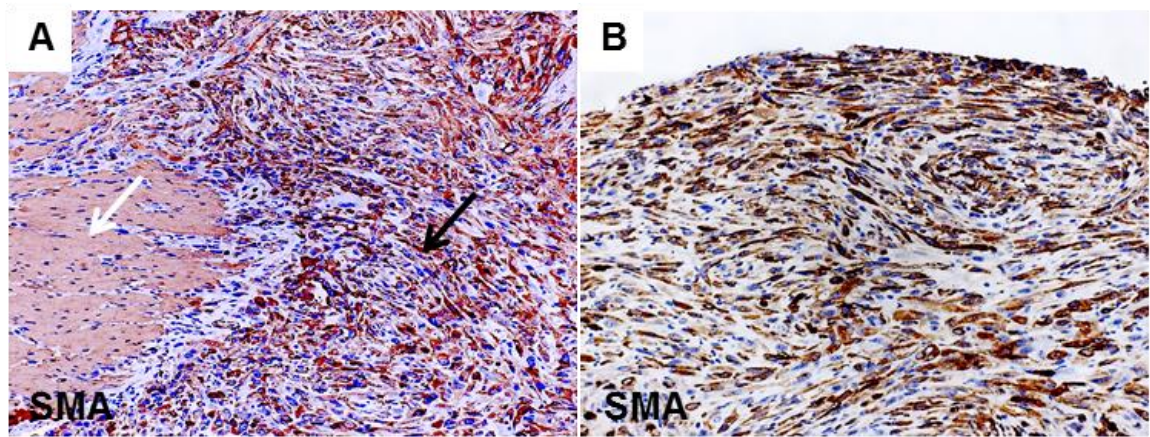


Figure 6-7: Smooth muscle actin staining on AdenoCre-induced $p53^{flox/flox}$ $Pten^{flox/flox}$ bladders at 3.5 months post injection

Immunohistochemistry for smooth muscle actin (SMA) on two representative bladder sections (A-B). Scale bar represents 200 μm in A and 100 μm in B.

6.3.2 Tumours in AdenoCre $p53^{R172H/R172H}$ $Pten^{flox/flox}$ bladders

We also analysed the effect of the dominant-negative $p53$ $R172H$ mutation in combination with $Pten$ deletion in the urothelium of $p53^{R172H/R172H}$ $Pten^{flox/flox}$ mice. Mutant $p53$ is also commonly found in human bladder cancer (Sidransky et al., 1991), but the effect of a dominant-negative mutation has never been analysed in the mouse bladder.

Bladders of $p53^{R172H/R172H}$ $Pten^{flox/flox}$ mice at 2-6 months of age (n=3), were injected with 2×10^9 pfu of Ad5CMVCre (Table 6-3).

Strikingly, AdenoCre $p53^{R172H/R172H}$ $Pten^{flox/flox}$ developed adverse effects as early as 1.7 months (n=2) and 2 months (n=1) post injection. This was one month earlier than AdenoCre $p53^{flox/flox}$ $Pten^{flox/flox}$ (Chapter 6.3.1). Two mice developed a lung tumour, and one mouse developed an additional lymphoma, while the third mouse presented with a big and fast growing soft tissue tumour in the flank.

Table 6-3: Summary of p53 and Pten deleted mice injected with AdenoCre

Mouse bladders were injected with 2×10^9 pfu Ad5CMVCre-eGFP with 10% Polybrene. Asterisks indicate cause of death or termination of the experiment due to signs of illness

Genotype	ID	Time post injection	Non-urothelial tumours	Urothelial abnormalities (H&E)	Bladder tumour (H&E)	Tumour origin in muscle (IHC)
$p53^{R172H/R172H}$ $Pten^{flox/flox}$ (n=3)	1	1.7 months	Lung tumour*	Hyperplasia, pleomorphism	Yes	Yes
	2	1.7 months	Large pelvic tumour*	Hyperplasia, pleomorphism	Yes	Yes
	3	2 months	Lung tumour, Lymphoma*	Hyperplasia, pleomorphism	Yes	Yes

In order to see whether the bladders had developed urothelial abnormalities or tumours, we examined H&E-stained sections (Figure 6-8).

Bladders presented with a hyperplastic urothelium (A). This was, however, without increased proliferation as indicated by Ki67 immunohistochemistry (B).

The surrounding muscle showed a similar histological phenotype as $p53^{flox/flox}$ $Pten^{flox/flox}$, including poorly differentiated cells with pleomorphism and frequent mitoses (C, arrows). In contrast to the hyperplastic urothelium, these tumours underneath were highly proliferative as indicated by Ki67 immunohistochemistry (D).

p53 was highly upregulated in these muscle tumours (E) compared to a representative area of the muscle that was not affected by the tumour (E, insert), indicating that the R172H mutant form of p53 was expressed upon AdenoCre recombination.

Tumours were positive for smooth muscle actin (SMA) (F), indicating that the origin of these tumours was likely to be the bladder muscle.

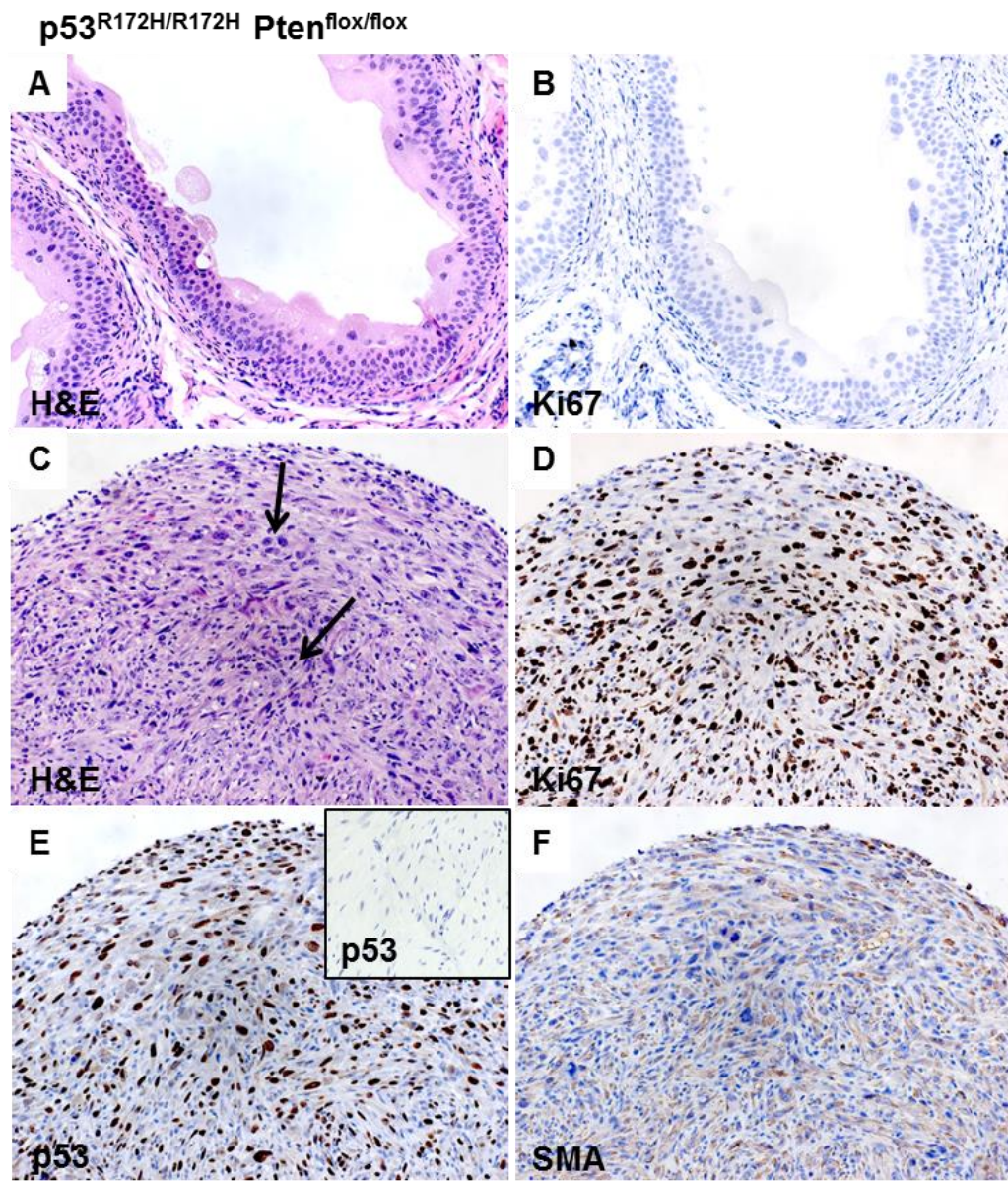


Figure 6-8: Histology of AdenoCre-induced $p53^{R172H/R172H}$ $Pten^{flox/flox}$ bladders at 1.7 months post injection

Representative bladder sections stained by H&E (A, C), Ki67 (B, D), p53 (E) and smooth muscle actin (SMA) (F). Non-tumorous area of the muscle stained by p53 (E, insert). Scale bar represents 100 μ m in A-F.

We also examined the lung lesions that had developed in 2 out of 3 AdenoCre $p53^{R172H/R172H}$ $Pten^{flox/flox}$ mice (Figure 6-9).

The lung harboured one large mass of tumour cells as well as multiple small lesions as visualised by H&E (A, arrows), accompanied by a large number of small dark-nucleated immune cells. Ki67 staining indicated high proliferative activity in these areas (B).

p53 expression was absent, suggesting that both copies of mutant p53 may have been lost as a characteristic of advanced grade and stage of the primary tumour (C).

Tumours were negative for smooth muscle actin (SMA) (D), indicating that these lesions were most likely lung primary, and not metastatic from the bladder muscle.

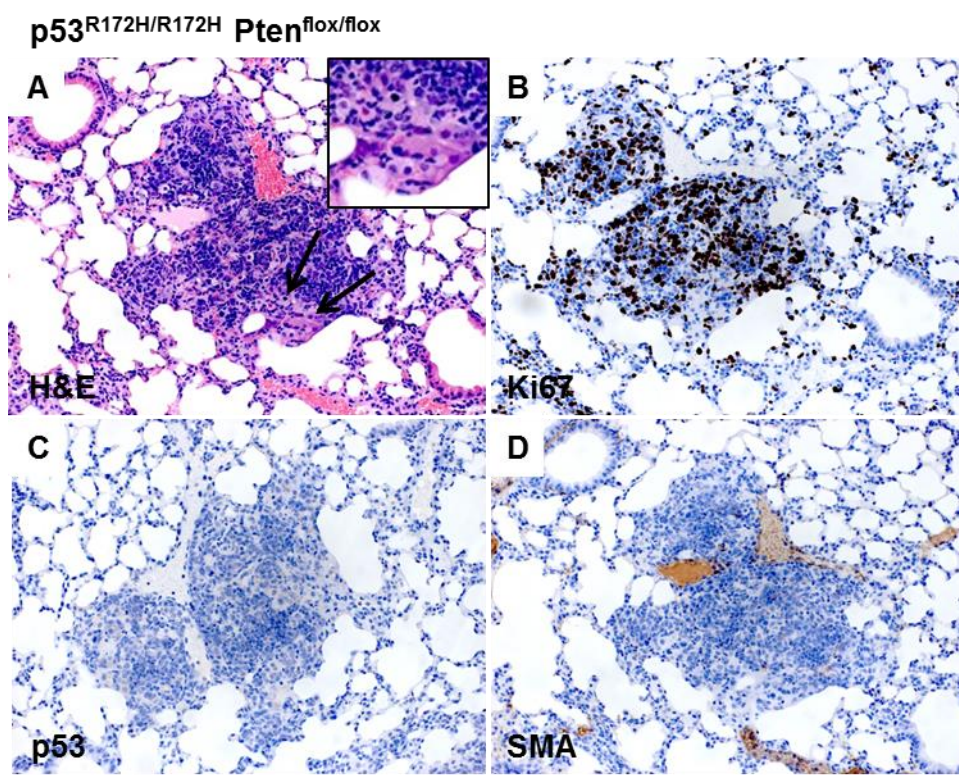


Figure 6-9: Histology of an AdenoCre-induced $p53^{R172H/R172H}$ $Pten^{flox/flox}$ lung at 1.7 months post injection

Representative lung sections stained by H&E (A), Ki67 (B), p53 (C) and smooth muscle actin (SMA) (D). Scale bar represents 100 μ m in A-D.

We also examined the grossly normal looking livers of AdenoCre $p53^{R172H/R172H}$ $Pten^{flox/flox}$ mice that had been sacrificed due to lung tumour formation (Figure 6-10).

As visualised by H&E, the livers harboured multiple areas of small dark cells surrounding the blood vessels (A, arrows). Ki67 staining indicated high proliferative potential of these areas (B).

Together with the presence of primary tumours in various organs (Figure 6-9), these results indicate that the adenovirus may have accessed the blood stream, distributed throughout the body, and recombined tissue at distant sites leading to tumour formation outside of the bladder.

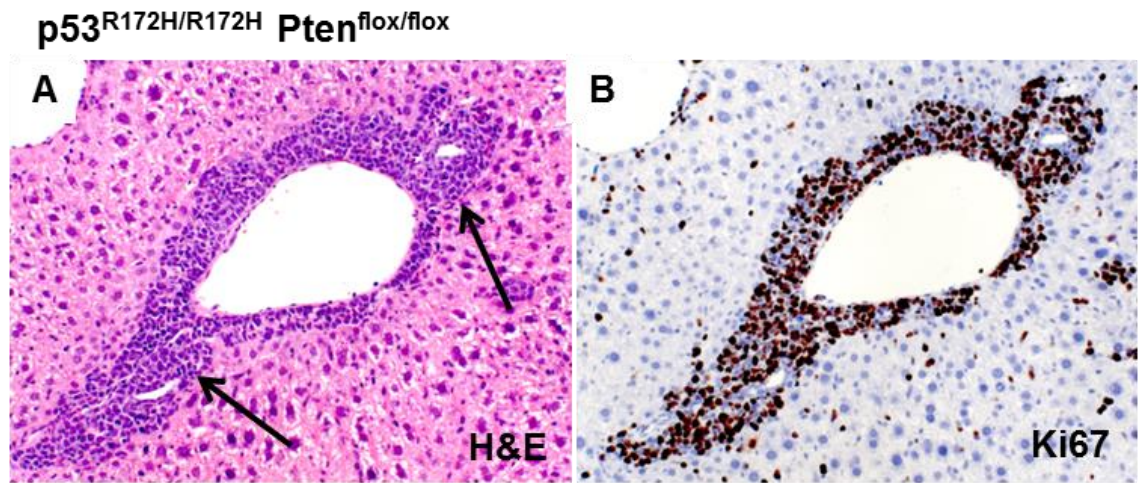


Figure 6-10: Histology of an AdenoCre-induced $p53^{R172H/R172H}$ $Pten^{flox/flox}$ liver at 1.7 months post injection
Representative liver sections stained by H&E (A) and Ki67 (B). Scale bar represents 100 μ m in A-B.

6.4 Exophytic tumours in AdenoCre β -catenin^{exon3/exon3} $Hras^{G12V/G12V}$ bladders

In a previous study we have generated mice with β -catenin and $Hras$ activation, $UroII\text{Cre } \beta\text{-catenin}^{\text{exon3/exon3}} Hras^{\text{Q61L}}$, which reliably produced tumours by 8 months of age (Ahmad et al., 2011b). Mice had to be sacrificed at 8 months due to clinical signs of illness such as haematuria or abdominal swelling. No metastases were found in these mice, and the tumours showed histological characteristics of low-grade, non-invasive urothelial carcinoma.

We aimed to refine this model of Wnt activation in order to allow more time for β -catenin and $Hras$ activated tumours to grow and adopt invasive behaviour. Since AdenoCre infection allows recombination in a smaller number of cells (Puzio-Kuter et al., 2009, Seager et al., 2010), we wished to assess whether these fewer lesions may allow models to survive longer and therefore the tumours would have the potential to progress and eventually metastasise.

We generated a cohort without $UroII\text{Cre}$, where AdenoCre was used to induce β -catenin^{exon3/exon3} $Hras^{G12V/G12V}$. We injected n=9 bladders with 2×10^9 pfu of Ad5CMVCre-eGFP of mice that were 2 months of age (Table 6-4).

Two out of eight β -catenin^{exon3/exon3} $Hras^{G12V/G12V}$ mice had to be killed due to pelvic tumour formation after 2 and 3.5 months respectively (Figure 6-16). Two mice developed a large liver tumour after 6.5 and 9 months respectively. One mouse developed a pancreatic tumour after 9.3 months (Figure 6-12).

Table 6-4: Summary of β -catenin and Hras mutant mice injected with AdenoCre

Mouse bladders were injected with 2×10^9 pfu Ad5CMVCre-eGFP with 10% Polybrene. Asterisks indicate cause of death or termination of the experiment due to signs of illness. u= detected by ultrasound

Genotype	ID	Time post injection	Non-urothelial tumours	Urothelial abnormalities (H&E)	Bladder tumour	Invasion (H&E)
<i>B-catenin^{exon3/exon3}</i> <i>Hras^{G12V/G12V}</i> (n=9)	1	2 months	Pelvic tumour*	Regional hypertrophy	Exophytic tumour (H&E)	None
	2	3.5 months	Pelvic tumour*	Regional hypertrophy	Exophytic tumour (H&E)	None
	3	6.5 months	Liver tumour*	Regional hypertrophy	Exophytic tumour (H&E)	None
	4	9.3 months	Pancreas tumour*	Regional hypertrophy	Exophytic tumour (H&E)	None
	5	8 months	None	unknown	Exophytic tumour (u)	unknown
	6	8 months	None	unknown	Thickened urothelium (u)	unknown
	7	8 months	None	unknown	Thickened urothelium (u)	unknown
	8	9 months	Liver tumour	unknown	Exophytic tumour (u)	unknown
	9	9 months	None	unknown	Exophytic tumour (u)	unknown

The bladders of three sacrificed *B-catenin^{exon3/exon3}* *Hras^{G12V/G12V}* animals were analysed by H&E (n=3) (Figure 6-11). Bladders had developed regional hyperplastic lesions (A, arrows) as well as low-grade exophytic tumours (C, arrows).

To visualise cells that had been transformed, we performed β -catenin immunohistochemistry as it was done previously in *UroIIcre B-catenin^{exon3/exon3}* mice (Ahmad et al., 2011a).

A marked upregulation of nuclear β -catenin was observed in *B-catenin^{exon3/exon3}* *Hras^{G12V/G12}* bladders (n=3) (Figure 6-11). The staining revealed multiple areas with nuclear β -catenin expression within the hyperplastic lesion (B, arrows), as

well as positivity throughout the entire tumour (D, arrows), indicating that the tumour originated from recombined cells. Furthermore, stromal β -catenin activation was observed (B, circled), indicating that recombination had not only occurred in the urothelium but also in surrounding tissue layers such as the connective tissue.

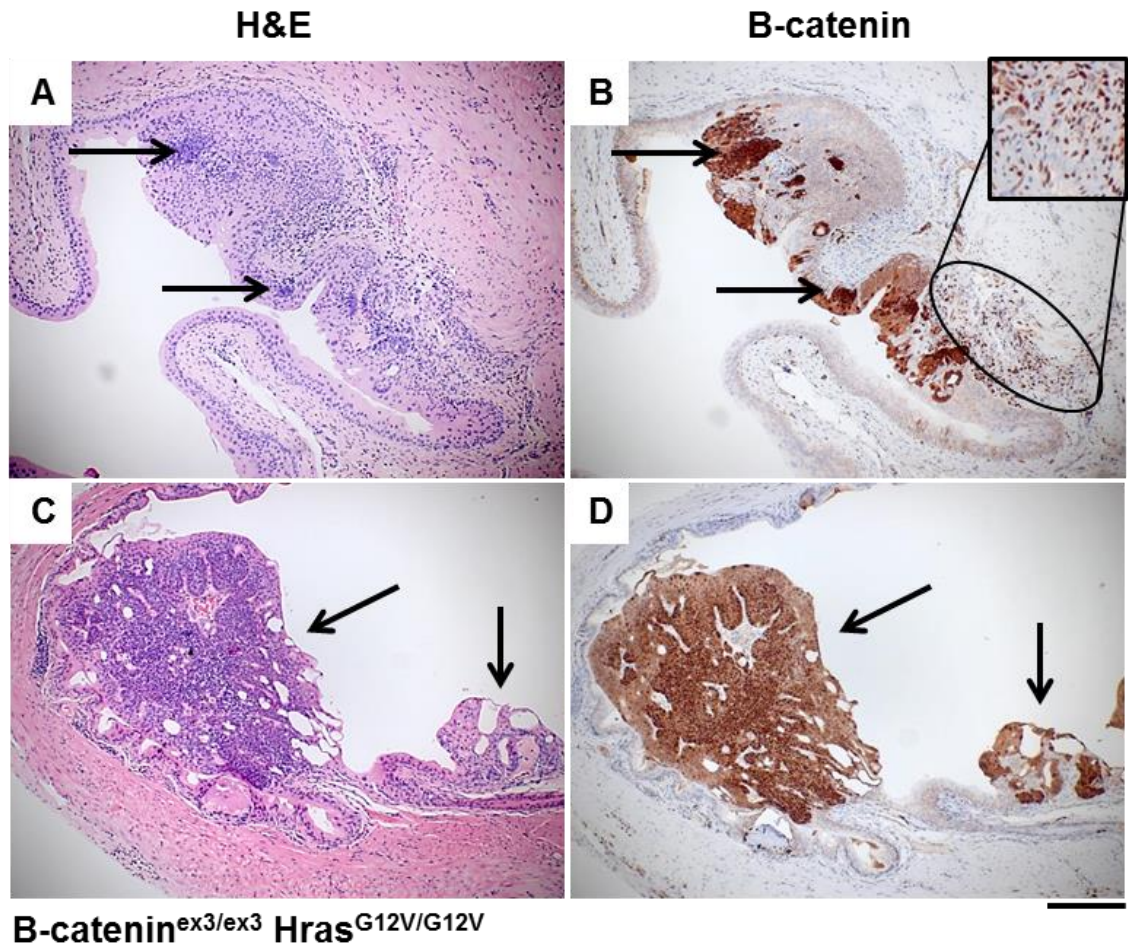


Figure 6-11: AdenoCre β -catenin^{exon3/exon3} Hras^{G12V/G12V} bladders at 2 months (A-B) and 3.5 months (C-D) post injection

Representative bladder sections stained by H&E (A, C) and immunohistochemistry for β -catenin (B, D). Scale bar represents 200 μ m (A-D).

The two tumours that developed in the liver and pancreas in two animals, respectively, were also assessed by H&E and β -catenin immunohistochemistry (Figure 6-12). Both organs harboured large mass of tumour cells as visualised by H&E (A, B). β -catenin immunohistochemistry revealed nuclear β -catenin translocation in both tumours (C, D), indicating that the neoplasms in these distant organs were caused by AdenoCre recombination.

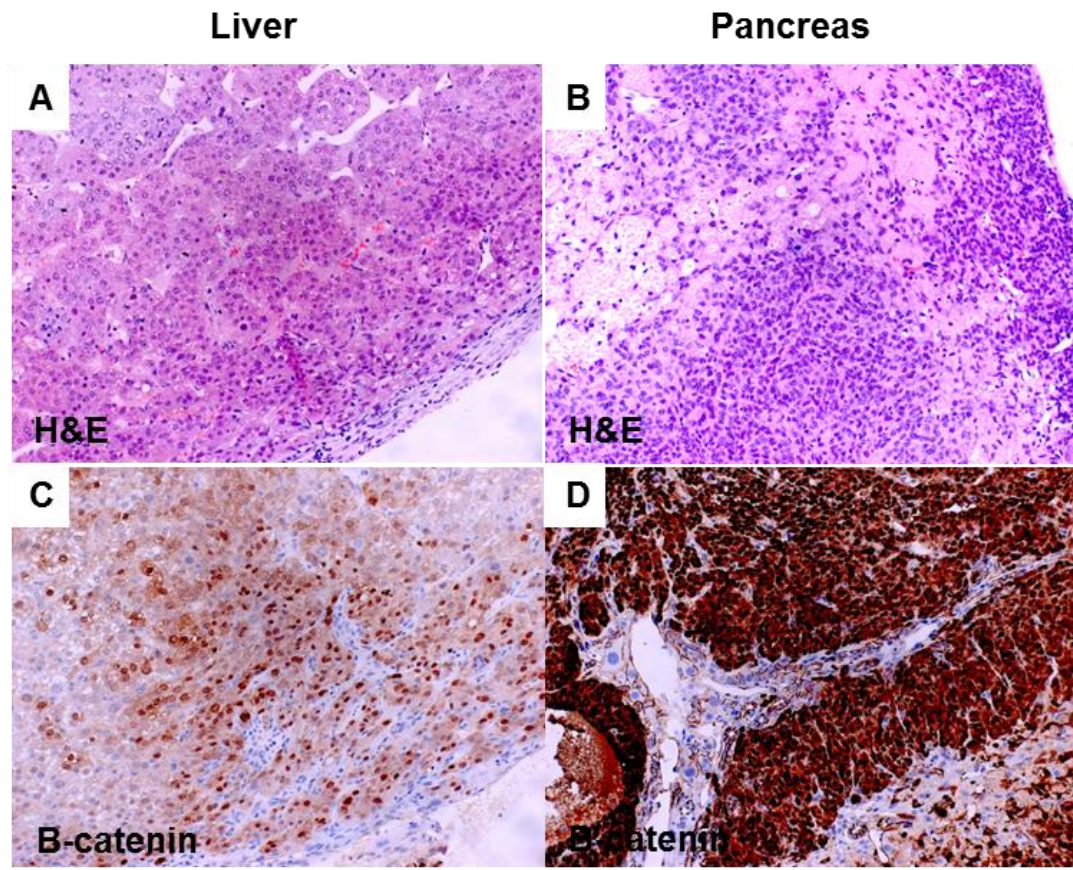


Figure 6-12: AdenoCre β -catenin^{exon3/exon3} Hras^{G12V/G12V} tumours in liver and pancreas
Representative sections of hepatic tumour (A, C) and pancreatic tumour (B, D) stained by H&E (A, B) and immunohistochemistry for β -catenin (C, D). Scale bar represents 100 μ m (A-D).

The alive remaining $n=5$ and otherwise healthy animals were examined by ultrasound at 8 months post infection (Figure 6-13). Four out of five β -catenin^{exon3/exon3} Hras^{G12V/G12V} animals harboured small bladder tumours of 4-5 mm in size (B, arrow), whereas no bladder thickening was observed in *Wild type* controls (A).

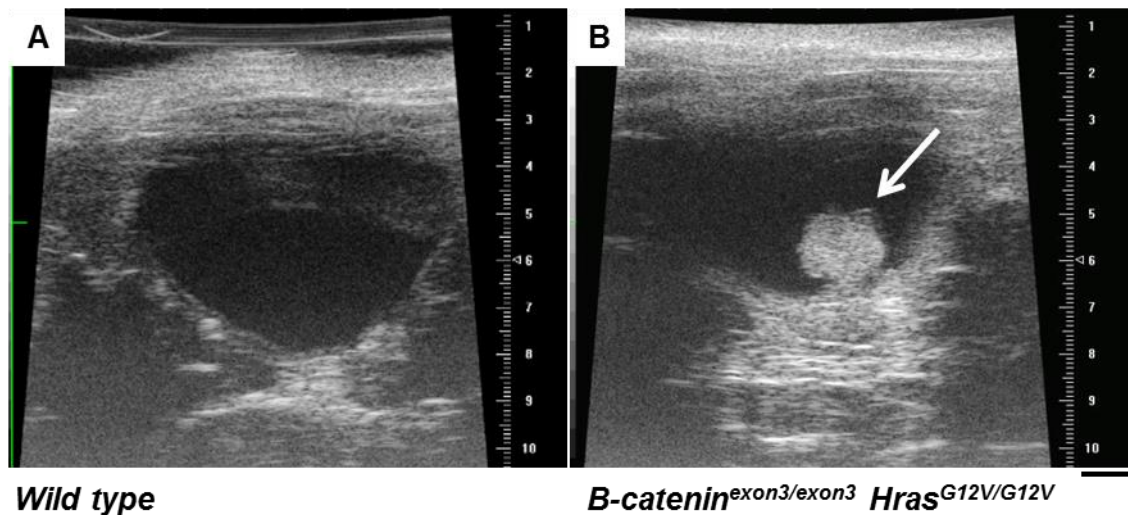


Figure 6-13: Ultrasound of AdenoCre β -catenin^{exon3/exon3} Hras^{G12V/G12V} bladders at 8 months post injection
 Representative bladders of non-injected *Wild type* (A) and AdenoCre-injected β -catenin^{exon3/exon3} Hras^{G12V/G12V} (B). Scale bar represents 1 mm (A-B).

Bladder tumours had formed only in 7 of 9 animals (78%). Following tumour detection via ultrasound imaging, β -catenin^{exon3/exon3} Hras^{G12V/G12V} bladders were harvested between 8-9 months post injection. The H&E-stained bladders presented regional hypertrophic lesions as well as small low-grade exophytic tumours that were not obviously different in size, stage or histological grade to the exophytic tumours observed at 3 months post injection (Figure 6-11).

6.5 Hypertrophy in AdenoCre *Hras*^{+G12V} *Pten*^{flox/flox} bladders

We also analysed the effect of the *Hras* mutation in combination with *Pten* deletion in the urothelium of *Hras*^{+G12V} *Pten*^{flox/flox} mice. *HRAS* mutation and loss of *P TEN* are both frequently found in human bladder tumours (*Hras* in 15-40% and *Pten* in 30%) (Jebar et al., 2005, Aveyard et al., 1999). However, co-occurrence of these mutations have been shown to be rare (Jebar et al., 2005) suggesting some redundancy between these pathways. In a mouse model of prostate cancer, it has been shown that *Pten* deletion and KRAS activation cooperate to promote EMT and metastatic progression (Mulholland et al., 2012). Also, it was shown that loss of *Pten* cooperates with HRAS activation to promote the development of melanoma and its metastasis (Kim, 2010). Furthermore, the combination of *Pten* and *Kras* mutation dramatically accelerated the development of endometrial cancer (Kim et al., 2010). However, in the bladder the combined effect of *Hras* and *Pten* mutation has never been analysed.

We generated *Hras*^{+G12V} *Pten*^{flox/flox} mice (n=9) and injected them with 2x10⁹ pfu of Ad5CMVCre-eGFP at 2-3 month of age (Table 6-5). We also generated *Pten*^{flox/flox} mice (n=8) to see the effect of *Pten* deletion by itself in the urothelium upon AdenoCre transduction.

None of the animals showed any adverse effect or clinical signs of bladder tumours at 6.5 months post infection.

Table 6-5: Summary of *Hras* and *Pten* mutant mice injected with AdenoCre
 Mouse bladders were injected with 2x10⁹ pfu Ad5CMVCre-eGFP with 10% Polybrene

Genotype	n	Time post injection	Non-urothelial tumours	Urothelial abnormalities (H&E)	Bladder tumour (H&E)
<i>Pten</i> ^{flox/flox}	8	8 months	None	Occasional mild hyperplasia	None
<i>Hras</i> ^{+G12V} <i>Pten</i> ^{flox/flox}	9	8 months	None	Occasional mild hyperplasia	None

In order to assess tumour development, two animals from the AdenoCre $Hras^{+/G12V} Pten^{flox/flox}$ cohort were examined by ultrasound imaging (Figure 6-14). Bladders of $Hras^{+/G12V} Pten^{flox/flox}$ presented with a normal bladder wall and no indication of tumours or irregularities in thickness (B) compared to non-injected *Wild type* controls (A). Since the double mutants did not show any urothelial abnormalities, mice with single mutation (AdenoCre $Pten^{flox/flox}$) were not examined by ultrasound.

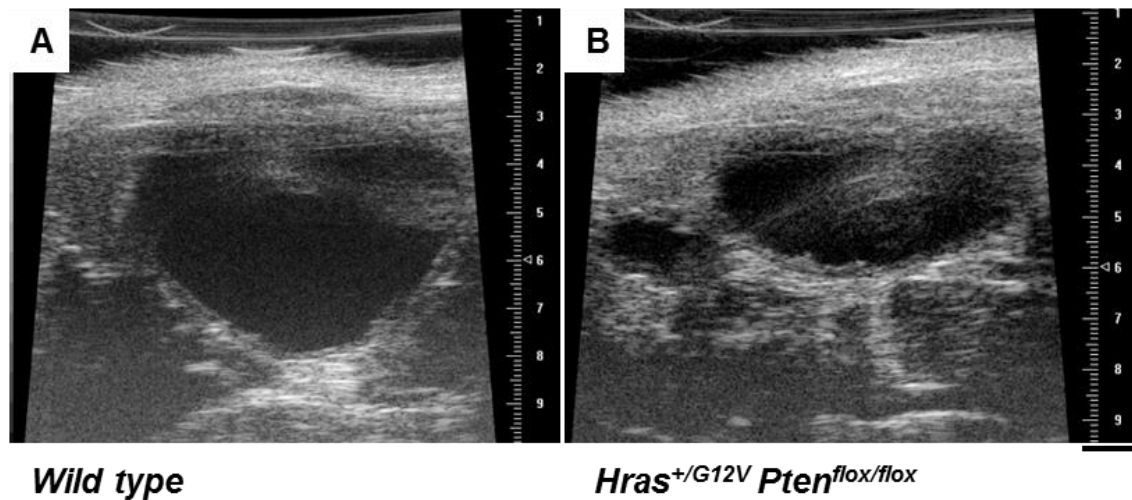


Figure 6-14: Ultrasound of AdenoCre $Hras^{+/G12V} Pten^{flox/flox}$ bladders at 6.5 months post injection

Bladders of non-injected *Wild type* (A) and AdenoCre-injected $Hras^{+/G12V} Pten^{flox/flox}$ (B). Scale bar represents 1 mm (A-B).

Both the *Pten*^{flox/flox} and the *Hras*^{+G12V} *Pten*^{flox/flox} cohort were sacrificed at 8 months post injection, a time point where *Uro11Cre*-driven *Hras* mutant bladders had presented hyperplasia and/or low-grade non-invasive urothelial carcinoma (Zhang et al., 2001, Ahmad et al., 2011b).

Histological features were analysed by H&E (Figure 6-15). We did not detect any indication of bladder tumour formation or any major cellular abnormalities in *Pten*^{flox/flox} (A) or *Hras*^{+G12V} *Pten*^{flox/flox} bladders (B) apart from occasional mild hypertrophy (C, D), which may be an effect of *Pten* deletion as described in Chapter 3, Figure 3-3 c, g, and by others (Tsuruta, 2006).

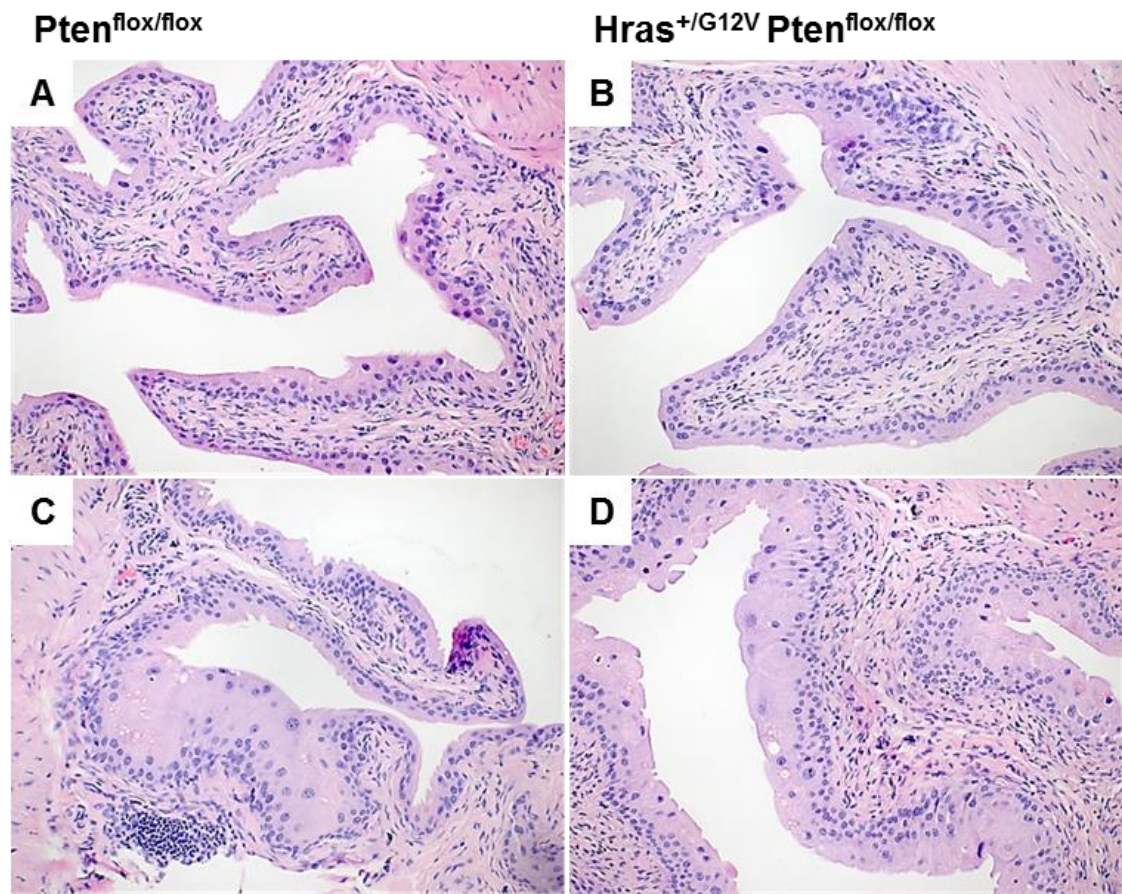


Figure 6-15: Histology of AdenoCre *Pten*^{flox/flox} and *Hras*^{+G12V} *Pten*^{flox/flox} bladders at 8 months post injection

Representative bladder sections stained by H&E. Scale bar represents 100 μ m (A-D).

6.6 AdenoCre off-target effects: soft tissue tumours and other non-urothelial tumours

A number of animals developed tumours in the soft tissue of the pelvic region as well as in organs other than the bladder upon AdenoCre incubation (Table 6-6 and Figure 6-16).

Two out of nine *B-catenin*^{exon3/exon3} *Hras*^{G12V/G12V} mice (22%) (B, C), five out of five *p53*^{flox/flox} *Pten*^{flox/flox} (100%) (A) and one out of three *p53*^{R172H/R172H} *Pten*^{flox/flox} mice (33%) (not shown) produced tumours in the pelvic soft tissue close to the AdenoCre injection site. Pelvic soft tissue tumours were not adherent to any internal organs, and presented fast growth behaviour.

One out of nine *B-catenin*^{exon3/exon3} *Hras*^{G12V/G12V} mice (11%) developed a pancreatic tumour, and two out of nine (22%) developed a hepatic tumour (Figure 6-12).

Two out of three *p53*^{R172H/R172H} *Pten*^{flox/flox} mice (67%) developed a lung tumour (Figure 6-9) and one out of three (33%) developed a lymphoma (not shown).

Table 6-6: Summary of non-urothelial tumours upon AdenoCre injection

Mouse bladders were injected with 2x10⁹ pfu Ad5CMVCre-eGFP with 10% Polybrene

Genotype	n	Pelvic tumour	Pancreas tumour	Liver tumour	Lung tumour	Lymphoma
<i>B-cat</i> ^{exon3/exon3} <i>Hras</i> ^{G12V/G12V}	9	2 (22%)	1 (11%)	2 (22%)	None	None
<i>p53</i> ^{flox/flox} <i>Pten</i> ^{flox/flox}	5	5 (100%)	None	None	None	None
<i>p53</i> ^{R172H/R172H} <i>Pten</i> ^{flox/flox}	3	1 (33%)	None	None	2 (67%)	1 (33%)

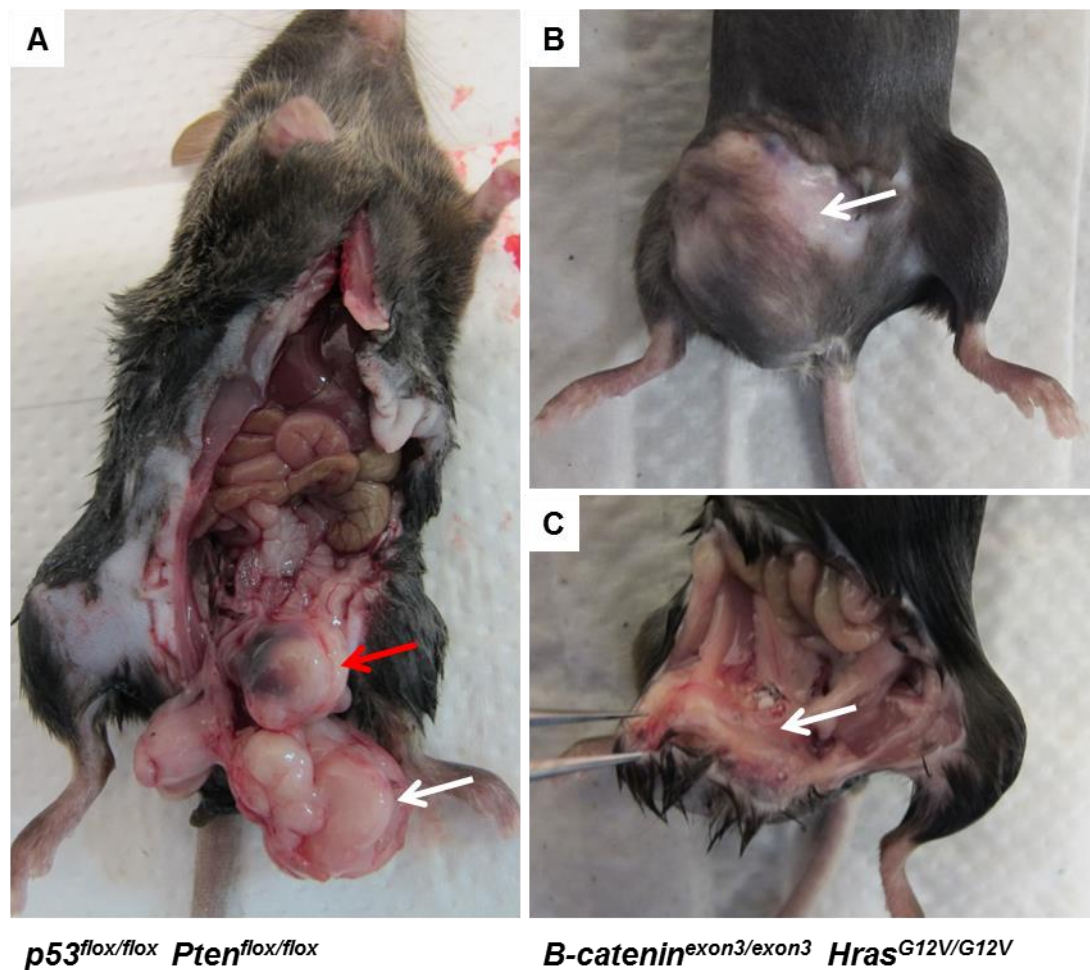


Figure 6-16: Pelvic tumour formation at 2.8 -3.5 post AdenoCre injection

Male $p53^{flox/flox} Pten^{flox/flox}$ mouse with a bladder tumour (A, red arrow) and a soft tissue tumour (A, white arrow). Female $\beta\text{-catenin}^{\text{exon3/exon3}} Hras^{G12V/G12V}$ with soft tissue tumour (B, C, white arrows; bladder removed).

In order to characterise the cellular morphology as well as the origin of the pelvic tumours from $\beta\text{-catenin}^{\text{exon3/exon3}} Hras^{G12V/G12V}$ mice, we performed H&E and immunohistochemistry.

H&E-stained sections presented features of invasive, keratin-rich squamous cell carcinomas (Figure 6-17). The pelvic tumours showed glandular areas (A, circled) mixed with regions of squamous metaplasia and poorly differentiated of cells (A). Keratinisation was observed in some regions of the tumours (A, arrow).

We observed pan-CK positivity along the borders of the glandular structures (B, dotted line), indicating that these tumour cells could potentially be of basal cell origin.

β -catenin was highly upregulated in the nuclei of the tumour cells but not in the adjacent stroma (C, arrows), indicating that AdenoCre-dependent recombination had occurred.

Tumours were highly proliferative along the borders but not inside of the glandular structures as indicated by expression of Ki67 (D, arrows).

In comparison to the pelvic tumours from $p53^{flox/flox} Pten^{flox/flox}$ mice, these β -catenin^{exon3/exon3} Hras^{G12V/G12V} tumours have different characteristics, such as the keratinisation and glandular structure which were not observed in $p53^{flox/flox} Pten^{flox/flox}$. This may indicate that the different histological phenotype is due to different nature of mutation and altered signalling in the tissue.

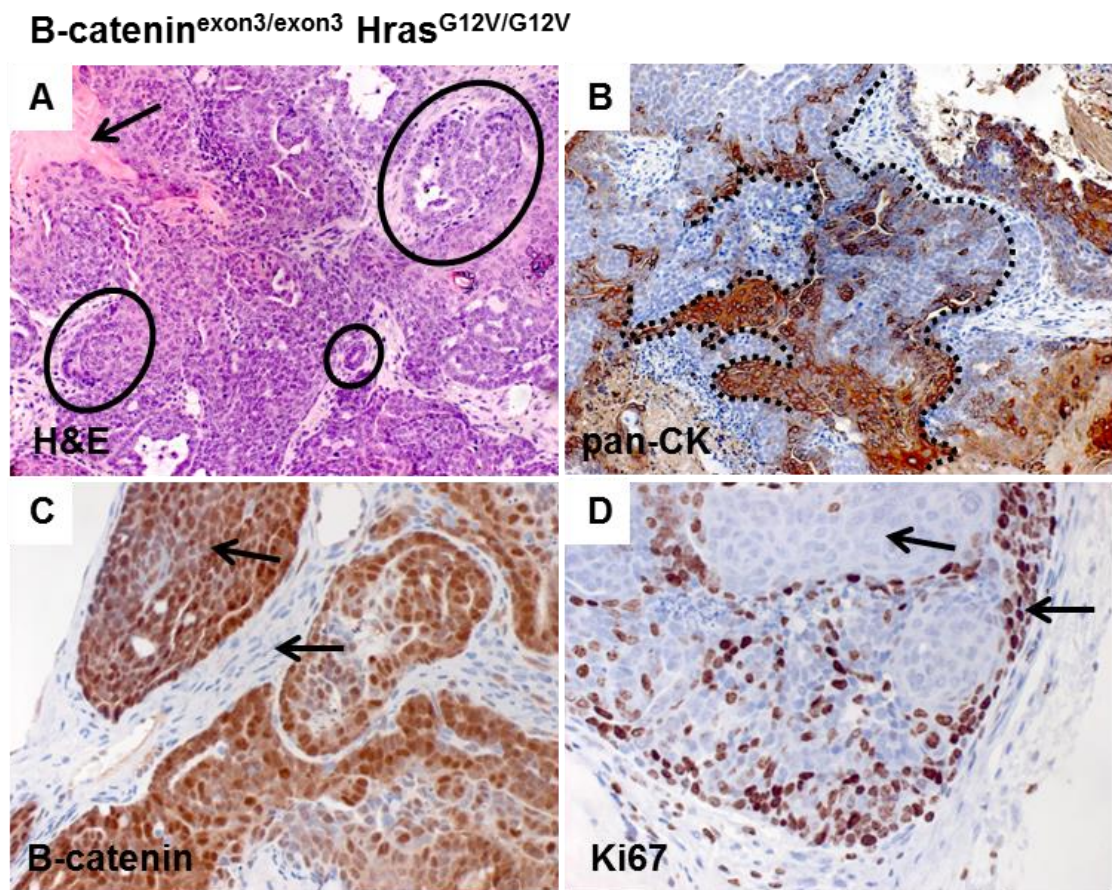


Figure 6-17: Histology of pelvic tumours at 2.8 -3.5 post AdenoCre injection
 Representative photos of pelvic tumour sections of AdenoCre β -catenin^{exon3/exon3} Hras^{G12V/G12V} stained by H&E (A), pan-CK (B), β -catenin (C) and Ki67 (D). Scale bar represents 100 μ m in A-B and 50 μ m in C-D).

6.7 The use of LentiCre as an alternative to AdenoCre

In order to explore an alternative for AdenoCre-mediated recombination, we tested Cre delivery via lentivirus (LentiCre) (Kumar et al., 2008). Lentiviruses are routinely used as vectors to transduce cells and tissues (Heldt and Ressler, 2009). In contrast to adenoviruses, lentiviruses integrate into the host genome resulting in stable transgenic Cre expression (Naldini et al., 1996). Lentiviruses also detain host immune response after infection, a defence mechanism which aims to eliminate transiently infected cells from the microenvironment (Brody and Crystal, 1994).

In order to test the effectiveness of lentivirus in mediating recombination via Cre recombinase, we injected n=3 *B-catenin*^{exon3/exon3} *Hras*^{G12V/G12V} mice with 4x10⁶ pfu LentiCre to analyse the recombination efficiency. At the time of writing at six months post injection, the LentiCre-injected mice are healthy and show no clinical signs of illness.

6.8 Establishment of techniques to assess growth and invasion *in vitro*

6.8.1 Development of an organotypic collagen-I invasion assay

It is yet unclear whether invasion can be detected using ultrasound. In order to develop a platform from which tumour invasion can be addressed at the cellular level, we adapted an organotypic collagen-I assay to murine primary bladder cancer cells in collaboration with Dr Paul Timpson (Garvan Institute, Sydney, Australia). This fibroblast-containing collagen-I assay had previously been used to assess invasion of pancreatic ductal adenocarcinoma and melanoma cells (Timpson et al., 2011). In the assay, cells with invasive behaviour migrate out into the matrix along a nutrient gradient, which is created by placing the matrices on a grid that is in contact with DMEM media only from the bottom.

We sought for a suitable cell type to model tumour invasion in collagen-I. *B-catenin*^{exon3/exon3} *Hras*^{G12V/G12V} is not a model of muscle-invasive bladder cancer *per se*. In our previous study, *B-catenin* and *Hras* activation (*Uro11Cre B-catenin*^{exon3/exon3} *Hras*^{Q61L}), resulted in non-invasive papillary carcinomas with no signs of invasion (Ahmad et al., 2011b). Also, unpublished data from our group of mice with *B-catenin* and *Hras* activation using *Uro11Cre* (*Uro11Cre B-catenin*^{exon3/exon3} *Hras*^{G12V/G12V}), did not obviously exhibit an invasive cancer phenotype.

Instead, the highly invasive human bladder cancer cell line EJ138 was chosen to test the system (Figure 6-18). EJ138 is in fact T24 (or sometimes referred to as MGH-U1), which has been shown by isoenzyme analysis and HLA profiles (O'Toole et al., 1983).

Invasion of EJ138 (4×10^4 seeded cells) into the collagen-I matrix containing human telomerase-immortalised fibroblasts (TIFFs) was clearly detectable after 14 days by H&E staining (A). Ki67 staining showed strong proliferation of invading cells (B). The direction of cell migration is indicated by the black arrows (A-C).

To visualise migrating cells in the matrix, Fascin expression levels were analysed. Fascin has been reported to be expressed in various stages of bladder tumours and is associated with cell dedifferentiation (Karasavvidou et al., 2008).

Invading cells close to the matrix surface expressed Fascin (C, black arrow); however, the expression was reduced in cells that migrated deeper into the collagen-I matrix (C, red arrow).

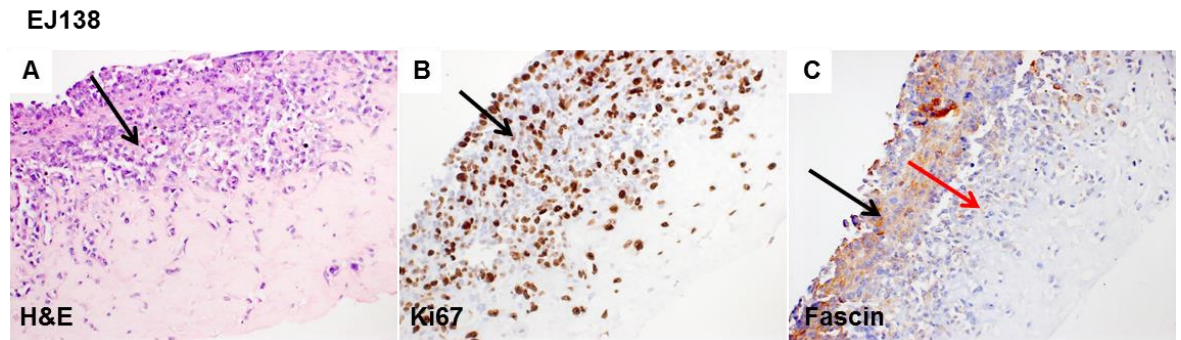


Figure 6-18: EJ138 human cell line migrating into organotypic collagen-I matrix

Representative section of EJ138 cells after 14 days of migration into collagen-I matrix stained by H&E (A) Ki67 (B) and Fascin (C). Scale bar represents 100 μ m (A-C).

This organotypic assay was subsequently used to assess migration of cancer cells derived from murine OH-BBN driven bladder tumours, where invasion had been demonstrated by H&E and immunohistochemistry (Chapter 5).

Migration of OH-BBN-driven *Wild type*, *Tg(Uro11-hFGFR3IIIbS249C)* and *Uro11Cre Pten^{flox/flox}* tumours was examined in matrices containing normal human fibroblasts (NHF) or human telomerase-immortalised fibroblasts (TIFFs). Because the culture was contaminated it was not possible to assess invasion in these assays.

6.8.2 Development of an *ex vivo* assay to test the effects of therapeutic drugs

6.8.2.1 Sphere culture

In order to examine the potential of urothelial cells to form 3D spheres in Matrigel, we used three bladder cell cultures with different growth characteristics. We examined the growth of normal murine *Wild type* urothelial cells, cells from a murine non-invasive tumour, and cells of a human invasive bladder carcinoma cell line. Murine cells from normal bladders and bladder tumours were scraped off the urothelium and pooled. Based on established sphere culture protocols of intestinal crypts and adenoma (Sansom laboratory, BICR), urothelial spheres were grown in Matrigel with ADF media without growth factors (Figure 6-19).

The urothelium of n=9 *Wild type* mouse bladders was scraped off and pooled, processed into single cells, and resuspended in Matrigel and distributed into 10 wells. These *Wild type* cells did not form spheres after 9 days in culture (A) and died after the first passaging.

Pieces of bladder tumours from *UroIIcre B-catenin^{exon3/exon3} Hras^{G12V/G12V}* (n=3) were processed into single cells, resuspended in Matrigel and distributed into 10 wells. Tumour cells formed spheres of a variety of different shapes, including perfectly round (B, white arrow), polarised (not shown), or blobbing and sprouting (B, yellow arrow) as early as after 3 days in culture. We were able to passage *UroIIcre B-catenin^{exon3/exon3} Hras^{G12V/G12V}* formed spheres up to 7 times, freeze and recover for another 4 passages until all cells had died.

The highly invasive human bladder cancer cell line EJ138 (passage 34 upon arrival) was processed into single cells, resuspended in Matrigel and distributed into 10 wells. EJ138 formed sphere-like structures with outgrowths of stretched differentiated cells (C, arrows). Cells were viable after passaging, freezing and recovering without impairment of secondary sphere formation.

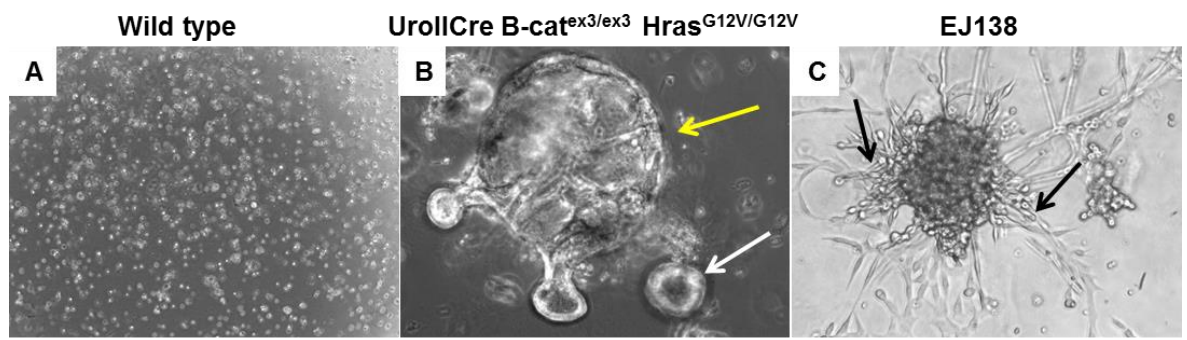


Figure 6-19: Matrigel culture of wild type urothelium, non-invasive tumour, and invasive tumour

Representative bright field photos of *Wild type* urothelium (A), *Uro11Cre β-catenin^{exon3/exon3} Hras^{G12V/G12V}* bladder tumour (B) and EJ138 cell line (C) after 3 days in Matrigel culture. Scale bar represents 10 μm (A-C).

6.8.2.2 Optimisation of sphere culture

Upon successful culture of *Uro11Cre β-catenin^{exon3/exon3} Hras^{G12V/G12V}* tumour spheres, where a variety of different shapes had formed after 3 days in culture (Chapter 6.8.2.1), we sought to define the optimal growth conditions by testing different growth factors using this cell type (Figure 6-20).

A piece of *Uro11Cre β-catenin^{exon3/exon3} Hras^{G12V/G12V}* bladder tumour (n=1) was processed into single cells, resuspended in Matrigel. In a triplicate experiment the addition of 50 ng/ml recombinant human EGF (hEGF) in ADF media resulted in a mild increase in the number of tumour spheres of *Uro11Cre β-catenin^{exon3/exon3} Hras^{G12V/G12V}* (B) compared to wells where no growth factors had been added (None) (A).

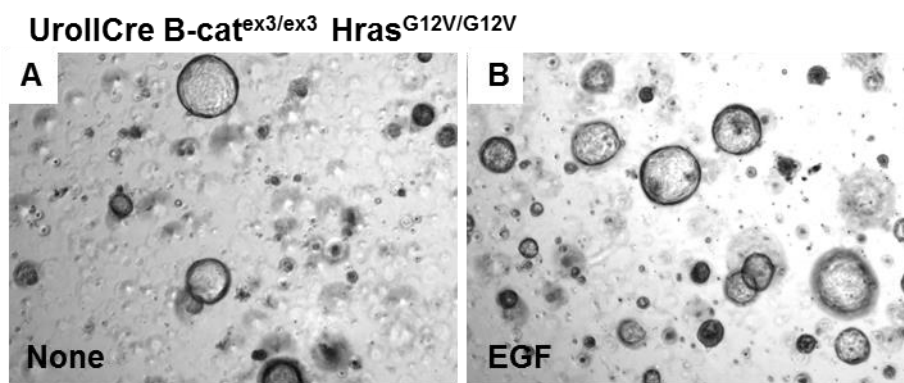


Figure 6-20: Effect of EGF on *Uro11Cre β-catenin^{exon3/exon3} Hras^{G12V/G12V}* tumour sphere culture
Representative bright field photos of *Uro11Cre β-catenin^{exon3/exon3} Hras^{G12V/G12V}* sphere culture with no addition of growth factors (A) and supplemented with hEGF (B) after 3 days in Matrigel. Scale bar represents 10 μm (A-B).

Next, we tested the effect of a number of other growth factors on sphere formation, including mouse Sonic hedgehog (mShh), human tumour growth factor alpha (hTGF- α), human fibroblast growth factor 16 (hFGF16), human keratinocyte growth factor (hKGF, also known as FGF7), as well as a TNF- α inducing salt compound, lithium chloride (LiCl) (Figure 6-21). We examined the growth of a hyperproliferative urothelium where no tumours are expected of mice with a heterozygous *Hras* mutation; *UroIIcre Hras*^{+/*G12V*} (compare H&E of *UroIIcre Hras*^{+/*G12V*} in Chapter 4, Figure 4-7 A).

Pooled urothelium of n=9 *UroIIcre Hras*^{+/*G12V*} bladders was processed into single cells, resuspended in Matrigel and distributed into 12 wells. Growth factor addition was carried out in duplicate wells.

The addition of 10mM LiCl to ADF media resulted in a mild decrease in the number of spheres (Figure 6-21 B) compared to wells where no growth factors had been added (None) (A).

The addition of 25ng/ml of recombinant hTGF- α , or 20ng/ml of hFGF16 had no obvious effect on the number or size of *UroIIcre Hras*^{+/*G12V*} spheres (D and E respectively).

The addition of 50ng/ml recombinant mShh, or 20 ng/ml hKGF, also known as FGF7, resulted in an increase in the number and size of spheres (C and F respectively).

In summary, this result shows that the addition of 50ng/ml mShh and 20ng/ml KGF/FGF7 to the media may enhance sphere number and size, and is therefore likely to improve growth conditions for spheres from non-tumourous urothelial tissue.

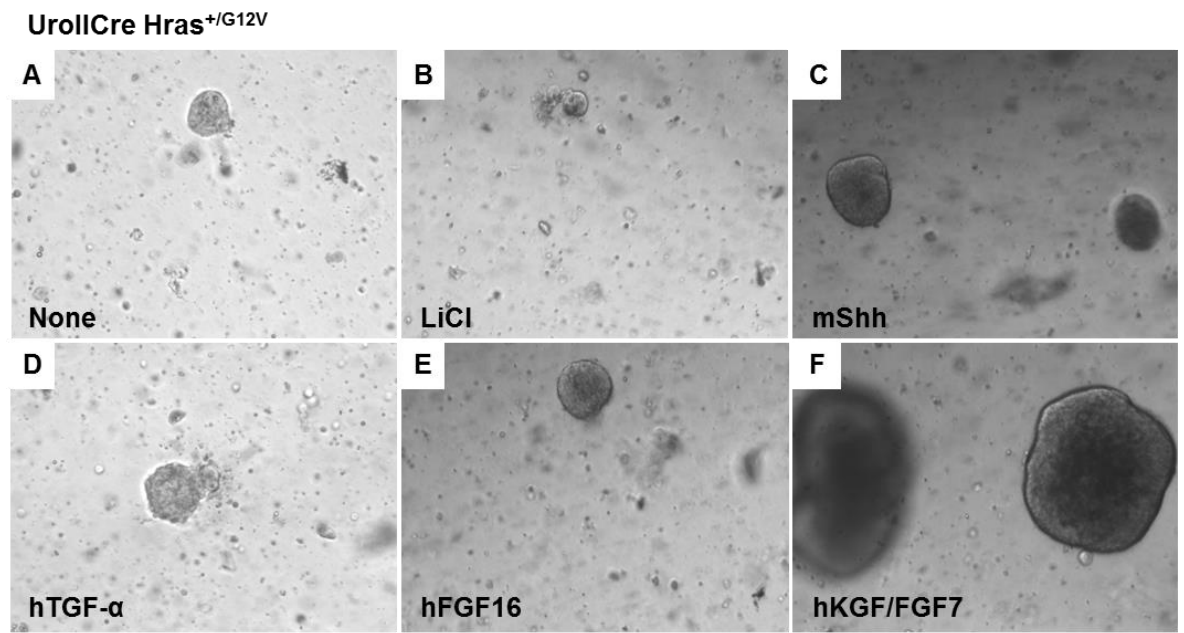


Figure 6-21: Effect of different growth factors on *Uro11Cre Hras^{+G12V}* sphere culture

Representative bright field photos of *Uro11Cr Hras^{+G12V}* sphere culture with no addition of growth factors (A) and supplemented with 10mM LiCl (B), 50ng/ml mShh (C), 25ng/ml hTGF- α (D), 20ng/ml hFGF16 (E), 20ng/ml hKGF/FGF7 (F) after 11 days in Matrigel. Scale bar represents 10 μ m (A-F).

6.8.2.3 Sphere culture of OH-BBN-induced bladder tumours

Next, we sought to examine the growth of cells derived from invasive mouse bladder tumours in Matrigel. Invasive tumours had been established in *Wild type* and *Tg(Uroll-hFGFR3IIIbS249C)* mutant mice by OH-BBN treatment for 10+10 weeks (Chapter 5; compare H&E in Figure 5-6)

Cells from macroscopically thickened bladders of *Wild type* and *Tg(Uroll-hFGFR3IIIbS249C)* were processed into single cells, resuspended in Matrigel and distributed into 8 wells per genotype. Matrigel with ADF media was supplemented with 50ng/ml mShh and 20ng/ml KGF/FGF7 (Figure 6-22).

Cultures from OH-BBN-treated *Wild type* bladders (n=3) showed little sphere formation after 3 days (A) and died by 14 days (C). After 3 days, spheres were as few as 1 sphere in 8 wells, which were generated from one half of a bladder.

OH-BBN *Tg(Uroll-hFGFR3IIIbS249C)* cultures (n=8) showed a larger number of spheres after 3 days (B) compared to OH-BBN *Wild type* (A). OH-BBN *Tg(Uroll-hFGFR3IIIbS249C)* spheres grew up to 3-times of the initial diameter size in 11 days (day 14 in culture) (D).

OH-BBN cultures of *Pten^{flox/flox}* (n=1) and *Tg(Uroll-hFGFR3IIIbS249C) Pten^{flox/flox}* (n=1) under the same conditions failed to form spheres after 3 days and died by 22 days in culture (data not shown).

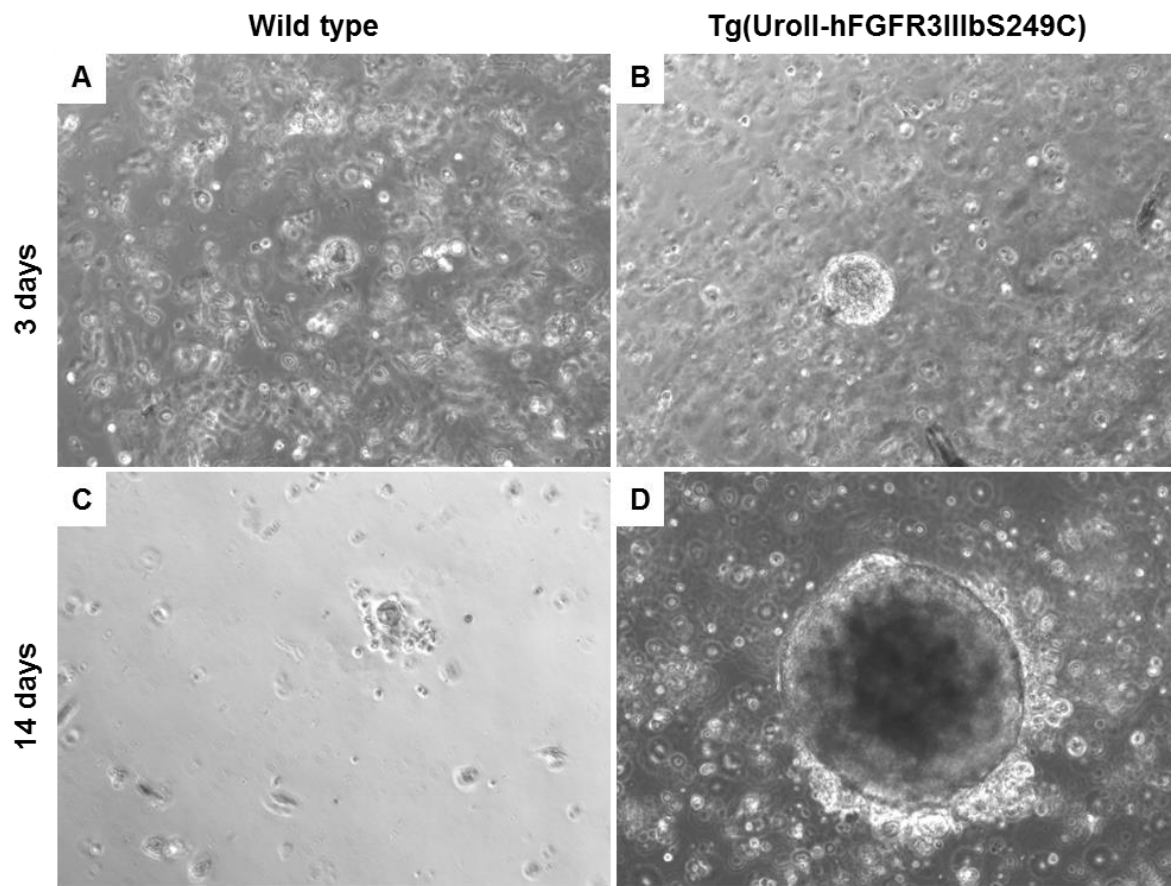


Figure 6-22: Sphere culture of OH-BBN-treated *Wild type* and *Tg(Uro11-hFGFR3IIIbS249C)* after 3 and 14 days

Representative bright field photos of OH-BBN-treated *Wild type* (A, C) and *Tg(Uro11-hFGFR3IIIbS249C)* (B, D) sphere culture supplemented with mShh and hKGF/FGF7 after 3 days (A, B) and 14 days (C, D) in Matrigel. Scale bar represents 10 μm (A-D).

In summary, cells derived from the OH-BBN-induced invasive mouse bladder tumours of *Wild type*, *FGFR3* mutant, *Pten* deletion, or a combination thereof, formed only very few spheres in Matrigel.

6.8.2.4 Organotypic slice culture

A major disadvantage of the Matrigel culture is the fact that urothelial cells are disconnected from their natural environment of the surrounding stroma and the bladder muscle. We therefore sought to develop a technique where the urothelium or the tumour cells can be cultured with a minimum of distortion of the natural signalling from surrounding tissue.

We aimed to establish an organotypic bladder slice culture to grow bladder tumour explants *ex vivo* in order to examine the effect of inhibitor treatment in real time. These experiments were performed in collaboration with Prof Cathy Mendelsohn's lab at Columbia University, New York, USA.

In a pilot experiment we cultured bladder slices of normal bladders on membrane culture inserts soaked in basal conditional media supplemented with recombinant rat glial cell line-derived neurotrophic factor (rGDNF), human hepatocyte growth factor (hHGF), and human keratinocyte growth factor (hKGF, also known as FGF7) as previously described (Batourina et al., 2012).

Bladders of established reporter lines were used, including *Uro11a-GFP-Cre-ERT2 mCherry* (*Uro11a-GCE; mCherry*), *K5-CreERT mTomato/mGFP* (*K5-CreERT mT/mG*), and *Shh-Cre YFP*. *Uro11a-GCE; mCherry* expresses an eGFP-Cre-ERT2 fusion protein under the Uroplakin IIIa (Uro11a) promoter. mCherry is expressed upon tamoxifen induction in this model (Gandhi et al., 2013). *K5-CreERT mTomato/mGFP* expresses a Cre-ERT2 fusion protein under the Cytokeratin-5 (K5) promoter. mTomato is expressed before tamoxifen induction, mGFP is expressed afterwards (Gandhi et al., 2013). *Shh-Cre YFP* expresses Cre and YFP under the Sonic hedgehog (Shh) promoter (Gandhi et al., 2013).

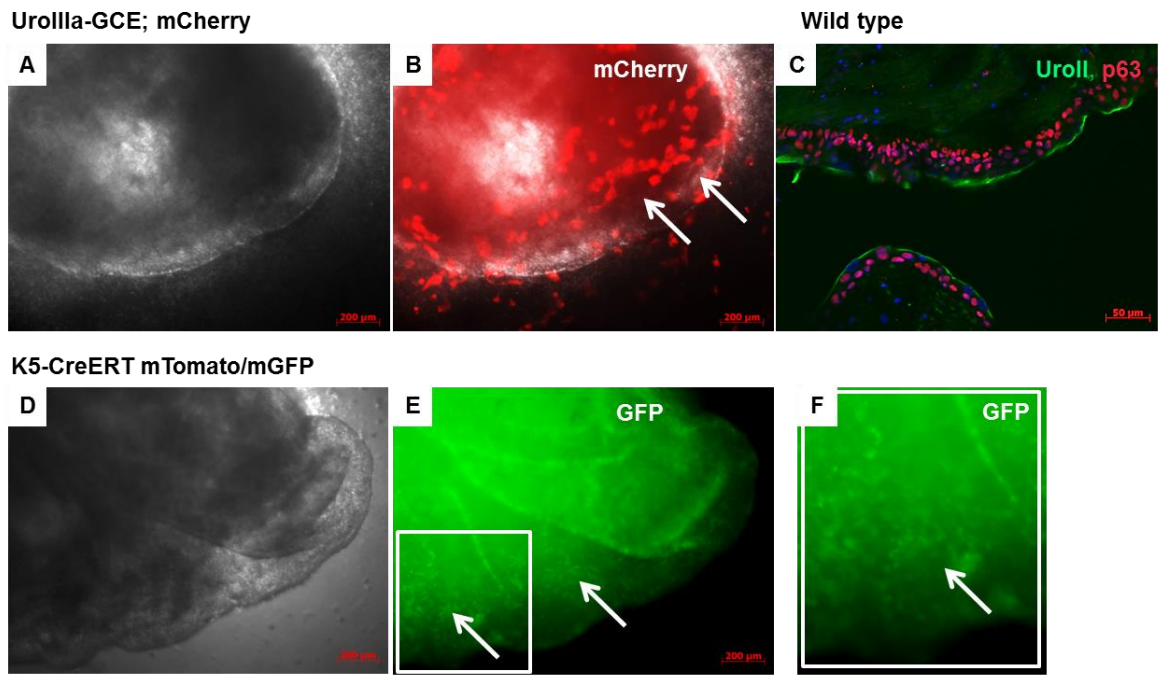
Bladder explants were analysed under a fluorescent microscope, and immunohistochemistry was subsequently performed on paraffin-embedded sections of the explants (Figure 6-23).

Tamoxifen-induced *Uro11a-GCE; mCherry* bladders (A, B) showed overall healthy appearance until termination of the experiment at day 14 in culture. Uroplakin11a-expressing cells were detected by mCherry-positivity (B, arrows).

In order to see whether the cultured organotypic slices maintain the bladder morphology, immunohistochemistry was performed on paraffin-embedded sections of *Wild type* bladder explants after 8 days in culture (C). We observed p63-positivity in basal and intermediate cells (C, red), as well as Uro11-positivity in umbrella cells of the explant (C, green). This was similar to *Wild type* bladders that are processed directly from the animal (Chapter 3, compare Figure 3-7).

Tamoxifen-induced *K5-CreERT mT/mG* bladders (D, E, F) showed overall healthy appearance until termination of the experiment at day 12 in culture. Keratin5-expressing cells were detected by GFP-positivity (E, arrows, magnified in F, arrows).

Bladder explants of *Shh-Cre YFP* mice were viable for 21 days in culture until termination of the experiment (data now shown).

**Figure 6-23: Organotypic slice culture of fluorescent reporter bladders**

Representative photos of slice culture of a tamoxifen-induced *Uro11a-GFP-Cre-ERT2 mCherry* under bright field (A) and red channel (B). Immunohistochemistry for Uroplakin III (green) and p63 (red) on section of paraffin-embedded organotypic bladder slice from *Wild type* (C). Representative photos of slice culture of a tamoxifen-induced *K5-CreERT mTomato/mGFP* under bright field (D) and green channel (E). GFP expression of same animal at higher magnification (white insert in E) (F). Scale bar represents 200 µm in A-B and D-E, 100 µm in F, and 50 µm in C.

6.8.2.5 Organotypic slice culture of OH-BBN-induced bladder tumours

In order to test whether the effect of therapeutic drugs can be assessed by the organotypic slice assay, we set out to culture explants of OH-BBN-induced tumours that we treated with the FGFR3 inhibitor R3Mab.

R3Mab is a monoclonal antibody against wild type and mutant forms of FGFR3, which has been shown to exhibit anti-tumour activity against bladder carcinoma and multiple myeloma xenografts in mice (Qing et al., 2009). The control antibody is a non-functional version of the R3Mab molecule that is dissolved in the same buffer.

We used OH-BBN-induced *Tg(Uro11-hFGFR3IIIbS249C)* bladder tumours (n=2) and OH-BBN-induced *Wild type* control bladders (n=6) to be subjected to 10nM R3Mab or 10nM of a control antibody mixed into basal conditional media for 4 days starting from the first day of culture. Explants were paraffin-embedded and stained by H&E to analyse a potential inhibitory effect of R3Mab on invasion.

We encountered difficulties in the interpretation of the H&E results on the effect of R3Mab, since both OH-BBN-induced *Wild type* and *Tg(Uro11-hFGFR3IIIbS249C)* tumour slices showed signs of urothelial cell disintegration and tumour cell disintegration in the H&E stained sections (Figure 6-24).

Regarding the orientation of the tissues, a minimal layer of coherent cells (A, arrow) was visible and defined as the urothelium. Dotted lines represent the invasive edge down to which urothelial cells have migrated. In panel (B), the urothelium is most likely located above the fine dotted line with invading tumour cells between the two dotted lines, and striated muscle below the thick dotted line. A clear cut of striated muscle can be identified in (C, arrow). The formation of blood vessels was visible in (D, arrow).

In OH-BBN-induced *Wild type* and *Tg(Uro11-hFGFR3IIIbS249C)* bladder slices, tumour cells were visible far beyond the urothelial lining in deep layers of the bladder (dotted lines in A, C and B, D, respectively). No obvious difference in the overall depth of invasion was observed comparing the two genotypes.

Comparing OH-BBN-induced *Wild type* tumour slices that had been treated with Control- or R3Mab antibody, no obvious difference in the overall depth of invasion was observed (A, C).

Similarly, in OH-BBN-induced *Tg(Uroll-hFGFR3IIIbS249C)* tumour slices that had been treated with Control- or R3Mab antibody, no obvious difference in the overall depth of invasion was observed (B, D).

R3Mab treatment for 14 days resulted in further disintegration of the urothelium within the tumour slice and greater difficulties in interpreting H&E results in terms of an inhibitory effect on invasion (data not shown).

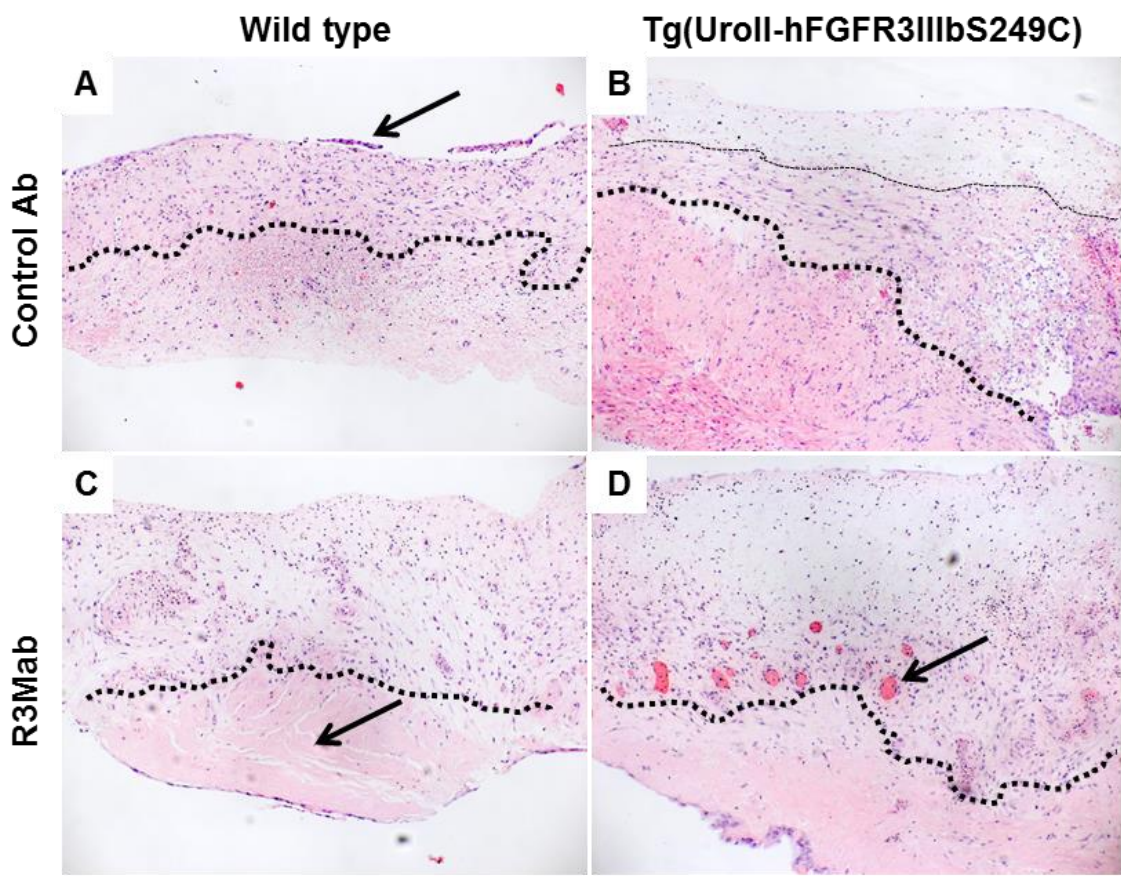


Figure 6-24: Organotypic slice culture of *Wild type* and *Tg(Uroll-hFGFR3IIIbS249C)* tumours treated with FGFR3 inhibitor (R3Mab)

Representative H&E sections of paraffin-embedded organotypic bladder slices from OH-BBN-induced *Wild type* (A, C) and *Tg(Uroll-hFGFR3IIIbS249C)* (B, D) tumours that were treated with control antibody (A, B) or R3Mab antibody (C, D). Scale bar represents 200 μ m (A-D).

6.9 Discussion

In this chapter we examined the effectiveness of AdenoCre to generate urothelial tumours with different combinations of genetic mutations. We replaced UroIICre-driven recombination by AdenoCre delivery. Furthermore, we tested fluorescent imaging and ultrasound imaging in the mouse bladder in order to detect and monitor tumour development and progression in living animals. Moreover, we tested *in vitro* systems such as an organotypic collagen-I assay, 3D sphere culture, and an organotypic slice culture to assess cell migration and the effect of therapeutic drugs *ex vivo*.

6.9.1 Recombination

In order to assess the recombination efficiency at a cellular level, we performed lacZ staining as well as immunohistochemistry for GFP, RFP and β -catenin (Figure 6-2). We showed that GFP immunohistochemistry can be used to detect infected cells; however the staining is not sufficient to specify recombination. RFP and lacZ detection was discontinued due to unspecific staining. In this study, AdenoCre recombination was most effectively detected by β -catenin staining in the presence of a β -catenin^{exon3/exon3} activating mutation. The exact percentage of successfully recombined cells could not be determined in our experiments. It has been shown that viral transduction efficiency can be influenced by the pH, as well as by addition of calcium phosphate (Jackson, 2001), which poses a chance to optimise recombination rates for future experiments.

Some studies have shown that urothelial stem cells, or at least a subgroup thereof, may reside in the basal cell compartment (Kurzrock et al., 2008, Gaisa et al., 2011, Shin et al., 2011, Chan et al., 2009b, Gandhi et al., 2013). From this study it appears that the incidence of stem cell recombination upon adenovirus infection may be very low. However, it is unknown at this point whether more than one type of urothelial progenitors exists, and whether urothelial stem cells are the cancer initiating cells in the bladder.

AdenoCre penetration has previously been assessed in human ureters (Chester et al., 2003). In the study, intact normal human ureters were transduced *ex vivo*

with Adv-cmv- β -gal viral solution and stained for β -galactosidase activity. Immersion with Adv-cmv- β -gal resulted in transduction of the most superficial layers of the urothelium only, with no obvious time dependence of viral exposure. Taken into account that those experiments were performed on human ureters, the results could indicate that deeper layers may not be transduced using adenoviral Cre infection in mice. However, in contrast to the human urothelium which consists of seven layers on average, the mouse urothelium is composed of only three layers, which could help the virus to penetrate deeper layers. In the first publication using AdenoCre in the mouse bladder, it was described that the entire urothelium can be targeted with 10% recombination efficiency using a titre of 1×10^9 pfu (Puzio-Kuter et al., 2009). Our results did not recapitulate these data. In our hands, AdenoCre recombination was mainly observed in umbrella and intermediate cells, consistent with previous suggestions in human ureters (Chester et al., 2003).

Comparing the recombination efficiency of AdenoCre and UroIICre, it is evident that UroIICre promotes recombination in the majority of cells in the urothelium (Figure 3-2) whereas AdenoCre mediates recombination only in a small number of cells (Figure 6-2). UroIICre recombination was predominantly observed in umbrella and intermediate cells, whereas basal cells showed fewer cells with GFP-positivity (Figure 3-2). AdenoCre recombination was mainly observed in umbrella and intermediate cells (Figure 6-2). Therefore, the basal cell compartment may not have been effectively targeted yet in our models. It would be interesting to utilise a Cre promoter that drives the expression of the recombinase in the basal cell layer given that the cancer cell of origin may reside therein. A study on urothelial regeneration has utilised a tamoxifen-inducible Sonic hedgehog-Cre (ShhCreER), where recombination in the basal cell compartment of the urothelium was reported (Shin et al., 2011). ShhCreER has not yet been tested in controlling the expression of bladder-specific mutations. Furthermore to the comparison of AdenoCre and UroIICre recombination, both systems promoted the growth of exophytic papillary tumours in *β -catenin* and *Hras* mutated bladders (Chapter 6.4 and (Ahmad et al., 2011b). However, AdenoCre-driven tumours seemed to be smaller in size compared to *UroIICre β -catenin^{exon3/exon3} Hras^{Q61L}* bladders upon dissection at 8 months. This may indicate that the fewer number of recombined cells by AdenoCre results in fewer

tumours or a smaller tumour mass combined. By defining a suitable and potent combination of genetic mutations, this may pose an opportunity to potentially study metastatic progression before the urothelial tumour reaches a lethal size.

6.9.2 *In vivo* imaging

In order to monitor tumour progression in living animals, we tested fluorescent imaging and ultrasound imaging in the mouse bladder (Table 6-7).

Table 6-7: Summary of *in vivo* imaging techniques tested in the study

<i>In vivo</i> imaging	Purpose	Result
IVIS	Tumour monitoring, metastatic spread	High background signal in reporter mice without tumours
Ultrasound	Tumour monitoring	Successful tumour detection and monitoring

Monitoring of AdenoCre -induced tumours *in vivo* was assessed by IVIS Spectrum (Figure 6-1). We were confronted with high background signal from the guts and urine, which made assessment difficult at both RFP and GFP wavelengths. It may be possible to reduce the background signal from the guts by feeding an alfalfa-free diet, which may help to obtain a clearer RFP signal from the bladder (Inoue et al., 2008). Furthermore, it is possible that collective RFP emission from a tumour cell mass may result in a stronger signal. However, bladder tumours with an RFP reporter construct were not available at the time of experiments. Moreover, it is possible that the expression level of the RFP reporter is particularly low in the bladder and that changing to a different reporter system such as an *mTomato* or *mCherry* line could be an alternative to potentially enhance the signal from the bladder (Muzumdar et al., 2007), (<http://www.gudmap.org>).

Using ultrasound imaging we were able to monitor tumour progression *in vivo* (Figure 6-3). Bladder wall thickening, as well as tumours as small as 0.5 mm in diameter, can be detected and the growth can be monitored. This is consistent

with a previous study where tumours as small as 0.53 mm³ were detected using this method (Patel et al., 2010). However, it is as yet unclear whether invasion can be addressed by this method. Ultrasound imaging could further be improved by targeted contrast enhancement (Chan et al., 2011).

6.9.3 AdenoCre

We have confirmed that orthotopic AdenoCre injection mediates recombination in the bladder, leading to tumours with different combinations of genetic mutations. The combination of *β-catenin* and *Hras* mutation caused exophytic papillary tumours in the urothelium as early as 3.5 months post injection in *β-catenin^{exon3/exon3} Hras^{G12V/G12V}*. AdenoCre-driven tumours seemed to be smaller in size, compared to *UroIICre β-catenin^{exon3/exon3} Hras^{Q61L}* bladders, upon dissection at 8 months (Ahmad et al., 2011b). This may reflect the smaller number of cells that was likely to be recombined by AdenoCre compared to broad recombination in umbrella and intermediate cells using UroIICre. Bladder tumours had formed only in 7 of 9 animals (78%). Whether these tumours will develop muscle-invasive potential or metastatic disease has to be tested in future experiments.

Hras activation in combination with *Pten* deletion did not produce tumours or any cellular abnormalities by 8 months in *Hras^{G12V/G12V} Pten^{flox/flox}*, indicating that AdenoCre-induced *Pten* deletion on its own or in combination with *Hras* is insufficient to induce urothelial tumourigenesis. This is in accordance with the findings in Chapter 3, where a mouse model of co-activated MAPK/AKT signalling through FGFR3 in combination with *Pten* deletion (*UroIICre Fgfr3^{+ /K644E} Pten^{flox/flox}*) presented a hypertrophic urothelium but did not result in carcinoma development (Chapter 3). As speculated before, this may be due to redundant pathway activation (Jebar et al., 2005). Mutual exclusivity of *Pten* and *Ras* pathways has also been demonstrated in skin papilloma formation (Mao et al., 2004). Alternatively, it is possible that the AdenoCre induction was incomplete.

p53 and *Pten* deletion in combination, *p53^{flox/flox} Pten^{flox/flox}*, caused tumours in the bladder as reported before (Puzio-Kuter et al., 2009). However, in the study by Puzio-Kuter it was not fully clarified whether these tumours were of epithelial- or muscle origin. Based on our immunohistochemistry and histological observations, we and other groups (Yang et al., 2013) define these tumours as of

non-urothelial origin. Due to AdenoCre recombination in the muscle upon needle insertion, these tumours seem to have originated in the striated muscle or other soft tissue surrounding the injection site. Our tumours were negative for urothelial markers such as CK5 and p63, which is in accordance with the work done by Yang, where pan-cytokeratin was used to demonstrate non-urothelial origin. Furthermore, our tumours resemble the appearance of the sarcomas in the $p53^{flox/flox} Kras^{+/LSLG12D}$ mouse model generated by Kirsch that were also positive for smooth muscle actin (SMA) (Kirsch et al., 2007). In contrast to Puzio-Kuter, we did not observe metastasis in the $p53^{flox/flox} Pten^{flox/flox}$ model.

$p53$ dominant-negative mutation and $Pten$ deletion in combination, $p53^{R172H/R172H} Pten^{flox/flox}$, caused tumours in the bladder muscle that were similar to the ones observed in $p53$ and $Pten$ deficient mice; however the tumour onset was 1 month earlier, indicating that a homozygous dominant-negative $p53$ mutation may promote faster tumour growth than homozygous $p53$ deletion.

An issue of AdenoCre infection was the frequent observation of non-urothelial tumours. Depending on the type of mutations that were introduced, we observed sarcoma formation in the bladder muscle, tumours in other areas of the pelvic region, as well as tumours in distant organs. For example, AdenoCre-injected $p53^{R172H/R172H} Pten^{flox/flox}$ mice developed lymphoma, lung tumours, and soft tissue tumours in the pelvis. In our hands all $p53^{flox/flox} Pten^{flox/flox}$ mice (n=5) developed soft tissue sarcomas in the bladder muscle, which was not reported in the original study where the AdenoCre-mediated $p53 Pten$ mouse model was first described (Puzio-Kuter et al., 2009). However, pelvic soft tissue tumours with similar histology have been observed in $p53^{flox/flox} Kras^{+/LSLG12D}$ bladders after 8.46×10^8 pfu AdenoCre treatment using catheterisation and urethral suture (Yang et al., 2013). Similar to our sarcomas in $p53^{flox/flox} Pten^{flox/flox}$, Yang also observed invasion of these tumours into adipose tissue and striated muscle layers at 4-8 weeks post AdenoCre exposure. Our β -catenin^{exon3/exon3} $Hras^{G12V/G12V}$ mice developed tumours in the liver and pancreas, as well as keratin-rich squamous cell carcinomas in the pelvic region. Based on histological observations and immunohistochemistry these distant growths were primary tumours (Figure 6-9). Furthermore, transformed cells were particularly present nearby blood vessels (Figure 6-10), suggesting presence of the adenovirus in the blood stream, which has led to recombination in distant sites outside of the bladder.

Mouse sarcomas induced by AdenoCre were originally described in $p53^{flox/flox}$ $Kras^{+/LSLG12D}$ mice (Kirsch et al., 2007). Soft tissue sarcomas in our cohorts generally developed in the pelvic region around the area of injection. We speculate that the exposed muscle tissue around the entry site of the needle is infected by AdenoCre and undergoes recombination. The issue with sarcoma formation is that these growths occur before the development of urothelial tumours, which may be due to the different proliferation rates of the two tissues. To overcome soft tissue sarcoma development, the technique of virus delivery needs to be improved. However, both methods, orthotopic instillation (this study, (Puzio-Kuter et al., 2009)) and catheterisation (Yang et al., 2013), have led to the formation of sarcomas. It would be possible to surgically remove pelvic sarcomas in order to allow more time for urothelial pathogenesis to occur. However, non-urothelial tumours such as in the liver, lung or pancreas were not easy to detect at an early stage and most likely difficult to remove without risking the wellbeing of the animal. Another possible modification of the technique could be the use Matrigel to solidify the virus solution in order to reduce virus influx into the blood stream. It could also be considered to pre-treat the urothelium with chemical agents in order to increase the transduction efficiency.

The virus titre is a parameter that needs to be chosen carefully in order to allow sufficient but specific recombination in the urothelium. The bladder lining is equipped with an effective defence barrier, the urothelial plaques made of a thick polyglucan layer and crystallised Uroplakin particles, which reduce the absorption of toxic substances that are present in the urine. We speculated that this natural barrier may also hamper the viral infection process, and that a high virus titre would be beneficial to maximise transduction. Furthermore, in case of a not completely voided bladder, the dilution of urine may pose a second hurdle to the amount of virus needed. Therefore, it needs to be ensured that the bladder has been sufficiently voided of urine before virus injection. The virus titre can also be adjusted according to the nature of the targeted mutations. For example, if a model of metastasis is desired, it may be beneficial to select “strong” tumourigenesis-inducing mutations in combination with a low virus titre. This would ensure recombination in only a small number of cells and therefore allow more time for metastasis to occur.

When AdenoCre was introduced for the first time as a driver of recombination in $p53^{flox/flox} Pten^{flox/flox}$ mice, a titre of 1×10^9 pfu was used (Puzio-Kuter et al., 2009). This resulted in a recombination efficiency of 10% of successfully transduced urothelial cells (Puzio-Kuter et al., 2009). In a different study with $p53^{flox/flox} Kras^{+/LSLG12D}$ mutant mice, a titre of 8.5×10^8 pfu was administered by catheterisation (Yang et al., 2013). This method resulted in higher recombination efficiency, however, the procedure is more time consuming and only female mice could be used for catheter instillation. Furthermore, this method has been shown to also result in soft tissue sarcomas (Yang et al., 2013) and would therefore not pose an advantage to our current surgical method of AdenoCre delivery. In our study, we used twice the amount of virus (2×10^9 pfu) as Puzio-Kuter to induce tumourigenesis in the same $p53^{flox/flox} Pten^{flox/flox}$ mouse model (Figure 6-5). Our $p53^{flox/flox} Pten^{flox/flox}$ mice developed tumours by 3 months post injection, while Puzio-Kuter reported tumours by 6 months post injection. However, our $p53^{flox/flox} Pten^{flox/flox}$ tumours arose in the muscle where recombination had taken place. It is possible that a lower AdenoCre titre may result in a higher rate of urothelial tumours rather than sarcomas as reported by Puzio-Kuter (Puzio-Kuter et al., 2009).

As an alternative to AdenoCre-mediated recombination we tested LentiCre-mediated Cre delivery in a still ongoing experiment. As a consequence of virus integration into the genome, the possibility of insertional mutagenesis cannot be excluded. LentiCre is currently not commercially available at the same high titre as AdenoCre.

Overall, AdenoCre has the advantage of recombining a small number of cells that are surrounded by a normal tissue environment, which would allow examination of signalling interaction between tumour and host tissue. In this matter, AdenoCre represents an interesting tool for modelling bladder cancer. The technique could also allow lineage tracing of cancer stem cells in a developing bladder tumour. However, at this point AdenoCre also comes with the disadvantage of frequent non-urothelial tumour formation in adjacent soft tissue or distant organs which precede the emergence of urothelial tumours and remains to be addressed in future experiments.

6.9.4 *In vitro* models

In order to assess transformation and cell migration as well as to test therapeutic drugs, we tested *ex vivo* techniques and assays including a Collagen-I invasion assay, 3D sphere culture and an organotypic slice culture (Table 6-8).

Table 6-8: Summary of *in vitro* techniques tested in the study

<i>In vitro</i> system	Purpose	Result
Collagen-I invasion	Proof of invasive potential	Invasion assay ready for human cell lines; needs to be optimised for mouse primary tumour cells
3D sphere formation	Drug treatment assessed by renewal capacity	Successful sphere formation in Wnt activation model; needs to be optimised for other genotypes
Organotypic slice culture	Drug treatment assessed by invasion	Length of treatment to be kept at a minimum; orientation of slice during embedding is of importance

Invasion at the cellular level was assessed using an organotypic collagen-I assay (Figure 6-18). We were able to detect migration of a human bladder cancer cell line into the matrix; however the system needs to be optimised for murine tissues. An issue with optimising the assay conditions is the current lack of a positive control of an invading mouse tumour. At the time of writing this assay is being repeated with a new set of OH-BBN-induced bladder tumours.

A 3D tumour sphere culture assay was developed in order to test the effects of therapeutic drugs by assessing the sphere formation and renewal capacity in Matrigel (Figure 6-19 to Figure 6-22). Murine Wnt-activated tumours as well as invasive human cell lines were capable of growing and renewing in Matrigel conditions with ADF media (Figure 6-20). In contrast, tumours of other genotypes, including OH-BBN-induced *Wild type Tg(Uro11-hFGFR3IIIbS249C)* and *Uro11Cre Pten^{flox/flox}* showed reduced sphere formation and renewal (Figure 6-22). *Wild type* urothelial cells completely failed to form spheres (Figure 6-19). It is

possible that adult *Wild type* urothelial cells do not have sufficient renewal capacity to form spheres. On the other hand, these cells may need special media conditions and a particular supply of growth factors, which was not further tested. In future experiments the diameters of spheres could be considered to be measured by ImageJ software. However, the number of urothelial cells from normal bladders was generally low, and therefore cells from multiple bladders had to be pooled in order to reach sufficient material to be plated. Therapeutic drugs were not tested in this assay due to the low rate of tumour sphere formation. Although the 3D sphere culture assay has successfully been used for drug screening in tumour spheres derived from other tissues such as the breast (Kim and Alexander, 2013), it may not be suitable for application in the bladder.

Organotypic slice culture was developed in order to test the effects of therapeutic drugs on invasion under natural conditions of a generally intact organ environment (Figure 6-23). In this slice culture system, normal bladder explants were viable for up to 21 days. However, slices of tumours quickly showed signs of urothelial cell and tumour cell disintegration, which made the interpretation of the results on the effect of R3Mab difficult (Figure 6-24). The orientation of the tumour slice in paraffin and properly cut sections are of great importance in order to analyse the depth of tumour cell invasion or impairment thereof. At the time of writing, this FGFR3 inhibition assay is being repeated in a new set of OH-BBN-induced *Fgfr3*-mutant bladder tumours.

6.9.5 Future work

For *in vivo* imaging it would be interesting to assess tumour growth or drug response in a three dimensional (3D) space. Therefore, it would be essential to work out volume measurements in the ultrasound software.

Regarding viral Cre injections, we are awaiting the results of the LentiCre experiment (Chapter 6.7), which will shed light on the effectiveness of LentiCre as an alternative to AdenoCre. Recombination efficiency and tumour development can be assessed in direct comparison with the AdenoCre-injected *B-catenin^{exon3/exon3} Hras^{G12V/G12V}* mice. Furthermore, AdenoCre could also be a useful tool for lineage tracing of cancer stem cells in a developing bladder tumour and potentially during metastatic spread.

For the *in vitro* assays, it would be essential to optimise the collagen-I assay using a positive control of invasive mouse tumour cells, as well as to optimise the organotypic slice culture conditions to impede the disintegration of the tissue in the culture in order to test therapeutic drugs.

6.9.6 Conclusion

We have validated the effectiveness of AdenoCre to generate urothelial tumours in mice with *B-catenin*^{exon3/exon3} *Hras*^{G12V/G12V} mutation and used ultrasound to monitor the growing tumours *in vivo*. Furthermore, we tested *in vitro* systems such as an organotypic collagen-I assay, 3D sphere culture, and an organotypic slice culture, which may become useful applications to assess cell migration and the effect of therapeutic drugs *ex vivo*.

Chapter 7

Final Discussion

7.1 Summary of the findings

The overall aim of this study was to examine the role of *FGFR3* mutation in bladder cancer initiation and progression by using mice as a model organism.

Firstly, we demonstrated that *Fgfr3* and *Pten* mutations cooperatively promote morphological changes of the urothelium, but not when mutated individually (Chapter 3). Our results provided functional evidence that supports the hypothesis that upregulation of FGFR3 signalling plays a causative role in urothelial pathogenesis of non-invasive bladder cancer together with upregulated PI3K-AKT signalling. However, mice still did not develop urothelial cell carcinoma.

Therefore, we searched for cooperating mutations of urothelial tumourigenesis in mice with *FGFR3*, *PTEN* or *RAS* mutation using Sleeping Beauty (SB) insertional mutagenesis (Chapter 4). The SB system failed to produce bladder tumours in *Fgfr3* as well as in *Hras* mutant mice and may therefore constitute an inefficient tool in the bladder to induce urothelial tumourigenesis. Furthermore, it is possible that other more realistic mutations are required to drive cancer in the bladder. In mice with *Pten* deletion, one tumour was generated and general hypertrophy with cellular abnormalities was observed in all samples. No direct association between *Fgfr3* and *Pten* mutations was found; however, SB mutagenesis supported that *Fgfr3* and *Pten* cooperation may merge at the signalling downstream.

Thirdly, we compared two point mutations, *S249C* and *K644E*, in *FGFR3* and *Fgfr3* respectively in the otherwise normal urothelium *in vivo*, and demonstrated that an *FGFR3 S249C* mutation alone does not lead to tumourigenesis, similar to *Fgfr3 K644E* mutation alone (Chapter 5). Differential effects between *K644E* and *S249C* on the cellular architecture were only apparent in combination with another mutation such as *Pten* deletion. Furthermore, we compared *S249C* and *K644E*, as well as the effect of *Pten* deletion and *Fgfr3-Pten* double mutation in OH-BBN-induced tumours (Chapter 5). Our results indicated that *Fgfr3* mutation may have an effect on tumour progression of established neoplasms.

Lastly, we validated the effectiveness of AdenoCre to generate urothelial tumours in mice with β -catenin^{exon3/exon3} Hras^{G12V/G12V} mutation and used ultrasound imaging to detect and monitor tumour development and progression *in vivo* (Chapter 6). Moreover, we tested *in vitro* systems such as an organotypic collagen-I assay, 3D sphere culture, and an organotypic slice culture, which may become useful applications to assess cell migration and the effect of therapeutic drugs *ex vivo*.

Taken together, our data supported previous evidence of functional involvement of FGFR3 in the development and progression of urothelial cell carcinoma. Furthermore, technological improvement of our *in vivo* and *in vitro* models may create useful tools to generate and assess invasive bladder cancer, and to perform preclinical drug testing.

7.2 Contribution of FGFR3 to tumour initiation, progression and invasion

Regarding tumour initiation, FGFR3 seems unlikely to be the sole driver of bladder tumourigenesis. This is in accordance with the current understanding of cancer biology where multiple ‘hits’ to DNA are required for a tumour to arise. Interestingly, *in vitro*, a single *FGFR3* mutation is able to induce morphological transformation, cell proliferation, and anchorage independent growth (di Martino et al., 2009). However, in mice we showed that a single mutation in the kinase domain of the receptor, *K644E*, was insufficient to promote cancer formation (Ahmad et al., 2011c). Similarly, a mutation in the linker region of the Ig-like domains in FGFR3, *S249C*, on its own did not lead to tumour initiation in the mouse bladder (Chapter 5). These results strongly suggest that FGFR3 needs a cooperating mutation to induce urothelial tumourigenesis.

It has been suggested that *FGFR3* mutation is an early event during bladder cancer development (Knowles, 2007, Zieger et al., 2005, Bakkar et al., 2003) due to the fact that *FGFR3* is found mutated in 60-80% of non-invasive bladder cancers including papilloma, PUNLMP, and low- and high-grade papillary carcinoma (Billerey et al., 2001, Cappellen et al., 1999, Tomlinson et al., 2007a, van Rhijn et al., 2012, van Rhijn et al., 2002). The urothelia of our mouse models with *Fgfr3* mutation and activated PI3K/AKT signalling showed

histological features comparable with hyperplasia and dysplasia, which are regarded as early stages bladder cancer pathogenesis in humans (Chapter 3). The model supports that these early-stage lesions with *FGFR3* mutation are unlikely to progress, as they did not produce tumours in the life time of the animal models up to 18 months (Chapter 3).

In terms of tumour progression of established neoplasms, we showed *in vivo* that *FGFR3 S249C* mutation can have an effect on cancer progression and invasion upon carcinogen-induced tumorigenesis (Chapter 5). Similar observations were made with a kinase domain mutation, *Fgfr3 K644E*, supporting the tumour-promoting properties of activated FGFR3 signalling (Chapter 5). Previous studies have linked *FGFR3* mutation to the development of early papillary lesions; however, the progression of advanced bladder cancer seemed to be unaffected by the presence of *FGFR3* mutations (Zieger et al., 2005). It would therefore be interesting to sequence our OH-BBN-induced tumours with *FGFR3*- or *Fgfr3*-mutant status in order to obtain information on potential cancer initiating mutations or cooperating mutations.

Mechanistically, the role of FGFR3 in bladder cancer is still being debated. It was proposed that FGFR3 can promote cellular proliferation and provide a growth advantage while apoptotic mechanisms and genomic stability are still maintained (Bakkar et al., 2003). This was supported in cell culture studies, where increased FGFR signalling provided a proliferation and survival advantage to urothelial cells (di Martino et al., 2009). FGFR3 may also bypass the cell cycle checkpoint at G1, which could promote the development of benign precursor lesions that may be able to progress due to accumulated replicative stress (Bartkova et al., 2005, Zieger et al., 2005). Our results potentially support the concept of FGFR3 in promoting cellular proliferation and/or providing a growth advantage to urothelial cells, since *FGFR3*-mutant bladders were linked to a significantly higher incidence of tumours compared to *Wild type* upon carcinogen treatment (Chapter 5). To further elucidate the mechanism behind FGFR3-dependent progression in OH-BBN-induced tumours, it would be essential to analyse alterations in the pathways downstream of *FGFR3 S249C* mutant signalling. It would also be interesting to investigate further to our experiments on γ H2aX phosphorylation in *FGFR3-S249C* and *Wild type* bladders (Chapter 5), whether the presence of an *FGFR3* mutation can alter the sensitivity to DNA

damage or the DNA repair machinery in *FGFR3*-mutant cells in a larger number of samples.

7.3 Tumour progression across pathogenesis pathways

The current model of two independent pathogenesis pathways of urothelial cell carcinoma has been suggested based on histological and genomic analysis of non-invasive and invasive tumours (Knowles, 2008, Lindgren et al., 2012). A question of immense clinical relevance remains: that is whether these pathways can overlap, or whether tumours can stage progress across these pathways to adopt a more aggressive phenotype and growth behaviour.

Indication of potential overlap of the tumourigenesis pathways comes from a study in mice where SV40T was overexpressed under the Uro11 promoter (Cheng et al., 2003). Cheng reported that the majority of mice developed CIS that evolved into high-grade, superficial papillary tumours before a small fraction of them advanced to invasive and metastatic cancer. This suggests that a fraction of CIS may constitute precursors of high-grade, papillary tumours with increased risk of progressing to invasive and metastatic disease. This could also fit with the study by Choi, where muscle-invasive bladder cancer was suggested to be subcategorised into basal-, luminal-, and p53-like tumours based on their immunohistochemical expression pattern (Choi et al., 2014). In this model, luminal-like tumours were enriched with *FGFR3* mutations amongst others, and could therefore potentially represent a subset of muscle-invasive tumours that have derived from non-invasive papillary tumours where *FGFR3* mutations are frequent (van Rhijn et al., 2012, Billerey et al., 2001, Hernandez et al., 2006).

FGFR3 has been associated with non-invasive low grade/stage pTa tumours. However, in muscle-invasive bladder tumours, *FGFR3* is mutated in only 10-15% of the cases (Billerey et al., 2001). This could indicate that non-invasive lesions with *FGFR3* mutation never progress to invasive tumours, and that invasive lesions arise predominantly from wild type *FGFR3* cells (Tomlinson et al., 2007a). It is possible that a subset of *FGFR3*-mutated invasive lesions may acquire *FGFR3* mutation later during stage progression (Choi et al., 2014, Sjobahl et al., 2012). However, it is also possible that the mutant *FGFR3* allele is lost during potential stage progression from non-invasive to invasive tumours.

Studies showed that non-invasive papillary carcinomas can indeed progress to a higher grade (Zieger et al., 2000, Herr, 2000, Cheng et al., 1999, Leblanc et al., 1999). It was also demonstrated that human *FGFR3*-mutant tumours can progress and acquire a CIS gene signature following the muscle-invasive pathway (Zieger et al., 2005). However, the presence of *FGFR3* mutation did not seem to be directly involved in the cancer progression (Zieger et al., 2005). This observation could potentially be explained under the hypothesis that the tumours were part of the 10-15% muscle-invasive tumour subset that carries *FGFR3* mutation (Billerey et al., 2001).

Our data indicates that *FGFR3* mutation can be functionally involved in urothelial changes that may represent early changes in human urothelial papilloma (Chapter 3) as well as in cancer progression of OH-BBN-induced tumours (Chapter 5). Whether superficial papillary tumours with *FGFR3* mutation can progress towards the muscle-invasive pathogenesis pathway where the receptor mutation then promotes tumour progression and invasion requires further experiments.

7.4 Cooperating mutations

Mutations that cooperate with activated *FGFR3* in the formation and progression of urothelial cell carcinoma have not fully been discovered.

Our previous data suggested that one of the potential candidates of *FGFR3*-cooperating mutations could be a component of the PI3K/AKT pathway (Ahmad et al., 2011c). Moreover, we have shown in mice that AKT pathway activation through *Pten* deletion together with *FGFR3* activation induced global hypertrophy with several cellular characteristics indicative of abnormal differentiation, which was overall similar to the early histopathological changes seen in human urothelial papilloma (Chapter 3 and 4). The morphological changes were likely to be caused cooperatively by *Fgfr3* and *Pten*. Potential cooperation of the PI3K/AKT and the FGFR signalling pathways is supported by the fact that *FGFR3* and *PIK3CA* mutations often co-occur in human bladder tumours across all stages and grades (Lopez-Knowles et al., 2006, Kompier et al., 2010, Duenas et al., 2013). However, the PI3K/AKT pathway may not be the only signalling pathway that is potentially able to cooperate with *FGFR3* activation.

FGFR3-cooperating mutations within the RAS/MAPK pathway were not identified in our models. Mice that carried heterozygous *Fgfr3* and *Hras* mutation in combination showed no urothelial abnormalities at 12 months apart from occasionally mild hyperplasia (Chapter 4). Although RAS/MAPK signalling cannot be fully excluded as a potential functional cooperator, co-occurrence of *FGFR3* and *RAS* mutations in human bladder tumours have been shown to be rare events, possibly due to redundancy of pathway activation (Kompier et al., 2010, Jebar et al., 2005, Juanpere et al., 2012, Ahmad et al., 2011c).

7.5 Current models of bladder cancer

Mice have been shown to resemble human urothelial cell carcinoma better than any other available laboratory animal by sharing many histological features with human bladder cancer, and by recapitulating tumour development in well-defined stages (Chan et al., 2009a). Recently, we presented for the first time a mouse model with *Fgfr3* mutation in the bladder (Ahmad et al., 2011c). Here we present a mouse model where the bladder of *Fgfr3 Pten* double mutant mice showed histological features that may be comparable with those of early urothelial papilloma in humans (Chapter 3). Furthermore, our results suggested that *FGFR3* activation can have an effect on progression in an invasive model of carcinogen-induced bladder cancer (Chapter 5), in which the effect of signalling inhibitors could be tested *in vivo* in future experiments. The use of a recently published AdenoCre technique to allow tissue-specific recombination in a small number of cells in order to generate tumours of the bladder has been evaluated in this study. The technique requires technological improvement but could potentially help to refine existing mouse models of bladder cancer, and could also allow lineage tracing of cancer stem cells in a developing urothelial tumour. Our results emphasise the importance of *in vivo* tumour models in cancer research to investigate the mechanisms of cancer development and progression. However, the bladder also poses a challenge as a target organ of cancer research in mice, since it is slowly proliferative (Stewart et al., 1980), which makes it a slow system to model tumour development. Therefore, it may be crucial to introduce mutations that promote proliferation in order to drive bladder tumourigenesis. Depending on the promoter that is used, this may promote earlier tumour formation in other organs that proliferate more quickly than the bladder as we have shown before (Ahmad et al., 2011c). Furthermore, stem cells

of the bladder have not been clearly identified, which may create ambiguity of which promoters are the most suitable ones to induce mutations in the putative stem cells of the mouse urothelium.

With the objective to assess tumour behaviour such as proliferation, renewal, invasion, as well as to test the effect of therapeutic drugs on cancer cells, the necessity of *in vitro* assays becomes evident. Our *in vitro* assays, including sphere formation, Collagen-I invasion, and organotypic slice culture are currently under development (Chapter 6). The assays can potentially be valuable in order to test therapeutic drugs as well as to study the characteristics of cancer cells *ex vivo*. Similar organotypic cell culture systems that serve as experimental intermediates towards living organisms have been tested with tumour cells derived from other organs, such as from pancreas, skin, intestine and breast (Kim and Alexander, 2013, Timpson et al., 2011, Sato et al., 2009). Cultures of cells derived from the normal urothelium or from bladder tumours have also been described previously (Chen et al., 2012, Shin et al., 2011, Batourina et al., 2012). However, these culturing systems appear to be more difficult compared to cultures of other organs, since they require FACS-based cell sorting of the urothelium, complex growth conditions specific to the nature of cell type, as well as a large number of urothelial cells with sufficient proliferative potential.

7.6 FGFR3 as a biomarker in bladder cancer

Biomarkers in cancer research are defined by the National Cancer Research Institute (NCI) as “A biological molecule found in blood, other body fluids, or tissues that is a sign of a normal or abnormal process, or of a condition or disease. A biomarker may be used to see how well the body responds to a treatment for a disease or condition.” (NCI Dictionary of Cancer Terms, National Cancer Institute, 2014).

Biomarkers can be categorised as (1) diagnostic, (2) prognostic or (3) predictive. Diagnostic biomarkers help to identify the current condition, such as early- or late-stage disease. Prognostic biomarkers help to forecast whether the cancer is likely to progress or whether it is stable in the absence of treatment. Predictive biomarkers help to predict how well a patient will respond to treatment.

Since recurrence is a major issue of bladder cancer management, there is great interest in developing urine-based tests to reduce the necessity of expensive cystoscopic surveillance. *FGFR3* has been examined as a diagnostic biomarker in urine (van Rhijn et al., 2003); however, due to lack of sensitivity and/or specificity, the tests are still not standard use in the clinic.

To date there are no validated prognostic molecular biomarkers available in bladder cancer (di Martino et al., 2012). However, several studies have examined the prognostic value of *FGFR3* in terms of recurrence, progression and survival of bladder cancer patients. *FGFR3* mutation is generally associated with favourable disease characteristics as it is linked to low grade/stage pTa tumours (van Rhijn et al., 2012, Billerey et al., 2001, Hernandez et al., 2006), whereas p53 expression is generally associated with higher stage and grade and worse clinical outcome (Schmitz-Drager et al., 2000, Malats et al., 2005).

We have demonstrated that *FGFR3* mutation alone is unlikely to drive tumourigenesis in the bladder (Ahmad et al., 2011, and Chapter 5 in this study). However, we showed that *FGFR3* activation can play a causative role in urothelial pathogenesis of non-invasive bladder cancer in cooperation with upregulated PI3K-AKT signalling in mice (Chapter 3). Since the animal model did not produce tumours in the life time up to 18 months, we concluded that these early-stage lesions with *FGFR3* mutation are unlikely to progress. This is in accordance with a rather good prognosis that is generally associated with the presence of *FGFR3* mutation in urothelial tumours (van Rhijn et al., 2012). In contrast, our model of invasive bladder cancer induced by carcinogen treatment suggests that presence of *FGFR3* mutation may constitute a rather bad prognosis, since *FGFR3*-mutant mice showed a 4.4-fold higher incidence of invasive bladder tumours than carcinogen-treated *Wild type* mice (Chapter 5). These results suggest context-dependence in terms of *FGFR3* mutation as a biomarker of progression. In order to clinically translate these observations to predict patient prognosis, further experiments would be essential to clearly define the effects of activated *FGFR3* signalling in bladder cancer.

The prognostic value of *FGFR3* as a biomarker of recurrence, which is generally associated with non-invasive low-grade Ta tumours, is still a matter of debate (Knowles, 2008). Some studies reported association of *FGFR3* mutation in non-

invasive tumours with low risk of recurrence (van Rhijn et al., 2001). Other groups have confirmed association of *FGFR3* mutation with non-invasive papillary tumours of low grade, however, with a higher risk of recurrence (Hernandez et al., 2006). Conversely, non-invasive papillary tumours of high grade were not associated with recurrence or progression in patients (Hernandez et al., 2006, Hernandez et al., 2005). Other studies have found no association between *FGFR3* mutational status and recurrence, progression or muscle invasion (Ploussard et al., 2011).

In conclusion, further research is required in order to validate *FGFR3* mutation as a prognostic biomarker in urothelial cell carcinoma. Since the effect of activated *FGFR3* signalling may be context-dependent, the prognosis of patients with *FGFR3*-mutated tumours should be assessed with caution.

7.7 *FGFR3*-targeted therapy

The wide availability of inhibitors specific to FGF signalling may provide an opportunity for *FGFR3*-targeted translation using our *in vivo* models with *FGFR3* mutation for preclinical experiments. We have shown that *FGFR3* mutation can play a functional role in bladder cancer, which suggests the possibility of *FGFR3* inhibition as a therapeutic strategy.

FGFR3-inhibiting drugs have been suggested as a therapeutic option in urothelial cell carcinoma (Lamont et al., 2011, Tomlinson et al., 2007b, Network, 2014). Several novel drugs against FGFRs including R3Mab, NVP-BGJ398, and AZD4547 have been shown to be effective in cell lines and xenograft models (Qing et al., 2009, Guagnano et al., 2011, Gavine et al., 2012). All of the named drugs are currently being used in clinical trials (Brooks et al., 2012, Liang et al., 2013).

Our *UroIIICre Fgfr3^{+K644E} Pten^{flox/flox}* mouse model indicated potential cooperation of the PI3K/AKT and the FGFR signalling pathways. Analysis of human bladder tumours supports that mutations in *FGFR3* and PI3K/AKT pathway genes are co-associated (Lopez-Knowles et al., 2006, Kompier et al., 2010, Duenas et al., 2013), which represents a therapeutic opportunity for combinatorial inhibitors. Combinatorial targeting is a valid approach for cancers with multiple activated signalling pathways, and has been shown to be successful in models of breast

cancer, where FGFR and PI3K/mTOR signalling were targeted in combination (Issa et al., 2013). In order to generate an *in vivo* model for combinatorial drug testing, our *FGFR3*-mutant mice can be crossed to any available mouse model carrying candidate mutations that cooperate with FGFR3 in tumourigenesis.

Interestingly, two studies have reported tumour suppressive properties of FGFR3. In one, FGFR3 protein expression was downregulated in colorectal cancer (Sonvilla et al., 2010). In a second study, FGFR3 overexpression had tumour suppressive effects on pancreatic cancer (PDAC) cell lines (Lafitte et al., 2013). Although yet unclear, it is possible that FGFR3 can either promote or suppress tumour development or progression in a context-dependent manner. Therefore FGFR3-targeted therapy needs to be considered individually with caution.

Altogether, for a translational benefit, further studies of the FGFR3 signalling pathway and its inhibitors are essential and will aid the development of therapies for both non muscle-invasive and muscle-invasive bladder cancer with deregulation of FGF signalling.

7.8 Future direction

Resistance to therapy is a major challenge of cancer treatment (Bambury and Rosenberg, 2013). Often patients first respond to a given drug and subsequently relapse. This is mostly due to the emergence of cellular mechanisms in the tumour to escape the effects of the drug, such as the generation of efflux pumps, alteration of the DNA repair machinery and modulation of apoptosis and survival pathways (Drayton and Catto, 2012, Herrera-Abreu et al., 2013, Chell et al., 2013). It would therefore be essential to elucidate resistance mechanisms in detail, and to test drug combinations that collectively target pathways that are used as escape routes. To this matter, it would also be vitally important to identify cooperating mutations in bladder cancer, to understand which pathways are co-activated and to identify drug targets within these pathways. Comprehensive knowledge of the molecular mechanisms underlying bladder cancer development and progression would also facilitate the identification of patients who are most likely to respond to treatment.

FGFR3 mutation or overexpression in the context of dissemination and metastasis formation is largely unknown. However, FGF signalling has been implicated in the regulation of EMT (Cheng et al., 2013, Tomlinson et al., 2012), a process that is strongly associated with invasion and formation of distant metastasis (Thiery, 2002). Our data suggests that *FGFR3* can have an effect on tumour progression of existing neoplasms. It would therefore be interesting to investigate further whether *FGFR3* can also play a role in the metastatic process in late-stage disease. Two recent publications reported upregulated *FGFR3* expression in bladder cancer metastases (Guancial et al., 2014b, Turo et al., 2014).

The tumour microenvironment has been implicated to play a role in cancer progression, metastasis and drug resistance (Sung et al., 2007). The stroma, as part of the microenvironment, secretes a variety of cytokines such as FGF ligands and interleukins that stimulate proliferation (Tlsty and Coussens, 2006, Cheng et al., 2013). Furthermore, it can host inflammatory processes that may influence tumour proliferation (Tlsty and Coussens, 2006). It would therefore be important to examine the role of the stroma in urothelial cell carcinoma and its potential contribution to the development or progression of bladder tumours.

7.9 Significance

Bladder cancer is a major health issue worldwide that causes considerable morbidity and mortality due to ineffective or insufficient therapeutic strategies. This study focused on the role of *FGFR3* signalling in cancer initiation, invasion and progression with the objective to generate models that can answer questions of basic science as well as to aid preclinical drug testing.

From the basic science question our data supported previous evidence of a functional role of *FGFR3* in initiating changes towards superficial urothelial carcinoma. Our data also suggested a potential role of *FGFR3* in progression of established neoplasms in mice. We showed that *FGFR3* activation plays a causative role in urothelial pathogenesis of non-invasive bladder cancer in cooperation with *Pten* loss *in vivo*. Furthermore, we present indication of functional involvement of *FGFR3 S249C* mutation in progression and invasion of carcinogen-induced tumours.

Our findings may also be of clinical relevance. It has previously been believed that the presence of an *FGFR3* mutation is a favourable prognostic factor since it is associated with superficial papillary tumours with low potential to progress. However, our data suggested that *FGFR3* mutation in an established tumour can act as a tumour promoter with worse prognosis than *FGFR3* wild type.

FGFR3 may therefore constitute a promising drug target. Given the wide availability of inhibitors specific to FGF signalling, our *FGFR3* mouse models together with technological improvement of our *in vitro* assays may provide a platform for *FGFR3*-targeted translation in urothelial disease.

References

- ADAR, R., MONSONEGO-ORNAN, E., DAVID, P. & YAYON, A. 2002. Differential activation of cysteine-substitution mutants of fibroblast growth factor receptor 3 is determined by cysteine localization. *J Bone Miner Res*, 17, 860-8.
- AHMAD, I., BARNETSON, R. J. & KRISHNA, N. S. 2008. Keratinizing squamous metaplasia of the bladder: a review. *Urol Int*, 81, 247-51.
- AHMAD, I., IWATA, T. & LEUNG, H. Y. 2012a. Mechanisms of FGFR-mediated carcinogenesis. *Biochim Biophys Acta*, 1823, 850-60.
- AHMAD, I., MORTON, J. P., SINGH, L. B., RADULESCU, S. M., RIDGWAY, R. A., PATEL, S., WOODGETT, J., WINTON, D. J., TAKETO, M. M., WU, X. R., LEUNG, H. Y. & SANSOM, O. J. 2011a. beta-Catenin activation synergizes with PTEN loss to cause bladder cancer formation. *Oncogene*, 30, 178-89.
- AHMAD, I., PATEL, R., LIU, Y., SINGH, L. B., TAKETO, M. M., WU, X. R., LEUNG, H. Y. & SANSOM, O. J. 2011b. Ras mutation cooperates with beta-catenin activation to drive bladder tumorigenesis. *Cell Death Dis*, 2, e124.
- AHMAD, I., SANSOM, O. J. & LEUNG, H. Y. 2012b. Exploring molecular genetics of bladder cancer: lessons learned from mouse models. *Dis Model Mech*, 5, 323-32.
- AHMAD, I., SINGH, L. B., FOTH, M., MORRIS, C. A., TAKETO, M. M., WU, X. R., LEUNG, H. Y., SANSOM, O. J. & IWATA, T. 2011c. K-Ras and {beta}-catenin mutations cooperate with Fgfr3 mutations in mice to promote tumorigenesis in the skin and lung, but not in the bladder. *Dis Model Mech*, 4, 548-55.
- AL HUSSAIN, T. O. & AKHTAR, M. 2013. Molecular basis of urinary bladder cancer. *Adv Anat Pathol*, 20, 53-60.
- ALI, S. H. & DECAPRIO, J. A. 2001. Cellular transformation by SV40 large T antigen: interaction with host proteins. *Semin Cancer Biol*, 11, 15-23.
- ALLENSPACH, E. J., MAILLARD, I., ASTER, J. C. & PEAR, W. S. 2002. Notch signaling in cancer. *Cancer Biol Ther*, 1, 466-76.
- ALTSCHUL, S. F., GISH, W., MILLER, W., MYERS, E. W. & LIPMAN, D. J. 1990. Basic local alignment search tool. *J Mol Biol*, 215, 403-10.
- AMANN, T., BATAILLE, F., SPRUSS, T., DETTMER, K., WILD, P., LIEDTKE, C., MUHLBAUER, M., KIEFER, P., OEFNER, P. J., TRAUTWEIN, C., BOSSERHOFF, A. K. & HELLERBRAND, C. 2010. Reduced expression of fibroblast growth factor receptor 2IIIb in hepatocellular carcinoma induces a more aggressive growth. *Am J Pathol*, 176, 1433-42.
- ANDERSON, R. D., HASKELL, R. E., XIA, H., ROESSLER, B. J. & DAVIDSON, B. L. 2000. A simple method for the rapid generation of recombinant adenovirus vectors. *Gene Ther*, 7, 1034-8.
- ANTON, M. & GRAHAM, F. L. 1995. Site-specific recombination mediated by an adenovirus vector expressing the Cre recombinase protein: a molecular switch for control of gene expression. *J Virol*, 69, 4600-6.
- ASKHAM, J. M., PLATT, F., CHAMBERS, P. A., SNOWDEN, H., TAYLOR, C. F. & KNOWLES, M. A. 2010. AKT1 mutations in bladder cancer: identification of a novel oncogenic mutation that can co-operate with E17K. *Oncogene*, 29, 150-5.
- AVEYARD, J. S., SKILLETER, A., HABUCHI, T. & KNOWLES, M. A. 1999. Somatic mutation of PTEN in bladder carcinoma. *Br J Cancer*, 80, 904-8.

- AYALA DE LA PENA, F., KANASAKI, K., KANASAKI, M., TANGIRALA, N., MAEDA, G. & KALLURI, R. 2011. Loss of p53 and acquisition of angiogenic microRNA profile are insufficient to facilitate progression of bladder urothelial carcinoma in situ to invasive carcinoma. *J Biol Chem*, 286, 20778-87.
- BABJUK, M., OOSTERLINCK, W., SYLVESTER, R., KAASINEN, E., BOHLE, A. & PALOU-REDORTA, J. 2008. EAU guidelines on non-muscle-invasive urothelial carcinoma of the bladder. *Eur Urol*, 54, 303-14.
- BAKKAR, A. A., WALLERAND, H., RADVANYI, F., LAHAYE, J. B., PISSARD, S., LECERF, L., KOUYOUMDJIAN, J. C., ABBOU, C. C., PAIRON, J. C., JAURAND, M. C., THIERY, J. P., CHOPIN, D. K. & DE MEDINA, S. G. 2003. FGFR3 and TP53 gene mutations define two distinct pathways in urothelial cell carcinoma of the bladder. *Cancer Res*, 63, 8108-12.
- BAMBURY, R. M. & ROSENBERG, J. E. 2013. Advanced Urothelial Carcinoma: Overcoming Treatment Resistance through Novel Treatment Approaches. *Front Pharmacol*, 4, 3.
- BARKER, N., VAN ES, J. H., KUIPERS, J., KUJALA, P., VAN DEN BORN, M., COZIJSSEN, M., HAEGEBARTH, A., KORVING, J., BEGTHEL, H., PETERS, P. J. & CLEVERS, H. 2007. Identification of stem cells in small intestine and colon by marker gene Lgr5. *Nature*, 449, 1003-1007.
- BARTKOVA, J., HOREJSI, Z., KOED, K., KRAMER, A., TORT, F., ZIEGER, K., GULDBERG, P., SEHESTED, M., NESLAND, J. M., LUKAS, C., ORNTOFT, T., LUKAS, J. & BARTEK, J. 2005. DNA damage response as a candidate anti-cancer barrier in early human tumorigenesis. *Nature*, 434, 864-70.
- BATOURINA, E., GANDHI, D., MENDELSON, C. L. & MOLOTKOV, A. 2012. Organotypic culture of the urogenital tract. *Methods Mol Biol*, 886, 45-53.
- BECCI, P. J., THOMPSON, H. J., STRUM, J. M., BROWN, C. C., SPORN, M. B. & MOON, R. C. 1981. N-butyl-N-(4-hydroxybutyl)nitrosamine-induced urinary bladder cancer in C57BL/6 X DBA/2 F1 mice as a useful model for study of chemoprevention of cancer with retinoids. *Cancer Res*, 41, 927-32.
- BERNARD-PIERROT, I., BRAMS, A., DUNOIS-LARDE, C., CAILLAULT, A., DIEZ DE MEDINA, S. G., CAPPELLEN, D., GRAFF, G., THIERY, J. P., CHOPIN, D., RICOL, D. & RADVANYI, F. 2006. Oncogenic properties of the mutated forms of fibroblast growth factor receptor 3b. *Carcinogenesis*, 27, 740-7.
- BERX, G. & VAN ROY, F. 2009. Involvement of members of the cadherin superfamily in cancer. *Cold Spring Harb Perspect Biol*, 1, a003129.
- BILLEREY, C., CHOPIN, D., AUBRIOT-LORTON, M. H., RICOL, D., GIL DIEZ DE MEDINA, S., VAN RHIJN, B., BRALET, M. P., LEFRERE-BELDA, M. A., LAHAYE, J. B., ABBOU, C. C., BONAVENTURE, J., ZAFRANI, E. S., VAN DER KWAST, T., THIERY, J. P. & RADVANYI, F. 2001. Frequent FGFR3 mutations in papillary non-invasive bladder (pTa) tumors. *Am J Pathol*, 158, 1955-9.
- BILLOTTET, C., TUEFFERD, M., GENTIEN, D., RAPINAT, A., THIERY, J. P., BROET, P. & JOUANNEAU, J. 2008. Modulation of several waves of gene expression during FGF-1 induced epithelial-mesenchymal transition of carcinoma cells. *J Cell Biochem*, 104, 826-39.
- BLAVERI, E., BREWER, J. L., ROYDASGUPTA, R., FRIDLAND, J., DEVRIES, S., KOPPIE, T., PEJAVAR, S., MEHTA, K., CARROLL, P., SIMKO, J. P. & WALDMAN, F. M. 2005. Bladder cancer stage and outcome by array-based comparative genomic hybridization. *Clin Cancer Res*, 11, 7012-22.
- BOHM, M., KIRCH, H., OTTO, T., RUBBEN, H. & WIELAND, I. 1997. Deletion analysis at the DEL-27, APC and MTS1 loci in bladder cancer: LOH at the DEL-27 locus on 5p13-12 is a prognostic marker of tumor progression. *Int J Cancer*, 74, 291-5.

- BOLDRUP, L., COATES, P. J., GU, X. & NYLANDER, K. 2007. DeltaNp63 isoforms regulate CD44 and keratins 4, 6, 14 and 19 in squamous cell carcinoma of head and neck. *J Pathol*, 213, 384-91.
- BOTTCHER, R. T. 2005. Fibroblast Growth Factor Signaling during Early Vertebrate Development. *Endocrine Reviews*, 26, 63-77.
- BRENNAN, P., BOGILLOT, O., CORDIER, S., GREISER, E., SCHILL, W., VINEIS, P., LOPEZ-ABENTE, G., TZONOU, A., CHANG-CLAUDE, J., BOLM-AUDORFF, U., JOCKEL, K. H., DONATO, F., SERRA, C., WAHRENDORF, J., HOURS, M., T'MANNETJE, A., KOGEVINAS, M. & BOFFETTA, P. 2000. Cigarette smoking and bladder cancer in men: a pooled analysis of 11 case-control studies. *Int J Cancer*, 86, 289-94.
- BRODY, S. L. & CRYSTAL, R. G. 1994. Adenovirus-mediated in vivo gene transfer. *Ann N Y Acad Sci*, 716, 90-101; discussion 101-3.
- BROOKS, A. N., KILGOUR, E. & SMITH, P. D. 2012. Molecular pathways: fibroblast growth factor signaling: a new therapeutic opportunity in cancer. *Clin Cancer Res*, 18, 1855-62.
- BROWN, B., LINDBERG, K., REING, J., STOLZ, D. B. & BADYLAK, S. F. 2006. The basement membrane component of biologic scaffolds derived from extracellular matrix. *Tissue Eng*, 12, 519-26.
- BURGER, M., CATTO, J. W., DALBAGNI, G., GROSSMAN, H. B., HERR, H., KARAKIEWICZ, P., KASSOUF, W., KIEMENEY, L. A., LA VECCHIA, C., SHARIAT, S. & LOTAN, Y. 2013. Epidemiology and risk factors of urothelial bladder cancer. *Eur Urol*, 63, 234-41.
- CADINANOS, J. & BRADLEY, A. 2007. Generation of an inducible and optimized piggyBac transposon system. *Nucleic Acids Res*, 35, e87.
- CAIRNS, P., EVRON, E., OKAMI, K., HALACHMI, N., ESTELLER, M., HERMAN, J. G., BOSE, S., WANG, S. I., PARSONS, R. & SIDRANSKY, D. 1998. Point mutation and homozygous deletion of PTEN/MMAC1 in primary bladder cancers. *Oncogene*, 16, 3215-8.
- CAIRNS, P., PROCTOR, A. J. & KNOWLES, M. A. 1991. Loss of heterozygosity at the RB locus is frequent and correlates with muscle invasion in bladder carcinoma. *Oncogene*, 6, 2305-9.
- CAIRNS, P., SHAW, M. E. & KNOWLES, M. A. 1993. Initiation of bladder cancer may involve deletion of a tumour-suppressor gene on chromosome 9. *Oncogene*, 8, 1083-5.
- CAIRNS, P., TOKINO, K., EBY, Y. & SIDRANSKY, D. 1994. Homozygous deletions of 9p21 in primary human bladder tumors detected by comparative multiplex polymerase chain reaction. *Cancer Res*, 54, 1422-4.
- CAMPBELL, S. L., KHOSRAVI-FAR, R., ROSSMAN, K. L., CLARK, G. J. & DER, C. J. 1998. Increasing complexity of Ras signaling. *Oncogene*, 17, 1395-413.
- CAPECCHI, M. R. 1994. Targeted gene replacement. *Sci Am*, 270, 52-9.
- CAPPELLEN, D., DE OLIVEIRA, C., RICOL, D., DE MEDINA, S., BOURDIN, J., SASTRE-GARAU, X., CHOPIN, D., THIERY, J. P. & RADVANYI, F. 1999. Frequent activating mutations of FGFR3 in human bladder and cervix carcinomas. *Nat Genet*, 23, 18-20.
- CAPPELLEN, D., GIL DIEZ DE MEDINA, S., CHOPIN, D., THIERY, J. P. & RADVANYI, F. 1997. Frequent loss of heterozygosity on chromosome 10q in muscle-invasive transitional cell carcinomas of the bladder. *Oncogene*, 14, 3059-66.
- CARLSON, C. M., DUPUY, A. J., FRITZ, S., ROBERG-PEREZ, K. J., FLETCHER, C. F. & LARGAESPADA, D. A. 2003. Transposon mutagenesis of the mouse germline. *Genetics*, 165, 243-56.

- CASTILLO-MARTIN, M., DOMINGO-DOMENECH, J., KARNI-SCHMIDT, O., MATOS, T. & CORDON-CARDO, C. 2010. Molecular pathways of urothelial development and bladder tumorigenesis. *Urologic Oncology: Seminars and Original Investigations*, 28, 401-408.
- CATTO, J. W. F., MIAH, S., OWEN, H. C., BRYANT, H., MYERS, K., DUDZIEC, E., LARRE, S., MILO, M., REHMAN, I., ROSARIO, D. J., DI MARTINO, E., KNOWLES, M. A., MEUTH, M., HARRIS, A. L. & HAMDY, F. C. 2009. Distinct MicroRNA Alterations Characterize High- and Low-Grade Bladder Cancer. *Cancer Research*, 69, 8472-8481.
- CHAFFER, C. L., BRENNAN, J. P., SLAVIN, J. L., BLICK, T., THOMPSON, E. W. & WILLIAMS, E. D. 2006. Mesenchymal-to-epithelial transition facilitates bladder cancer metastasis: role of fibroblast growth factor receptor-2. *Cancer Res*, 66, 11271-8.
- CHAN, E., PATEL, A., HESTON, W. & LARCHIAN, W. 2009a. Mouse orthotopic models for bladder cancer research. *BJU International*, 104, 1286-1291.
- CHAN, E. S., PATEL, A. R., LARCHIAN, W. A. & HESTON, W. D. 2011. In vivo targeted contrast enhanced micro-ultrasound to measure intratumor perfusion and vascular endothelial growth factor receptor 2 expression in a mouse orthotopic bladder cancer model. *J Urol*, 185, 2359-65.
- CHAN, H. M., NARITA, M., LOWE, S. W. & LIVINGSTON, D. M. 2005. The p400 E1A-associated protein is a novel component of the p53 --> p21 senescence pathway. *Genes Dev*, 19, 196-201.
- CHAN, K. S., ESPINOSA, I., CHAO, M., WONG, D., AILLES, L., DIEHN, M., GILL, H., PRESTI, J., CHANG, H. Y., VAN DE RIJN, M., SHORTLIFFE, L. & WEISSMAN, I. L. 2009b. Identification, molecular characterization, clinical prognosis, and therapeutic targeting of human bladder tumor-initiating cells. *Proceedings of the National Academy of Sciences*, 106, 14016-14021.
- CHATTERJEE, S. J., GEORGE, B., GOEBELL, P. J., ALAVI-TAFRESHI, M., SHI, S. R., FUNG, Y. K., JONES, P. A., CORDON-CARDO, C., DATAR, R. H. & COTE, R. J. 2004. Hyperphosphorylation of pRb: a mechanism for RB tumour suppressor pathway inactivation in bladder cancer. *J Pathol*, 203, 762-70.
- CHELL, V., BALMANNO, K., LITTLE, A. S., WILSON, M., ANDREWS, S., BLOCKLEY, L., HAMPSON, M., GAVINE, P. R. & COOK, S. J. 2013. Tumour cell responses to new fibroblast growth factor receptor tyrosine kinase inhibitors and identification of a gatekeeper mutation in FGFR3 as a mechanism of acquired resistance. *Oncogene*, 32, 3059-70.
- CHELLAIAH, A. T., MCEWEN, D. G., WERNER, S., XU, J. & ORNITZ, D. M. 1994. Fibroblast growth factor receptor (FGFR) 3. Alternative splicing in immunoglobulin-like domain III creates a receptor highly specific for acidic FGF/FGF-1. *J Biol Chem*, 269, 11620-7.
- CHEN, Z., DING, W., XU, K., TAN, J., SUN, C., GOU, Y., TONG, S., XIA, G., FANG, Z. & DING, Q. 2012. The 1973 WHO Classification is more suitable than the 2004 WHO Classification for predicting prognosis in non-muscle-invasive bladder cancer. *PLoS One*, 7, e47199.
- CHENG, J., HUANG, H., PAK, J., SHAPIRO, E., SUN, T. T., CORDON-CARDO, C., WALDMAN, F. M. & WU, X. R. 2003. Allelic loss of p53 gene is associated with genesis and maintenance, but not invasion, of mouse carcinoma in situ of the bladder. *Cancer Res*, 63, 179-85.
- CHENG, J., HUANG, H., ZHANG, Z. T., SHAPIRO, E., PELLICER, A., SUN, T. T. & WU, X. R. 2002. Overexpression of epidermal growth factor receptor in urothelium elicits urothelial hyperplasia and promotes bladder tumor growth. *Cancer Res*, 62, 4157-63.

- CHENG, L., NEUMANN, R. M., WEAVER, A. L., SPOTTS, B. E. & BOSTWICK, D. G. 1999. Predicting cancer progression in patients with stage T1 bladder carcinoma. *J Clin Oncol*, 17, 3182-7.
- CHENG, T., ROTH, B., CHOI, W., BLACK, P. C., DINNEY, C. & MCCONKEY, D. J. 2013. Fibroblast growth factor receptors-1 and -3 play distinct roles in the regulation of bladder cancer growth and metastasis: implications for therapeutic targeting. *PLoS One*, 8, e57284.
- CHESI, M. 2001. Activated fibroblast growth factor receptor 3 is an oncogene that contributes to tumor progression in multiple myeloma. *Blood*, 97, 729-736.
- CHESTER, J. D., KENNEDY, W., HALL, G. D., SELBY, P. J. & KNOWLES, M. A. 2003. Adenovirus-mediated gene therapy for bladder cancer: efficient gene delivery to normal and malignant human urothelial cells in vitro and ex vivo. *Gene Ther*, 10, 172-9.
- CHEUNG, W. L., ALBADINE, R., CHAN, T., SHARMA, R. & NETTO, G. J. 2009. Phosphorylated H2AX in noninvasive low grade urothelial carcinoma of the bladder: correlation with tumor recurrence. *J Urol*, 181, 1387-92.
- CHO, J. Y., GUO, C., TORELLO, M., LUNSTRUM, G. P., IWATA, T., DENG, C. & HORTON, W. A. 2004. Defective lysosomal targeting of activated fibroblast growth factor receptor 3 in achondroplasia. *Proc Natl Acad Sci U S A*, 101, 609-14.
- CHOI, S. H., BYUN, Y. & LEE, G. 2009. Expressions of uroplakins in the mouse urinary bladder with cyclophosphamide-induced cystitis. *J Korean Med Sci*, 24, 684-9.
- CHOI, W., PORTEN, S., KIM, S., WILLIS, D., PLIMACK, E. R., HOFFMAN-CENSITS, J., ROTH, B., CHENG, T., TRAN, M., LEE, I. L., MELQUIST, J., BONDARUK, J., MAJEWSKI, T., ZHANG, S., PRETZSCH, S., BAGGERLY, K., SIEFKER-RADTKE, A., CZERNIAK, B., DINNEY, C. P. & MCCONKEY, D. J. 2014. Identification of distinct Basal and luminal subtypes of muscle-invasive bladder cancer with different sensitivities to frontline chemotherapy. *Cancer Cell*, 25, 152-65.
- CHOI, W., SHAH, J. B., TRAN, M., SVATEK, R., MARQUIS, L., LEE, I. L., YU, D., ADAM, L., WEN, S., SHEN, Y., DINNEY, C., MCCONKEY, D. J. & SIEFKER-RADTKE, A. 2012. p63 expression defines a lethal subset of muscle-invasive bladder cancers. *PLoS One*, 7, e30206.
- CLASSON, M. & HARLOW, E. 2002. The retinoblastoma tumour suppressor in development and cancer. *Nat Rev Cancer*, 2, 910-7.
- COHEN, S. M., WITTENBERG, J. F. & BRYAN, G. T. 1976. Effect of avitaminosis A and hypervitaminosis A on urinary bladder carcinogenicity of N-(4-(5-Nitro-2-furyl)-2-thiazolyl)formamide. *Cancer Res*, 36, 2334-9.
- COLLIER, L. S., CARLSON, C. M., RAVIMOHAN, S., DUPUY, A. J. & LARGAESPADA, D. A. 2005. Cancer gene discovery in solid tumours using transposon-based somatic mutagenesis in the mouse. *Nature*, 436, 272-6.
- COLQUHOUN, A. J. & MELLON, J. K. 2002. Epidermal growth factor receptor and bladder cancer. *Postgrad Med J*, 78, 584-9.
- COLVIN, J. S., BOHNE, B. A., HARDING, G. W., MCEWEN, D. G. & ORNITZ, D. M. 1996. Skeletal overgrowth and deafness in mice lacking fibroblast growth factor receptor 3. *Nat Genet*, 12, 390-7.
- COPELAND, N. G. & JENKINS, N. A. 2010. Harnessing transposons for cancer gene discovery. *Nature Reviews Cancer*, 10, 696-706.
- CUNNINGHAM, D. L., SWEET, S. M., COOPER, H. J. & HEATH, J. K. 2010. Differential phosphoproteomics of fibroblast growth factor signaling:

- identification of Src family kinase-mediated phosphorylation events. *J Proteome Res*, 9, 2317-28.
- CZERNIAK, B., COHEN, G. L., ETKIND, P., DEITCH, D., SIMMONS, H., HERZ, F. & KOSS, L. G. 1992. Concurrent mutations of coding and regulatory sequences of the Ha-ras gene in urinary bladder carcinomas. *Hum Pathol*, 23, 1199-204.
- D'AVIS, P. Y., ROBERTSON, S. C., MEYER, A. N., BARDWELL, W. M., WEBSTER, M. K. & DONOGHUE, D. J. 1998. Constitutive activation of fibroblast growth factor receptor 3 by mutations responsible for the lethal skeletal dysplasia thanatophoric dysplasia type I. *Cell Growth Differ*, 9, 71-8.
- DAHIA, P. L. 2000. PTEN, a unique tumor suppressor gene. *Endocr Relat Cancer*, 7, 115-29.
- DAVIDSON, B. L., ALLEN, E. D., KOZARSKY, K. F., WILSON, J. M. & ROESSLER, B. J. 1993. A model system for in vivo gene transfer into the central nervous system using an adenoviral vector. *Nat Genet*, 3, 219-23.
- DAVIDSON, D., BLANC, A., FILION, D., WANG, H., PLUT, P., PFEFFER, G., BUSCHMANN, M. D. & HENDERSON, J. E. 2005. Fibroblast growth factor (FGF) 18 signals through FGF receptor 3 to promote chondrogenesis. *J Biol Chem*, 280, 20509-15.
- DENG, C., WYNshaw-BORIS, A., ZHOU, F., KUO, A. & LEDER, P. 1996. Fibroblast growth factor receptor 3 is a negative regulator of bone growth. *Cell*, 84, 911-21.
- DENZINGER, S., MOHREN, K., KNUECHEL, R., WILD, P. J., BURGER, M., WIELAND, W. F., HARTMANN, A. & STOEHR, R. 2006. Improved clonality analysis of multifocal bladder tumors by combination of histopathologic organ mapping, loss of heterozygosity, fluorescence in situ hybridization, and p53 analyses. *Hum Pathol*, 37, 143-51.
- DI COMO, C. J., URIST, M. J., BABAYAN, I., DROBNJAK, M., HEDVAT, C. V., TERUYA-FELDSTEIN, J., POHAR, K., HOOS, A. & CORDON-CARDO, C. 2002. p63 expression profiles in human normal and tumor tissues. *Clin Cancer Res*, 8, 494-501.
- DI MARTINO, E., L'HOTE, C. G., KENNEDY, W., TOMLINSON, D. C. & KNOWLES, M. A. 2009. Mutant fibroblast growth factor receptor 3 induces intracellular signaling and cellular transformation in a cell type- and mutation-specific manner. *Oncogene*, 28, 4306-16.
- DI MARTINO, E., TOMLINSON, D. C. & KNOWLES, M. A. 2012. A Decade of FGF Receptor Research in Bladder Cancer: Past, Present, and Future Challenges. *Adv Urol*, 2012, 429213.
- DIEZ DE MEDINA, S. G., CHOPIN, D., EL MARJOU, A., DELOUVEE, A., LAROCHELLE, W. J., HOZNEK, A., ABOU, C., AARONSON, S. A., THIERY, J. P. & RADVANYI, F. 1997. Decreased expression of keratinocyte growth factor receptor in a subset of human transitional cell bladder carcinomas. *Oncogene*, 14, 323-30.
- DING, S., WU, X., LI, G., HAN, M., ZHUANG, Y. & XU, T. 2005. Efficient Transposition of the piggyBac (PB) Transposon in Mammalian Cells and Mice. *Cell*, 122, 473-483.
- DRAYTON, R. M. & CATTO, J. W. 2012. Molecular mechanisms of cisplatin resistance in bladder cancer. *Expert Rev Anticancer Ther*, 12, 271-81.
- DUENAS, M., MARTINEZ-FERNANDEZ, M., GARCIA-ESCUADERO, R., VILLACAMPA, F., MARQUES, M., SAIZ-LADERA, C., DUARTE, J., MARTINEZ, V., GOMEZ, M. J., MARTIN, M. L., FERNANDEZ, M., CASTELLANO, D., REAL, F. X., RODRIGUEZ-PERALTO, J. L., DE LA ROSA, F. & PARAMIO, J. M. 2013.

- PIK3CA gene alterations in bladder cancer are frequent and associate with reduced recurrence in non-muscle invasive tumors. *Mol Carcinog*.
- DUNOIS-LARDE, C., LEVREL, O., BRAMS, A., THIERY, J. P. & RADVANYI, F. 2005. Absence of FGFR3 mutations in urinary bladder tumours of rats and mice treated with N-butyl-N-(4-hydroxybutyl)nitrosamine. *Mol Carcinog*, 42, 142-9.
- DUPUY, A. J., AKAGI, K., LARGAESPADA, D. A., COPELAND, N. G. & JENKINS, N. A. 2005. Mammalian mutagenesis using a highly mobile somatic Sleeping Beauty transposon system. *Nature*, 436, 221-226.
- DUPUY, A. J., FRITZ, S. & LARGAESPADA, D. A. 2001. Transposition and gene disruption in the male germline of the mouse. *Genesis*, 30, 82-8.
- DUPUY, A. J., ROGERS, L. M., KIM, J., NANNAPANENI, K., STARR, T. K., LIU, P., LARGAESPADA, D. A., SCHEETZ, T. E., JENKINS, N. A. & COPELAND, N. G. 2009. A modified sleeping beauty transposon system that can be used to model a wide variety of human cancers in mice. *Cancer Res*, 69, 8150-6.
- DUTT, A., RAMOS, A. H., HAMMERMAN, P. S., MERMEL, C., CHO, J., SHARIFNIA, T., CHANDE, A., TANAKA, K. E., STRANSKY, N., GREULICH, H., GRAY, N. S. & MEYERSON, M. 2011. Inhibitor-sensitive FGFR1 amplification in human non-small cell lung cancer. *PLoS One*, 6, e20351.
- EL-DEIRY, W. S., TOKINO, T., VELCULESCU, V. E., LEVY, D. B., PARSONS, R., TRENT, J. M., LIN, D., MERCER, W. E., KINZLER, K. W. & VOGELSTEIN, B. 1993. WAF1, a potential mediator of p53 tumor suppression. *Cell*, 75, 817-25.
- EL-MARJOU, A., DELOUVEE, A., THIERY, J. P. & RADVANYI, F. 2000. Involvement of epidermal growth factor receptor in chemically induced mouse bladder tumour progression. *Carcinogenesis*, 21, 2211-8.
- ERTURK, E., COHEN, S. M. & BRYAN, G. T. 1970. Induction, histogenesis, and isotransplantability of renal tumors induced by formic acid 2-[4-(5-nitro-2-furyl)-2-triazolyl]-hydrazide in rats. *Cancer Res*, 30, 2098-106.
- ESRIG, D., ELMAJIAN, D., GROSHEN, S., FREEMAN, J. A., STEIN, J. P., CHEN, S. C., NICHOLS, P. W., SKINNER, D. G., JONES, P. A. & COTE, R. J. 1994. Accumulation of nuclear p53 and tumor progression in bladder cancer. *N Engl J Med*, 331, 1259-64.
- FITZGERALD, J. M., RAMCHURREN, N., RIEGER, K., LEVESQUE, P., SILVERMAN, M., LIBERTINO, J. A. & SUMMERHAYES, I. C. 1995. Identification of H-ras mutations in urine sediments complements cytology in the detection of bladder tumors. *J Natl Cancer Inst*, 87, 129-33.
- FODDE, R. & BRABLETZ, T. 2007. Wnt/beta-catenin signaling in cancer stemness and malignant behavior. *Curr Opin Cell Biol*, 19, 150-8.
- FREIER, K., SCHWAENEN, C., STICHT, C., FLECHTENMACHER, C., MUHLING, J., HOFELE, C., RADLWIMMER, B., LICHTER, P. & JOOS, S. 2007. Recurrent FGFR1 amplification and high FGFR1 protein expression in oral squamous cell carcinoma (OSCC). *Oral Oncol*, 43, 60-6.
- FRESE, K. K. & TUVESON, D. A. 2007. Maximizing mouse cancer models. *Nat Rev Cancer*, 7, 645-58.
- FRESNO VARA, J. A., CASADO, E., DE CASTRO, J., CEJAS, P., BELDA-INIESTA, C. & GONZALEZ-BARON, M. 2004. PI3K/Akt signalling pathway and cancer. *Cancer Treat Rev*, 30, 193-204.
- FRIEDRICH, M. G., BLIND, C., MILDE-LANGOSCH, K., ERBERSDOBLER, A., CONRAD, S., LONING, T., HAMMERER, P. & HULAND, H. 2001. Frequent p16/MTS1 inactivation in early stages of urothelial carcinoma of the bladder is not associated with tumor recurrence. *Eur Urol*, 40, 518-24.

- FUKUSHIMA, S., HIROSE, M., TSUDA, H., SHIRAI, T. & HIRAO, K. 1976. Histological classification of urinary bladder cancers in rats induced by N-butyl-n-(4-hydroxybutyl)nitrosamine. *Gann*, 67, 81-90.
- GABRIEL, U., BOLENZ, C. & MICHEL, M. S. 2007. Experimental models for therapeutic studies of transitional cell carcinoma. *Anticancer Res*, 27, 3163-71.
- GAISA, N. T., GRAHAM, T. A., MCDONALD, S. A., CANADILLAS-LOPEZ, S., POULSOM, R., HEIDENREICH, A., JAKSE, G., TADROUS, P. J., KNUECHEL, R. & WRIGHT, N. A. 2011. The human urothelium consists of multiple clonal units, each maintained by a stem cell. *J Pathol*, 225, 163-71.
- GANDHI, D., MOLOTKOV, A., BATOURINA, E., SCHNEIDER, K., DAN, H., REILEY, M., LAUFER, E., METZGER, D., LIANG, F., LIAO, Y., SUN, T. T., ARONOW, B., ROSEN, R., MAUNEY, J., ADAM, R., ROSSELOT, C., VAN BATAVIA, J., MCMAHON, A., MCMAHON, J., GUO, J. J. & MENDELSON, C. 2013. Retinoid signaling in progenitors controls specification and regeneration of the urothelium. *Dev Cell*, 26, 469-82.
- GAO, J., HUANG, H.-Y., PAK, J., CHENG, J., ZHANG, Z.-T., SHAPIRO, E., PELLICER, A., SUN, T.-T. & WU, X.-R. 2004. p53 deficiency provokes urothelial proliferation and synergizes with activated Ha-ras in promoting urothelial tumorigenesis. *Oncogene*, 23, 687-696.
- GARCIA-CLOSAS, M., MALATS, N., SILVERMAN, D., DOSEMECI, M., KOGEVINAS, M., HEIN, D. W., TARDON, A., SERRA, C., CARRATO, A., GARCIA-CLOSAS, R., LLORETA, J., CASTANO-VINYALS, G., YEAGER, M., WELCH, R., CHANOCK, S., CHATTERJEE, N., WACHOLDER, S., SAMANIC, C., TORA, M., FERNANDEZ, F., REAL, F. X. & ROTHMAN, N. 2005. NAT2 slow acetylation, GSTM1 null genotype, and risk of bladder cancer: results from the Spanish Bladder Cancer Study and meta-analyses. *Lancet*, 366, 649-59.
- GARCIA DEL MURO, X., TORREGROSA, A., MUNOZ, J., CASTELLSAGUE, X., CONDOM, E., VIGUES, F., ARANCE, A., FABRA, A. & GERMA, J. R. 2000. Prognostic value of the expression of E-cadherin and beta-catenin in bladder cancer. *Eur J Cancer*, 36, 357-62.
- GARTSIDE, M. G., CHEN, H., IBRAHIMI, O. A., BYRON, S. A., CURTIS, A. V., WELLENS, C. L., BENGSTON, A., YUDT, L. M., ELISEENKOVA, A. V., MA, J., CURTIN, J. A., HYDER, P., HARPER, U. L., RIEDESEL, E., MANN, G. J., TRENT, J. M., BASTIAN, B. C., MELTZER, P. S., MOHAMMADI, M. & POLLOCK, P. M. 2009. Loss-of-function fibroblast growth factor receptor-2 mutations in melanoma. *Mol Cancer Res*, 7, 41-54.
- GAVINE, P. R., MOONEY, L., KILGOUR, E., THOMAS, A. P., AL-KADHIMI, K., BECK, S., ROONEY, C., COLEMAN, T., BAKER, D., MELLOR, M. J., BROOKS, A. N. & KLINOWSKA, T. 2012. AZD4547: an orally bioavailable, potent, and selective inhibitor of the fibroblast growth factor receptor tyrosine kinase family. *Cancer Res*, 72, 2045-56.
- GOETZ, R. & MOHAMMADI, M. 2013. Exploring mechanisms of FGF signalling through the lens of structural biology. *Nat Rev Mol Cell Biol*, 14, 166-80.
- GOMEZ-ROMAN, J. J., SAENZ, P., MOLINA, M., CUEVAS GONZALEZ, J., ESCUREDO, K., SANTA CRUZ, S., JUNQUERA, C., SIMON, L., MARTINEZ, A., GUTIERREZ BANOS, J. L., LOPEZ-BREA, M., ESPARZA, C. & VAL-BERNAL, J. F. 2005. Fibroblast growth factor receptor 3 is overexpressed in urinary tract carcinomas and modulates the neoplastic cell growth. *Clin Cancer Res*, 11, 459-65.
- GORDON, J. W. & RUDDLE, F. H. 1981. Integration and stable germ line transmission of genes injected into mouse pronuclei. *Science*, 214, 1244-6.

- GREENBLATT, M. S., BENNETT, W. P., HOLLSTEIN, M. & HARRIS, C. C. 1994. Mutations in the p53 tumor suppressor gene: clues to cancer etiology and molecular pathogenesis. *Cancer Res*, 54, 4855-78.
- GRIPPO, P. J. & SANDGREN, E. P. 2000. Highly invasive transitional cell carcinoma of the bladder in a simian virus 40 T-antigen transgenic mouse model. *Am J Pathol*, 157, 805-13.
- GUAGNANO, V., FURET, P., SPANKA, C., BORDAS, V., LE DOUGET, M., STAMM, C., BRUEGGEN, J., JENSEN, M. R., SCHNELL, C., SCHMID, H., WARTMANN, M., BERGHAUSEN, J., DRUECKES, P., ZIMMERLIN, A., BUSSIÈRE, D., MURRAY, J. & GRAUS PORTA, D. 2011. Discovery of 3-(2,6-dichloro-3,5-dimethoxy-phenyl)-1-{6-[4-(4-ethyl-piperazin-1-yl)-phenylamino]-pyrimidin-4-yl}-1-methyl-urea (NVP-BGJ398), a potent and selective inhibitor of the fibroblast growth factor receptor family of receptor tyrosine kinase. *J Med Chem*, 54, 7066-83.
- GUAGNANO, V., KAUFFMANN, A., WOHRLE, S., STAMM, C., ITO, M., BARYS, L., PORNON, A., YAO, Y., LI, F., ZHANG, Y., CHEN, Z., WILSON, C. J., BORDAS, V., LE DOUGET, M., GAITHER, L. A., BORAWSKI, J., MONAHAN, J. E., VENKATESAN, K., BRUMMENDORF, T., THOMAS, D. M., GARCIA-ECHEVERRIA, C., HOFMANN, F., SELLERS, W. R. & GRAUS-PORTA, D. 2012. FGFR genetic alterations predict for sensitivity to NVP-BGJ398, a selective pan-FGFR inhibitor. *Cancer Discov*, 2, 1118-33.
- GUANCIAL, E. A., BELLMUNT, J., YEH, S., ROSENBERG, J. E. & BERMAN, D. M. 2014a. The evolving understanding of microRNA in bladder cancer. *Urol Oncol*, 32, 41 e31-40.
- GUANCIAL, E. A., WERNER, L., BELLMUNT, J., BAMIAS, A., CHOUËIRI, T. K., ROSS, R., SCHUTZ, F. A., PARK, R. S., O'BRIEN, R. J., HIRSCH, M. S., BARLETTA, J. A., BERMAN, D. M., LIS, R., LODA, M., STACK, E. C., GARRAWAY, L. A., RIESTER, M., MICHOR, F., KANTOFF, P. W. & ROSENBERG, J. E. 2014b. FGFR3 expression in primary and metastatic urothelial carcinoma of the bladder. *Cancer Med*, 3, 835-44.
- GUNTHER, J. H., JURCZOK, A., WULF, T., BRANDAU, S., DEINERT, I., JOCHAM, D. & BOHLE, A. 1999. Optimizing syngeneic orthotopic murine bladder cancer (MB49). *Cancer Res*, 59, 2834-7.
- GUO, C. C., FINE, S. W. & EPSTEIN, J. I. 2006. Noninvasive squamous lesions in the urinary bladder: a clinicopathologic analysis of 29 cases. *Am J Surg Pathol*, 30, 883-91.
- HABUCHI, T. 2005. Origin of multifocal carcinomas of the bladder and upper urinary tract: molecular analysis and clinical implications. *Int J Urol*, 12, 709-16.
- HABUCHI, T., KINOSHITA, H., YAMADA, H., KAKEHI, Y., OGAWA, O., WU, W. J., TAKAHASHI, R., SUGIYAMA, T. & YOSHIDA, O. 1994. Oncogene amplification in urothelial cancers with p53 gene mutation or MDM2 amplification. *J Natl Cancer Inst*, 86, 1331-5.
- HACOHEN, N., KRAMER, S., SUTHERLAND, D., HIROMI, Y. & KRASNOW, M. A. 1998. sprouty encodes a novel antagonist of FGF signaling that patterns apical branching of the Drosophila airways. *Cell*, 92, 253-63.
- HAFNER, C., KNUECHEL, R., STOEHR, R. & HARTMANN, A. 2002. Clonality of multifocal urothelial carcinomas: 10 years of molecular genetic studies. *Int J Cancer*, 101, 1-6.
- HAFNER, C., KNUECHEL, R., ZANARDO, L., DIETMAIER, W., BLASZYK, H., CHEVILLE, J., HOFSTAEDTER, F. & HARTMANN, A. 2001. Evidence for oligoclonality and tumor spread by intraluminal seeding in multifocal

- urothelial carcinomas of the upper and lower urinary tract. *Oncogene*, 20, 4910-5.
- HART, K. C., ROBERTSON, S. C. & DONOGHUE, D. J. 2001. Identification of tyrosine residues in constitutively activated fibroblast growth factor receptor 3 involved in mitogenesis, Stat activation, and phosphatidylinositol 3-kinase activation. *Mol Biol Cell*, 12, 931-42.
- HART, K. C., ROBERTSON, S. C., KANEMITSU, M. Y., MEYER, A. N., TYNAN, J. A. & DONOGHUE, D. J. 2000. Transformation and Stat activation by derivatives of FGFR1, FGFR3, and FGFR4. *Oncogene*, 19, 3309-20.
- HARTMANN, A., ROSNER, U., SCHLAKE, G., DIETMAIER, W., ZAAK, D., HOFSTAEDTER, F. & KNUECHEL, R. 2000. Clonality and genetic divergence in multifocal low-grade superficial urothelial carcinoma as determined by chromosome 9 and p53 deletion analysis. *Lab Invest*, 80, 709-18.
- HAWLEY, S. P., WILLS, M. K. & JONES, N. 2010. Adenovirus-mediated genetic removal of signaling molecules in cultured primary mouse embryonic fibroblasts. *J Vis Exp*.
- HE, F., MO, L., ZHENG, X. Y., HU, C., LEPOR, H., LEE, E. Y., SUN, T. T. & WU, X. R. 2009. Deficiency of pRb family proteins and p53 in invasive urothelial tumorigenesis. *Cancer Res*, 69, 9413-21.
- HE, Z., KOSINSKA, W., ZHAO, Z. L., WU, X. R. & GUTTENPLAN, J. B. 2012. Tissue-specific mutagenesis by N-butyl-N-(4-hydroxybutyl)nitrosamine as the basis for urothelial carcinogenesis. *Mutat Res*, 742, 92-5.
- HELDT, S. A. & RESSLER, K. J. 2009. The Use of Lentiviral Vectors and Cre/loxP to Investigate the Function of Genes in Complex Behaviors. *Front Mol Neurosci*, 2, 22.
- HENRIQUEZ, N. V., VAN OVERVELD, P. G., QUE, I., BUIJS, J. T., BACHELIER, R., KAIJZEL, E. L., LOWIK, C. W., CLEZARDIN, P. & VAN DER PLUIJM, G. 2007. Advances in optical imaging and novel model systems for cancer metastasis research. *Clin Exp Metastasis*, 24, 699-705.
- HERNANDEZ, S., LOPEZ-KNOWLES, E., LLORETA, J., KOGEVINAS, M., AMOROS, A., TARDON, A., CARRATO, A., SERRA, C., MALATS, N. & REAL, F. X. 2006. Prospective study of FGFR3 mutations as a prognostic factor in nonmuscle invasive urothelial bladder carcinomas. *J Clin Oncol*, 24, 3664-71.
- HERNANDEZ, S., LOPEZ-KNOWLES, E., LLORETA, J., KOGEVINAS, M., JARAMILLO, R., AMOROS, A., TARDON, A., GARCIA-CLOSAS, R., SERRA, C., CARRATO, A., MALATS, N. & REAL, F. X. 2005. FGFR3 and Tp53 mutations in T1G3 transitional bladder carcinomas: independent distribution and lack of association with prognosis. *Clin Cancer Res*, 11, 5444-50.
- HERR, H. W. 2000. Tumor progression and survival of patients with high grade, noninvasive papillary (TaG3) bladder tumors: 15-year outcome. *J Urol*, 163, 60-1; discussion 61-2.
- HERRERA-ABREU, M. T., PEARSON, A., CAMPBELL, J., SHNYDER, S. D., KNOWLES, M. A., ASHWORTH, A. & TURNER, N. C. 2013. Parallel RNA Interference Screens Identify EGFR Activation as an Escape Mechanism in FGFR3-Mutant Cancer. *Cancer Discov*, 3, 1058-71.
- HO, P. L., LAY, E. J., JIAN, W., PARRA, D. & CHAN, K. S. 2012. Stat3 activation in urothelial stem cells leads to direct progression to invasive bladder cancer. *Cancer Res*, 72, 3135-42.
- HSIEH, J. K., CHAN, F. S., O'CONNOR, D. J., MITTNACHT, S., ZHONG, S. & LU, X. 1999. RB regulates the stability and the apoptotic function of p53 via MDM2. *Mol Cell*, 3, 181-93.

- HUGHES, S. E. 1997. Differential expression of the fibroblast growth factor receptor (FGFR) multigene family in normal human adult tissues. *J Histochem Cytochem*, 45, 1005-19.
- HUMPHRAY, S. J., OLIVER, K., HUNT, A. R., PLUMB, R. W., LOVELAND, J. E., HOWE, K. L., ANDREWS, T. D., SEARLE, S., HUNT, S. E., SCOTT, C. E., JONES, M. C., AINSCOUGH, R., ALMEIDA, J. P., AMBROSE, K. D., ASHWELL, R. I., BABBAGE, A. K., BABBAGE, S., BAGGULEY, C. L., BAILEY, J., BANERJEE, R., BARKER, D. J., BARLOW, K. F., BATES, K., BEASLEY, H., BEASLEY, O., BIRD, C. P., BRAY-ALLEN, S., BROWN, A. J., BROWN, J. Y., BURFORD, D., BURRILL, W., BURTON, J., CARDER, C., CARTER, N. P., CHAPMAN, J. C., CHEN, Y., CLARKE, G., CLARK, S. Y., CLEE, C. M., CLEGG, S., COLLIER, R. E., CORBY, N., CROSIER, M., CUMMINGS, A. T., DAVIES, J., DHAMI, P., DUNN, M., DUTTA, I., DYER, L. W., EARTHROWL, M. E., FAULKNER, L., FLEMING, C. J., FRANKISH, A., FRANKLAND, J. A., FRENCH, L., FRICKER, D. G., GARNER, P., GARNETT, J., GHORI, J., GILBERT, J. G., GLISON, C., GRAFHAM, D. V., GRIBBLE, S., GRIFFITHS, C., GRIFFITHS-JONES, S., GROCOCK, R., GUY, J., HALL, R. E., HAMMOND, S., HARLEY, J. L., HARRISON, E. S., HART, E. A., HEATH, P. D., HENDERSON, C. D., HOPKINS, B. L., HOWARD, P. J., HOWDEN, P. J., HUCKLE, E., JOHNSON, C., JOHNSON, D., JOY, A. A., KAY, M., KEENAN, S., KERSHAW, J. K., KIMBERLEY, A. M., KING, A., KNIGHTS, A., LAIRD, G. K., LANGFORD, C., LAWLOR, S., LEONGAMORNLETT, D. A., LEVERSHA, M., LLOYD, C., LLOYD, D. M., LOVELL, J., MARTIN, S., MASHREGHI-MOHAMMADI, M., MATTHEWS, L., MCLAREN, S., MCLAY, K. E., et al. 2004. DNA sequence and analysis of human chromosome 9. *Nature*, 429, 369-74.
- INOUE, Y., IZAWA, K., KIRYU, S., TOJO, A. & OHTOMO, K. 2008. Diet and abdominal autofluorescence detected by in vivo fluorescence imaging of living mice. *Mol Imaging*, 7, 21-7.
- ISSA, A., GILL, J. W., HEIDEMAN, M. R., SAHIN, O., WIEMANN, S., DEY, J. H. & HYNES, N. E. 2013. Combinatorial targeting of FGF and ErbB receptors blocks growth and metastatic spread of breast cancer models. *Breast Cancer Res*, 15, R8.
- IVICS, Z., HACKETT, P. B., PLASTERK, R. H. & IZSVAK, Z. 1997. Molecular reconstruction of Sleeping Beauty, a Tc1-like transposon from fish, and its transposition in human cells. *Cell*, 91, 501-10.
- IWATA, T., CHEN, L., LI, C., OVCHINNIKOV, D. A., BEHRINGER, R. R., FRANCOMANO, C. A. & DENG, C. X. 2000. A neonatal lethal mutation in FGFR3 uncouples proliferation and differentiation of growth plate chondrocytes in embryos. *Hum Mol Genet*, 9, 1603-13.
- IWATA, T. & HEVNER, R. F. 2009. Fibroblast growth factor signaling in development of the cerebral cortex. *Dev Growth Differ*, 51, 299-323.
- IYER, G. & MILOWSKY, M. I. 2012. Fibroblast growth factor receptor-3 in urothelial tumorigenesis. *Urol Oncol*.
- JACKSON, E. L. 2001. Analysis of lung tumor initiation and progression using conditional expression of oncogenic K-ras. *Genes & Development*, 15, 3243-3248.
- JACQUEMIER, J., ADELAIDE, J., PARC, P., PENAULT-LLORCA, F., PLANCHE, J., DELAPEYRIERE, O. & BIRNBAUM, D. 1994. Expression of the FGFR1 gene in human breast-carcinoma cells. *Int J Cancer*, 59, 373-8.
- JANG, J. H., SHIN, K. H. & PARK, J. G. 2001. Mutations in fibroblast growth factor receptor 2 and fibroblast growth factor receptor 3 genes associated with human gastric and colorectal cancers. *Cancer Res*, 61, 3541-3.

- JEBAR, A. H., HURST, C. D., TOMLINSON, D. C., JOHNSTON, C., TAYLOR, C. F. & KNOWLES, M. A. 2005. FGFR3 and Ras gene mutations are mutually exclusive genetic events in urothelial cell carcinoma. *Oncogene*, 24, 5218-5225.
- JONES, T. D., WANG, M., EBLE, J. N., MACLENNAN, G. T., LOPEZ-BELTRAN, A., ZHANG, S., COCCO, A. & CHENG, L. 2005. Molecular evidence supporting field effect in urothelial carcinogenesis. *Clin Cancer Res*, 11, 6512-9.
- JUANPERE, N., AGELL, L., LORENZO, M., DE MUGA, S., LOPEZ-VILARO, L., MURILLO, R., MOJAL, S., SERRANO, S., LORENTE, J. A., LLORETA, J. & HERNANDEZ, S. 2012. Mutations in FGFR3 and PIK3CA, singly or combined with RAS and AKT1, are associated with AKT but not with MAPK pathway activation in urothelial bladder cancer. *Hum Pathol*, 43, 1573-82.
- JURCZOK, A., FORNARA, P. & SOLING, A. 2008. Bioluminescence imaging to monitor bladder cancer cell adhesion in vivo: a new approach to optimize a syngeneic, orthotopic, murine bladder cancer model. *BJU Int*, 101, 120-4.
- KAGAN, J., LIU, J., STEIN, J. D., WAGNER, S. S., BABKOWSKI, R., GROSSMAN, B. H. & KATZ, R. L. 1998. Cluster of allele losses within a 2.5 cM region of chromosome 10 in high-grade invasive bladder cancer. *Oncogene*, 16, 909-13.
- KALLIONIEMI, A., KALLIONIEMI, O. P., CITRO, G., SAUTER, G., DEVRIES, S., KERSCHMANN, R., CAROLL, P. & WALDMAN, F. 1995. Identification of gains and losses of DNA sequences in primary bladder cancer by comparative genomic hybridization. *Genes Chromosomes Cancer*, 12, 213-9.
- KANG, J., LEE, S. Y., KIM, Y. J., PARK, J. Y., KWON, S. J., NA, M. J., LEE, E. J., JEON, H. S. & SON, J. W. 2012. microRNA-99b acts as a tumor suppressor in non-small cell lung cancer by directly targeting fibroblast growth factor receptor 3. *Exp Ther Med*, 3, 149-153.
- KARASAVVIDOU, F., BARBANIS, S., PAPPA, D., MOUTZOURIS, G., TZORTZIS, V., MELEKOS, M. D. & KOUKOULIS, G. 2008. Fascin determination in urothelial carcinomas of the urinary bladder: a marker of invasiveness. *Arch Pathol Lab Med*, 132, 1912-5.
- KARNI-SCHMIDT, O., CASTILLO-MARTIN, M., SHEN, T. H., GLADOUN, N., DOMINGO-DOMENECH, J., SANCHEZ-CARBAYO, M., LI, Y., LOWE, S., PRIVES, C. & CORDON-CARDO, C. 2011. Distinct expression profiles of p63 variants during urothelial development and bladder cancer progression. *Am J Pathol*, 178, 1350-60.
- KATOH, M. 2013. Functional and cancer genomics of ASXL family members. *Br J Cancer*, 109, 299-306.
- KATOH, M. & NAKAGAMA, H. 2013. FGF Receptors: Cancer Biology and Therapeutics. *Med Res Rev*.
- KENG, V. W., VILLANUEVA, A., CHIANG, D. Y., DUPUY, A. J., RYAN, B. J., MATISE, I., SILVERSTEIN, K. A., SARVER, A., STARR, T. K., AKAGI, K., TESSAROLLO, L., COLLIER, L. S., POWERS, S., LOWE, S. W., JENKINS, N. A., COPELAND, N. G., LLOVET, J. M. & LARGAESPADA, D. A. 2009. A conditional transposon-based insertional mutagenesis screen for genes associated with mouse hepatocellular carcinoma. *Nat Biotechnol*, 27, 264-74.
- KHANDELWAL, P., ABRAHAM, S. N. & APODACA, G. 2009. Cell biology and physiology of the uroepithelium. *Am J Physiol Renal Physiol*, 297, F1477-501.
- KIKUCHI, E., XU, S., OHORI, M., MATEI, C., LUPU, M., MENENDEZ, S., KOUTCHER, J. A. & BOCHNER, B. H. 2003. Detection and quantitative analysis of early

- stage orthotopic murine bladder tumor using in vivo magnetic resonance imaging. *J Urol*, 170, 1375-8.
- KIM, I., MOON, S., YU, K., KIM, U. & KOH, G. Y. 2001. A novel fibroblast growth factor receptor-5 preferentially expressed in the pancreas(1). *Biochim Biophys Acta*, 1518, 152-6.
- KIM, M. 2010. Cooperative interactions of PTEN deficiency and RAS activation in melanoma metastasis. *Small GTPases*, 1, 161-164.
- KIM, S. & ALEXANDER, C. M. 2013. Tumorsphere assay provides more accurate prediction of in vivo responses to chemotherapeutics. *Biotechnol Lett*.
- KIM, T. H., WANG, J., LEE, K. Y., FRANCO, H. L., BROADDUS, R. R., LYDON, J. P., JEONG, J. W. & DEMAYO, F. J. 2010. The Synergistic Effect of Conditional Pten Loss and Oncogenic K-ras Mutation on Endometrial Cancer Development Occurs via Decreased Progesterone Receptor Action. *J Oncol*, 2010, 139087.
- KIRSCH, D. G., DINULESCU, D. M., MILLER, J. B., GRIMM, J., SANTIAGO, P. M., YOUNG, N. P., NIELSEN, G. P., QUADE, B. J., CHABER, C. J., SCHULTZ, C. P., TAKEUCHI, O., BRONSON, R. T., CROWLEY, D., KORSMEYER, S. J., YOON, S. S., HORNICEK, F. J., WEISSLEDER, R. & JACKS, T. 2007. A spatially and temporally restricted mouse model of soft tissue sarcoma. *Nat Med*, 13, 992-7.
- KNOWLES, M. A. 2007. Role of FGFR3 in urothelial cell carcinoma: biomarker and potential therapeutic target. *World Journal of Urology*, 25, 581-593.
- KNOWLES, M. A. 2008. Molecular pathogenesis of bladder cancer. *International Journal of Clinical Oncology*, 13, 287-297.
- KNOWLES, M. A., PLATT, F. M., ROSS, R. L. & HURST, C. D. 2009. Phosphatidylinositol 3-kinase (PI3K) pathway activation in bladder cancer. *Cancer and Metastasis Reviews*, 28, 305-316.
- KNOWLES, M. A. & WILLIAMSON, M. 1993. Mutation of H-ras is infrequent in bladder cancer: confirmation by single-strand conformation polymorphism analysis, designed restriction fragment length polymorphisms, and direct sequencing. *Cancer Res*, 53, 133-9.
- KOGEVINAS, M., T MANNETJE, A., CORDIER, S., RANFT, U., GONZALEZ, C. A., VINEIS, P., CHANG-CLAUDE, J., LYNGE, E., WAHRENDORF, J., TZONOU, A., JOCKEL, K. H., SERRA, C., PORRU, S., HOURS, M., GREISER, E. & BOFFETTA, P. 2003. Occupation and bladder cancer among men in Western Europe. *Cancer Causes Control*, 14, 907-14.
- KOMPIER, L. C., LURKIN, I., VAN DER AA, M. N., VAN RHIJN, B. W., VAN DER KWAST, T. H. & ZWARTHOFF, E. C. 2010. FGFR3, HRAS, KRAS, NRAS and PIK3CA mutations in bladder cancer and their potential as biomarkers for surveillance and therapy. *PLoS One*, 5, e13821.
- KONG, X. T. 2004. Roles of uroplakins in plaque formation, umbrella cell enlargement, and urinary tract diseases. *The Journal of Cell Biology*, 167, 1195-1204.
- KORKOLOPOULOU, P., LEVIDOU, G., TRIGKA, E. A., PREKETE, N., KARLOU, M., THYMARA, I., SAKELLARIOU, S., FRAGKOU, P., ISAIADIS, D., PAVLOPOULOS, P., PATSOURIS, E. & SAETTA, A. A. 2012. A comprehensive immunohistochemical and molecular approach to the PI3K/AKT/mTOR (phosphoinositide 3-kinase/v-akt murine thymoma viral oncogene/mammalian target of rapamycin) pathway in bladder urothelial carcinoma. *BJU Int*, 110, E1237-48.
- KOVALENKO, D., YANG, X., NADEAU, R. J., HARKINS, L. K. & FRIESEL, R. 2003. Sef inhibits fibroblast growth factor signaling by inhibiting FGFR1 tyrosine

- phosphorylation and subsequent ERK activation. *J Biol Chem*, 278, 14087-91.
- KUMAR, M. S., ERKELAND, S. J., PESTER, R. E., CHEN, C. Y., EBERT, M. S., SHARP, P. A. & JACKS, T. 2008. Suppression of non-small cell lung tumor development by the let-7 microRNA family. *Proc Natl Acad Sci U S A*, 105, 3903-8.
- KUNII, K., DAVIS, L., GORENSTEIN, J., HATCH, H., YASHIRO, M., DI BACCO, A., ELBI, C. & LUTTERBACH, B. 2008. FGFR2-amplified gastric cancer cell lines require FGFR2 and Erbb3 signaling for growth and survival. *Cancer Res*, 68, 2340-8.
- KUNZE, E., GRAEWE, T., SCHERBER, S., WEBER, J. & GELLHAR, P. 1989. Cell cycle dependence of N-methyl-N-nitrosourea-induced tumour development in the proliferating, partially resected rat urinary bladder. *Br J Exp Pathol*, 70, 125-42.
- KURZROCK, E. A., LIEU, D. K., DEGRAFFENRIED, L. A., CHAN, C. W. & ISSEROFF, R. R. 2008. Label-retaining cells of the bladder: candidate urothelial stem cells. *Am J Physiol Renal Physiol*, 294, F1415-21.
- KWABI-ADDO, B., OZEN, M. & ITTMANN, M. 2004. The role of fibroblast growth factors and their receptors in prostate cancer. *Endocr Relat Cancer*, 11, 709-24.
- LAEDERICH, M. B. & HORTON, W. A. 2012. FGFR3 targeting strategies for achondroplasia. *Expert Rev Mol Med*, 14, e11.
- LAFITTE, M., MORANVILLIER, I., GARCIA, S., PEUCHANT, E., IOVANNA, J., ROUSSEAU, B., DUBUS, P., GUYONNET-DUPERAT, V., BELLEANNEE, G., RAMOS, J., BEDEL, A., DE VERNEUIL, H., MOREAU-GAUDRY, F. & DABERNAT, S. 2013. FGFR3 has tumor suppressor properties in cells with epithelial phenotype. *Mol Cancer*, 12, 83.
- LAMONT, F. R., TOMLINSON, D. C., COOPER, P. A., SHNYDER, S. D., CHESTER, J. D. & KNOWLES, M. A. 2011. Small molecule FGF receptor inhibitors block FGFR-dependent urothelial carcinoma growth in vitro and in vivo. *Br J Cancer*, 104, 75-82.
- LANDER, E. S., LINTON, L. M., BIRREN, B., NUSBAUM, C., ZODY, M. C., BALDWIN, J., DEVON, K., DEWAR, K., DOYLE, M., FITZHUGH, W., FUNKE, R., GAGE, D., HARRIS, K., HEAFORD, A., HOWLAND, J., KANN, L., LEHOCZKY, J., LEVINE, R., MCEWAN, P., MCKERNAN, K., MELDRIM, J., MESIROV, J. P., MIRANDA, C., MORRIS, W., NAYLOR, J., RAYMOND, C., ROSETTI, M., SANTOS, R., SHERIDAN, A., SOUGNEZ, C., STANGE-THOMANN, N., STOJANOVIC, N., SUBRAMANIAN, A., WYMAN, D., ROGERS, J., SULSTON, J., AINSCOUGH, R., BECK, S., BENTLEY, D., BURTON, J., CLEE, C., CARTER, N., COULSON, A., DEADMAN, R., DELOUKAS, P., DUNHAM, A., DUNHAM, I., DURBIN, R., FRENCH, L., GRAFHAM, D., GREGORY, S., HUBBARD, T., HUMPHRAY, S., HUNT, A., JONES, M., LLOYD, C., MCMURRAY, A., MATTHEWS, L., MERCER, S., MILNE, S., MULLIKIN, J. C., MUNGALL, A., PLUMB, R., ROSS, M., SHOWNKEEN, R., SIMS, S., WATERSTON, R. H., WILSON, R. K., HILLIER, L. W., MCPHERSON, J. D., MARRA, M. A., MARDIS, E. R., FULTON, L. A., CHINWALLA, A. T., PEPIN, K. H., GISH, W. R., CHISSOE, S. L., WENDL, M. C., DELEHAUNTY, K. D., MINER, T. L., DELEHAUNTY, A., KRAMER, J. B., COOK, L. L., FULTON, R. S., JOHNSON, D. L., MINX, P. J., CLIFTON, S. W., HAWKINS, T., BRANSCOMB, E., PREDKI, P., RICHARDSON, P., WENNING, S., SLEZAK, T., DOGGETT, N., CHENG, J. F., OLSEN, A., LUCAS, S., ELKIN, C., UBERBACHER, E., FRAZIER, M., et al. 2001. Initial sequencing and analysis of the human genome. *Nature*, 409, 860-921.

- LEBLANC, B., DUCLOS, A. J., BENARD, F., COTE, J., VALIQUETTE, L., PAQUIN, J. M., MAUFFETTE, F., FAUCHER, R. & PERREAULT, J. P. 1999. Long-term followup of initial Ta grade 1 transitional cell carcinoma of the bladder. *J Urol*, 162, 1946-50.
- LESCHE, R., GROSZER, M., GAO, J., WANG, Y., MESSING, A., SUN, H., LIU, X. & WU, H. 2002. Cre/loxP-mediated inactivation of the murine Pten tumor suppressor gene. *genesis*, 32, 148-149.
- LI, C., CHEN, L., IWATA, T., KITAGAWA, M., FU, X. Y. & DENG, C. X. 1999. A Lys644Glu substitution in fibroblast growth factor receptor 3 (FGFR3) causes dwarfism in mice by activation of STATs and ink4 cell cycle inhibitors. *Hum Mol Genet*, 8, 35-44.
- LI, C., SCOTT, D. A., HATCH, E., TIAN, X. & MANSOUR, S. L. 2007. Dusp6 (Mkp3) is a negative feedback regulator of FGF-stimulated ERK signaling during mouse development. *Development*, 134, 167-76.
- LI, W., LIU, M., FENG, Y., HUANG, Y. F., XU, Y. F., CHE, J. P., WANG, G. C. & ZHENG, J. H. 2013. High expression of Notch ligand Jagged2 is associated with the metastasis and recurrence in urothelial carcinoma of bladder. *Int J Clin Exp Pathol*, 6, 2430-40.
- LIANES, P., ORLOW, I., ZHANG, Z. F., OLIVA, M. R., SARKIS, A. S., REUTER, V. E. & CORDON-CARDO, C. 1994. Altered patterns of MDM2 and TP53 expression in human bladder cancer. *J Natl Cancer Inst*, 86, 1325-30.
- LIANG, G., CHEN, G., WEI, X., ZHAO, Y. & LI, X. 2013. Small molecule inhibition of fibroblast growth factor receptors in cancer. *Cytokine Growth Factor Rev*, 24, 467-75.
- LIANG, Q., KONG, J., STALKER, J. & BRADLEY, A. 2009. Chromosomal mobilization and reintegration of Sleeping Beauty and PiggyBac transposons. *genesis*, 47, 404-408.
- LIN, J. H., ZHAO, H. & SUN, T. T. 1995. A tissue-specific promoter that can drive a foreign gene to express in the suprabasal urothelial cells of transgenic mice. *Proc Natl Acad Sci U S A*, 92, 679-83.
- LINDGREN, D., SJODAHL, G., LAUSS, M., STAAF, J., CHEBIL, G., LOVGREN, K., GUDJONSSON, S., LIEBERG, F., PATSCHAN, O., MANSSON, W., FERNO, M. & HOGLUND, M. 2012. Integrated genomic and gene expression profiling identifies two major genomic circuits in urothelial carcinoma. *PLoS One*, 7, e38863.
- LIU, G., MCDONNELL, T. J., MONTES DE OCA LUNA, R., KAPOOR, M., MIMS, B., EL-NAGGAR, A. K. & LOZANO, G. 2000. High metastatic potential in mice inheriting a targeted p53 missense mutation. *Proc Natl Acad Sci U S A*, 97, 4174-9.
- LOGIE, A. 2005. Activating mutations of the tyrosine kinase receptor FGFR3 are associated with benign skin tumors in mice and humans. *Human Molecular Genetics*, 14, 1153-1160.
- LOPEZ-KNOWLES, E., HERNANDEZ, S., MALATS, N., KOGEVINAS, M., LLORETA, J., CARRATO, A., TARDON, A., SERRA, C. & REAL, F. X. 2006. PIK3CA mutations are an early genetic alteration associated with FGFR3 mutations in superficial papillary bladder tumors. *Cancer Res*, 66, 7401-4.
- LORD, C. J. & ASHWORTH, A. 2012. The DNA damage response and cancer therapy. *Nature*, 481, 287-94.
- LOSKOG, A., NINALGA, C., HEDLUND, T., ALIMOHAMMADI, M., MALMSTROM, P. U. & TOTTERMAN, T. H. 2005. Optimization of the MB49 mouse bladder cancer model for adenoviral gene therapy. *Lab Anim*, 39, 384-93.
- LU, M. L., WIKMAN, F., ORNTOFT, T. F., CHARYTONOWICZ, E., RABBANI, F., ZHANG, Z., DALBAGNI, G., POHAR, K. S., YU, G. & CORDON-CARDO, C.

2002. Impact of alterations affecting the p53 pathway in bladder cancer on clinical outcome, assessed by conventional and array-based methods. *Clin Cancer Res*, 8, 171-9.
- LUCHE, H., WEBER, O., NAGESWARA RAO, T., BLUM, C. & FEHLING, H. J. 2007. Faithful activation of an extra-bright red fluorescent protein in "knock-in" Cre-reporter mice ideally suited for lineage tracing studies. *Eur J Immunol*, 37, 43-53.
- LUO, G., IVICS, Z., IZSVAK, Z. & BRADLEY, A. 1998. Chromosomal transposition of a Tc1/mariner-like element in mouse embryonic stem cells. *Proc Natl Acad Sci U S A*, 95, 10769-73.
- LYONS, S. K. 2005. Advances in imaging mouse tumour models in vivo. *J Pathol*, 205, 194-205.
- MACHER-GOEPFINGER, S., BERMEJO, J. L., SCHIRMACHER, P., PAHERNIK, S., HOHENFELLNER, M. & ROTH, W. 2013. Senescence-associated protein p400 is a prognostic marker in renal cell carcinoma. *Oncol Rep*, 30, 2245-53.
- MAEHAMA, T. & DIXON, J. E. 1998. The tumor suppressor, PTEN/MMAC1, dephosphorylates the lipid second messenger, phosphatidylinositol 3,4,5-trisphosphate. *J Biol Chem*, 273, 13375-8.
- MALATS, N., BUSTOS, A., NASCIMENTO, C. M., FERNANDEZ, F., RIVAS, M., PUENTE, D., KOGEVINAS, M. & REAL, F. X. 2005. P53 as a prognostic marker for bladder cancer: a meta-analysis and review. *Lancet Oncol*, 6, 678-86.
- MANN, K. M., WARD, J. M., YEW, C. C., KOVOCHICH, A., DAWSON, D. W., BLACK, M. A., BRETT, B. T., SHEETZ, T. E., DUPUY, A. J., CHANG, D. K., BIANKIN, A. V., WADDELL, N., KASSAHN, K. S., GRIMMOND, S. M., RUST, A. G., ADAMS, D. J., JENKINS, N. A. & COPELAND, N. G. 2012. Sleeping Beauty mutagenesis reveals cooperating mutations and pathways in pancreatic adenocarcinoma. *Proc Natl Acad Sci U S A*, 109, 5934-41.
- MAO, J. H., TO, M. D., PEREZ-LOSADA, J., WU, D., DEL ROSARIO, R. & BALMAIN, A. 2004. Mutually exclusive mutations of the Pten and ras pathways in skin tumor progression. *Genes Dev*, 18, 1800-5.
- MARCH, H. N., RUST, A. G., WRIGHT, N. A., TEN HOEVE, J., DE RIDDER, J., ELDRIDGE, M., VAN DER WEYDEN, L., BERNS, A., GADIOT, J., UREN, A., KEMP, R., ARENDS, M. J., WESSELS, L. F., WINTON, D. J. & ADAMS, D. J. 2011. Insertional mutagenesis identifies multiple networks of cooperating genes driving intestinal tumorigenesis. *Nat Genet*, 43, 1202-9.
- MARQUIS, L., TRAN, M., CHOI, W., LEE, I. L., HUSZAR, D., SIEFKER-RADTKE, A., DINNEY, C. & MCCONKEY, D. J. 2012. p63 expression correlates with sensitivity to the Eg5 inhibitor ZD4877 in bladder cancer cells. *Cancer Biol Ther*, 13, 477-86.
- MARSH, S. K., BANSAL, G. S., ZAMMIT, C., BARNARD, R., COOPE, R., ROBERTS-CLARKE, D., GOMM, J. J., COOMBES, R. C. & JOHNSTON, C. L. 1999. Increased expression of fibroblast growth factor 8 in human breast cancer. *Oncogene*, 18, 1053-60.
- MARTINIOVA, L., SCHIMEL, D., LAI, E. W., LIMPUANGTHIP, A., KVETNANSKY, R. & PACAK, K. 2010. In vivo micro-CT imaging of liver lesions in small animal models. *Methods*, 50, 20-5.
- MARZIONI, D., LORENZI, T., MAZZUCHELLI, R., CAPPARUCCIA, L., MORRONI, M., FIORINI, R., BRACALENTI, C., CATALANO, A., DAVID, G., CASTELLUCCI, M., MUZZONIGRO, G. & MONTIRONI, R. 2009. Expression of basic fibroblast growth factor, its receptors and syndecans in bladder cancer. *Int J Immunopathol Pharmacol*, 22, 627-38.

- MATSUMOTO, M., OHTSUKI, Y., OCHII, K., SEIKE, Y., ISEDA, N., SASAKI, T., OKADA, Y., KURABAYASHI, A. & FURIHATA, M. 2004. Fibroblast growth factor receptor 3 protein expression in urothelial carcinoma of the urinary bladder, exhibiting no association with low-grade and/or non-invasive lesions. *Oncol Rep*, 12, 967-71.
- MCCORMICK, D. L., RONAN, S. S., BECCI, P. J. & MOON, R. C. 1981. Influence of total dose and dose schedule on induction of urinary bladder cancer in the mouse by N-butyl-N-(4-hydroxybutyl)nitrosamine. *Carcinogenesis*, 2, 251-4.
- MEIER, Y., ZODAN, T., LANG, C., ZIMMERMANN, R., KULLAK-UBLICK, G. A., MEIER, P. J., STIEGER, B. & PAULI-MAGNUS, C. 2008. Increased susceptibility for intrahepatic cholestasis of pregnancy and contraceptive-induced cholestasis in carriers of the 1331T>C polymorphism in the bile salt export pump. *World J Gastroenterol*, 14, 38-45.
- MHAWECH-FAUCEGLIA, P., CHENEY, R. T., FISCHER, G., BECK, A. & HERRMANN, F. R. 2006. FGFR3 and p53 protein expressions in patients with pTa and pT1 urothelial bladder cancer. *Eur J Surg Oncol*, 32, 231-7.
- MIKI, T., BOTTARO, D. P., FLEMING, T. P., SMITH, C. L., BURGESS, W. H., CHAN, A. M. & AARONSON, S. A. 1992. Determination of ligand-binding specificity by alternative splicing: two distinct growth factor receptors encoded by a single gene. *Proc Natl Acad Sci U S A*, 89, 246-50.
- MO, L., CHENG, J., LEE, E. Y., SUN, T. T. & WU, X. R. 2005. Gene deletion in urothelium by specific expression of Cre recombinase. *Am J Physiol Renal Physiol*, 289, F562-8.
- MO, L., ZHENG, X., HUANG, H. Y., SHAPIRO, E., LEPOR, H., CORDON-CARDO, C., SUN, T. T. & WU, X. R. 2007. Hyperactivation of Ha-ras oncogene, but not Ink4a/Arf deficiency, triggers bladder tumorigenesis. *J Clin Invest*, 117, 314-25.
- MOLL, R., DIVO, M. & LANGBEIN, L. 2008. The human keratins: biology and pathology. *Histochem Cell Biol*, 129, 705-33.
- MONTIRONI, R., MAZZUCHELLI, R., SCARPELLI, M., LOPEZ-BELTRAN, A. & CHENG, L. 2008. Morphological diagnosis of urothelial neoplasms. *J Clin Pathol*, 61, 3-10.
- MORRIS, R. J. & POTTEN, C. S. 1994. Slowly cycling (label-retaining) epidermal cells behave like clonogenic stem cells in vitro. *Cell Prolif*, 27, 279-89.
- MULHOLLAND, D. J., KOBAYASHI, N., RUSCETTI, M., ZHI, A., TRAN, L. M., HUANG, J., GLEAVE, M. & WU, H. 2012. Pten loss and RAS/MAPK activation cooperate to promote EMT and metastasis initiated from prostate cancer stem/progenitor cells. *Cancer Res*, 72, 1878-89.
- MUNRO, J., STEEGHS, K., MORRISON, V., IRELAND, H. & PARKINSON, E. K. 2001. Human fibroblast replicative senescence can occur in the absence of extensive cell division and short telomeres. *Oncogene*, 20, 3541-52.
- MURPHY, T., DARBY, S., MATHERS, M. E. & GNANAPRAGASAM, V. J. 2010. Evidence for distinct alterations in the FGF axis in prostate cancer progression to an aggressive clinical phenotype. *J Pathol*, 220, 452-60.
- MUZUMDAR, M. D., TASIC, B., MIYAMICHI, K., LI, L. & LUO, L. 2007. A global double-fluorescent Cre reporter mouse. *Genesis*, 45, 593-605.
- NAGY, A. 2000. Cre recombinase: the universal reagent for genome tailoring. *Genesis*, 26, 99-109.
- NAIDU, R., WAHAB, N. A., YADAV, M., KUTTY, M. K. & NAIR, S. 2001. Detection of amplified int-2/FGF-3 gene in primary breast carcinomas using differential polymerase chain reaction. *Int J Mol Med*, 8, 193-8.

- NAIMI, B., LATIL, A., FOURNIER, G., MANGIN, P., CUSSENOT, O. & BERTHON, P. 2002. Down-regulation of (IIIb) and (IIIc) isoforms of fibroblast growth factor receptor 2 (FGFR2) is associated with malignant progression in human prostate. *Prostate*, 52, 245-52.
- NAKOPOULOU, L., ZERVAS, A., GAKIOPOULOU-GIVALOU, H., CONSTANTINIDES, C., DOUMANIS, G., DAVARIS, P. & DIMOPOULOS, C. 2000. Prognostic value of E-cadherin, beta-catenin, P120ctn in patients with transitional cell bladder cancer. *Anticancer Res*, 20, 4571-8.
- NALDINI, L., BLOMER, U., GALLAY, P., ORY, D., MULLIGAN, R., GAGE, F. H., VERMA, I. M. & TRONO, D. 1996. In vivo gene delivery and stable transduction of nondividing cells by a lentiviral vector. *Science*, 272, 263-7.
- NASKI, M. C., WANG, Q., XU, J. & ORNITZ, D. M. 1996. Graded activation of fibroblast growth factor receptor 3 by mutations causing achondroplasia and thanatophoric dysplasia. *Nat Genet*, 13, 233-7.
- NETWORK, T. C. G. A. R. 2014. Comprehensive molecular characterization of urothelial bladder carcinoma. *Nature*, 507, 315-22.
- NICOLIS, S. K. 2007. Cancer stem cells and "stemness" genes in neuro-oncology. *Neurobiol Dis*, 25, 217-29.
- NIEGISCHE, G., LORCH, A., DROLLER, M. J., LAVERY, H. J., STENSLAND, K. D. & ALBERS, P. 2013. Neoadjuvant chemotherapy in patients with muscle-invasive bladder cancer: which patients benefit? *Eur Urol*, 64, 355-7.
- O'TOOLE, C. M., POVEY, S., HEPBURN, P. & FRANKS, L. M. 1983. Identity of some human bladder cancer cell lines. *Nature*, 301, 429-30.
- ODA, K., MATSUOKA, Y., FUNAHASHI, A. & KITANO, H. 2005. A comprehensive pathway map of epidermal growth factor receptor signaling. *Mol Syst Biol*, 1, 2005 0010.
- OGAWA, K., UZVOLGYI, E., ST JOHN, M. K., DE OLIVEIRA, M. L., ARNOLD, L. & COHEN, S. M. 1998. Frequent p53 mutations and occasional loss of chromosome 4 in invasive bladder carcinoma induced by N-butyl-N-(4-hydroxybutyl)nitrosamine in B6D2F1 mice. *Mol Carcinog*, 21, 70-9.
- OHTANI, M., KAKIZOE, T., NISHIO, Y., SATO, S., SUGIMURA, T., FUKUSHIMA, S. & NIIJIMA, T. 1986. Sequential changes of mouse bladder epithelium during induction of invasive carcinomas by N-butyl-N-(4-hydroxybutyl)nitrosamine. *Cancer Res*, 46, 2001-4.
- OLIVEIRA, P. A., COLACO, A., DE LA CRUZ, P. L. & LOPES, C. 2006. Experimental bladder carcinogenesis-rodent models. *Exp Oncol*, 28, 2-11.
- ONEYAMA, C., IKEDA, J., OKUZAKI, D., SUZUKI, K., KANOU, T., SHINTANI, Y., MORII, E., OKUMURA, M., AOZASA, K. & OKADA, M. 2011. MicroRNA-mediated downregulation of mTOR/FGFR3 controls tumor growth induced by Src-related oncogenic pathways. *Oncogene*, 30, 3489-501.
- OOI, A., HERZ, F., II, S., CORDONCARDO, C., FRADET, Y. & MAYALL, B. 1994. Ha-ras codon 12 mutation in papillary tumors of the urinary-bladder - a retrospective study. *Int J Oncol*, 4, 85-90.
- OOTTAMASATHIEN, S., WANG, Y., WILLIAMS, K., FRANCO, O. E., WILLS, M. L., THOMAS, J. C., SABA, K., SHARIF-AFSHAR, A. R., MAKARI, J. H., BHOWMICK, N. A., DEMARCO, R. T., HIPKENS, S., MAGNUSON, M., BROCK, J. W., 3RD, HAYWARD, S. W., POPE, J. C. T. & MATUSIK, R. J. 2007. Directed differentiation of embryonic stem cells into bladder tissue. *Dev Biol*, 304, 556-66.
- OZAKI, K., SUKATA, T., YAMAMOTO, S., UWAGAWA, S., SEKI, T., KAWASAKI, H., YOSHITAKE, A., WANIBUCHI, H., KOIDE, A., MORI, Y. & FUKUSHIMA, S. 1998. High susceptibility of p53(+/-) knockout mice in N-butyl-N-(4-

- hydroxybutyl)nitrosamine urinary bladder carcinogenesis and lack of frequent mutation in residual allele. *Cancer Res*, 58, 3806-11.
- PARKIN, D. M. 2011. 2. Tobacco-attributable cancer burden in the UK in 2010. *Br J Cancer*, 105 Suppl 2, S6-S13.
- PARKIN, D. M., BRAY, F., FERLAY, J. & PISANI, P. 2005. Global cancer statistics, 2002. *CA Cancer J Clin*, 55, 74-108.
- PATEL, A. R., CHAN, E. S., HANSEL, D. E., POWELL, C. T., HESTON, W. D. & LARCHIAN, W. A. 2010. Transabdominal micro-ultrasound imaging of bladder cancer in a mouse model: a validation study. *Urology*, 75, 799-804.
- PIGNON, J. C., GRISANZIO, C., GENG, Y., SONG, J., SHIVDASANI, R. A. & SIGNORETTI, S. 2013. p63-expressing cells are the stem cells of developing prostate, bladder, and colorectal epithelia. *Proc Natl Acad Sci U S A*, 110, 8105-10.
- PLOUSSARD, G., SOLIMAN, H., DUBOSQ, F., MERIA, P., VERINE, J., DESGRAND-CHAMPS, F., DETHE, H. & MONGIAT-ARTUS, P. 2011. The prognostic value of FGFR3 mutational status for disease recurrence and progression depends on allelic losses at 9p22. *Am J Cancer Res*, 1, 498-507.
- POLLOCK, P. M., GARTSIDE, M. G., DEJEZA, L. C., POWELL, M. A., MALLON, M. A., DAVIES, H., MOHAMMADI, M., FUTREAL, P. A., STRATTON, M. R., TRENT, J. M. & GOODFELLOW, P. J. 2007. Frequent activating FGFR2 mutations in endometrial carcinomas parallel germline mutations associated with craniosynostosis and skeletal dysplasia syndromes. *Oncogene*, 26, 7158-62.
- POWERS, C. J., MCLESKEY, S. W. & WELLSTEIN, A. 2000. Fibroblast growth factors, their receptors and signaling. *Endocr Relat Cancer*, 7, 165-97.
- PROST, S., SHEAHAN, S., RANNIE, D. & HARRISON, D. J. 2001. Adenovirus-mediated Cre deletion of floxed sequences in primary mouse cells is an efficient alternative for studies of gene deletion. *Nucleic Acids Res*, 29, E80.
- PUNYAVORAVUT, V. & NELSON, S. D. 1999. Diffuse bony metastasis from transitional cell carcinoma of urinary bladder: a case report and review of literature. *J Med Assoc Thai*, 82, 839-43.
- PUZIO-KUTER, A. M., CASTILLO-MARTIN, M., KINKADE, C. W., WANG, X., SHEN, T. H., MATOS, T., SHEN, M. M., CORDON-CARDO, C. & ABATE-SHEN, C. 2009. Inactivation of p53 and Pten promotes invasive bladder cancer. *Genes Dev*, 23, 675-80.
- QING, J., DU, X., CHEN, Y., CHAN, P., LI, H., WU, P., MARSTERS, S., STAWICKI, S., TIEN, J., TOTPAL, K., ROSS, S., STINSON, S., DORNAN, D., FRENCH, D., WANG, Q. R., STEPHAN, J. P., WU, Y., WIESMANN, C. & ASHKENAZI, A. 2009. Antibody-based targeting of FGFR3 in bladder carcinoma and t(4;14)-positive multiple myeloma in mice. *J Clin Invest*, 119, 1216-29.
- REDDY, E. P., REYNOLDS, R. K., SANTOS, E. & BARBACID, M. 1982. A point mutation is responsible for the acquisition of transforming properties by the T24 human bladder carcinoma oncogene. *Nature*, 300, 149-52.
- REYA, T. & CLEVERS, H. 2005. Wnt signalling in stem cells and cancer. *Nature*, 434, 843-50.
- ROIDL, A., FOO, P., WONG, W., MANN, C., BECHTOLD, S., BERGER, H. J., STREIT, S., RUHE, J. E., HART, S., ULLRICH, A. & HO, H. K. 2010. The FGFR4 Y367C mutant is a dominant oncogene in MDA-MB453 breast cancer cells. *Oncogene*, 29, 1543-52.

- ROMANO, R. A., ORTT, K., BIRKAYA, B., SMALLEY, K. & SINHA, S. 2009. An active role of the DeltaN isoform of p63 in regulating basal keratin genes K5 and K14 and directing epidermal cell fate. *PLoS One*, 4, e5623.
- ROOS, W. P. & KAINA, B. 2006. DNA damage-induced cell death by apoptosis. *Trends Mol Med*, 12, 440-50.
- ROSS, R. L., ASKHAM, J. M. & KNOWLES, M. A. 2013. PIK3CA mutation spectrum in urothelial carcinoma reflects cell context-dependent signaling and phenotypic outputs. *Oncogene*, 32, 768-76.
- RUSSELL, T. D., FISCHER, A., BEEMAN, N. E., FREED, E. F., NEVILLE, M. C. & SCHAACK, J. 2003. Transduction of the mammary epithelium with adenovirus vectors in vivo. *J Virol*, 77, 5801-9.
- SAAM, J. R. & GORDON, J. I. 1999. Inducible gene knockouts in the small intestinal and colonic epithelium. *J Biol Chem*, 274, 38071-82.
- SAHADEVAN, K., DARBY, S., LEUNG, H. Y., MATHERS, M. E., ROBSON, C. N. & GNANAPRAGASAM, V. J. 2007. Selective over-expression of fibroblast growth factor receptors 1 and 4 in clinical prostate cancer. *J Pathol*, 213, 82-90.
- SAID, N., FRIERSON, H. F., SANCHEZ-CARBAYO, M., BREKKEN, R. A. & THEODORESCU, D. 2013. Loss of SPARC in bladder cancer enhances carcinogenesis and progression. *J Clin Invest*, 123, 4089.
- SAMUELSON, A. V., NARITA, M., CHAN, H. M., JIN, J., DE STANCHINA, E., MCCURRACH, M. E., FUCHS, M., LIVINGSTON, D. M. & LOWE, S. W. 2005. p400 is required for E1A to promote apoptosis. *J Biol Chem*, 280, 21915-23.
- SANDILANDS, E., AKBARZADEH, S., VECCHIONE, A., MCEWAN, D. G., FRAME, M. C. & HEATH, J. K. 2007. Src kinase modulates the activation, transport and signalling dynamics of fibroblast growth factor receptors. *EMBO Rep*, 8, 1162-9.
- SANGAR, V. K., RAGAVAN, N., MATANHELIA, S. S., WATSON, M. W. & BLADES, R. A. 2005. The economic consequences of prostate and bladder cancer in the UK. *BJU Int*, 95, 59-63.
- SATO, T., VRIES, R. G., SNIPPERT, H. J., VAN DE WETERING, M., BARKER, N., STANGE, D. E., VAN ES, J. H., ABO, A., KUJALA, P., PETERS, P. J. & CLEVERS, H. 2009. Single Lgr5 stem cells build crypt-villus structures in vitro without a mesenchymal niche. *Nature*, 459, 262-5.
- SAVAGNER, P., VALLES, A. M., JOUANNEAU, J., YAMADA, K. M. & THIERY, J. P. 1994. Alternative splicing in fibroblast growth factor receptor 2 is associated with induced epithelial-mesenchymal transition in rat bladder carcinoma cells. *Mol Biol Cell*, 5, 851-62.
- SAYAN, A. E., D'ANGELO, B., SAYAN, B. S., TUCCI, P., CIMINI, A., CERÙ, M. P., KNIGHT, R. A. & MELINO, G. 2010. p73 and p63 regulate the expression of fibroblast growth factor receptor 3. *Biochemical and Biophysical Research Communications*, 394, 824-828.
- SCHMALHOFER, O., BRABLETZ, S. & BRABLETZ, T. 2009. E-cadherin, beta-catenin, and ZEB1 in malignant progression of cancer. *Cancer Metastasis Rev*, 28, 151-66.
- SCHMITZ-DRAGER, B. J., GOEBELL, P. J., EBERT, T. & FRADET, Y. 2000. p53 immunohistochemistry as a prognostic marker in bladder cancer. Playground for urology scientists? *Eur Urol*, 38, 691-9; discussion 700.
- SCOTET, E. & HOUSSAINT, E. 1995. The choice between alternative IIIb and IIIc exons of the FGFR-3 gene is not strictly tissue-specific. *Biochim Biophys Acta*, 1264, 238-42.

- SEAGER, C., PUZIO-KUTER, A. M., CORDON-CARDO, C., MCKIERNAN, J. & ABATE-SHEN, C. 2010. Mouse Models of Human Bladder Cancer as a Tool for Drug Discovery.
- SHARIAT, S. F., KIM, J., RAPTIDIS, G., AYALA, G. E. & LERNER, S. P. 2003. Association of p53 and p21 expression with clinical outcome in patients with carcinoma in situ of the urinary bladder. *Urology*, 61, 1140-5.
- SHIN, K., LEE, J., GUO, N., KIM, J., LIM, A., QU, L., MYSOREKAR, I. U. & BEACHY, P. A. 2011. Hedgehog/Wnt feedback supports regenerative proliferation of epithelial stem cells in bladder. *Nature*, 472, 110-4.
- SHINAGARE, A. B., RAMAIYA, N. H., JAGANNATHAN, J. P., FENNESSY, F. M., TAPLIN, M. E. & VAN DEN ABBEELE, A. D. 2011. Metastatic pattern of bladder cancer: correlation with the characteristics of the primary tumor. *AJR Am J Roentgenol*, 196, 117-22.
- SIDRANSKY, D., FROST, P., VON ESCHENBACH, A., OYASU, R., PREISINGER, A. C. & VOGELSTEIN, B. 1992. Clonal origin bladder cancer. *N Engl J Med*, 326, 737-40.
- SIDRANSKY, D., VON ESCHENBACH, A., TSAI, Y. C., JONES, P., SUMMERHAYES, I., MARSHALL, F., PAUL, M., GREEN, P., HAMILTON, S. R., FROST, P. & ET AL. 1991. Identification of p53 gene mutations in bladder cancers and urine samples. *Science*, 252, 706-9.
- SIMON, R., ELTZE, E., SCHAFER, K. L., BURGER, H., SEMJONOW, A., HERTLE, L., DOCKHORN-DWORNICZAK, B., TERPE, H. J. & BOCKER, W. 2001. Cytogenetic analysis of multifocal bladder cancer supports a monoclonal origin and intraepithelial spread of tumor cells. *Cancer Res*, 61, 355-62.
- SIMONEAU, M., LARUE, H., ABOULKASSIM, T. O., MEYER, F., MOORE, L. & FRADET, Y. 2000. Chromosome 9 deletions and recurrence of superficial bladder cancer: identification of four regions of prognostic interest. *Oncogene*, 19, 6317-23.
- SJODAHL, G., LAUSS, M., LOVGREN, K., CHEBIL, G., GUDJONSSON, S., VEERLA, S., PATSCHAN, O., AINE, M., FERNO, M., RINGNER, M., MANSSON, W., LIEBERG, F., LINDGREN, D. & HOGLUND, M. 2012. A molecular taxonomy for urothelial carcinoma. *Clin Cancer Res*, 18, 3377-86.
- SLEEMAN, M., FRASER, J., MCDONALD, M., YUAN, S., WHITE, D., GRANDISON, P., KUMBLE, K., WATSON, J. D. & MURISON, J. G. 2001. Identification of a new fibroblast growth factor receptor, FGFR5. *Gene*, 271, 171-82.
- SOLOWAY, M. S. 1977. Intravesical and systemic chemotherapy of murine bladder cancer. *Cancer Res*, 37, 2918-29.
- SONVILLA, G., ALLERSTORFER, S., HEINZLE, C., STATTNER, S., KARNER, J., KLIMPFINGER, M., WRBA, F., FISCHER, H., GAUGLHOFER, C., SPIEGL-KREINECKER, S., GRASL-KRAUPP, B., HOLZMANN, K., GRUSCH, M., BERGER, W. & MARIAN, B. 2010. Fibroblast growth factor receptor 3-IIIc mediates colorectal cancer growth and migration. *Br J Cancer*, 102, 1145-56.
- SPRUCK, C. H., 3RD, OHNESEIT, P. F., GONZALEZ-ZULUETA, M., ESRIG, D., MIYAO, N., TSAI, Y. C., LERNER, S. P., SCHMUTTE, C., YANG, A. S., COTE, R. & ET AL. 1994. Two molecular pathways to transitional cell carcinoma of the bladder. *Cancer Res*, 54, 784-8.
- STARR, T. K., ALLAEI, R., SILVERSTEIN, K. A., STAGGS, R. A., SARVER, A. L., BERGEMANN, T. L., GUPTA, M., O'SULLIVAN, M. G., MATISE, I., DUPUY, A. J., COLLIER, L. S., POWERS, S., OBERG, A. L., ASMANN, Y. W., THIBODEAU, S. N., TESSAROLLO, L., COPELAND, N. G., JENKINS, N. A., CORMIER, R. T. & LARGAESPADA, D. A. 2009. A transposon-based genetic

- screen in mice identifies genes altered in colorectal cancer. *Science*, 323, 1747-50.
- STEIN, J. P., GINSBERG, D. A., GROSSFELD, G. D., CHATTERJEE, S. J., ESRIG, D., DICKINSON, M. G., GROSHEN, S., TAYLOR, C. R., JONES, P. A., SKINNER, D. G. & COTE, R. J. 1998. Effect of p21WAF1/CIP1 expression on tumor progression in bladder cancer. *J Natl Cancer Inst*, 90, 1072-9.
- STEINBERG, G. D., BRENDLER, C. B., SQUIRE, R. A. & ISAACS, J. T. 1991. Experimental intravesical therapy for superficial transitional cell carcinoma in a rat bladder tumor model. *J Urol*, 145, 647-53.
- STEWART, F. A., DENEKAMP, J. & HIRST, D. G. 1980. Proliferation kinetics of the mouse bladder after irradiation. *Cell Tissue Kinet*, 13, 75-89.
- STOEHR, R., HARTMANN, A., HIENDLMEYER, E., MURLE, K., WIELAND, W. & KNUECHEL, R. 2000. Oligoclonality of early lesions of the urothelium as determined by microdissection-supported genetic analysis. *Pathobiology*, 68, 165-72.
- SUMMERHAYES, I. C. & FRANKS, L. M. 1979. Effects of donor age on neoplastic transformation of adult mouse bladder epithelium in vitro. *J Natl Cancer Inst*, 62, 1017-23.
- SUNG, S. Y., HSIEH, C. L., WU, D., CHUNG, L. W. & JOHNSTONE, P. A. 2007. Tumor microenvironment promotes cancer progression, metastasis, and therapeutic resistance. *Curr Probl Cancer*, 31, 36-100.
- SYLVESTER, R. J., VAN DER MEIJDEN, A. P., OOSTERLINCK, W., WITJES, J. A., BOUFFIOUX, C., DENIS, L., NEWLING, D. W. & KURTH, K. 2006. Predicting recurrence and progression in individual patients with stage Ta T1 bladder cancer using EORTC risk tables: a combined analysis of 2596 patients from seven EORTC trials. *Eur Urol*, 49, 466-5; discussion 475-7.
- TAKAHASHI, T., HABUCHI, T., KAKEHI, Y., MITSUMORI, K., AKAO, T., TERACHI, T. & YOSHIDA, O. 1998. Clonal and chronological genetic analysis of multifocal cancers of the bladder and upper urinary tract. *Cancer Res*, 58, 5835-41.
- TAVORMINA, P. L., SHIANG, R., THOMPSON, L. M., ZHU, Y. Z., WILKIN, D. J., LACHMAN, R. S., WILCOX, W. R., RIMOIN, D. L., COHN, D. H. & WASMUTH, J. J. 1995. Thanatophoric dysplasia (types I and II) caused by distinct mutations in fibroblast growth factor receptor 3. *Nat Genet*, 9, 321-8.
- TAYLOR, J. G. T., CHEUK, A. T., TSANG, P. S., CHUNG, J. Y., SONG, Y. K., DESAI, K., YU, Y., CHEN, Q. R., SHAH, K., YOUNGBLOOD, V., FANG, J., KIM, S. Y., YEUNG, C., HELMAN, L. J., MENDOZA, A., NGO, V., STAUDT, L. M., WEI, J. S., KHANNA, C., CATCHPOOLE, D., QUALMAN, S. J., HEWITT, S. M., MERLINO, G., CHANOCK, S. J. & KHAN, J. 2009. Identification of FGFR4-activating mutations in human rhabdomyosarcomas that promote metastasis in xenotransplanted models. *J Clin Invest*, 119, 3395-407.
- THEODOROU, V., BOER, M., WEIGELT, B., JONKERS, J., VAN DER VALK, M. & HILKENS, J. 2004. Fgf10 is an oncogene activated by MMTV insertional mutagenesis in mouse mammary tumors and overexpressed in a subset of human breast carcinomas. *Oncogene*, 23, 6047-55.
- THIERY, J. P. 2002. Epithelial-mesenchymal transitions in tumour progression. *Nat Rev Cancer*, 2, 442-54.
- TIMPSON, P., MCGHEE, E. J., ERAMI, Z., NOBIS, M., QUINN, J. A., EDWARD, M. & ANDERSON, K. I. 2011. Organotypic collagen I assay: a malleable platform to assess cell behaviour in a 3-dimensional context. *J Vis Exp*, e3089.
- TLSTY, T. D. & COUSSENS, L. M. 2006. Tumor stroma and regulation of cancer development. *Annu Rev Pathol*, 1, 119-50.

- TOMLINSON, D. C., BALDO, O., HARNDEN, P. & KNOWLES, M. A. 2007a. FGFR3 protein expression and its relationship to mutation status and prognostic variables in bladder cancer. *J Pathol*, 213, 91-8.
- TOMLINSON, D. C., BAXTER, E. W., LOADMAN, P. M., HULL, M. A. & KNOWLES, M. A. 2012. FGFR1-induced epithelial to mesenchymal transition through MAPK/PLCgamma/COX-2-mediated mechanisms. *PLoS One*, 7, e38972.
- TOMLINSON, D. C., HURST, C. D. & KNOWLES, M. A. 2007b. Knockdown by shRNA identifies S249C mutant FGFR3 as a potential therapeutic target in bladder cancer. *Oncogene*, 26, 5889-99.
- TOMLINSON, D. C., L'HOTE, C. G., KENNEDY, W., PITT, E. & KNOWLES, M. A. 2005. Alternative splicing of fibroblast growth factor receptor 3 produces a secreted isoform that inhibits fibroblast growth factor-induced proliferation and is repressed in urothelial carcinoma cell lines. *Cancer Res*, 65, 10441-9.
- TOMLINSON, D. C., LAMONT, F. R., SHNYDER, S. D. & KNOWLES, M. A. 2009. Fibroblast growth factor receptor 1 promotes proliferation and survival via activation of the mitogen-activated protein kinase pathway in bladder cancer. *Cancer Res*, 69, 4613-20.
- TONG, G. X., YEE, H., CHIRIBOGA, L., HERNANDEZ, O. & WAISMAN, J. 2005. Fascin-1 expression in papillary and invasive urothelial carcinomas of the urinary bladder. *Hum Pathol*, 36, 741-6.
- TOYODA, T., AKAGI, J., CHO, Y. M., MIZUTA, Y., ONAMI, S., SUZUKI, I. & OGAWA, K. 2013. Detection of gamma-H2AX, a Biomarker for DNA Double-strand Breaks, in Urinary Bladders of N-Butyl-N-(4-Hydroxybutyl)-Nitrosamine-Treated Rats. *J Toxicol Pathol*, 26, 215-21.
- TSURUTA, H. 2006. Hyperplasia and Carcinomas in Pten-Deficient Mice and Reduced PTEN Protein in Human Bladder Cancer Patients. *Cancer Research*, 66, 8389-8396.
- TUMBAR, T. 2004. Defining the Epithelial Stem Cell Niche in Skin. *Science*, 303, 359-363.
- TURNER, N. & GROSE, R. 2010. Fibroblast growth factor signalling: from development to cancer. *Nat Rev Cancer*, 10, 116-29.
- TURO, R., HARNDEN, P., THYGESEN, H., FLEISCHMANN, A., THALMANN, G. N., SEILER, R., CROSS, W. R. & KNOWLES, M. A. 2014. FGFR3 expression in primary invasive bladder cancers and matched lymph node metastases. *J Urol*.
- UREN, A. G., MIKKERS, H., KOOL, J., VAN DER WEYDEN, L., LUND, A. H., WILSON, C. H., RANCE, R., JONKERS, J., VAN LOHUIZEN, M., BERNS, A. & ADAMS, D. J. 2009. A high-throughput splinkerette-PCR method for the isolation and sequencing of retroviral insertion sites. *Nat Protoc*, 4, 789-98.
- VAN DER FLIER, L. G. & CLEVERS, H. 2009. Stem cells, self-renewal, and differentiation in the intestinal epithelium. *Annu Rev Physiol*, 71, 241-60.
- VAN RHIJN, B. W., LURKIN, I., CHOPIN, D. K., KIRKELS, W. J., THIERY, J. P., VAN DER KWAST, T. H., RADVANYI, F. & ZWARTHOFF, E. C. 2003. Combined microsatellite and FGFR3 mutation analysis enables a highly sensitive detection of urothelial cell carcinoma in voided urine. *Clin Cancer Res*, 9, 257-63.
- VAN RHIJN, B. W., LURKIN, I., RADVANYI, F., KIRKELS, W. J., VAN DER KWAST, T. H. & ZWARTHOFF, E. C. 2001. The fibroblast growth factor receptor 3 (FGFR3) mutation is a strong indicator of superficial bladder cancer with low recurrence rate. *Cancer Res*, 61, 1265-8.

- VAN RHIJN, B. W., MONTIRONI, R., ZWARTHOF, E. C., JOBSIS, A. C. & VAN DER KWAST, T. H. 2002. Frequent FGFR3 mutations in urothelial papilloma. *J Pathol*, 198, 245-51.
- VAN RHIJN, B. W., VAN DER KWAST, T. H., LIU, L., FLESHNER, N. E., BOSTROM, P. J., VIS, A. N., ALKHATEEB, S. S., BANGMA, C. H., JEWETT, M. A., ZWARTHOF, E. C., ZLOTTA, A. R. & BAPAT, B. 2012. The FGFR3 mutation is related to favorable pT1 bladder cancer. *J Urol*, 187, 310-4.
- VAN RHIJN, B. W., VAN DER KWAST, T. H., VIS, A. N., KIRKELS, W. J., BOEVE, E. R., JOBSIS, A. C. & ZWARTHOF, E. C. 2004. FGFR3 and P53 characterize alternative genetic pathways in the pathogenesis of urothelial cell carcinoma. *Cancer Res*, 64, 1911-4.
- VERANIC, P., ROMIH, R. & JEZERNIK, K. 2004. What determines differentiation of urothelial umbrella cells? *Eur J Cell Biol*, 83, 27-34.
- VOGELSTEIN, B., LANE, D. & LEVINE, A. J. 2000. Surfing the p53 network. *Nature*, 408, 307-10.
- VON DER MAASE, H., HANSEN, S. W., ROBERTS, J. T., DOGLIOTTI, L., OLIVER, T., MOORE, M. J., BODROGI, I., ALBERS, P., KNUTH, A., LIPPERT, C. M., KERBRAT, P., SANCHEZ ROVIRA, P., WERSALL, P., CLEALL, S. P., ROYCHOWDHURY, D. F., TOMLIN, I., VISSEREN-GRUL, C. M. & CONTE, P. F. 2000. Gemcitabine and cisplatin versus methotrexate, vinblastine, doxorubicin, and cisplatin in advanced or metastatic bladder cancer: results of a large, randomized, multinational, multicenter, phase III study. *J Clin Oncol*, 18, 3068-77.
- VON DER MAASE, H., SENGELOV, L., ROBERTS, J. T., RICCI, S., DOGLIOTTI, L., OLIVER, T., MOORE, M. J., ZIMMERMANN, A. & ARNING, M. 2005. Long-term survival results of a randomized trial comparing gemcitabine plus cisplatin, with methotrexate, vinblastine, doxorubicin, plus cisplatin in patients with bladder cancer. *J Clin Oncol*, 23, 4602-8.
- WALLERAND, H., BAKKAR, A. A., DE MEDINA, S. G., PAIRON, J. C., YANG, Y. C., VORDOS, D., BITTARD, H., FAUCONNET, S., KOUYOUMDJIAN, J. C., JAURAND, M. C., ZHANG, Z. F., RADVANYI, F., THIERY, J. P. & CHOPIN, D. K. 2005. Mutations in TP53, but not FGFR3, in urothelial cell carcinoma of the bladder are influenced by smoking: contribution of exogenous versus endogenous carcinogens. *Carcinogenesis*, 26, 177-84.
- WANG, D. S., RIEGER-CHRIST, K., LATINI, J. M., MOINZADEH, A., STOFFEL, J., PEZZA, J. A., SAINI, K., LIBERTINO, J. A. & SUMMERHAYES, I. C. 2000. Molecular analysis of PTEN and MXI1 in primary bladder carcinoma. *Int J Cancer*, 88, 620-5.
- WANG, H., LEAV, I., IBARAGI, S., WEGNER, M., HU, G. F., LU, M. L., BALK, S. P. & YUAN, X. 2008. SOX9 is expressed in human fetal prostate epithelium and enhances prostate cancer invasion. *Cancer Res*, 68, 1625-30.
- WANG, H., XIE, H., ZHANG, H., DAS, S. K. & DEY, S. K. 2006. Conditional gene recombination by adenovirus-driven Cre in the mouse uterus. *Genesis*, 44, 51-6.
- WATANABE, T., SHINOHARA, N., SAZAWA, A., HARABAYASHI, T., OGISO, Y., KOYANAGI, T., TAKIGUCHI, M., HASHIMOTO, A., KUZUMAKI, N., YAMASHITA, M., TANAKA, M., GROSSMAN, H. B. & BENEDICT, W. F. 2000. An improved intravesical model using human bladder cancer cell lines to optimize gene and other therapies. *Cancer Gene Ther*, 7, 1575-80.
- WATERSTON, R. H., LINDBLAD-TOH, K., BIRNEY, E., ROGERS, J., ABRIL, J. F., AGARWAL, P., AGARWALA, R., AINSCOUGH, R., ALEXANDERSSON, M., AN, P., ANTONARAKIS, S. E., ATTWOOD, J., BAERTSCH, R., BAILEY, J., BARLOW, K., BECK, S., BERRY, E., BIRREN, B., BLOOM, T., BORK, P.,

- BOTCHERBY, M., BRAY, N., BRENT, M. R., BROWN, D. G., BROWN, S. D., BULT, C., BURTON, J., BUTLER, J., CAMPBELL, R. D., CARNINCI, P., CAWLEY, S., CHIAROMONTE, F., CHINWALLA, A. T., CHURCH, D. M., CLAMP, M., CLEE, C., COLLINS, F. S., COOK, L. L., COPLEY, R. R., COULSON, A., COURONNE, O., CUFF, J., CURWEN, V., CUTTS, T., DALY, M., DAVID, R., DAVIES, J., DELEHAUNTY, K. D., DERI, J., DERMITZAKIS, E. T., DEWEY, C., DICKENS, N. J., DIEKHANS, M., DODGE, S., DUBCHAK, I., DUNN, D. M., EDDY, S. R., ELNITSKI, L., EMES, R. D., ESWARA, P., EYRAS, E., FELSENFELD, A., FEWELL, G. A., FLICEK, P., FOLEY, K., FRANKEL, W. N., FULTON, L. A., FULTON, R. S., FUREY, T. S., GAGE, D., GIBBS, R. A., GLUSMAN, G., GNERRE, S., GOLDMAN, N., GOODSTADT, L., GRAFHAM, D., GRAVES, T. A., GREEN, E. D., GREGORY, S., GUIGO, R., GUYER, M., HARDISON, R. C., HAUSSLER, D., HAYASHIZAKI, Y., HILLIER, L. W., HINRICHS, A., HLAVINA, W., HOLZER, T., HSU, F., HUA, A., HUBBARD, T., HUNT, A., JACKSON, I., JAFFE, D. B., JOHNSON, L. S., JONES, M., JONES, T. A., JOY, A., KAMAL, M., KARLSSON, E. K., et al. 2002. Initial sequencing and comparative analysis of the mouse genome. *Nature*, 420, 520-62.
- WEINER, L. P. 2008. Definitions and criteria for stem cells. *Methods Mol Biol*, 438, 3-8.
- WESCHE, J., HAGLUND, K. & HAUGSTEN, E. M. 2011. Fibroblast growth factors and their receptors in cancer. *Biochem J*, 437, 199-213.
- WILLIAMS, P. D., LEE, J. K. & THEODORESCU, D. 2008. Molecular credentialing of rodent bladder carcinogenesis models. *Neoplasia*, 10, 838-46.
- WU, X., OBATA, T., KHAN, Q., HIGHSHAW, R. A., DE VERE WHITE, R. & SWEENEY, C. 2004. The phosphatidylinositol-3 kinase pathway regulates bladder cancer cell invasion. *BJU Int*, 93, 143-50.
- XIN, L., LUKACS, R. U., LAWSON, D. A., CHENG, D. & WITTE, O. N. 2007. Self-renewal and multilineage differentiation in vitro from murine prostate stem cells. *Stem Cells*, 25, 2760-9.
- YAMAMOTO, S., CHEN, T., MURAI, T., MORI, S., MORIMURA, K., OOHARA, T., MAKINO, S., TATEMATSU, M., WANIBUCHI, H. & FUKUSHIMA, S. 1997. Genetic instability and p53 mutations in metastatic foci of mouse urinary bladder carcinomas induced by N-butyl-N-(4-hydroxybutyl)nitrosamine. *Carcinogenesis*, 18, 1877-82.
- YAMAMOTO, S., MASUI, T., MURAI, T., MORI, S., OOHARA, T., MAKINO, S., FUKUSHIMA, S. & TATEMATSU, M. 1995. Frequent mutations of the p53 gene and infrequent H- and K-ras mutations in urinary bladder carcinomas of NON/Shi mice treated with N-butyl-N-(4-hydroxybutyl)nitrosamine. *Carcinogenesis*, 16, 2363-8.
- YAMAMOTO, S., TATEMATSU, M., YAMAMOTO, M., FUKAMI, H. & FUKUSHIMA, S. 1998. Clonal analysis of urothelial carcinomas in C3H/HeN<-->BALB/c chimeric mice treated with N-butyl-N-(4-hydroxybutyl)nitrosamine. *Carcinogenesis*, 19, 855-60.
- YANG, X., LA ROSA, F. G., GENOVA, E. E., HUBER, K., SCHAACK, J., DEGREGORI, J., SERKOVA, N. J., LI, Y., SU, L. J., KESSLER, E. & FLAIG, T. W. 2013. Simultaneous Activation of Kras and Inactivation of p53 Induces Soft Tissue Sarcoma and Bladder Urothelial Hyperplasia. *PLoS One*, 8, e74809.
- YAO, R., LEMON, W. J., WANG, Y., GRUBBS, C. J., LUBET, R. A. & YOU, M. 2004. Altered gene expression profile in mouse bladder cancers induced by hydroxybutyl(butyl)nitrosamine. *Neoplasia*, 6, 569-77.
- YOHN, N. L., BINGAMAN, C. N., DUMONT, A. L. & YOO, L. I. 2011. Phosphatidylinositol 3'-kinase, mTOR, and glycogen synthase kinase-3beta

- mediated regulation of p21 in human urothelial carcinoma cells. *BMC Urol*, 11, 19.
- YOO, L. I., LIU, D. W., LE VU, S., BRONSON, R. T., WU, H. & YUAN, J. 2006. Pten deficiency activates distinct downstream signaling pathways in a tissue-specific manner. *Cancer Res*, 66, 1929-39.
- ZAYED, H., IZSVAK, Z., KHARE, D., HEINEMANN, U. & IVICS, Z. 2003. The DNA-bending protein HMGB1 is a cellular cofactor of Sleeping Beauty transposition. *Nucleic Acids Res*, 31, 2313-22.
- ZHANG, Y., WANG, Z., YU, J., SHI, J., WANG, C., FU, W., CHEN, Z. & YANG, J. 2012. Cancer stem-like cells contribute to cisplatin resistance and progression in bladder cancer. *Cancer Lett*, 322, 70-7.
- ZHANG, Z. T., PAK, J., HUANG, H. Y., SHAPIRO, E., SUN, T. T., PELLICER, A. & WU, X. R. 2001. Role of Ha-ras activation in superficial papillary pathway of urothelial tumor formation. *Oncogene*, 20, 1973-80.
- ZHANG, Z. T., PAK, J., SHAPIRO, E., SUN, T. T. & WU, X. R. 1999. Urothelium-specific expression of an oncogene in transgenic mice induced the formation of carcinoma in situ and invasive transitional cell carcinoma. *Cancer Res*, 59, 3512-7.
- ZHU, X., KANAI, Y., SAITO, A., KONDO, Y. & HIROHASHI, S. 2000. Aberrant expression of beta-catenin and mutation of exon 3 of the beta-catenin gene in renal and urothelial carcinomas. *Pathol Int*, 50, 945-52.
- ZIEGER, K., DYRSKJOT, L., WIUF, C., JENSEN, J. L., ANDERSEN, C. L., JENSEN, K. M. & ORNTOF, T. F. 2005. Role of activating fibroblast growth factor receptor 3 mutations in the development of bladder tumors. *Clin Cancer Res*, 11, 7709-19.
- ZIEGER, K., WOLF, H., OLSEN, P. R. & HOJGAARD, K. 2000. Long-term follow-up of noninvasive bladder tumours (stage Ta): recurrence and progression. *BJU Int*, 85, 824-8.

Appendices

Appendix 1 – Publications

FOTH M, AHMAD I, VAN RHIJN BW, VAN DER KWAST T, BERGMAN AM, KING L, RIDGWAY R, LEUNG HY, FRASER S, SANSOM OJ, IWATA T. 2014. Fibroblast growth factor receptor 3 activation plays a causative role in urothelial cancer pathogenesis in cooperation with Pten loss in mice. *J Pathol*, Epub 2014 Mar 31. doi: 10.1002/path.4334.